VOT 71458

AN APPROACH TO JOINT ROUGHNESS MEASUREMENT IN ROCK – A COMPARATIVE STUDY

(SATU PENDEKATAN KAEDAH PENGUKURAN KEKASARAN KEKAR DALAM BATUAN – KAJIAN PERBANDINGAN)

MOHD FOR BIN MOHD AMIN
MUSHAIRRY BIN MUSTAFFAR
TEO KING BENG

RESEARCH VOT NO:
71458

Jabatan Geoteknik dan Pengangkutan
Fakulti Kejuruteraan Awam
Universiti Teknologi Malaysia

2002

UNIVERSITI TEKNOLOGI MALAYSIA

BORANG PENGESAHAN
LAPORAN AKHIR PENYELIDIKAN

TAJUK PROJEK : AN APPROACH TO JOINT ROUGHNESS MEASUREMENT IN ROCK - A COMPARATIVE STUDY

Saya MOHD FOR MOHD AMIN
(HURUF BESAR)

Mengaku membenarkan Laporan Akhir Penyelidikan ini disimpan di Perpustakaan Universiti Teknologi Malaysia dengan syarat-syarat kegunaan seperti berikut : -

1. Laporan Akhir Penyelidikan adalah hakmilik Universiti Teknologi Malaysia.
2. Perpustakaan Universiti Teknologi Malaysia dibenarkan membuat salinan untuk tujuan rujukan sahaja.
3. Perpustakaan dibenarkan membuat penjualan salinan Laporan Akhir Penyelidikan ini bagi kategori TIDAK TERHAD.
4. Sila tandakan (/)

☐	**SULIT**	(Megandungi maklumat yang berdarjah keselamatan atau kepentingan Malaysia seperti yang termaktub di dalam **AKTA RAHSIA RASMI 1972**)
☐	**TERHAD**	(Mengandungi maklumat **TERHAD** yang telah ditentukan oleh organisasi/badan di mana penyelidikan dijalankan)
☑	**TIDAK TERHAD**	

.....
(TANDATANGAN KETUA PENYELIDIK)
MOHD FOR MOHD AMIN
Pensyarah
Jabatan Geoteknik & Pengangkutan
Fakulti Kej. Awam,
Universiti Teknologi Malaysia
Skudai
Nama & Cop Ketua Penyelidik

Tarikh : 20th. May 2004

CATATAN : Jika Lapotran Akhir Penyelidikan ini SULIT atau TERHAD, sila lampirkan surat daripada pihak berkuasa/organisasi berkenaan dengan menyatakan sekali sebab dan tempoh laporan ini perlu dikelaskan sebagai SULIT dan TERHAD.

TABLE OF CONTENTS

ABSTRAK

Kekuatan ricih satah kelemahan dalam batuan, seperti satah kekar, amat dipengaruhi oleh keadaan permukaannya. Oleh yang demikian, tekstur dan tahap kekasaran merupakan suatu aspek yang penting dalam penilaian kekuatan ricih satah kekar. Walaubagaimanapun, kaedah pengukuran kekasaran permukaan kekar yang sedia ada melibatkan prosedur kerja yang rumit dan memakan masa. Kajian ini cuba mengetengahkan satu kaedah alternatif yang menggunakan prinsip fotogrametri jarak dekat. Kesesuaian kaedah ini telah dikaji di makmal dengan menggunakan model fizikal permukaan kekar. Geometri kekasaran permukaan model tersebut, dalam bentuk ketinggian puncak dan palung, diukur dengan menggunakan kaedah fotogrametri dan kaedah biasa. Pengukuran dibuat pada titik-titik grid yang sama yang ditandakan pada permukaan model. Untuk tujuan perbandingan, data yang diperolehi daripada kaedah biasa digunakan sebagai rujukan. Perbandingan yang dibuat adalah dari segi nilai ketinggian puncak dan palung, bentuk profil, plotan 3 dimensi dan indeks-indeks kekasaran (iaitu sisihan piawai, kekasaran mutlak dan purata garis pertengahan). Bagi menilai kebolehgunaan kaedah ini, kerja pengukuran permukaan kekar di lapangan juga telah dilaksanakan. Hasil kajian jelas menunjukkan bahawa kaedah fotogrametri menampakkan beberapapa ciri positif sebagai suatu kaedah alternatif yang berpotensi. Perolehan tekstur permukaan kekar dengan menggunakan kamera digital membolehkan lebih banyak data diperolehi di lapangan dan data-data ini boleh disimpan untuk diproses kemudian. Secara amnya, boleh dirumuskan bahawa kaedah fotogrametri dapat mempermudahkan lagi kerja pengukuran kekasaran permukaan kekar di lapangan. Imej 3 dimensi bagi permukaan kekar yang diperolehi melalui kaedah ini boleh memberi gambaran yang lebih jelas dalam menilai kekuatan ricih kekar.

ABSTRACT

The shear strength of a weakness plane in rock such as joint, is greatly influenced by its surface condition. Therefore, surface texture and degree of roughness are important aspects to be considered in assessing the shear strength of joint. However, the present method for measuring surface texture are labourious and time consuming processes. This study highlights an alternative method of measurement using close-range photogrammetry. The suitability of the proposed method was verified in laboratory using a physical model of joint surface. The degree of roughness of the model surface, was measured using both photogrammetry and conventional method. All measurements were made on the same grid points marked on the model surface. Data obtained from both methods was compared in terms of peak and trough height, profile shape, 3-dimensional plot and roughness index (i.e. standard deviation, absolute roughness and central line average). In the comparison process, data obtained using conventional method is used as reference. To verify its practicality, the proposed method was used to measure joint surface in the field. The outcome of this study, clearly shows that photogrammetry exhibits several positive characteristics as an alternative method for measuring surface texture of joint in rock. The use of digital camera allows for a larger amount of field data to be collected and this data could be stored and processed at a later stage. Consequently, this facilitates joint survey work in the field. In addition, the 3-dimensional image of the joint surface which can be readily plotted using photgrammetry data, serves as a useful tool in providing vital information on the texture of the joint surface. The image can be used as tool in assessing the surface conditions, which is an important procedure for laboratory shear test on joint in rock.

CHAPTER I

INTRODUCTION

1.1 Introduction

Joints are planes of weakness or discontinuities in rock mass. In civil engineering construction, joints pose several problems particularly in work that are related to slope and underground excavation in rock. This is mainly due to the stability and strength of the jointed rock mass are largely controlled by the existing joints. As such, assessment on the shear strength of joint in rock mass is an important procedure in the design and planning of any civil structure that is associated with excvation in rock.

The texture of a joint surface has a significant influence on the shear strength and the mechanical behaviour of a rock block that slides along this joint plane (Richards and Cowland, 1982). As a natural fracture in rock, the texture and degree of roughness of joints vary significantly, depending of their mode of formation and geometrical position in the host rock. Consequently, the measurement of joint surface texture needs to be conducted on representative joint, particularly those that are critical to the proposed structure. The technique of measurement is important in ensuring the reliability of data which is acquired at minimal cost and time.

1.2 Background of research

Roughness profiler is an apparatus commonly used for measuring surface roughness of joint. Being a manually operated linear profiler, the measured data is subjected to random error and the number of sections that can be profiled is also limited. These problems arise due to the repetitive nature of the measuring process. As a result, this would mean insufficient data of lower accuracy to represent the actual texture of the measured surface. For field use, this profiler exhibits limited versatility. Field conditions may also affect the

operator's competency and subsequently, the quality of data collected. Hence, alternative methods for joint surface texture measurement is therefore essential. The method should be versatile for field use and able to acquire large number of data of sufficient accuracy at minimal time possible.

The principles of a number of methods in land surveying are of similar concept as surface texture measurement in rock and this in particular is close-range photogrammetry. In principle, close-range photogrammetry is a technique of obtaining the position, size and and shape of an object without directly measuring the object.

1.3 Significant of research

In the field, relevant data pertaining to joint surface texture is determined from representative joints exposed on the rock surface. Linear profiler is a tool normally used for obtaining the relevant data on surface texture. However, unfavourable field conditions and accessibility of representative joints may inhibit collection of sufficient and reliable data. In addition, measuring procedures are laborious and repeatitive particularly, when a large number of joints is involved. Occasionally, joints that are critical to the proposed structure may have to be sampled and assessed in detailed in laboratory. The process usualy associated with expensive sampling and testing methods. Hence, the reliability of data collected from the laboratory assessments must justify the cost that has been incurred. An alternative method, with appropriate characteristics, for joint surface measurement in laboratory and field would help to reduce some of the above-mentioned problems.

1.4 Objectives of research

The main objectives of this research are:

(i) To propose an alternative method for surface texture measurement of joint in rock.

(ii) To verify the suitability of close-range photogrammetry for measuring surface texture of joint in rock. Assessment on suitability will be based on the practicality, reliability of data and capability for automation of the proposed method.

(iii) To verify the versatility of the proposed method for field use, particularly on the measurement processes involved and time required to undertake the measurement.

1.5 Research scope and limitations

This study will be focussed on the following aspects:

(i) Exposed joint in granite rock. This is necessary as image processing in this study requires a well-textured joint surface which can be readily obtained from a coarse-grained rock with distinctive colour variation of its mafic minerals.

(ii) Joint surface selected for model casting and measurement is an unweathered joint. This ensures the surface roughness measured is representative of fresh joint in granite. Weathering may affect the surface texture of joint to a certain degree.

(iii) Measurements are made on small-scale roughness (scale of few mm to cm) for this is the type of roughness which has a significant effect on joint shear strength.

(iv) Systematic error of camera sensors (pixel size and lens distortion) will be disregarded.

(v) Images are acquired using medium resolution digital camera under normal lighting condition therefore, the effect of radiometric on the image will not be considered.

1.6 Research methodology

The main bulk of this study comprised laboratory and field work. In laboratory, surface measurements were conducted on a replica model of joint surface. This model was made by casting a suitable mix of plaster of Paris on a typical fresh joint in granite.

Geometrical measurement made on the model surface consists of height of peaks and troughs, measured at predetermined points marked on the model. Measurements were undertaken using both conventional profiler and close-range photogrammetry technique. Data obtained was processed accordingly and the geometrical data obtained using both methods was then compared in terms of accuracy. Once the suitability of photogrammetry technique had been verified, measurement on actual joint surface in granite was conducted at a selected site. This is to verify the versatility of this method for field use.

CHAPTER 2.0

LITERATURE REVIEW

2.1 Introduction

Joints are planes of weakness or discontinuities in rock mass. The term discontinuity is a collective term for all fractures and features in rock mass such as joints, faults and bedding planes that have zero or relatively low tensile strength (Brady & Brown, 1985). Joints are formed by tensile stress in the rock mass as such, its formation is associated with negligible amount of displacement. Joints are relatively small in size compared to faults and they can be of several metres in length. Being fracture planes, joints effect the strength and deformability of rock mass (Goodman & Richard, 1980).

Based on mode of formation, joints are classified as tension joint, shear joint, joint due to periodic sedimentation (Aydan & Kawamoto, 1990). For massive and strong rock like granite, joints may occur in several sets and this can be attributed to their mode of formation in this intrusive igneous rock. In granite, sets of joints are formed due to stresses induced during its cooling stage and also due to release of overburden stresses following the extrusion of this plutonic rock to the surface. Joint can also be classified as closed (matched joint) and opened joint. In addition, an opened joint may be unfilled (clean joint) or filled with infilling materials. These infillings may comprised weathered materials resulting from in-situ weathering of joint walls, in-washed sediments or secondary mineralisation (Chernychev & Dearman, 1991).

2.1.1 Roughness and texture of joint surface

Roughness of joint surface is the main factor that controls its shear strength especially in the case of undisplaced and interlocked joint. According to ISRM (1981) and Brady & Brown (1985), roughness of joint is a measure of the inherent surface uneveness and waviness (geometrical undulations) of this discontinuity with respect to its mean plane.

The importance of roughness declines with increasing joint opening/aperture, filling thickness or previous shear displacement. In other word roughness is an important aspect to be considered when assessing the mechanical properties of undisplaced matched joint.

The texture and feature that create roughness on joint surface depend on several factors and among these include types of joint, mode of formation, types and mineralogy of host rock. Perhaps, size of mineral grains of the host rock is the main factor to be considered when dealing with small scale roughness as discussed below. For rocks that exhibit coarse crystal grains with interlocking texture like granite, the effect of roughness can be significant to the shear strength of its joint. However, previous shear displacement and weathering may damage the surface texture of joint to a certain extent (Bells, 1992).

2.1.2 Scale of joint roughness

Scale is a factor that must be considered when assessing surface roughness of joint. Roughness of different scale will lead to different mode of shearing and level of shear strength. For instant, roughness of baselength 1mm will have a significant effect on the shear strength of a joint with 10cm baselength. However, for joint with baselength more than 10m, the effect of these small features on strength will be insignificant (Bandis, 1993). Similarly, joint surface with roughness of base length of 2m will induce minimal shearing resistance on a $1m^3$ block sliding on this joint but, will dictitate the sliding direction of the block. On the other hand, roughness of 2mm base length will affect the shear strength of the same sliding block but little influence on the shearing direction. It is due to these effect that roughness is usually classified into two main groups, based on scale (Barton, 1978):

a) Small scale roughness (few cm) – small scale surface irregularity or uneveness.
b) Large scale roughness (few m) – medium size surface irregularity or waviness.

The schematic presentation of different scale of discontinuity roughness sampled at different scales is shown in Figure 2.1. From this figure it can be summarised that

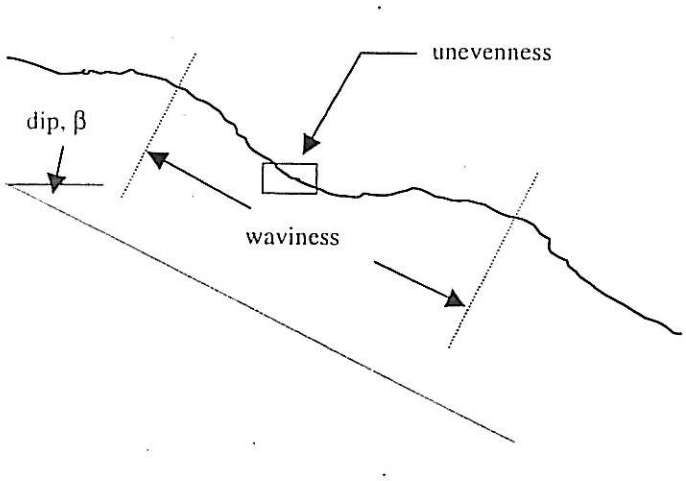

Figure 2.1: The schematic presentation of different scale of discontinuity roughness sampled at different scales (after Brady & Brown, 1983).

large scale roughness (waviness) affects the intial direction of shear displacement relative to the mean discontinuity plane, while small scale roughness (unevenness) affects the shear strength that would normally be sampled in a laboratory or medium scale *in situ* direct shear test (ISRM, 1981). The medium scale roughness can be further classified as *stepped*, *undulating* and *planar*. Combination of both these scales, small scale roughness is often classified as *rough*, *smooth* and *slickensided* as shown in Figure 2.2.

The different scale of waviness and unevenness each gives different effect on joint shear strength. Waviness which is first order asperities occurs as undulations on joint surface. This large scale roughness which, if interlocked and in contact, cause dilation during shear displacement since they are too large to be sheared off. Unevenness, which is second order asperities occurs as small scale features that tends to be damaged during shear displacement unless the discontinuity walls are of high strength and/or the stress levels are too low, so that dilation can also occur on these surface features. Small scale roughness has a significant impact on friction angle (Bells, 1993) consequently, the shear strength of a joint.

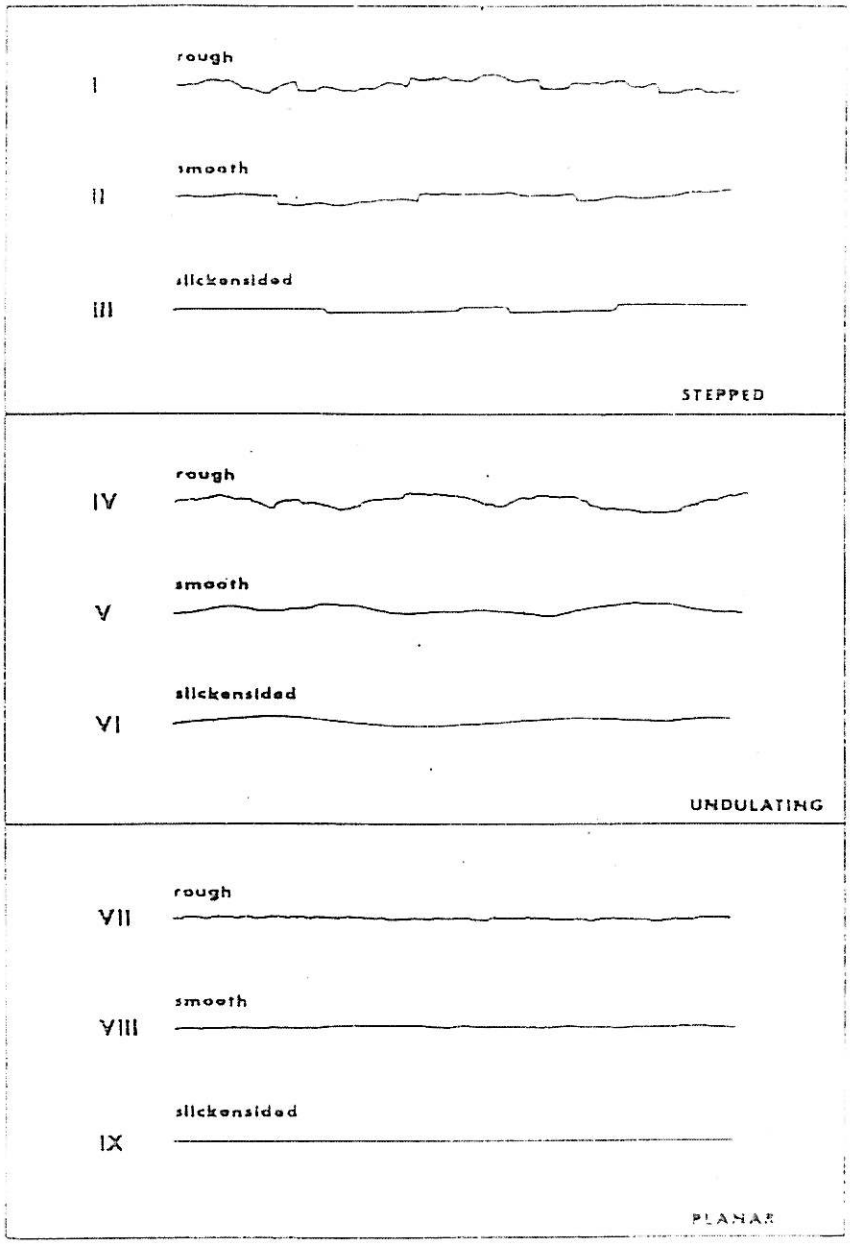

Figure 2.2: Typical roughness profiles and suggested nomenclature (after Brady & Brown, 1983).

As a summary, joints are the main source of instability in slope and underground excavation in rock. This is mainly due to the stability and strength of rock mass are largely controlled by the existing joints. In addition, roughness and texture of the joint surface dictates its shear strength. As such, assessment on joints, especially surface texture and shear strength, is an important procedure in designing and planning of any structure that is associated with excavation in jointed rock mass.

2.1.2.2 Methods for measuring roughness of joint surface

In general, type of method for measuring surface roughness depend on scale of roughness to measured and purpose of measurement. Measurement of a surface can be done in the form features along line as profile section or, as texture of the whole surface. If sliding direction of rock blocks on a joint plane is known, measurement of roughness of this joint is usually taken along lines, parallel to the sliding path. Since shearing of joint is a complex process that may involve dilation, compression as well as lateral displacement of the joint therefore, 3-dimensional surface measurement may be required. Such measurement is also necessary when input data like shear direction, amount of dilation and contact surface during shearing is required. Perhaps, this nature of surface measurement is usually associated with research work or when stability of joints in rock is a critical factor in a design of a structure.

Several methods are available for measuring surface texture of joints (ISRM, 1981):

a) Linear profiler – This simple apparatus is used to measure geometrical shape of joint surface at selected sections (see Figure 2.3). Measurement are made along lines that are parallel to sliding direction. This type of measurement is suitable for wedge failure formed by two intersecting joints. In this type of failure, the sliding direction is approximately along line of intersection of joints.

   Accessories and equipments required include segments of wooden plank (2m length), Brunton compass or clinometer and aluminium discs (5, 10, 20 and 40cm diameter).

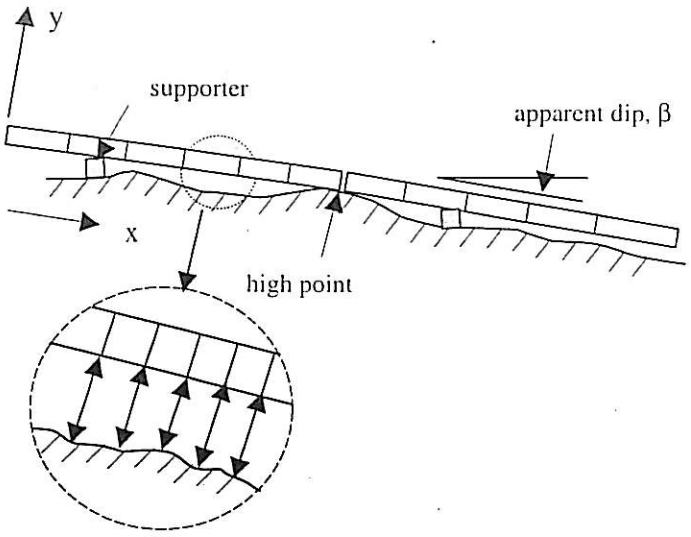

Figure 2.3: Measurement of joint surface roughness using linear pofiler (modified after ISRM, 1981).

Although measuring procedures are simple and straight forward however, they are tedious and repeatitive. Human judgements and working conditions, contribute to a certain degree, to the reliability of data.

b) Photogrammetry method – A technique adopted from photogrammetry in land survey, use for surface contouring of a large size joint surface. Accuracy of data is proportional to joint size hence, it is not suitable for small-scale surface features. The technique requires at least 4 coordinate points to establish the orientation of joint surface. To ensure the accuracy data, certain procedures must be undertaken: correction for lens distortion, selection of film type based on light intensity, correct positioning of camera stations and control targets.

Work involved are divided into two; data acquisition on site and data processing in laboratory. Equipments and accessories for field work and data processing include phototheodolite, light meter, stereoscopic plotter and stereo comparator. Figure 2.4 shows the general layout for photogrammetry method.

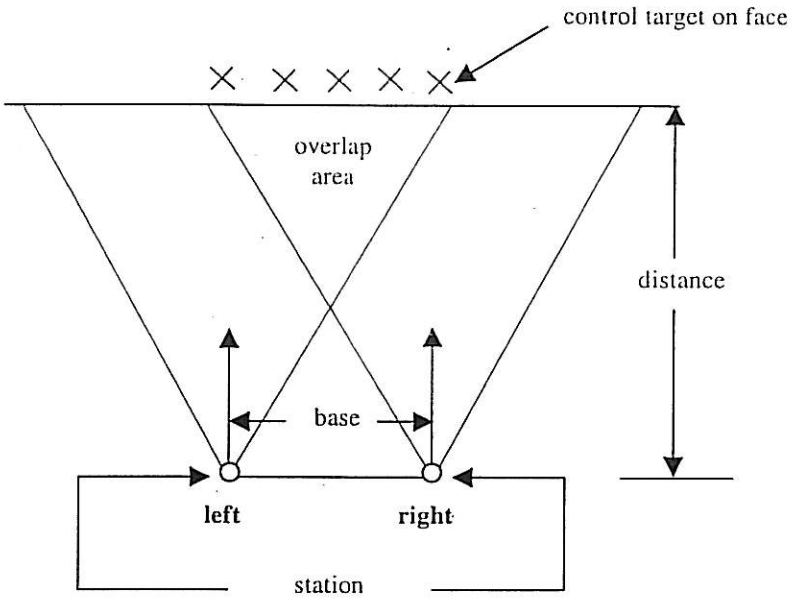

Figure 2.4: General equipment layout for photogrammetry method.

Besides the two methods proposed by ISRM (1981) above, several other methods have been proposed by other researchers that include profilograph technique (Fecker & Rengers, 1971) and 'shadow and photoanalysis' method (Franklin & Dusseault, 1989). General descriptions of these methods are discussed in Teo (2002). The use of highly sensitive sensors and laser beam have also been proposed for surface text measurement, mainly adopted from the field of metallurgy. However, due to involvement of highly sophisticated equipments, their application in the field engineering rock mechanics is unpractical and unjustifiable.

2.1.2.3 Weaknesses of the existing methods for joint surface measurement.

Common methods for joint surface measurement in rock usually consist of manually operated mechanical equipments and the associated measuring processes are tedious and repeatitive. Data acquired using equipment of these natures is subjected to error as well as human dependent. Associated work occasionally requires measurement to be

undertaken on site. This may induce further inconsistency into the collected data due to adverse working conditions and limited versatility of the equipment used.

Linear profiler although simple and practical it suffers from several shortcomings for measuring surface texture of joint. Some assembling work on the equipment is required (see ISRM, 1981 & Teo, 2002). Only limited number of profiles can be measured at given time hence, quantity of data may not be sufficient to represent the correct topography of joint surface. Since profiler has to be placed directly on the joint, measurement would be difficult for joints located at unfavorable position in the rock mass. Field conditions may also affect the operator's competency and subsequently, the quality of data collected.

Comparatively, photogrammetry techniques is better in terms of accuracy however, this method is time consuming and expensive. Most of the equipments used are highly specialised and would require trained personnel and hence rarely used in the field of engineering geology and rock mechanics.

As far as field and laboratory measurement of joint surface are concerned, the reliability of data collected must justify the cost and objective of the measurement. Alternative method must exhibit characteristics and versatility that are appropriate for the purpose and able to eliminate or reduce the associated problems.

2.1.3 Effect of surface roughness on mechanical properties of joint

Surface roughness characteristic of joint has a significant effect on its mechanical behaviour. Most importantly is the effect on shear strength which greatly dependent on frictional characteristics of the joint surface (Barton & Choubey, 1977; Piggott & Elsworth, 1995). In addition, different roughness features will result in different contact area between interfacing joint walls during shearing (Mohd Amin *et al.*, 2001; Power & Hencher, 1996).

2.1.3.1 Shear strength

The strength components when shearing occurs in smooth joint can be described using Coulomb's equation:

$$\tau = \sigma_n \tan \phi + c \qquad (2.1)$$

where;

τ = peak shear strength,

σ_n = acting normal stress,

ϕ = friction angle,

c = cohesion properties.

For rock joint, another strength component will be induced by the occurrence of surface roughness and this parameter is termed as roughness angle, *i*. Equation 2.1 will take the following form:

$$\tau = \sigma_n \tan (\phi_b + i) + c \qquad (2.2)$$

It can be seen that the frictional component for rough joint, the friction angle (ϕ) consists of basic friction angle (ϕ_b) and roughness angle (*i*). The latter is usually measured in the direction of shearing. Value of ϕ_b depends on the mineralogy of joint surface (i.e. the host rock) and *i* depends on the roughness charateristics of joint surface. Correlations between these parameters are depicted in Figure 2.5(a) and 2.5(b). From these figures it can be seen that higher shear strength exhibited by rough joint is mainly due to a larger value of *i* measured along sliding direction. If the joint surface is relatively strong or, acting normal stress is too low for the roughness features to be sheared off then, dilation of joint will occur. It is for this reason that the roughness angle, *i*, is also termed as dilation angle, i.e. the dip angle of the roughness profile in the direction of sliding, as shown in Figure 2.5(b).

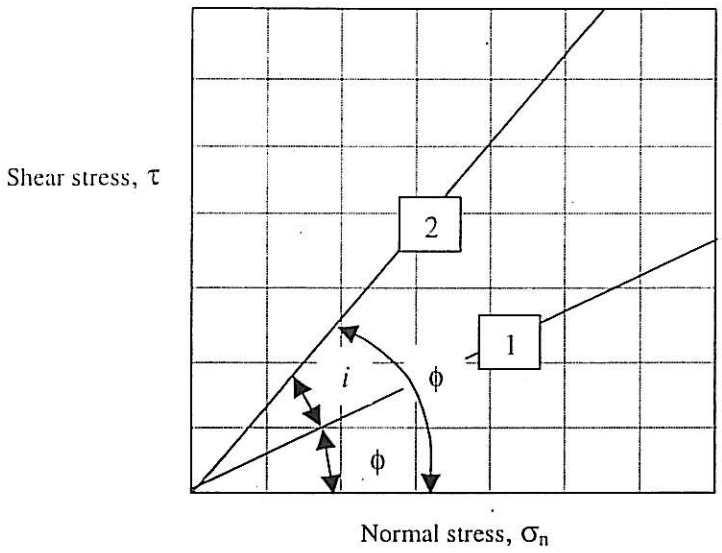

Figure 2.5(a): Relation between shear and normal stress for – [1] smooth surface and [2] rough surface.

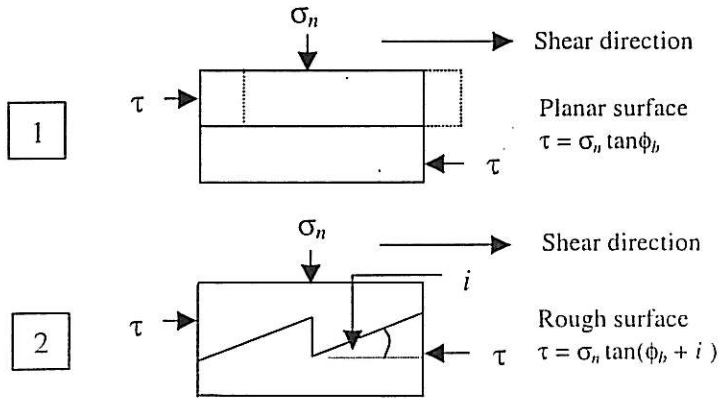

Figure 2.5(b): Effect of roughness on shear behaviour of joint.

For normal conditions and continuous joint, value of cohesion, c, is usually taken as zero. Cohesion will only occur when joint is not persistence or discontinuous, due to bridging between joint surfaces or occurrence of secondary mineralisation along joint (Hencher & Richards, 1989). In very rough and matching joint, interlocking of the surface features between interfacing joint may lead to some degree of cohesion. In situation where applied normal stress is relatively high, fracturing of surface features or asperities will take place

during shearing. The resulting fragments will affect the value of angle *I*, which usually taken as residual friction angle (Richards and Cowland, 1982).

In true situation, the behaviour of shearing joint is far more complex than what is depicted in Figure 2.5. Geometric features of the surface roughness vary considerably along any section on the surface and so does the roughness angle *i*. Patton (1966), in his attempt to simplify the complexity, proposed a refined classification for roughness based on angle *i* and this is shown in Figure 2.6. Asperity in the form of large undulations is termed as first order asperity (i.e. medium scale roughness) and small scale roughness is termed second order asperity.

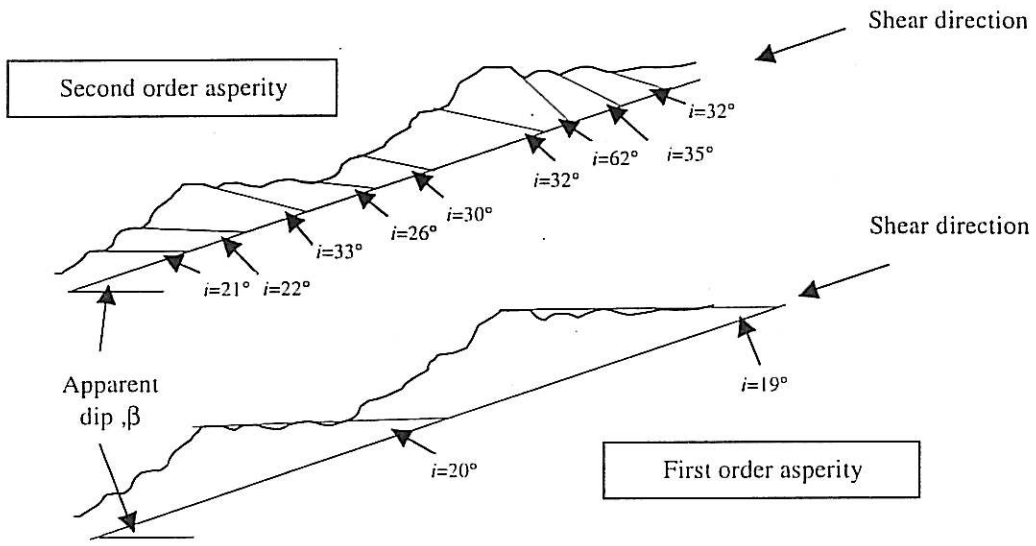

Figure 2.6: Value of roughness of dilation angle, *i*, based on Patton (1966).

Shear behaviour of a joint under low normal stress is affected by second order asperity. Asperity of this order will be sheared off if applied normal stress is higher than compressive strength of the asperity, i.e. compressive strength of the joint surface. In this situation shearing stress will be transferred to first order asperity which in turn, will also be sheared off if the prevailing normal stress is still too high. Shearing will continue with the shearing of the first order asperity and the condition is similar to sliding along a planar surface with broken fragments of the asperity remain on the surface. Value of *i*

will eventually reduced to zero and in return c starts to prevail. The residual friction angle, ϕ_r, will be higher than normal condition due to interlocking of the broken fragments (Richards & Cowland, 1982).

Detailed study conducted by Barton & Choubey (1977) on shear behaviour of joint shows that its peak shear strength is controlled by several parameters:

$$\tau = \sigma_n \tan [\, JRC \log_{10} (JCS/\sigma_n) + \phi_b \,] \qquad (2.3)$$

where,

τ = peak shear strength

σ_n = effective normal stress

JCS = joint wall compressive strength

JRC = joint roughness coefficient

ϕ_b = basic friction angle (measured using residual shear test on smooth, unweathered rock surface).

In their study, the value of *JRC* was in the range of between 0 and 20, for smooth to rough surface depending on the roughness measured (see Figure 2.7). *JCS* is the uniaxial compressive strength of fresh rock that contains the joint. Alternatively *JCS* can be approximated from Schmidt hammer or rebound hammer test on fresh rock block where, rebound number, R, can be correlated with *JCS*.

Figure 2.8 shows the application of this empirical correlations. In this figure correlation graphs are used for estimating peak shear strength based on *JRC*, as proposed by Barton and Choubey (1977). Value of *JRC* 20, 10 and 5 and, *JCS* 5, 10, 50 and 100 (in MPa) in the graph, show the effect of surface roughness and surface strength on peak shear strength of joint, repectively. Basic friction angle, ϕ_b, is taken as 30^0 in all these graphs but, for unweathered joint it is between 25^0 and 35^0 (Barton & Choubey, 1977).

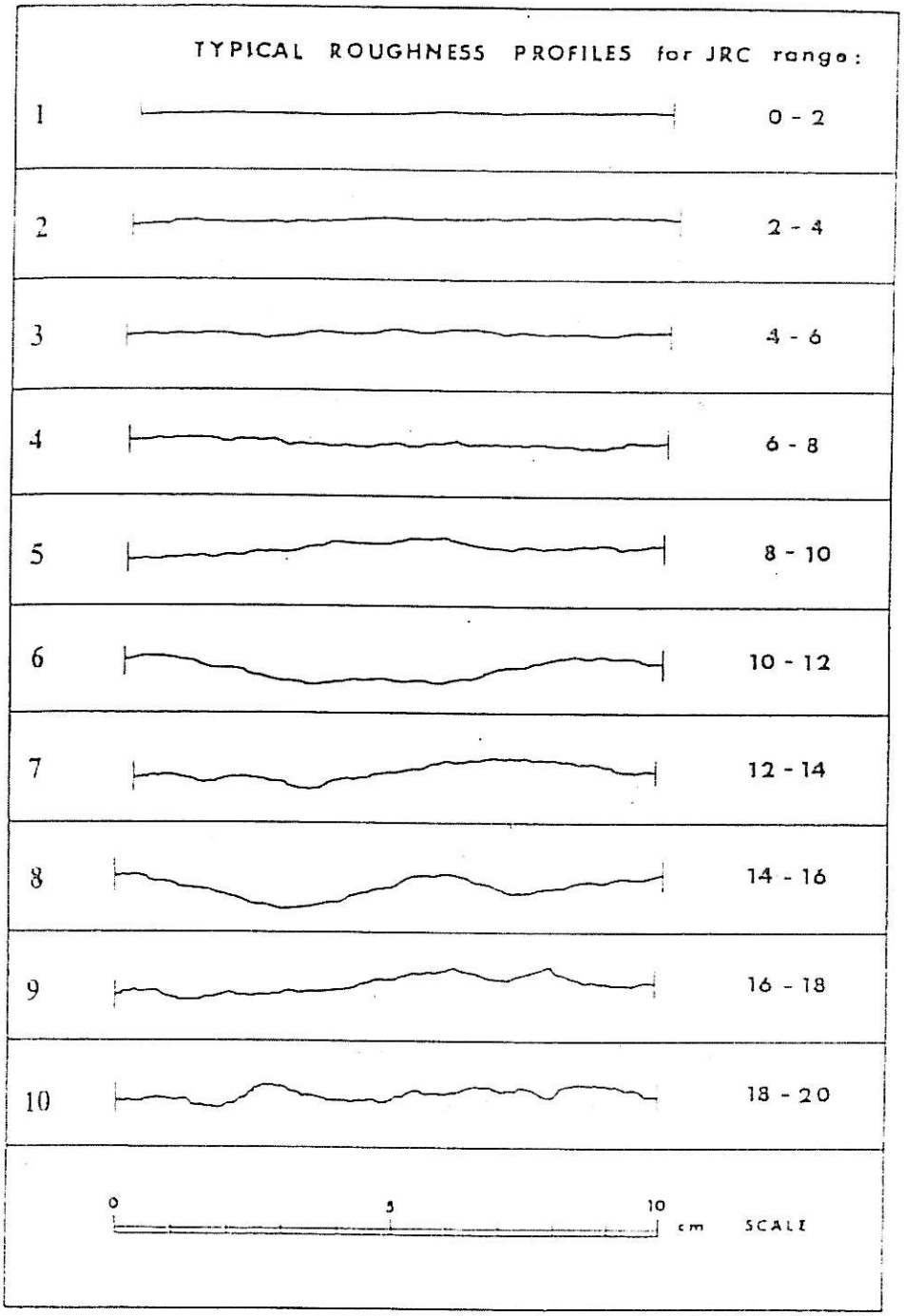

Figure 2.7: Roughness profiles and corresponding range of *JRC* values (after ISRM, 1981).

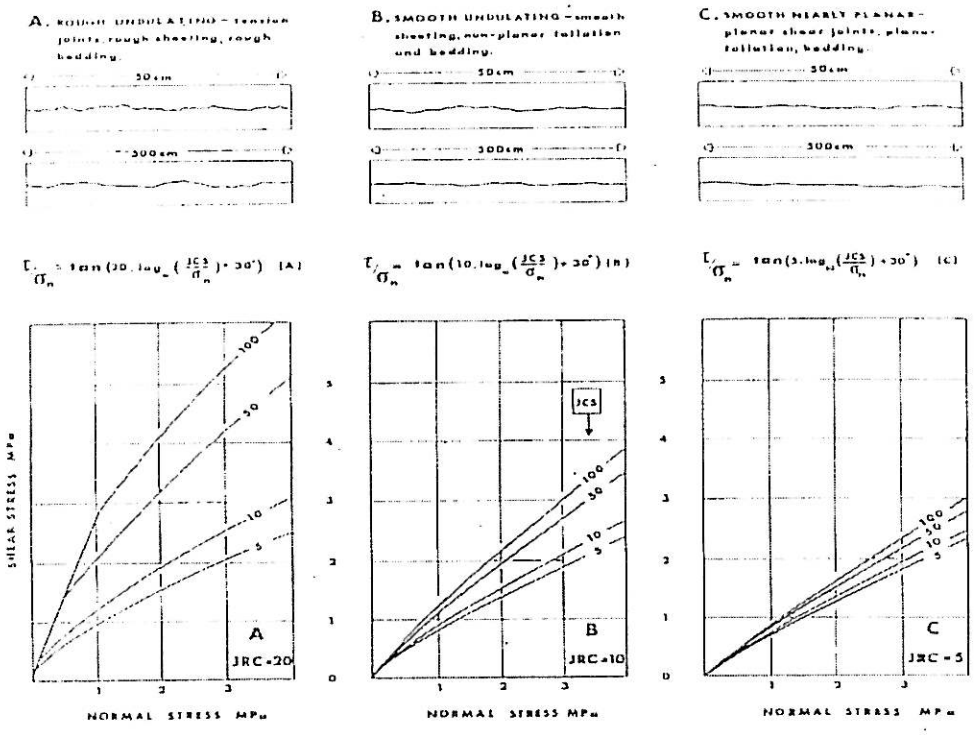

Figure 2.8: Method for estimating peak shear strength from roughness profile (JRC) and surface strength (JCS) of joint (after Barton Choubey, 1977).

Similar to Figure 2.5, Figure 2.8 signifies the effect of surface texture on shear strength of a joint. The curves in this figure show that as the degree of roughness (JRC) increases, the shear strength also increases. However, the effect becomes less significant as the value of JCS becomes smaller, as in smoother joint surface.

In laboratory shear test on rock joint, the acting normal stress is usually calculated as the applied normal load divided by the cross-sectional area of sample. The normal stress at subsequent shearing is calculated accordingly, taking into account the reduction in contact area as the joint blocks displace relative to each other. This may be true for smooth joints but for rough joints different situation may arise, as schematically shown in Figure 2.9. Not only the contact area changes throughout the shearing process, but it also depends on the amount of contact between peaks of the interfacing joint surfaces (Power

& Hencher, 1996). True contact area is actually much less than gross projected area. Figure 2.10 shows the difference between apparent contact area (i.e. cross-sectional of sample); contour contact area and true contact area (contact area at peaks of asperity) for interfacing rough joint surface. True contact area lies in the range between apparent and contour contact area. Total contact at asperity points is very small, according to Barton & Choubey (1977) it is about 1/10 to 1/1000 of the cross-sectional area of the sample. It is for this reason Barton & Choubey suggested that the ratio of contact area (gross/true) can be approximated by the value of JCS/σ_n.

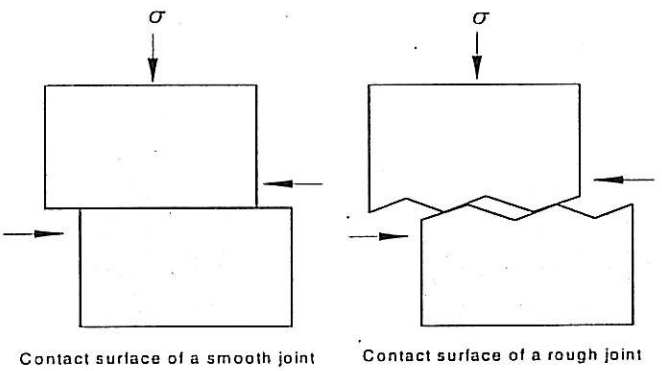

Figure 2.9: Contact area of joint during shear test

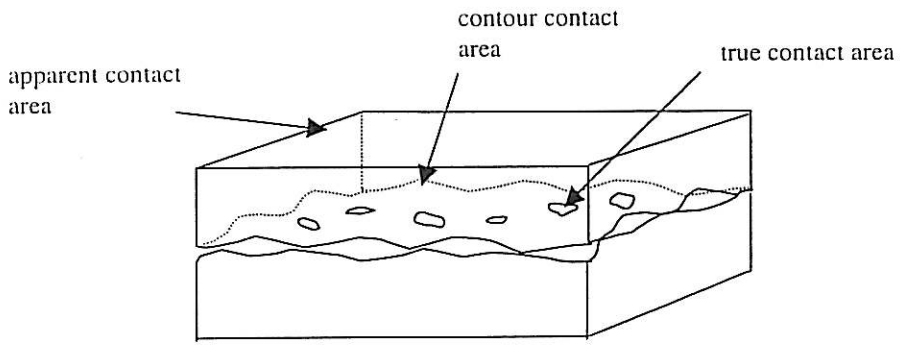

Figure 2.10: Contact area between two interfacing rough joint surfaces (Lama & Vutukuri, 1978).

Depending on strength of joint surface, distribution of asperity peaks and degree of roughness, asperity may deform in elastic or plastic manner or, fracture under loading.

Hence, contact area between joint surfaces varies invariably with applied load and throughout the shearing process (Lama & Vutukuri, 1978).

In this study, procedure for estimating the true contact area is also discussed. Such procedure is only possible if an accurate topography of the joint surface is available.

2.1.3.2 Joint dilation

When a rough, matching joint is subjected shear displacement, there is a tendency for joint to dilate in vertical direction. Dilation is mainly due to surface undulations, and the amount depends on strength of joint surface, level of normal stress and size of roughness. Figure 2.11 explains how asperity induces dilation into a displaced joint.

When joint is displaced in horizontal direction, u, over-riding between asperity results displacement in vertical direction, v_n. Volume change due to joint opening can be explained in terms of dilation angle d_n^0 (Bandis, 1993), as shown in the following equation:

$$d_n^0 = \text{arc tangent } (\mathrm{d}v_n / \mathrm{d}u) \qquad (2.4)$$

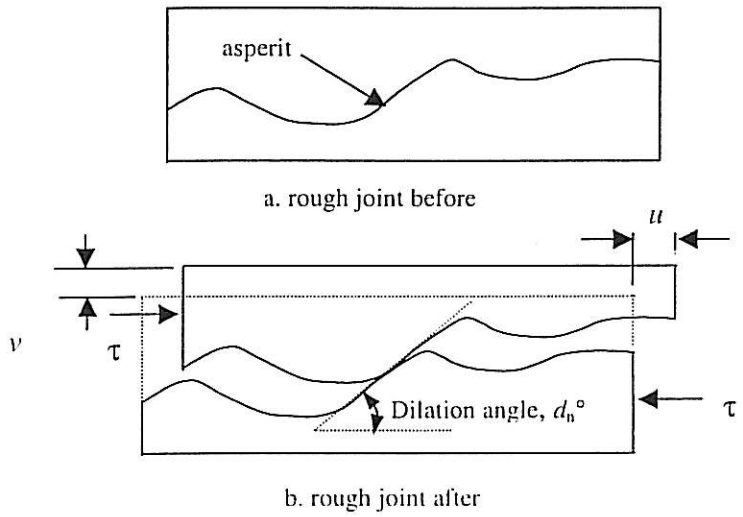

Figure 2.11: Effect of surface roughness on joint roughness.

On the other hand Barton and Choubey (1977), shows that dilation angle during shearing in a tilt test can be calculated as:

$$d_n^0 = \alpha - \phi_r \qquad (2.5)$$

where,

α = angle of inclination of a rough joint at a start of sliding.

ϕ_r = angle of inclination of a smooth joint at a start of sliding.

From equation 2.5, dilation angle is equal to roughness angle, *i* and the difference between α and ϕ_r is due to the factor of roughness. Again, the above explanations signify the importance of texture and roughness of a joint surface. In order to obtain a better estimate on dilation angle, assessment of joint surface is therefore important. The alternative method proposed in this study has the ability of providing correct and essential information pertaining to joint surface.

2.1.4 Effect of roughness scale

Roughness of different scale gives a different effect on shear strength of a joint. Pratt *et al.* (1974) in their study on the effect of scale of roughness on shear strength found that the strength reduced to about 40% when the area of a joint increases from 60cm^2 to 5000cm^2, indicating that shear test on smaller sample leads to a higher shear strength. This is related to fact that effect of roughness is greater in a smaller scale (Barton & Bandis, 1982). This effect is also studied by Barton & Choubey (1977) where, it is shown that value of *JRC* decreases with increasing scale of roughness.

Angle *i* also depends on the measured baselength, D, of joint where, *i* seems to increase with decreasing D (Bandis, 1993). This effect is depicted in Figure 2.12. Figure 2.13 highlights the effect of different size of joint sample on mode of failure under shear loading (Bandis *et al.* 1981).

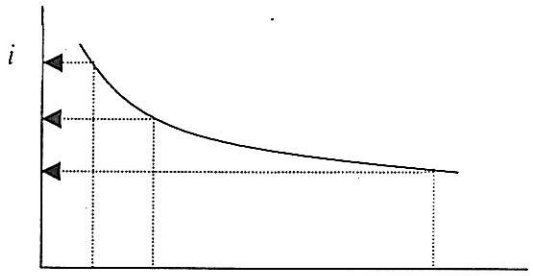

Figure 2.12: Effect of geometric scale of roughness (Bandis, 1993).

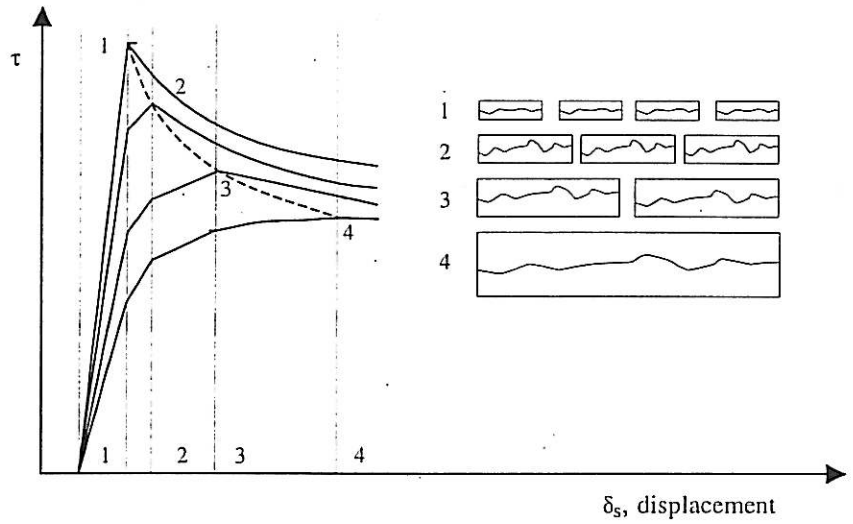

Figure 2.13: Effect of joint size on mode of failure under shear loading (Bandis *et al.*, 1981)

A correction factor for scale effect on joint roughness has been proposed by Bandis (1993) where, value of JRC_n in the field can be obtained from value of JRC_o in laboratory:

$$JRC_n = JRC_o \, [L_n / L_o]^{-0.02JRC0} \qquad (2.6)$$

where,

L_n = baselength of joint in the field.

L_o = baselength of joint in laboratory.

2.1.5 Analysis of joint surface roughness

Analysis on roughness is aimed at producing a numerical rating for the various surface texture of joint surface in rock. Several methods for assessing joint roughness have been used and these include statistical approach, geostatic, spectrum and slit island (Piggot and Elsworth, 1995). According to Bandis (1993), roughness can be evaluated quantitatively using the following methods:

a) Using the maximum or median roughness angle (equation 2.7):

$$i = \arctan (2a / L) \qquad (2.7)$$

where,

i = maximum or median roughness angle;

A = amplitude;

L = length of roughness.

b) Using the arithmetic mean of peak and trough at mean plane of joint surface.

c) Using a concept that the amplitude index is equal to the ratio of total projection length of asperities to total length of profile.

According to Goodman *et al.* (1972), the vertical measurements such as maximum, minimum, mean and standard deviation of roughness features joint surface can be used for evaluating the degree of roughness. As shown in Figure 2.14, the deviation of maximum height (+ ve) and minimum height (– ve) from mean height are termed as peak and trough, respectively. The standard deviation of a profile with respect to its mean height, at any selected section of a surface is the value of roughness of that surface.

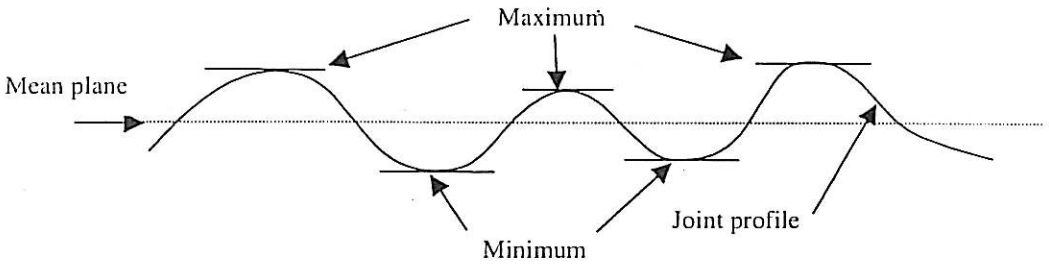

Figure 2.14: Assessment of joint roughness based on maximum height, minimum height and mean height (modified from Goodman *et al.*, 1972).

In the field of metallurgy, indexes used to describe surface roughness are based on data obtained from measurement using a linear profile, method that is also used in joint surface measurement in rock. Roughness indexes used can be divided into two categories: index for describing the roughness magnitude and index for describing surface texture of rough surface (Lamas, 1996).

Amongst the index in the first category are *absolute roughness*, *k*, *central line average*, *CLA*, and root mean square, z_1. Index *k* is often used in the study on hydraulic conductivity of joint and its value is the difference between the maximum height of peak and minimum height of trough of a profile:

$$k = \text{maximum } (y_j) - \text{minimum } (y_j) \qquad (2.8)$$

CLA is the arithmetic mean of asperity heights and is given as:

$$CLA = \frac{1}{L}\int_0^L |y|\,dx \approx \frac{1}{N}\sum_{j=1}^{N}|y_i| \qquad (2.9)$$

z_1 on the other hand, is given as:

$$z_1 = \left[\frac{1}{L}\int_0^L y^2 dx\right]^{1/2} \approx \left[\frac{1}{N}\sum_{j=1}^{N} y_j^2\right]^{1/2} \qquad (2.10)$$

where,

L = length of profile

N = number of divisions chosen for a profile length.

Another theory that was recently introduced for roughness measurement of joint surface is the fractal geometry. Its application in rock mechanics is introduced by Muralha (1991). Fractal geometry evaluates roughness in terms of fractal dimension, D, and is given as:

$$D = [\log N] / [\log (l/r)] \qquad (2.11)$$

where,

N = the number of fractal division

r = the ratio between a length and sub-units that makes the length.

A number of studies have been undertaken to establish correlation between fractal dimension and value of *JRC*. Among these include study conducted by Lamas (1996) who establish the relationship between *JRC* and fractal dimension (D) as given by the following equation:

$$JRC = 1195.38\ [D - 1] \qquad (2.12)$$

2.2 Photogrammetry

2.2.1 Introduction

Photogrammetry is defined as a technique of measuring photograph image that is specially acquired from a large distant (skies) using a matrix camera as in aerial photography (Abdul Hamid, 1990). The main objective is obtain the 3 dimensional image of an object acquired using photograph image. In other words, photogrammetry is a technique in mapping where observation and collection of data are undertaken directly on the acquired photograph without any direct measurement on the actual object.

Based on the system of data acquisition and procedure of analysis, photogrammetry can be divided into a number of categories:

1. Aerial photogrammetry: is a field in photogrammetry where the photograph image of a surface area on earth is acquired using a special aerial camera of high accuracy. For this aerial mapping purpose, the camera is attached to an aircraft.
2. Terrestrial photogrammetry: is a branch of photogrammetry where image of a surface area on earth is acquired using a camera mounted at a height from earth surface.
3. Remote sensing: is a field in photogrammetry where a systematic interpretation of an object, area or phenomenon is made based on their photographic images. Instruments used include a multi-spectral camera and infra-red sensors.

Photogrammetry is also classified based on the procedures of data analysis namely; analog, analytical and digital photogrammetry. In digital photogrammetry, analysis is undetaken using digital images, instead of photographs, using various computerised techniques (Krauss, 1993).

2.2.2 Basic theory in photogrammetry

In photogrammetry, photography is taken to be the point of projection of a 3-dimensional image on a plane. An image cannot be formed on a plane using one projection point thus,

an image is a representation of a 3-dimesional object on a plane. In order to produce a dimension or a drawing, a number of analysis must be undertaken either, in mathemetical or analog form. Usually a pair of overlapping photographs of an image is used in the analysis. A pair of overlapping photographs enables one to visualise the image in stereoscopic form and consequently, the relevant measurements of the object, in 3 dimensional, can be undertaken.

There are two types of stereo image used in aerial photogrammetry. The first type is a pair of photographs taken using a camera with its precise height (a priori) from a datum is known. The other type is photographs taken using a camera at an unknown height. In the former case, related measurement of earth must be carried out during image acquisition of an object so that camera position and orientation can be determined. In the latter case, measurements are undertaken on the object being photographed in order to determine the camera position (a posteriori), scale and position of the object (Dowman & Scott, 1980).

2.2.2.1 Definations

Figure 2.15 shows a number of important parameters & definations for a single photograph (Dowman & Scott, 1980). The centre point of a photograph is termed as *principal point*, *P*. It is a point for a line normal to the photograph which passes through the *perspective center* of the camera lens (S). The distance between the centre perpective and photograph, along this normal line, is termed as *principal distance*, *f*. When a camera is focussed at infinity, *f* is approximately equals to the focal length of the camera lens. The points of intersection between fiducial marks are the centre points of a photograph and the *principal points* are located at these points.

There are two type of system coordinate for an object being photographed and the photograph itself. The coordinate system of a photograph originates from the perspective centre , x- and y-axis are parallel to the axes of photograph and z-axis is located at the lens axis. Coordinates for the *principal point*, *P*, in this coordinate system is given as (0,

0, *f*). The position of *perspective centre*, *S*, need to be defined in terms of object coordinate system.

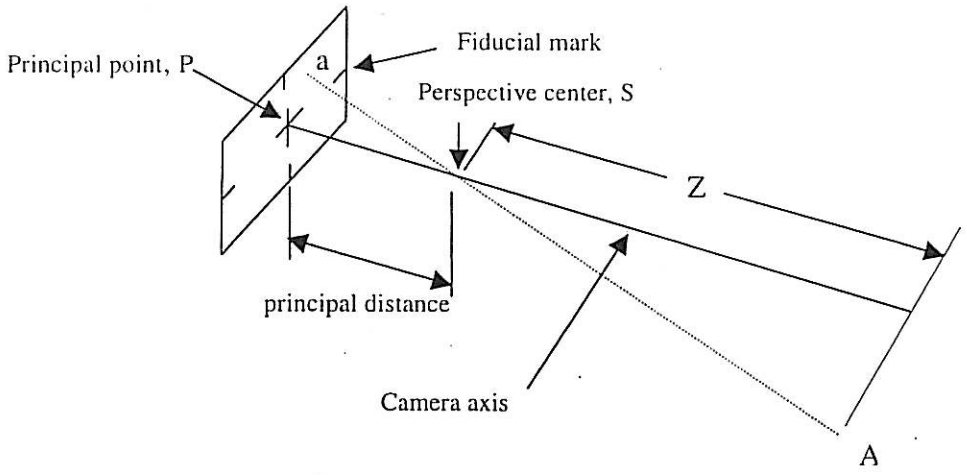

Figure 2.15: Single photograph (Dowman & Scott, 1980).

The horizontal distance parallel to the camera axis, measured between *S* and an object *A* (Figure 2.15), is termed as *Z*. Scale for any point on the object is given as value of ratio *f*/*Z*. For a normal photograph, scale for the image points usually vary due to the varying position of the points on the object, with respect to perspective centre of the camera.

Figure 2.16(a) shows a pair of photograph (photograph 1 and 2) for object point A. S_1 and S_2 are the perspective centre for the respective photograph, separated by a base length, *B*. Points a_1 and a_2 are the image point for point A on photograph 1 and 2, respectively. Each photograph displays its own coordinate system, i.e. (x_1, y_1, z_1) for photograph 1 and (x_2, y_2, z_2) for photograph 2. *X*-axis for both photographs is parallel to the camera base length, *B*. A system of model coordinate (*X*, *Y*, *Z*) that originates from S_1 is a common case in photogrammetry photography where axes for both cameras are normal to camera base, *B*. In the case of aerial photography, *Z* axis is the vertical height of the camera from earth surface.

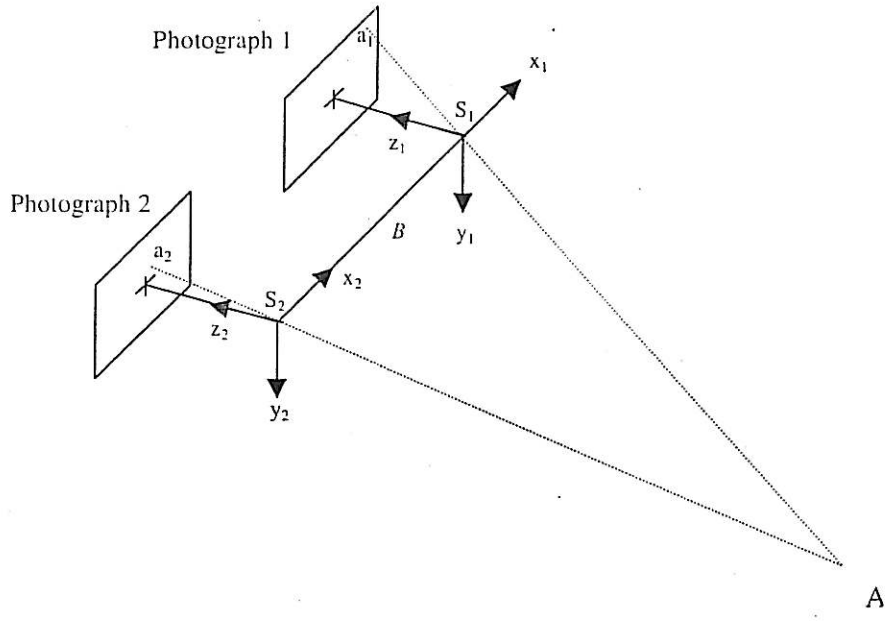

Figure 2.16(a): A paired photograph on a single plane.

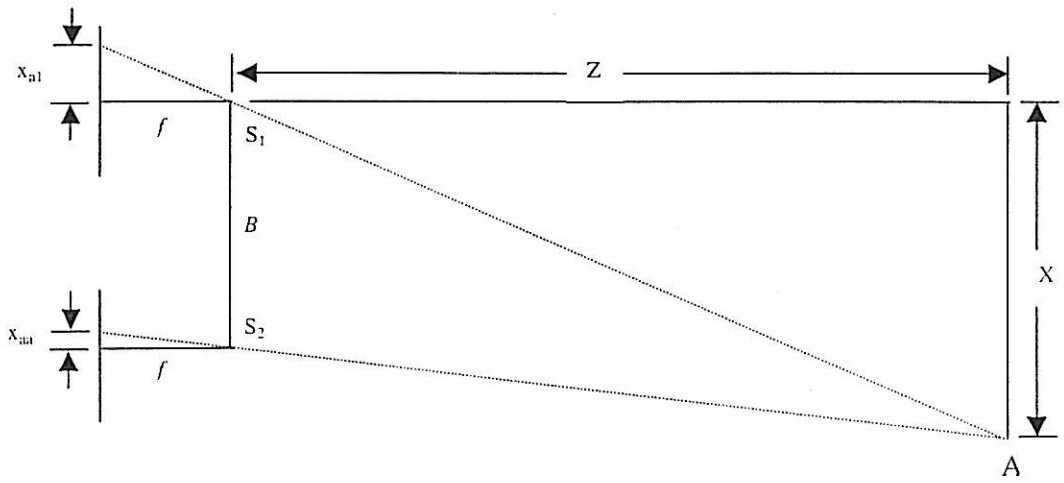

Figure 2.16(b): Parallax for a pair of photograph.

Image scale at a_1 and a_2 is the same (f/Z). Coordinates for these image points are (x_{a1}, y_{a1}, f) and (x_{a2}, y_{a2}, f) and if S_1 and S_2 are at the same level and base B is horizontal, then x axis is colinear and y_{a1} is similar to y_{a2} (Dowman & Scott, 1980). Figure 2.16(b) shows plane xz for the light projection of Figure 2.16(a). From these geometrical diagrams, the followings are obtained:

$$Z/B = f/(x_{a1} - y_{a2}) \tag{2.19}$$

$$Z = fB/(x_{a1}, -x_{a2}) \tag{2.20}$$

$$X = x_{a1} Z/f \tag{2.21}$$

$$Y = y_{a1} Z/f \tag{2.22}$$

Consequently, based on a pair of photographs that are acquired using the same camera focal length and position of perspective center and with a known base length, the position of point A can be determined by measuring the coordinates of same image point on both photographs.

2.2.4 Photogrammetry camera

In field of photogrammetry, type of camera used can be divided into two categories namely; matrix camera and non-matrix camera. Matrix camera is a specially designed camera for use in photogrammetry. At present, non-matrix camera has been widely used especially in close-range photogrametry. These include 35mm, video and digital camera for conventional use. However, the non-matrix camera needs to be calibrated accordingly for use in photogrammetry. Table 2.1 below oulines the difference between matrix and non-matrix camera.

Table 2.1: Differences between matrix and non-matrix camera (after Wolf, 1974)

Matrix camera	Non-matrix camera
Specially designed for use in photogrammetry	Camera for conventional used
Orientation of internal elements are known and stable	Orientation of internal elements are not known and unstable
Fixed focal length	Variable focal length
Contains fiducial points to show internal space orientation.	No fiducial points
Sensors are film-based.	Sensors are film-based or special sensors such as CCD.

2.2.5 Camera calibration.

Camera calibration is an essential process in photogrammetry and must be undertaken before a camera is used for the photography. Its main objective is to verify the precise value of the various camera constants. In general, the essential elements usually calibrated include the following (Abdul Hamid, 1990):

a) uni-value of focal length,
b) calibrated focal length,
c) average radial distortion of lens, and
d) tangential distortion.

2.2.6 Theoretical background of close-range photogrammetry.

Close-range photogrammetry implies that the object being photographed is at a distance less than 100m from the camera (Cooper & Robson, 1996). In this technique, image acquisition is undertaken around the object. In some cases, camera axes are parallel and pointing toward the center portion of the object. Based on the information related to the imaging processes and physical measurements undertaken, a mathematical model is developed using numerical method, to describe the object in three dimensions. Among the important theories are discussed in the following sections.

2.2.6.1 Conformal 3-dimensional transformation

If the origin of an axis (*XYZ*) is transformed to another position (X_o, Y_o, Z_o), and the scale for each axis is multiplied by λ and orientated by the amount of ω, φ and κ to form a second axis (*xyz*) (see Figure 2.17/Rajah2.21), the correlation between the first coordinate system (*XYZ*), for point A, and the second coordinate system (*xyz*) can be explained using a vector equation:

$$\mathbf{X} = \mathbf{X_o} + \lambda^{-1}\,\mathbf{R^t}\,\mathbf{x} \qquad (2.26a)$$

Transformation of the second coordinate system to the first coordinate can be summarised as follows:

$$\begin{bmatrix} X \\ Y \\ Z \end{bmatrix} = \begin{bmatrix} X_o \\ Y_o \\ Z_o \end{bmatrix} + \lambda^{-1} \begin{bmatrix} r_{11} & r_{21} & r_{31} \\ r_{12} & r_{22} & r_{32} \\ r_{13} & r_{23} & r_{33} \end{bmatrix} \begin{bmatrix} x \\ y \\ z \end{bmatrix}. \qquad (2.26b)$$

Element $\mathbf{R^t}$ is explained in (Teo King Beng, 2002). Inverse transformation (i.e. first to second coordinate) is $\mathbf{x} = \lambda\mathbf{R}(\mathbf{X} - \mathbf{X_o})$. Seven parameters, i.e. X_o, Y_o, Z_o, ω, φ, κ and λ, are involved in this transformation.

2.2.6.2 Intersection

If the external elements of orientation for two cameras and perspective center O_1 and O_2 are known (Figure 2.18) then, the space coordinate of an object (X_A,Y_A,Z_A) for point A, can be determined by measuring coordinate of photograph (x_1,y_1)(a_1) and (x_2,y_2)(a_2). Equation of co-linearity is the basis for this method, but due to the three unknown (X_A,Y_A,Z_A) and four equations, the least-square method is usually used. This process is termed as intersection (Cooper & Robson, 1996)

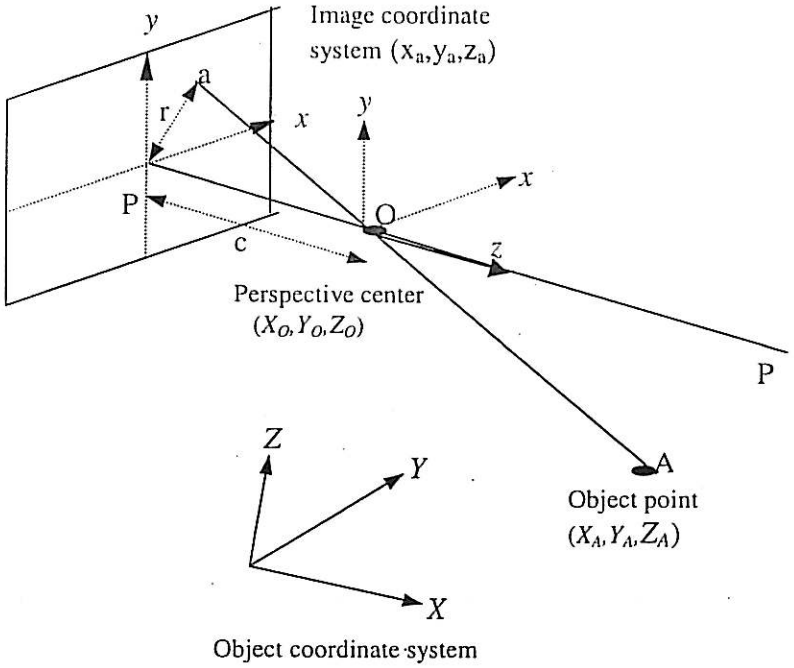

Figure 2.17: Transformation of perspective center (Cooper & Robson, 1996).

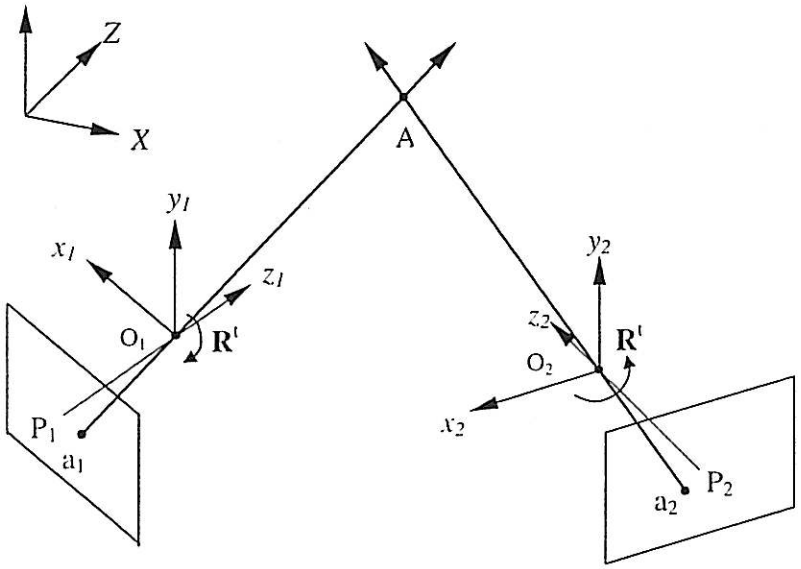

Figure 2.18: Intersection (Cooper & Robson, 1996).

Normally, intersection process is undertaken after resection where, the two processes is done separately. However, this procedure does not yield high accuracy for estimating object coordinate in the object space in close-range photogrammetry. A procedure, known as bundle adjustment, may be undertaken to obtain better accuracy.

At present, with the use of digital camera, bundle adjustment method enables a high accuracy data to be obtained within a short period of time.

2.2.7 Fundamentals of digital photogrammetry

The use of digital camera in close-range photogrammetry has becoming more popular. This is mainly due to its relatively cheap price and flexible and swift processing procedure of the digital images. The primary advantages of digital image compared to photograph image are as follows (Dowman, 1996):

a. Image can be displayed and measured accurately using computer monitor and softwares with no requirenment for optical and mechanical equipments.
b. Measuring system is stable and does not require calibration procedures.
c. Ability to produce enhanced image using image processing techniques.
d. Automated measurement can be undertaken.
e. Output can be obtained in real time or near real time.

2.2.7.1 Definition of digital photogrammetry image

Digital image is a two-dimensional matrix arrangement, G, produced by camera sensors. Each element in the matrix, g_{ij} (i = row, j = column), exhibits a different density which is the required essential information. These elements are termed as pixels. Each pixel exhibits different size ($\Delta x \times \Delta y$) depending on the size of the camera sensor. Δx can be of

similar length as Δy. This implies that a digital image is a sampling process based on the interval of Δx and Δy. Figure 2.19 shows the schematic presentation of digital image. Relationships between i, j, and x, y, can be obtained based on value of Δx and Δy for each pixel. Thus, the position of each pixel, in x and y direction, relative to the center coordinate of selected image, can be determined (Dowman, 1996).

Value of each pixel depends on the camera sensor being used. The range normally is between 0 and 255. For black and white image, value of 0 represents black and 255 represents white. Thus. value of pixel is better known as grey values. For coloured image, there are three sets of matrix representing the variations of red, green and blue colour, in a similar range.

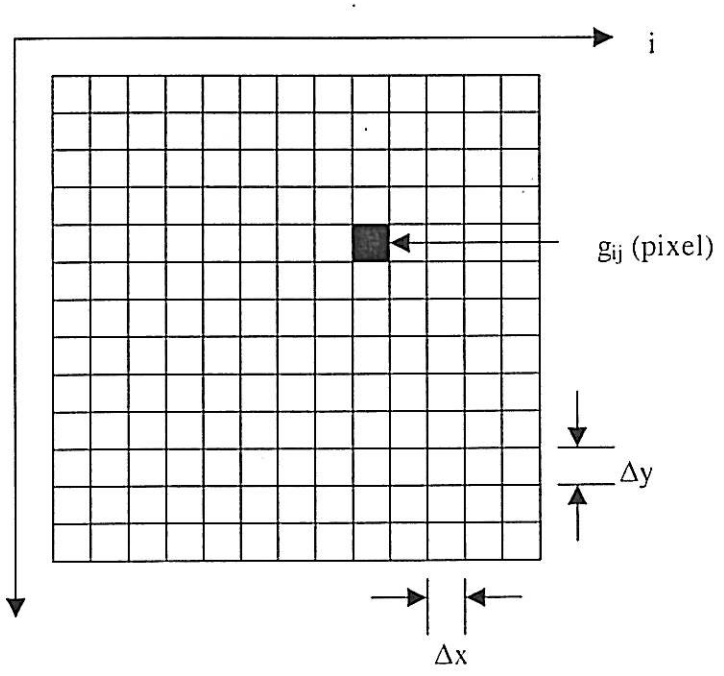

Figure 2.19: Definition of digital photogrammetry image (Dawman, 1996).

2.2.7.2 The advantages of close-range photogrammetry for measuring roughness of joint surface.

One of the main advantages of close-range photogrammetry is its relatively simple procedure for direct measurement of texture of joint surface. This is particularly essential when detailed information of a joint surface is required for specific purpose in laboratory work. If conventional method is used, it would be time consuming and only limited information of the surface texture can be obtained. By using photogrammetry method, detailed information of the joint surface can be obtained almost close to real-time (Mustaffar, 1999). This method can provide the coordinates of a surface in the form of digital data. As such, data can be used directly for the most important analysis in roughness assessment, i.e. statistical analysis. This method also allows for 3-D analysis of joint surface roughness be undertaken as proposed by Archambault *et al.* (1996).

CHAPTER III

MEASUREMENT OF JOINT SURFACE

3.1 Introduction

Methodology of this research is divided into two, firstly a comparative study on methods of measurement undertaken in the laboratory and secondly, measurement of joint surface in the field. Laboratory study involved measurement of joint surface using close-range photogrammetry and linear profiler method. To enable a detailed and accurate measurement could be undertaken using both methods, a model joint surface was used in the laboratory study. Comparison was made on data representing the surface texture of the model joint that comprised of surface profiles, 3-dimensional plots, contact area and a number of roughness index. Measurement of joint surface in the field, using close-range photogrammetry, is mainly to verify its practicality for the purpose.

3.2 Model of Joint Surface

The model joint surface is prepared by casting a slurry of suitable plaster material on a natural joint surface in rock. Suitable joint surface was selected from exposed joints found at Sunway Masai Granite Sdn. Bhd., Kota Masai Johor Bharu, Johor. An appropriate mix for the casting purpose was verified in the laboratory using various proportion of plaster of Paris, Ordinary Portland Cement and water. Based on the various mix tested, it shows that a mix of plaster of Paris with water ratio of 1:1 gives the best mix in terms of workability and consistency. The casting of the joint surface was undertaken using a wooden mould (270 × 270 × 40 mm) and according to the procedures as discussed by Teo King Beng (2002). Extra care was taken as to avoid any formation of air bubbles in the casting material particularly, at the interface between the cast and the rock. Once the cast had set, it was carefully removed from the rock surface and brought back to the lab. In the lab 15mm square grids, along x- and y-direction, were carefully marked on the model joint using black marker. The grid points were denoted as A to S in

x-direction and *1* to *19* in *y*-direction. For both directions there were 361 points of intersection between grid lines A to S and line 1 to 19 (see Figure 3.1). These grid points would be used as target points during the measuring processes.

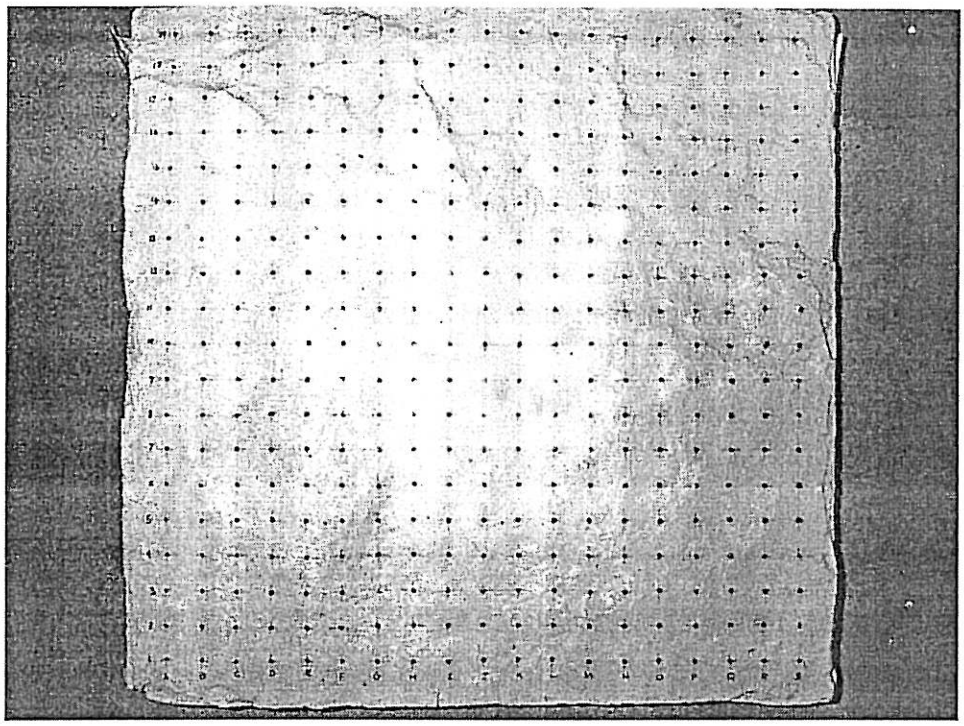

Figure 3.1: The model joint surface with the marked grid system

3.3 Measurement of Model Joint Surface using Profiler

A specially fabricated laboratory profiler has been used to measure the vertical height of all the 361 grid points. The height was measured using a dial gauge (accuracy 0.01mm) that was attached to the profiler. Figure 3.2 shows the setting of the model joint and dial gauge during laboratory profiling. By using the rotating wheel of the profiler, the dial gauge was positioned as close as possible at the grid points and the vertical height was read directly from the gauge. Measurement was undertaken in both *x*-direction and *y*-directions at grid points A1 to A19 and B1 to B19, respectively. 10 sets of reading were recorded for each grid point. The collected data was then analysed statistically to obtain

the final set of data representing the vertical height of all grid points on the model joint. The analysis of data is described in Teo King Beng (2002).

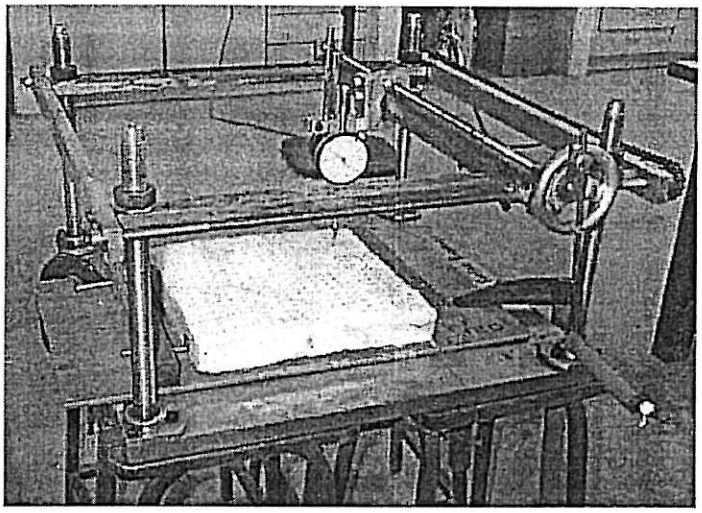

Figure 3.2: Specially fabricated profiler for laboratory measurement of model joint surface

3.4 Measurement of Model Joint Surface using Close-range Photogrammetry

Measurement of the model joint surface, using close-range photogrammetry, consists of three main procedures and these are:

(a) Determination of initial data.
(b) Image acquisition.
(c) Analysis and processing of image.

The processed data obtained from each procedure is used in the subsequent process. Figure 3.3 and Figure 3.4 show the main processes and the sequence of each associated sub-processes for measuring the texture of the model joint surface.

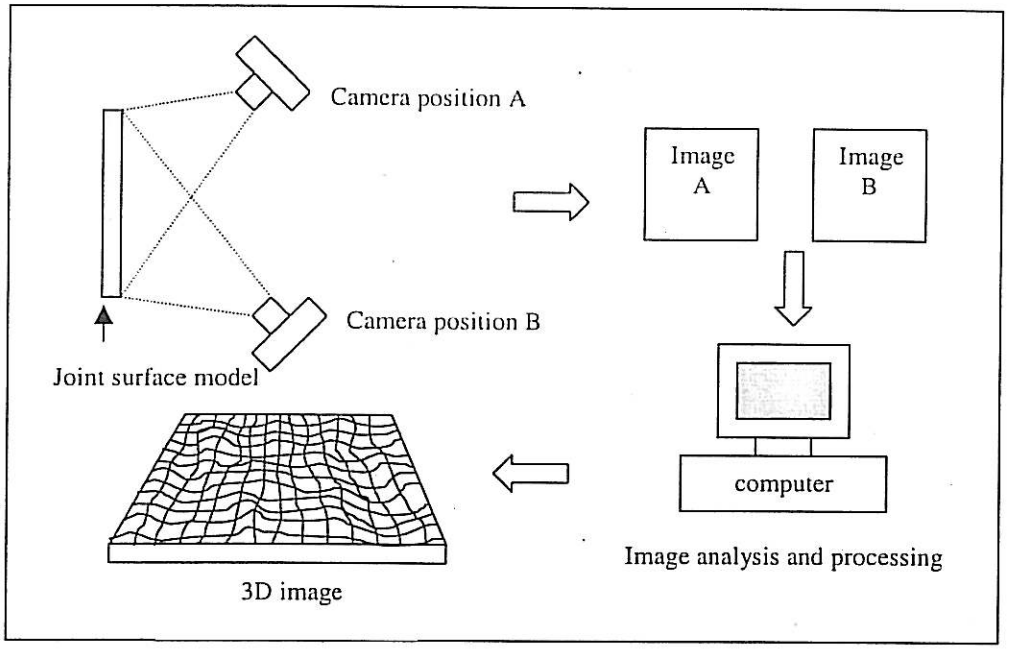

Figure 3.3: The main processes in the close-range photogrammetry

3.4.1 Determination of Initial Data

The camera used for the image acquisition need to be calibrated so that the essential parameters, such as pixel size, for the image processing procedure can be obtained. Two main processes involved in this procedure are:

(a) Determination of control points – This is a process of measuring fixed points which act as control points for the determination of the relative orientation of camera during image acquisition. A specially fabricated target plate, shown in Figure 3.5, is used in this process. The target plate consists of a thick plastic base and 36 number of screws of variable heights. The coordinates of the control points (the screws) were determined using a pair of theodolites that were positioned in a manner as shown in Figure 3.6. The procedures for determining the control points are discussed in detailed by Teo King Beng (2002). The coordinates for all the control points are listed in Appendix A.

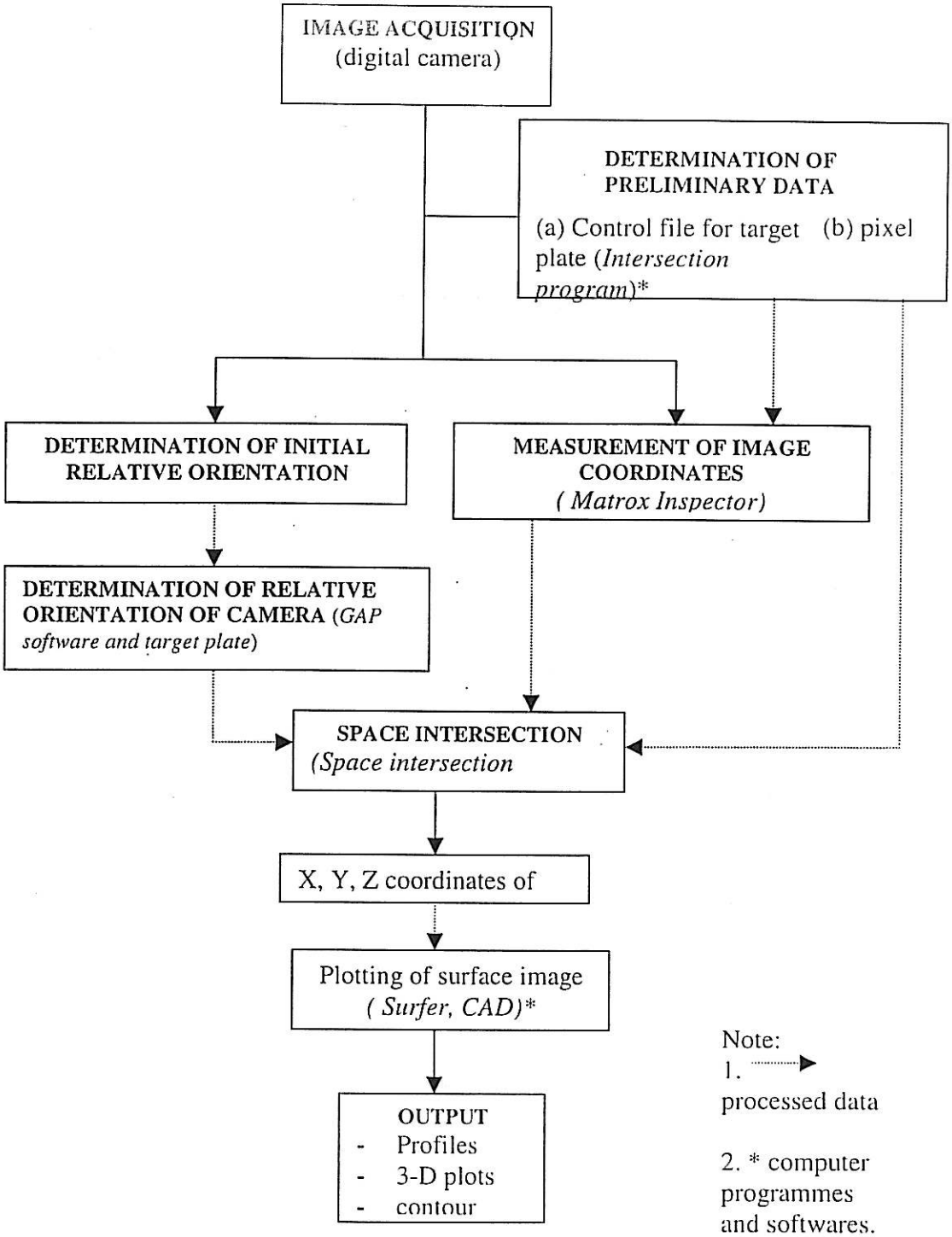

Figure 3.4: Flow charts representing the associated processes in the close-range photogrammetry

(b) Determination of the camera pixel size – This procedure is to determine accurately the dimension of pixel in the CCD (charge coupled device) sensor for the digital camera used. This data is used for measuring the image coordinates using Matrox Inspector programme. The data on pixel size is also essential for image matching and determination of 3D coordinates.

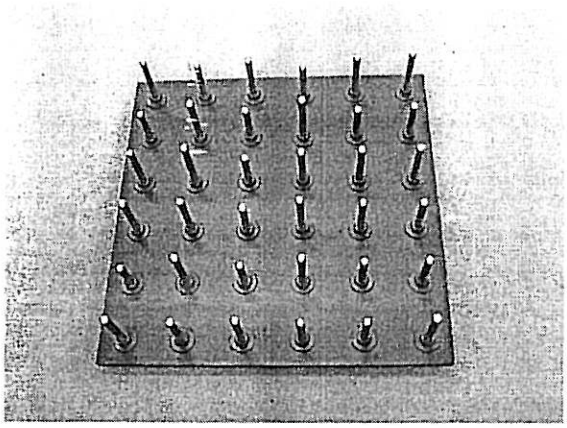

Figure 3.5: Target plate

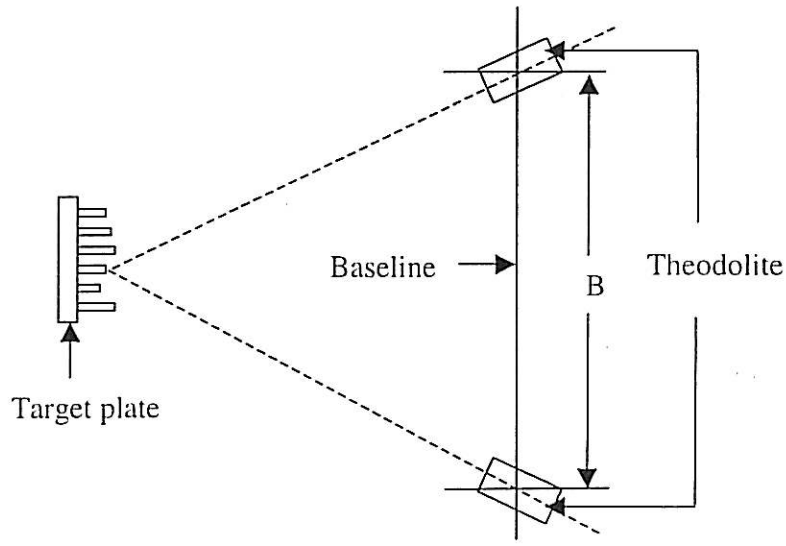

Figure 3.6: The positioning of the target plate and theodolites for measuring the control points

The size of camera sensor can be determined using the concept of congruent triangles. This is done by determining the size of an object (y), the distance between y and camera lens (a) and, focal length (f). The concept is schematically presented in Figure 3.7. In this procedure, a steel ruler is used as an object and dimension x is calculated using the following formula:

$$x = \frac{y \times f}{a} \tag{3.1}$$

The dimension of the sensor in y direction is determined in a similar manner.

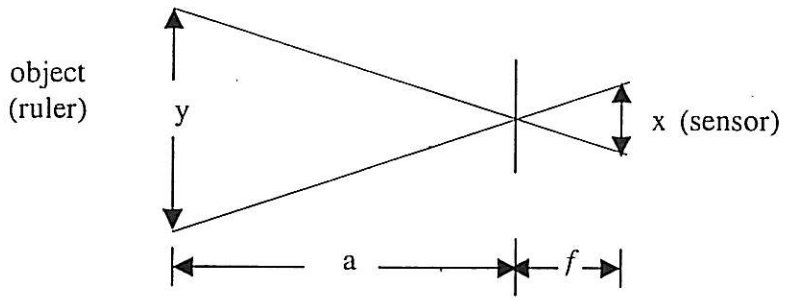

Figure 3.7: Determination of camera sensor size using congruent triangles concept

The specification of the camera used shows that the number of pixel in x and y direction is 1280 and 960, respectively. Therefore, the pixel size in any direction can be determined by dividing the length of the sensor by the number of pixels in that direction. The size of the CCD sensor and pixel for the digital camera used in the image acquisition is listed in Table 3.1 below.

Table 3.1: Size of CCD sensor and pixel for the digital camera used in image acquisition

CCD size in x axis	5.56 mm
CCD size in y axis	4.35 mm
Pixel size in x axis	0.0041 mm
Pixel size in y axis	0.0045 mm

3.4.2 Image Acquisition

The digital camera being used for the image acquisition is Kodak DC240 (Figure 3.8). This is a normal small format camera with the capability of acquiring image in digital form. Based on the manufacturer specification, each image is represented by 1.2 million pixels (1280 × 960) i.e., the number of pixel in the CCD sensor. Specifications for the Kodak DC 240 camera are enclosed in Appendix B.

Figure 3.8: Kodak digital camera DC 240 used in image acquisition

Figure 3.9 shows schematically the image acquisition procedure. During image acquisition, the camera lenses are set at maximum focal length (18mm). This setting will give a minimum

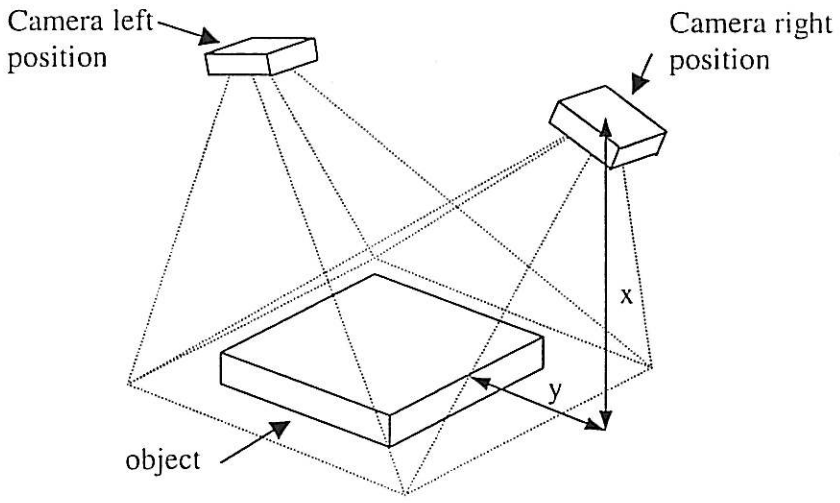

Figure 3.9: Positions of camera during image acquisition

3.4.3 Determination of Relative Orientation

Parameters that need to be determined in this part are ω, ϕ, κ, Xo, Y_o *and* Z_o for image acquired from each camera station. These parameters are determined using computer software namely GAP (General Adjustment Program). However, only one image is required by the program to determine the relevant parameters for the relative orientation.

For each camera position, values of Xo, Y_o *and* Z_o are established by measuring the distance x and y as shown in Figure 3.9. Since the camera is in vertical position relative to the object therefore, the camera rotation as denoted by ω, and κ, are assumed to be zero. Camera rotation, ϕ, is estimated based on the image being produced (see Figure 3.10). Angle x, in Figure 3.11 is the estimated value of angle ϕ.

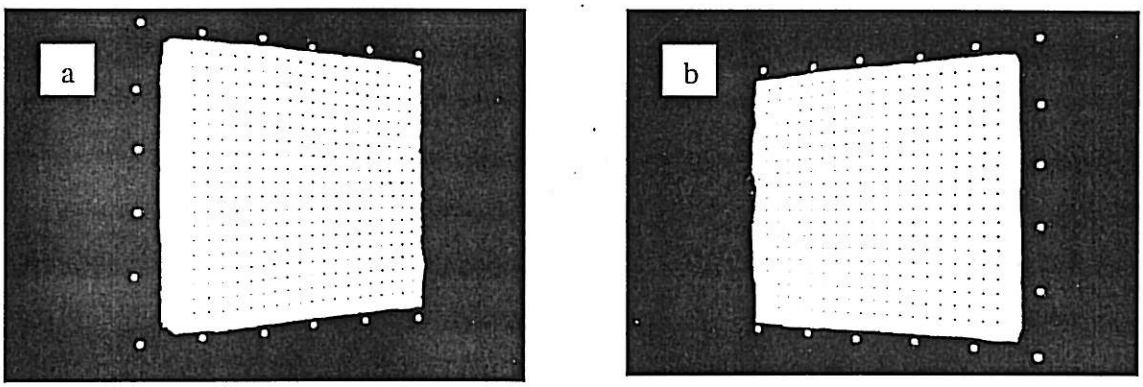

Figure 3.10: Image of surface model (a) left image (b) right image

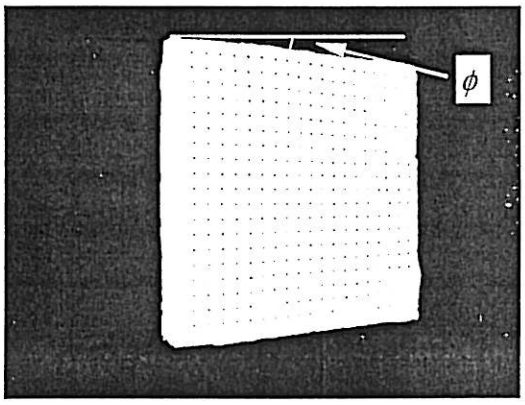

Figure 3.11: Estimation of angle of orientation of camera, ϕ.

3.4.4 Measurement of Image Coordinates

Coordinates of image are measured using a computer program namely Matrox Inspector. The measured coordinates are based on the positions of the grid points marked on the surface of the joint model, as discussed in Section 3.3. The use of Matrox Inspector would require the value of pixel size and the origin of coordinates. The origin for the coordinates is fixed at the lower left-hand corner of the image, i.e. according to format used in the Space Intersection program. As required by the program, the format for the image is also converted to JPEG file. The detailed description on the procedures for measurement of image coordinates is given in Teo King Beng (2002). Data obtained from this part of analysis is in the form of x and y coordinates for all the 361 grid points for each image (see Appendix C). These data are saved as txt fail and are used as input data for the next stage of data processing using Space Intersection Program.

3.4.5 Space Intersection

Space intersection is a process to obtain the 3D coordinates of an image. This process is undertaken using *Space Intersection* program (Mustaffar, 1997). The input data for this program consists of the relative orientation data obtained using GAP program and image coordinates obtained using Matrox Inspector. Output data obtained from processing using *Space Intersection* program is listed in Appendix F.

3.4.6 3 Dimensional Transformation

For comparison purpose, the coordinates of the grid points obtained using photogrammetry must be transformed into 3D coordinates. This is to ensure that the orientation of the surface profile of the model joint is similar to the profile obtained using laboratory profiler. The 3D transformation is undertaken using transformation matrix which involved 3 essential elements namely; rotation, scale and translation. Equation 3.2(a) below shows 9 non-linear equations involving 7 variables s (scale), ω, ϕ, κ, T_x, T_y and T_z (translation) for the process of 3D transformation (Wolf, 1983).

$$
\begin{aligned}
X_P &= s(m_{11}x_p + m_{21}y_p + m_{31}z_p) + T_x \\
Y_P &= s(m_{12}x_p + m_{22}y_p + m_{32}z_p) + T_y \\
Z_P &= s(m_{13}x_p + m_{23}y_p + m_{33}z_p) + T_z \\
X_Q &= s(m_{11}x_q + m_{21}y_q + m_{31}z_q) + T_x \\
Y_Q &= s(m_{12}x_q + m_{22}y_q + m_{32}z_q) + T_y \\
Z_Q &= s(m_{13}x_q + m_{23}y_q + m_{33}z_q) + T_z \\
X_R &= s(m_{11}x_r + m_{21}y_r + m_{31}z_r) + T_x \\
Y_R &= s(m_{12}x_r + m_{22}y_r + m_{32}z_r) + T_y \\
Z_R &= s(m_{13}x_r + m_{23}y_r + m_{33}z_r) + T_z
\end{aligned}
\tag{3.2a}
$$

The above equation can be rewritten in matrix form as follows:

$$X = sM^T X + T \tag{3.2b}$$

The equations in the complete matrix form are listed in Appendix D.

3.5 Procedure for Data Analysis

Data of the surface profile of the model joint obtained using profiler and close-range photogrammetry method are compared in order to verify the accuracy and validity of data. Comparison is based on several parameters but the main focus is on the value of the peaks and troughs that describe the roughness profile of the surface model. Data obtained using profiler method is used as datum in the comparison.

3.5.1 Comparison on Surface Profiles

For the data of surface profiles, comparison is made based on the grid lines in x and y directions (see Figure 3.1). A total number of 38 profiles in both directions (profile A to S and 1 to 19) have been compared individually and in similar direction. Although there are

changes in the major orientation, resulting from the 3D transformation, but the transformation is done roughly for the 4 reference control points do possess error (will be discussed in Section 4.3). Therefore, the profiles obtained using photogrammetry must be changed into 2D orientation (minor transformation) so that the difference in orientation will not affect the comparison result.

The process of 2D transformation, the transformation is undertaken in a linear manner with the profiles obtained using profiler taken as datum. Figure 3.12 shows the general procedure in the 2D transformation.

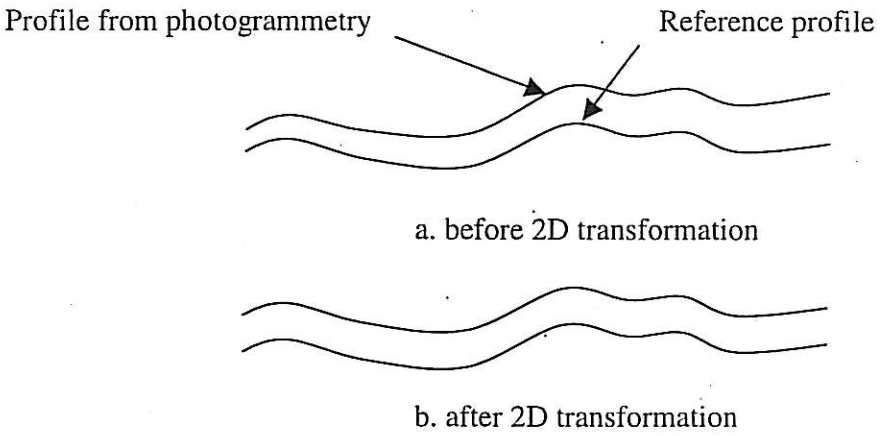

Figure 3.12: 2D transformation of the profiles obtained using photogrammetry

Detailed description on the 2D transformation is given in Teo King Beng (2002) and the process mainly involved Microsoft Excel Program.

3.5.2 Comparison of Roughness Index

The reason for using *roughness index* in the comparison process is mainly to verify any difference, in terms of roughness index, for the surface profiles obtained using profiler and photogrammetry methods. Three types of roughness index are used in the comparison process namely, absolute roughness index (k), Center Line Average (CLA)

and Standard Deviation (*SD*). The selected indexes are more suitable for this purpose because their values are more appropriate in describing the degree of roughness of a profile. It should be noted that the indexes normally used in describing the texture of joint surface are smaller in scale (Tze & Cruden, 1979; Lama, 1996) as compared to the distance between grid points on the model surface used in this study (i.e. 15mm). However, this comparison is mainly to verify the reliability and accuracy of data obtained using photogrammetry method.

Standard deviation index is an index proposed by Goodman *et al.* (1972) to describe the degree of roughness of surface profile (see Section 2.1.5). For the comparison process, this particular index is more suitable because it is not dependent of scale effect.

3.5.3 Comparison of Contact Surface Area

Data obtained using both profiler and photogrammetry methods are also analysed to determine the contact surface area of the model joint. For this comparison, it is assumed that when two interfacing matching joint blocks are sheared, the shear plane occurs at the mean plane (i.e. the plane represented by dashed line in Figure 3.13). In other words, this is a plane taken at the mean height of all the peaks and troughs that create the roughness of a joint surface (Mohd Amin et el., 2000 & 2001).

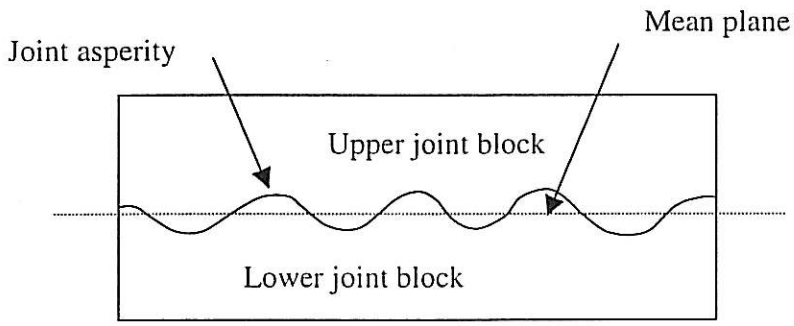

Figure 3.13: Area of contact at shearing plane (shown as line in 2 dimension)

Computer software, *Surfer*, is used to plot the mean planes for both data obtained using profiler and photogrammetry. The surface area of both mean planes is calculated and compared, with the area of plane based on data from profiler as datum. For further comparison, *Surfer* software is used to plot the contour and the orthographic projection (3D) of the joint surface using data from both methods.

3.6 Measurement of Joint Surface Texture in the Field using Close-range Photogrammetry

This procedure is mainly to verify the applicability and practicality of the close-range photogrammetry for measuring the texture of joint surface in the field. The field test was carried out at a granite quarry namely, Kamad Quarry Sdn. Bhd. It is located about 10 km from UTM Skudai, along the Skudai-Pontian trunk road. Exposed joint surface of a dislocated joint block was used as a sample in the measuring process.

A method has been proposed for projecting the grid points (texture) on the exposed joint surface (see Teo King Beng, 2002). However, due to insufficient intensity of grid points being projected on the joint surface in open condition, the method has been abandoned. Instead, a similar procedure as that used in the laboratory (Section 3.2) had been adopted for marking the grid points on the joint surface. A total number of 169 grid points (13 × 13) of 10 mm apart were marked on the joint surface. Before marking the grid points on the selected area of the joint surface, it was sprayed with white paint so that a better contrast of texture can be obtained. Figure 3.14 shows the acquisition of image of exposed joint in the field. Two images of the joint surface were acquired namely, left and right image. The data obtained (digital images) was then processed and analysed accordingly in the laboratory as discussed below.

3.6.1 Processing of Data

The same concept and procedure as those used in the laboratory work are adopted for the processing of field data. However, different computer software, known as *Photo*

Figure 3.14: Image acquisition of joint surface in the field

Modeler, is used in determining the coordinates of object and image. This software allows for the camera parameters to be determined more accurately during calibration process. Camera calibration is carried out by capturing the image of white A4 paper (known dimensions), using DC 240 digital camera from a pre-determined distance. The equipment layout is shown in Figure 3.15. Figure 3.16 shows the image of an A4 paper captured at a distance of 1 m from the camera. Based on the concept of equilateral triangles, the relevant camera parameters are determined using *Photo Modeler* software. The input data for the calibration is shown in Table 3.2.

Table 3.2: Input data for camera calibration using *Photo Moduler*.

No.	Parameters	Value
1	Size of object measured diagonally	175 mm
2	Lenses focal length during image acquisition	18 mm
3	Size of A4 paper	210 × 297 mm
4	The distance between paper and camera	1000 mm
5	File for image of A4 paper in JPEG format	

The relevant camera parameters obtained from calibration process using, *Photo Modeler*, are listed in Table 3.3

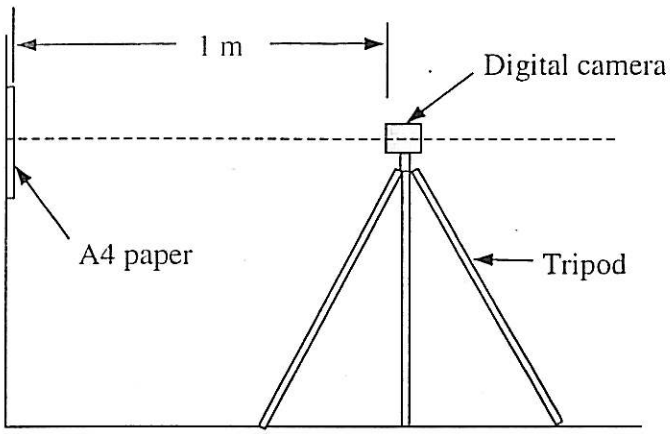

Figure 3.15: Equipments layout for camera calibration

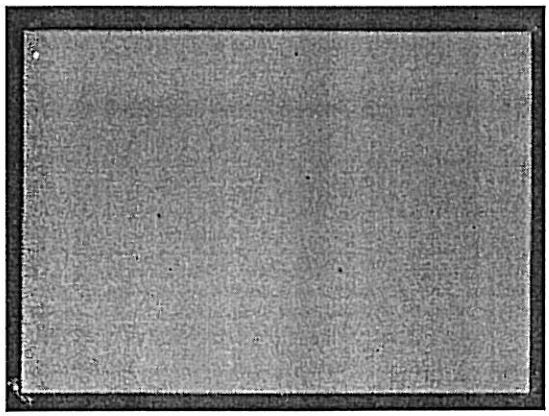

Figure 3.16: Image of A4 paper used camera calibration

Table 3.3: Camera parameters obtained from calibration.

Parameters	Value
Focal length of lenses	18 mm
Format size (sensor)	4.2624 mm (height) × 5.7094 mm (width)
Coordinate of primary point	2.8547 mm (x), 2.1312 mm (y)

For the *Photo Modeler*, the points to be measured must be marked manually so that the software can identified their positions (see Figure 3.17). This procedure is slightly different from the *Matrox Inspector* which can identified the locations of the points of interest (grid points) automatically. For the *Photo Modeler*, the marking of the position of the grid points must be carried out for both digital images (left and right images). The process of marking of the grid points on the computer screen starts with the left image (taken as reference) as shown in Figure 3.17. The marking sequence is done in left to right direction and begins with the top left point. Similar procedure is used for the right image as shown in Figure 3.18. Figure 3.19 shows the 3D projection of the actual joint surface measured in the field processed using *Photo Modeler*.

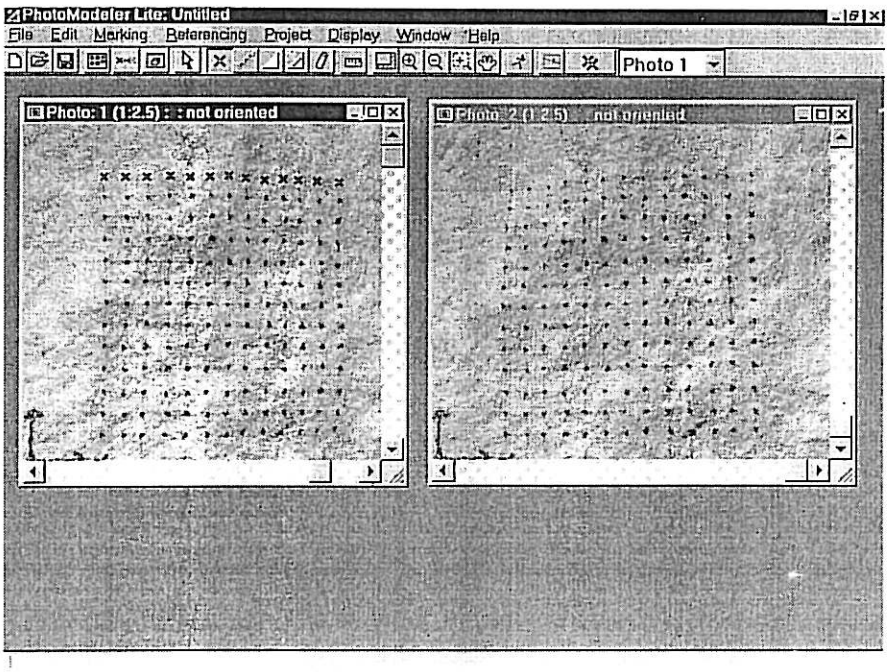

Figure 3.17: Marking of the locations of points to be measured for left image

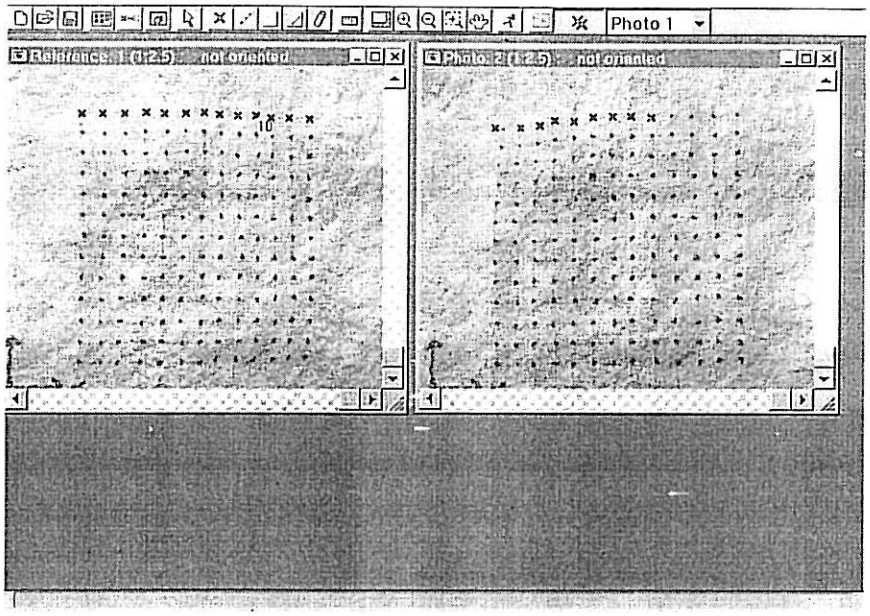

Figure 3.18: Marking of the locations of points to be measured for right image

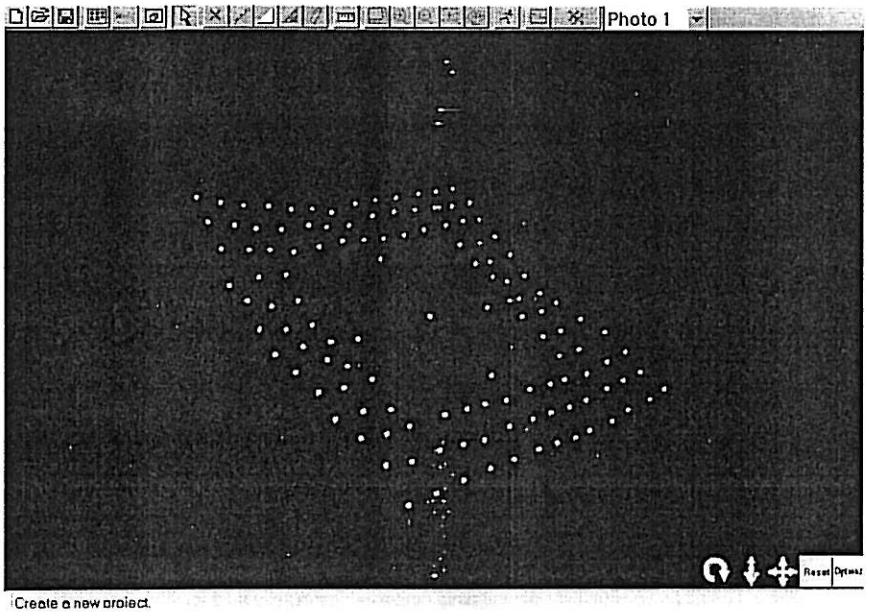

Figure 3.19: 3D projection of the joint surface being displayed in Photo Modeler

CHAPTER IV

ANALYSIS OF DATA AND RESULT

4.1 Introduction

This chapter discusses the associated processing and analysis of data representing the texture of joint surface, acquired using profiler and close-range photogrammetry. The output of this study and the comparison made on both methods, for the purpose of joint surface measurement, are also discussed. The following aspects are discussed:

a) Processing of data acquired using profiler method.
b) Processing of data acquired using close-range photogrammetry.
c) Comparison of linear profiles.
d) Plotted contour of the model joint.
e) 3D plot of the model joint.
f) Comparison on roughness indexes.
g) Comparison on contact surface.
h) Data from the measurement of joint surface in the field.

4.2 Result of Data Analysis for Profiler Method

As discussed in Chapter 3, the height of each grid point marked on the model joint has been measured 10 times using laboratory profiler. By using the statistical method for rejection of observation (see Section 3.3), data that does not meet the required accuracy is being eliminated. The process of elimination for the data is shown in Appendix E. For the analysis shown in the appendix, values listed in the first column are raw data from measurement using profiler method and values in column *y* (second column) are the results of subtracting the value of x_i with the average value for all the observed data, x (written as 'MIN' in the appendix). Values in z rows are the product of multiplying the value of standard deviation with values of critical distribution T, *f*. Accepted & rejected data is marked as 'accept' and 'rejected', respectively. Value of the first MIN is the average value for 10 observations and the second MIN is the value of final/ultimate data (height of grid) after the observation rejection process. If there is no rejected data then, the value of the first MIN is taken as the final/ultimate data. The processed data (ultimate data) for the profiler method is shown in Table 4.1.

4.3 Result of Data Analysis for Photogrammetry Method

In order for the numerical comparison to be made, data from photogrammetry method has been transformed into 3D form. This is to ensure that the orientation of the surface texture, produced by photogrammetry is similar to that of the profiler. This process is undertaken using matrix transformation that has been discussed in Section 3.4.6. The coordinates of the four grid points, that make up the corners of the model joint, i.e. point A1, A19, S19 and S1 (see Figure 4.1) have been taken as reference point in this transformation. The process for changing the orientation of the joint surface produced by photogrammetry (Surface A) to the orientation of joint surface produced by profiler (Surface B), and based on the 4 reference points, can be presented as one matrix

Table 4.1: The height (mm) of all grid points measured using profiler

Profile	1	2	3	4	5	6	7	8	9	10
A	31.44	31.31	31.06	30.90	31.79	31.53	31.50	32.75	33.51	31.91
B	31.53	31.90	30.96	31.58	32.85	33.62	31.24	31.65	31.23	31.01
C	33.01	33.35	32.85	31.67	32.18	31.81	32.48	31.65	30.20	30.58
D	33.07	33.38	33.64	32.27	32.01	31.98	32.84	33.79	30.91	31.11
E	32.51	33.04	34.56	34.16	33.98	33.70	33.54	33.75	30.78	30.37
F	32.35	32.11	30.58	31.96	32.43	33.24	31.17	29.17	29.70	30.01
G	32.12	27.75	26.90	26.92	27.85	31.41	29.64	29.56	29.21	29.25
H	31.31	27.74	27.00	26.93	27.18	26.62	26.90	27.56	28.26	28.77
I	29.75	27.70	26.61	26.92	27.56	26.67	26.51	26.94	28.37	28.92
J	27.67	27.34	27.00	27.95	27.92	27.60	27.20	27.12	27.61	28.07
K	27.18	27.31	26.99	26.81	27.59	26.23	26.34	26.75	26.90	26.92
L	26.22	26.94	26.85	26.62	27.32	26.51	27.24	27.66	27.61	27.81
M	29.24	29.77	27.42	28.12	27.66	28.10	28.64	28.77	28.35	28.18
N	29.64	29.36	29.69	27.48	27.57	28.11	28.32	28.55	28.53	27.59
O	28.54	28.79	29.16	27.44	27.58	27.02	26.96	27.91	28.59	27.78
P	28.97	29.36	29.37	0.29	27.43	28.32	27.34	27.93	28.83	28.26
Q	30.02	28.65	28.81	28.56	26.32	26.90	27.36	27.74	28.77	24.39
R	29.63	27.96	28.74	28.31	27.78	26.31	26.53	27.58	28.54	27.26
S	29.07	29.10	28.88	27.80	26.52	25.96	25.67	25.65	25.50	27.46
Profile	11	12	13	14	15	16	17	18	19	
A	32.60	33.02	32.75	32.97	32.53	32.69	32.30	27.99	26.13	
B	32.13	32.32	33.12	33.95	33.88	33.42	33.16	27.20	25.82	
C	31.94	32.04	32.42	33.16	33.11	33.39	32.12	28.68	25.69	
D	31.79	31.80	32.15	32.51	32.49	32.61	31.07	29.22	27.47	
E	31.25	31.34	33.13	33.78	33.65	32.56	31.43	29.46	28.95	
F	30.79	31.67	32.96	33.85	33.82	33.74	31.75	31.62	31.31	
G	29.98	31.31	31.88	33.26	33.85	33.29	33.27	32.71	32.89	
H	29.03	29.38	31.52	33.05	32.52	33.38	33.94	31.43	29.85	
I	29.45	29.47	31.26	32.19	32.58	31.86	29.28	28.68	28.85	
J	29.27	29.59	29.95	29.73	28.78	29.34	28.49	28.25	28.25	
K	28.09	26.97	26.59	27.33	24.45	26.32	27.69	27.78	27.31	
L	27.20	26.77	26.58	25.59	25.99	25.91	26.35	26.13	25.71	
M	26.48	25.98	25.47	25.35	24.56	25.20	25.65	25.05	24.49	
N	26.72	24.48	24.82	23.84	24.22	23.75	24.50	22.35	22.67	
O	25.76	22.86	22.67	22.53	22.84	21.55	20.87	20.43	20.82	
P	24.96	21.50	21.58	22.15	21.69	21.44	20.37	20.04	20.40	
Q	22.72	21.96	21.63	20.47	20.29	20.71	20.14	20.55	21.17	
R	28.05	25.46	20.71	19.59	20.04	20.95	20.91	21.29	21.49	
S	28.48	25.80	20.38	19.75	20.72	21.20	21.07	21.54	21.80	

transformation (Appendix D). Transformation of the remaining grid points is undertaken using this matrix transformation and the concept is schematically presented as Figure 4.1.

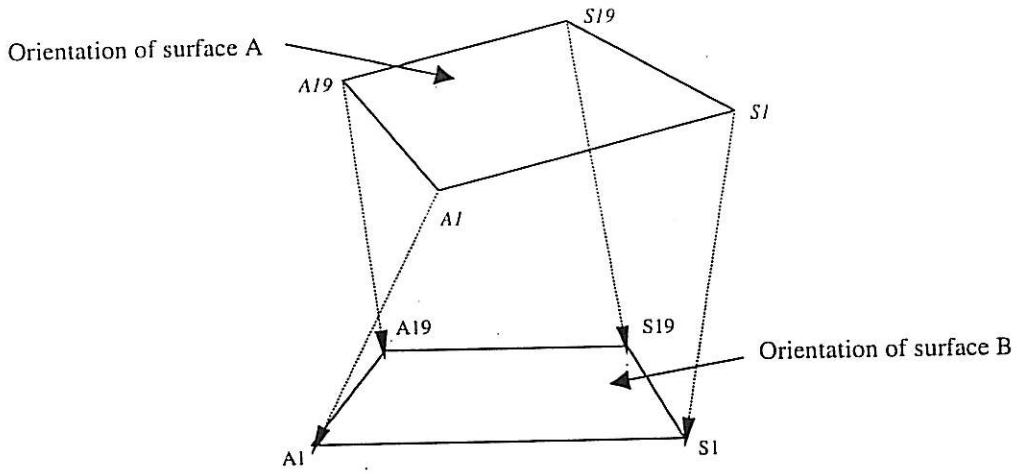

Figure 4.1: 3D transformation of the four corner grid points

Table 4.2 lists the heights of all the grid points, measured by photogrammetry method, after the 3D transformation. The raw data from the *Space Intersection* program, before the transformation, is listed in Appendix F.

4.4 Comparison of linear profiles

A total of 38 profiles, measured along x and y directions, have been compared in order to verify the versatility of close-range photogrammetry in obtaining the texture of a joint surface. To compare all the profiles obtained from both methods of measurement, minor transformation is carried out (see Section 3.5.1) on each profile obtained using photogrammetry. This is to ensure so that all profiles are of similar orientation. Table 4.4 shows the results obtained from the comparison analysis. Data in the first and second column is data from the profiler and photogrammetry method, respectively. The value of 'x' in Table 4.3 is the difference between the data from both methods. Value of +ve 'x' implies that point measured using photogrammetry is lower than the reference point and vice versa for the –ve 'x'. The value of difference shown the table is the maximum

Table 4.2: The height (mm) of all grid points measured using photogrammetry

Profile	1	2	3	4	5	6	7	8	9	10
A	31.44	31.42	31.03	31.11	31.57	31.10	30.89	31.79	32.02	30.61
B	31.35	31.59	31.07	31.35	31.75	32.17	30.59	30.17	30.10	29.94
C	32.03	32.55	31.85	31.07	31.31	31.44	31.47	30.58	29.53	29.31
D	31.96	32.12	32.54	31.38	31.00	31.01	31.13	31.68	29.14	29.87
E	31.12	31.85	32.81	32.15	32.15	31.97	31.36	31.64	29.78	28.53
F	31.33	30.88	29.85	30.59	31.21	31.55	29.78	28.35	28.47	28.62
G	30.83	28.06	27.43	27.66	27.86	30.08	28.97	28.07	27.91	28.25
H	30.36	27.68	27.22	27.25	27.27	26.78	26.69	27.22	27.35	27.16
I	29.08	28.09	26.87	26.80	27.24	26.51	26.81	26.28	27.13	27.84
J	27.73	27.76	27.36	27.62	26.98	26.96	26.69	26.49	26.64	27.03
K	27.34	27.87	27.40	26.88	27.06	26.48	26.34	26.23	26.15	26.16
L	27.20	27.54	27.22	26.99	27.87	26.63	27.23	26.64	26.22	26.50
M	28.96	29.41	27.47	27.66	27.49	27.75	27.69	27.37	26.85	26.95
N	29.02	28.84	28.86	26.96	27.19	27.44	27.73	27.66	27.27	26.73
O	28.51	28.54	28.45	27.27	27.04	26.74	26.36	27.04	27.19	26.65
P	28.40	28.44	29.09	28.17	27.13	27.63	27.09	26.69	27.33	26.66
Q	29.75	28.75	28.51	28.37	26.49	26.89	26.88	26.73	27.70	24.24
R	29.26	28.36	28.47	28.41	27.59	26.33	26.45	26.89	27.01	25.79
S	29.07	29.19	29.14	27.67	26.87	26.44	25.94	25.72	25.67	26.43
Profile	11	12	13	14	15	16	17	18	19	
A	31.36	31.23	31.38	31.08	30.73	30.85	30.33	27.08	26.13	
B	30.39	30.75	31.52	31.84	31.85	30.83	30.95	26.41	25.35	
C	30.37	30.46	30.66	30.97	31.00	31.19	30.20	27.65	25.36	
D	29.83	30.28	30.12	30.56	30.34	30.31	28.74	27.71	26.59	
E	29.54	29.78	31.41	31.34	31.25	30.06	28.89	27.37	26.89	
F	28.69	29.73	30.37	31.32	30.98	30.33	29.46	28.96	28.52	
G	28.35	29.47	29.80	30.66	31.04	30.56	29.98	29.63	29.72	
H	27.62	27.97	28.95	30.31	29.88	30.10	30.85	28.73	27.57	
I	27.66	28.19	28.86	29.75	29.62	29.74	27.47	26.43	26.64	
J	27.79	27.50	28.13	27.78	27.17	26.74	26.48	26.41	26.17	
K	26.94	26.37	25.82	25.79	24.09	25.18	25.88	25.75	25.72	
L	25.93	25.16	25.40	24.03	24.19	24.91	24.29	24.39	23.88	
M	25.64	25.21	24.76	24.62	24.37	24.69	24.78	24.16	23.36	
N	25.11	24.00	24.33	23.81	23.64	23.45	23.54	21.86	22.16	
O	25.20	23.39	22.39	22.26	23.00	21.50	20.99	20.78	21.25	
P	24.40	22.46	21.90	22.20	22.09	21.61	20.60	20.59	20.91	
Q	22.97	22.72	22.45	21.26	20.99	21.02	20.85	21.11	21.28	
R	26.82	24.94	21.56	20.65	21.06	21.82	20.81	21.64	21.43	
S	26.92	25.85	21.58	21.32	21.37	21.55	21.58	21.77	21.80	

difference between the compared profiles. Value of standard deviation is shown in the lower part of column '*x*'.

Graph 4.1 shows the typical shape of profiles along sections 1, 2, 3, R and S on the model joint obtained using both measurement methods. In the plot, the profile being compared is plotted separately so the difference in shape can be visualised. The lower curve (in dashed-line), show the error in the profile, obtained using photogrammetry, compared to profile obtained using profiler. The rest of the profiles is shown in Appendix G. Table 4.3 lists the estimated value of JRC for profiles 1, 2, 3, R and S, obtained using photogrammetry. These JRC values is estimated by visual comparison with the 10 standard profiles proposed by Barton and Choubey, as shown in Figure 2.7

Table 4.3: Estimation of *JRC* value based on visual comparison

Profile	JRC
1	8 - 10
2	10 - 12
3	10 - 12
R	10 - 12
S	10 - 12

Based on Table 4.4, the maximum and minimum standard deviation for all the profiles are 1.15 mm (for profile 19) and 0.35 mm (for profile 10), respectively. These profiles are then divided into two groups, i.e. profiles in *x* and *y* directions. Profiles from each groups are then analysed and the respective standard deviation is 0.66 mm for *x* direction and 0.54 mm for *y* direction. The standard deviation for all profiles (in *x* and *y* direction) is 0.61 mm.

Table 4.4: Results of Profiles Comparison

	1		x	2		x	3		x	4		x	5		x
A	31.44	32.44	-1.00	31.31	32.29	-0.98	31.06	31.91	-0.85	30.90	32.21	-1.31	31.79	32.57	-0.78
B	31.53	32.30	-0.77	31.90	32.56	-0.66	30.96	32.01	-1.04	31.58	32.61	-1.03	32.85	32.70	0.15
C	33.01	32.92	0.09	33.35	33.97	-0.63	32.85	33.16	-0.31	31.67	32.26	-0.59	32.18	32.20	-0.02
D	33.07	32.79	0.28	33.38	33.36	0.02	33.64	34.22	-0.57	32.27	32.75	-0.48	32.01	31.83	0.17
E	32.51	31.89	0.62	33.04	33.00	0.04	34.56	34.64	-0.08	34.16	33.93	0.23	33.98	32.93	1.05
F	32.35	32.05	0.30	32.11	31.60	0.51	30.58	30.38	0.20	31.96	31.72	0.25	32.43	31.94	0.49
G	32.12	31.49	0.63	27.75	27.52	0.23	26.90	26.90	0.00	26.92	27.51	-0.60	27.85	28.53	-0.68
H	31.31	30.97	0.35	27.74	27.00	0.75	27.00	26.63	0.37	26.93	26.98	-0.05	27.18	27.88	-0.70
I	29.75	29.64	0.11	27.70	27.62	0.09	26.61	26.15	0.46	26.92	26.38	0.54	27.56	27.80	-0.24
J	27.67	28.23	-0.56	27.34	27.16	0.18	27.00	26.90	0.10	27.95	27.63	0.33	27.92	27.48	0.44
K	27.18	27.78	-0.61	27.31	27.34	-0.02	26.99	27.01	-0.02	26.81	26.60	0.21	27.59	27.50	0.09
L	26.22	27.59	-1.37	26.94	26.88	0.06	26.85	26.78	0.07	26.62	26.81	-0.19	27.32	28.25	-0.93
M	29.24	29.29	-0.05	29.77	29.62	0.16	27.42	27.17	0.25	28.12	27.84	0.28	27.66	27.82	-0.17
N	29.64	29.30	0.34	29.36	28.81	0.54	29.69	29.24	0.45	27.48	26.88	0.60	27.57	27.46	0.10
O	28.54	28.73	-0.19	28.79	28.40	0.39	29.16	28.68	0.48	27.44	27.38	0.06	27.58	27.26	0.32
P	28.97	28.56	0.41	29.36	28.28	1.09	29.37	29.65	-0.28	28.70	28.75	-0.05	27.43	27.30	0.14
Q	30.02	29.86	0.15	28.65	28.75	-0.10	28.81	28.85	-0.03	28.56	29.10	-0.54	26.32	26.60	-0.29
R	29.63	29.31	0.31	27.96	28.20	-0.25	28.74	28.82	-0.08	28.31	29.21	-0.90	27.78	27.65	0.13
S	29.07	29.07	0.00	29.10	29.43	-0.33	28.88	29.84	-0.96	27.80	28.18	-0.39	26.52	26.87	-0.35
Standard deviation =			*0.56*			*0.50*			*0.47*			*0.54*			*0.50*

	6		x	7		x	8		x	9		x	10		x
A	31.53	32.30	-0.77	31.50	32.09	-0.59	32.75	32.89	-0.14	33.51	33.52	-0.01	31.91	31.91	0.00
B	33.62	33.30	0.32	31.24	31.73	-0.49	31.65	31.20	0.45	31.23	31.60	-0.37	31.01	31.23	-0.21
C	31.81	32.50	-0.69	32.48	32.54	-0.06	31.65	31.56	0.09	30.20	31.03	-0.83	30.58	30.59	0.00
D	31.98	32.01	-0.03	32.84	32.13	0.71	33.79	32.59	1.20	30.91	30.64	0.27	31.11	31.12	-0.01
E	33.70	32.91	0.79	33.54	32.29	1.24	33.75	32.49	1.25	30.78	31.28	-0.50	30.37	29.77	0.60
F	33.24	32.42	0.82	31.17	30.65	0.52	29.17	29.14	0.03	29.70	29.97	-0.27	30.01	29.84	0.16
G	31.41	30.88	0.53	29.64	29.77	-0.13	29.56	28.80	0.76	29.21	29.41	-0.20	29.25	29.46	-0.20
H	26.62	27.52	-0.90	26.90	27.42	-0.52	27.56	27.89	-0.33	28.26	28.85	-0.59	28.77	28.35	0.42
I	26.67	27.18	-0.51	26.51	27.48	-0.97	26.94	26.89	0.05	28.37	28.63	-0.26	28.92	29.02	-0.09
J	27.60	27.56	0.04	27.20	27.29	-0.09	27.12	27.04	0.07	27.61	28.14	-0.53	28.07	28.20	-0.13
K	26.23	27.01	-0.79	26.34	26.87	-0.53	26.75	26.72	0.03	26.90	27.65	-0.75	26.92	27.31	-0.40
L	26.51	27.10	-0.59	27.24	27.70	-0.46	27.66	27.06	0.60	27.61	27.72	-0.11	27.81	27.64	0.17
M	28.10	28.15	-0.05	28.64	28.09	0.54	28.77	27.73	1.04	28.35	28.35	-0.01	28.18	28.07	0.11
N	28.11	27.77	0.33	28.32	28.06	0.26	28.55	27.96	0.59	28.53	28.77	-0.25	27.59	27.84	-0.25
O	27.02	27.01	0.00	26.96	26.62	0.33	27.91	27.28	0.63	28.59	28.69	-0.10	27.78	27.74	0.04
P	28.32	27.83	0.49	27.34	27.29	0.05	27.93	26.88	1.05	28.83	28.83	0.00	28.26	27.74	0.53
Q	26.90	27.03	-0.13	27.36	27.01	0.35	27.74	26.85	0.89	28.77	29.20	-0.43	24.39	25.30	-0.91
R	26.31	26.40	-0.09	26.53	26.52	0.01	27.58	26.95	0.63	28.54	28.51	0.03	27.26	26.84	0.41
S	25.96	26.44	-0.48	25.67	25.94	-0.28	25.65	25.72	-0.07	25.50	27.17	-1.67	27.46	27.46	0.00
			0.54			0.54			0.49			0.43			0.35

	11		x	12		x	13		x	14		x	15		x
A	32.60	33.10	-0.50	33.02	33.43	-0.40	32.75	33.58	-0.83	32.97	34.08	-1.11	32.53	33.73	-1.21
B	32.13	32.08	0.05	32.32	32.80	-0.48	33.12	33.59	-0.47	33.95	34.63	-0.68	33.88	34.65	-0.77
C	31.94	32.00	-0.06	32.04	32.36	-0.33	32.42	32.59	-0.17	33.16	33.55	-0.39	33.11	33.59	-0.48
D	31.79	31.39	0.40	31.80	32.03	-0.23	32.15	31.92	0.22	32.51	32.93	-0.42	32.49	32.73	-0.24
E	31.25	31.04	0.20	31.34	31.38	-0.04	33.13	33.08	0.05	33.78	33.50	0.28	33.65	33.43	0.21
F	30.79	30.13	0.65	31.67	31.18	0.49	32.96	31.90	1.06	33.85	33.27	0.58	33.82	32.96	0.86
G	29.98	29.73	0.24	31.31	30.77	0.54	31.88	31.20	0.68	33.26	32.39	0.87	33.85	32.83	1.03
H	29.03	28.94	0.08	29.38	29.12	0.25	31.52	30.22	1.30	33.05	31.83	1.22	32.52	31.46	1.06
I	29.45	28.93	0.52	29.47	29.19	0.27	31.26	29.99	1.27	32.19	31.06	1.12	32.58	30.99	1.59
J	29.27	28.99	0.28	29.59	28.35	1.24	29.95	29.13	0.82	29.73	28.88	0.84	28.78	28.35	0.43
K	28.09	28.08	0.00	26.97	27.07	-0.10	26.59	26.69	-0.10	27.33	26.68	0.65	24.45	25.07	-0.62
L	27.20	27.01	0.19	26.77	25.71	1.06	26.58	26.13	0.44	25.59	24.71	0.88	25.99	24.96	1.03
M	26.48	26.66	-0.17	25.98	25.61	0.37	25.47	25.36	0.10	25.35	25.09	0.27	24.56	24.94	-0.38
N	26.72	26.07	0.64	24.48	24.25	0.23	24.82	24.80	0.02	23.84	24.06	-0.23	24.22	24.00	0.22
O	25.76	26.10	-0.34	22.86	23.49	-0.63	22.67	22.72	-0.05	22.53	22.30	0.23	22.84	23.16	-0.33
P	24.96	25.24	-0.28	21.50	22.41	-0.91	21.58	22.10	-0.53	22.15	22.04	0.12	21.69	22.05	-0.36
Q	22.72	23.74	-1.02	21.96	22.52	-0.56	21.63	22.51	-0.89	20.47	20.89	-0.42	20.29	20.74	-0.45
R	28.05	27.53	0.52	25.46	24.59	0.87	20.71	21.49	-0.79	19.59	20.07	-0.47	20.04	20.61	-0.57
S	28.48	27.58	0.90	25.80	25.35	0.45	20.38	21.38	-1.00	19.75	20.52	-0.77	20.72	20.72	0.00
			0.46			*0.59*			*0.72*			*0.69*			*0.76*

	16		x	17		x	18		x	19		x
A	32.69	33.85	-1.17	32.30	33.23	-0.93	27.99	29.28	-1.28	26.13	28.13	-2.00
B	33.42	33.63	-0.21	33.16	33.69	-0.52	27.20	28.49	-1.28	25.82	27.35	-1.53
C	33.39	33.79	-0.40	32.12	32.78	-0.65	28.68	29.60	-0.93	25.69	27.36	-1.68
D	32.61	32.71	-0.10	31.07	31.16	-0.09	29.22	29.54	-0.32	27.47	28.59	-1.12
E	32.56	32.26	0.30	31.43	31.14	0.29	29.46	29.08	0.38	28.95	28.89	0.06
F	33.74	32.33	1.41	31.75	31.56	0.19	31.62	30.55	1.07	31.31	30.52	0.79
G	33.29	32.36	0.93	33.27	31.91	1.35	32.71	31.10	1.62	32.89	31.72	1.18
H	33.38	31.70	1.67	33.94	32.62	1.31	31.43	30.08	1.35	29.85	29.57	0.29
I	31.86	31.14	0.73	29.28	29.08	0.20	28.68	27.66	1.03	28.85	28.64	0.21
J	29.34	27.94	1.39	28.49	27.93	0.56	28.25	27.51	0.73	28.25	28.17	0.08
K	26.32	26.18	0.13	27.69	27.17	0.52	27.78	26.73	1.05	27.31	27.72	-0.41
L	25.91	25.71	0.19	26.35	25.42	0.92	26.13	25.25	0.88	25.71	25.88	-0.17
M	25.20	25.29	-0.09	25.65	25.75	-0.10	25.05	24.89	0.16	24.49	25.36	-0.87
N	23.75	23.85	-0.10	24.50	24.34	0.16	22.35	22.47	-0.12	22.67	24.16	-1.49
O	21.55	21.70	-0.15	20.87	21.64	-0.77	20.43	21.26	-0.84	20.82	23.25	-2.43
P	21.44	21.61	-0.17	20.37	21.08	-0.71	20.04	20.95	-0.91	20.40	22.91	-2.51
Q	20.71	20.82	-0.11	20.14	21.17	-1.03	20.55	21.35	-0.81	21.17	23.28	-2.11
R	20.95	21.42	-0.48	20.91	20.97	-0.07	21.29	21.76	-0.48	21.49	23.43	-1.95
S	21.20	20.95	0.25	21.07	21.58	-0.51	21.54	21.77	-0.23	21.80	23.80	-2.00
			0.72			0.71			0.94			1.15

	A		x	B		x	C		x	D		x	E		x
1	31.44	31.44	0.00	31.53	31.35	0.17	33.01	33.03	-0.02	33.07	33.96	-0.89	32.51	32.52	0.00
2	31.31	31.51	-0.20	31.90	31.69	0.21	33.35	33.55	-0.21	33.38	34.12	-0.73	33.04	33.29	-0.25
3	31.06	31.20	-0.15	30.96	31.27	-0.31	32.85	32.85	0.01	33.64	34.54	-0.90	34.56	34.28	0.28
4	30.90	31.38	-0.47	31.58	31.65	-0.07	31.67	32.07	-0.40	32.27	33.38	-1.10	34.16	33.65	0.51
5	31.79	31.93	-0.14	32.85	32.15	0.69	32.18	32.31	-0.13	32.01	33.00	-0.99	33.98	33.68	0.30
6	31.53	31.55	-0.02	33.62	32.67	0.95	31.81	32.44	-0.63	31.98	33.01	-1.03	33.70	33.54	0.16
7	31.50	31.42	0.07	31.24	31.19	0.04	32.48	32.47	0.00	32.84	33.13	-0.29	33.54	32.96	0.58
8	32.75	32.41	0.33	31.65	30.87	0.79	31.65	31.58	0.07	33.79	33.68	0.11	33.75	33.27	0.47
9	33.51	32.73	0.78	31.23	30.90	0.33	30.20	30.53	-0.33	30.91	31.14	-0.23	30.78	31.44	-0.66
10	31.91	31.41	0.50	31.01	30.84	0.17	30.58	30.31	0.27	31.11	31.87	-0.75	30.37	30.23	0.14
11	32.60	32.25	0.36	32.13	31.39	0.73	31.94	31.37	0.57	31.79	31.83	-0.03	31.25	31.27	-0.03
12	33.02	32.20	0.82	32.32	31.85	0.47	32.04	31.46	0.57	31.80	32.28	-0.48	31.34	31.55	-0.20
13	32.75	32.44	0.30	33.12	32.72	0.39	32.42	31.66	0.77	32.15	32.12	0.02	33.13	33.21	-0.08
14	32.97	32.23	0.74	33.95	33.14	0.81	33.16	31.97	1.19	32.51	32.56	-0.05	33.78	33.17	0.61
15	32.53	31.98	0.55	33.88	33.25	0.62	33.11	32.00	1.12	32.49	32.34	0.15	33.65	33.11	0.53
16	32.69	32.19	0.50	33.42	32.33	1.09	33.39	32.19	1.20	32.61	32.31	0.30	32.56	31.96	0.60
17	32.30	31.75	0.55	33.16	32.55	0.62	32.12	31.20	0.92	31.07	30.74	0.33	31.43	30.82	0.61
18	27.99	28.59	-0.60	27.20	28.11	-0.91	28.68	28.65	0.03	29.22	29.71	-0.49	29.46	29.33	0.12
19	26.13	27.73	-1.60	25.82	27.15	-1.33	25.69	26.36	-0.68	27.47	28.59	-1.12	28.95	28.89	0.06
Standard deviation =			*0.60*			*0.63*			*0.61*			*0.50*			*0.36*

	F		x	G		x	H		x	I		x	J		x
1	32.35	32.33	0.02	32.12	30.83	1.30	31.31	29.56	1.76	29.75	28.88	0.87	27.67	27.33	0.34
2	32.11	31.98	0.13	27.75	28.23	-0.48	27.74	27.12	0.62	27.70	28.06	-0.36	27.34	27.50	-0.16
3	30.58	31.05	-0.47	26.90	27.79	-0.89	27.00	26.91	0.09	26.61	27.00	-0.39	27.00	27.23	-0.23
4	31.96	31.89	0.08	26.92	28.19	-1.27	26.93	27.19	-0.25	26.92	27.10	-0.18	27.95	27.64	0.31
5	32.43	32.61	-0.19	27.85	28.57	-0.72	27.18	27.45	-0.27	27.56	27.71	-0.15	27.92	27.14	0.79
6	33.24	33.05	0.19	31.41	30.97	0.44	26.62	27.21	-0.59	26.67	27.15	-0.47	27.60	27.26	0.34
7	31.17	31.38	-0.21	29.64	30.03	-0.40	26.90	27.36	-0.46	26.51	27.61	-1.10	27.20	27.12	0.07
8	29.17	30.05	-0.88	29.56	29.31	0.25	27.56	28.13	-0.57	26.94	27.25	-0.31	27.12	27.06	0.05
9	29.70	30.27	-0.57	29.21	29.34	-0.13	28.26	28.51	-0.25	28.37	28.26	0.11	27.61	27.35	0.26
10	30.01	30.52	-0.51	29.25	29.85	-0.59	28.77	28.56	0.21	28.92	29.14	-0.21	28.07	27.88	0.19
11	30.79	30.69	0.10	29.98	30.13	-0.15	29.03	29.27	-0.24	29.45	29.13	0.32	29.27	28.78	0.49
12	31.67	31.83	-0.16	31.31	31.42	-0.11	29.38	29.86	-0.48	29.47	29.82	-0.36	29.59	28.63	0.96
13	32.96	32.57	0.39	31.88	31.94	-0.05	31.52	31.08	0.43	31.26	30.66	0.60	29.95	29.40	0.55
14	33.85	33.62	0.22	33.26	32.97	0.29	33.05	32.69	0.36	32.19	31.72	0.47	29.73	29.19	0.54
15	33.82	33.38	0.45	33.85	33.53	0.32	32.52	32.50	0.02	32.58	31.75	0.83	28.78	28.72	0.06
16	33.74	32.83	0.91	33.29	33.23	0.06	33.38	32.97	0.41	31.86	32.04	-0.17	29.34	28.43	0.91
17	31.75	32.06	-0.32	33.27	32.82	0.44	33.94	33.96	-0.02	29.28	29.93	-0.65	28.49	28.31	0.18
18	31.62	31.66	-0.05	32.71	32.65	0.06	31.43	32.09	-0.66	28.68	29.07	-0.38	28.25	28.37	-0.13
19	31.31	31.32	-0.01	32.89	32.92	-0.02	29.85	31.17	-1.31	28.85	29.44	-0.59	28.25	28.27	-0.02
			0.42			0.48			0.48			0.48			0.36

	K		x	L		x	M		x	N		x	O		x
1	27.18	26.84	0.34	26.22	26.20	0.02	29.24	28.96	0.29	29.64	29.62	0.02	28.54	29.21	-0.66
2	27.31	27.48	-0.17	26.94	26.70	0.25	29.77	29.47	0.30	29.36	29.44	-0.08	28.79	29.18	-0.39
3	26.99	27.14	-0.15	26.85	26.53	0.32	27.42	27.60	-0.18	29.69	29.46	0.22	29.16	29.03	0.14
4	26.81	26.73	0.08	26.62	26.45	0.17	28.12	27.86	0.26	27.48	27.56	-0.09	27.44	27.78	-0.35
5	27.59	27.03	0.56	27.32	27.49	-0.17	27.66	27.76	-0.10	27.57	27.79	-0.22	27.58	27.50	0.09
6	26.23	26.56	-0.34	26.51	26.41	0.10	28.10	28.09	0.02	28.11	28.04	0.07	27.02	27.14	-0.12
7	26.34	26.54	-0.20	27.24	27.16	0.07	28.64	28.09	0.54	28.32	28.33	-0.01	26.96	26.69	0.26
8	26.75	26.55	0.20	27.66	26.73	0.94	28.77	27.83	0.94	28.55	28.26	0.29	27.91	27.31	0.60
9	26.90	26.58	0.32	27.61	26.47	1.14	28.35	27.39	0.96	28.53	27.87	0.65	28.59	27.40	1.19
10	26.92	26.71	0.20	27.81	26.90	0.91	28.18	27.55	0.63	27.59	27.33	0.25	27.78	26.80	0.98
11	28.09	27.61	0.48	27.20	26.48	0.72	26.48	26.30	0.18	26.72	25.71	1.00	25.76	25.29	0.47
12	26.97	27.15	-0.18	26.77	25.87	0.89	25.98	25.95	0.04	24.48	24.60	-0.12	22.86	23.42	-0.56
13	26.59	26.72	-0.13	26.58	26.27	0.31	25.47	25.56	-0.10	24.82	24.93	-0.11	22.67	22.36	0.31
14	27.33	26.80	0.53	25.59	25.05	0.53	25.35	25.49	-0.13	23.84	24.41	-0.57	22.53	22.16	0.37
15	24.45	25.23	-0.78	25.99	25.37	0.62	24.56	25.30	-0.74	24.22	24.24	-0.02	22.84	22.85	-0.01
16	26.32	26.43	-0.12	25.91	26.25	-0.34	25.20	25.69	-0.49	23.75	24.05	-0.30	21.55	21.28	0.27
17	27.69	27.24	0.44	26.35	25.78	0.56	25.65	25.85	-0.20	24.50	24.14	0.36	20.87	20.71	0.15
18	27.78	27.24	0.54	26.13	26.04	0.09	25.05	25.29	-0.24	22.35	22.46	-0.11	20.43	20.44	-0.01
19	27.31	27.32	-0.01	25.71	25.68	0.03	24.49	24.56	-0.07	22.67	22.76	-0.09	20.82	20.85	-0.03
			0.37			*0.41*			*0.45*			*0.36*			*0.44*

	P		x	Q		x	R		x	S		x
1	28.97	29.00	-0.02	30.02	29.75	0.27	29.63	29.26	0.37	29.07	29.07	0.00
2	29.36	28.98	0.38	28.65	28.71	-0.06	27.96	28.36	-0.40	29.10	29.19	-0.09
3	29.37	29.57	-0.20	28.81	28.43	0.38	28.74	28.47	0.27	28.88	29.14	-0.26
4	28.70	28.59	0.11	28.56	28.26	0.31	28.31	28.41	-0.11	27.80	27.67	0.12
5	27.43	27.48	-0.05	26.32	26.33	-0.02	27.78	27.59	0.19	26.52	26.87	-0.35
6	28.32	27.93	0.40	26.90	26.70	0.20	26.31	26.33	-0.03	25.96	26.44	-0.48
7	27.34	27.32	0.01	27.36	26.65	0.72	26.53	26.45	0.08	25.67	25.94	-0.28
8	27.93	26.87	1.06	27.74	26.46	1.28	27.58	26.89	0.69	25.65	25.72	-0.07
9	28.83	27.44	1.39	28.77	27.39	1.38	28.54	27.01	1.53	25.50	25.67	-0.17
10	28.26	26.71	1.55	24.39	23.89	0.50	27.26	25.79	1.46	27.46	26.43	1.03
11	24.96	24.39	0.57	22.72	22.58	0.14	28.05	26.82	1.24	28.48	26.92	1.56
12	21.50	22.39	-0.89	21.96	22.30	-0.34	25.46	24.94	0.52	25.80	25.85	-0.05
13	21.58	21.77	-0.19	21.63	21.98	-0.35	20.71	21.56	-0.85	20.38	21.58	-1.20
14	22.15	22.01	0.15	20.47	20.76	-0.29	19.59	20.65	-1.06	19.75	21.32	-1.57
15	21.69	21.83	-0.14	20.29	20.44	-0.15	20.04	21.06	-1.02	20.72	21.37	-0.65
16	21.44	21.29	0.15	20.71	20.44	0.27	20.95	21.82	-0.88	21.20	21.55	-0.35
17	20.37	20.22	0.15	20.14	20.23	-0.09	20.91	20.81	0.10	21.07	21.58	-0.51
18	20.04	20.15	-0.11	20.55	20.45	0.10	21.29	21.64	-0.35	21.54	21.77	-0.23
19	20.40	20.41	-0.01	21.17	20.58	0.59	21.49	21.43	0.05	21.80	21.80	0.00
			0.60			0.50			0.79			0.69

Graph 4.1: Typical Profile Along Section 1, 2, 3, R and S

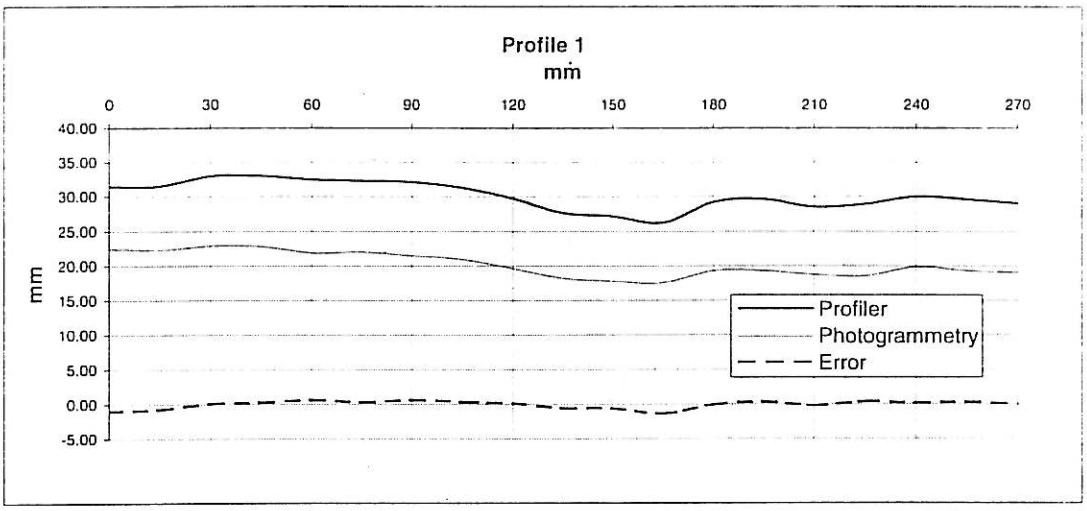

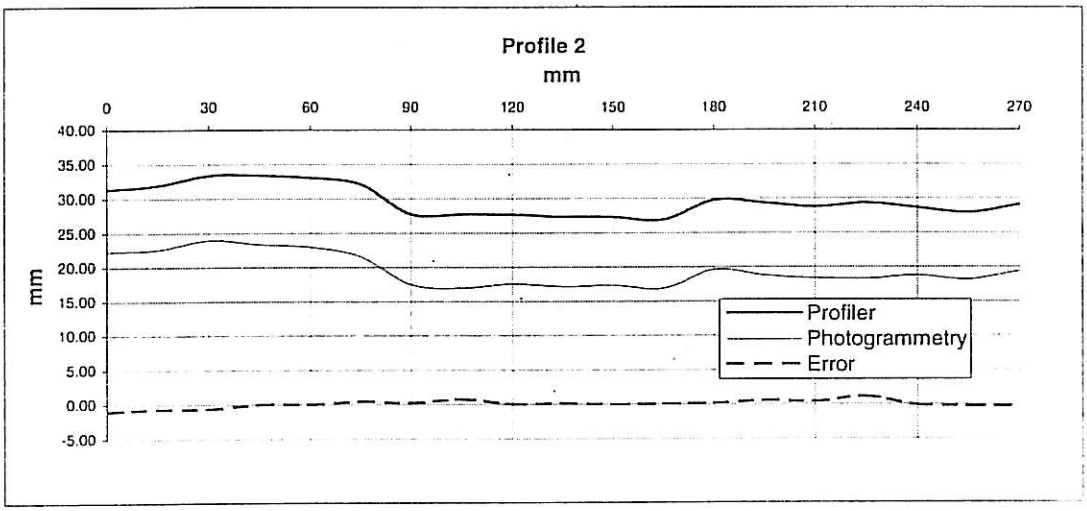

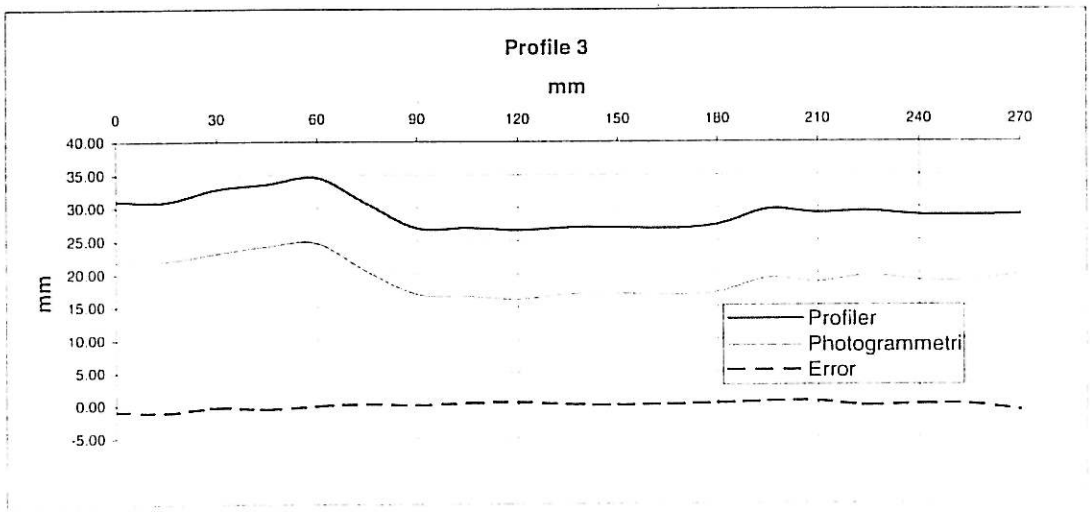

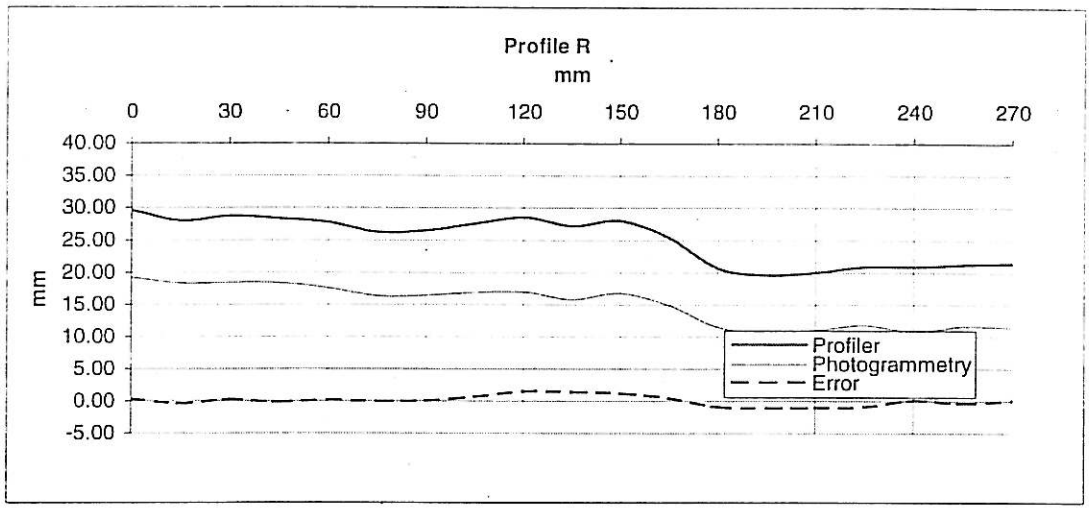
Profile R
mm
0
30
60
90
120
150
180
210
240
270
40.00
35.00
30.00
25.00
20.00
15.00
10.00
5.00
0.00
-5.00
mm
Profiler
Photogrammetry
Error

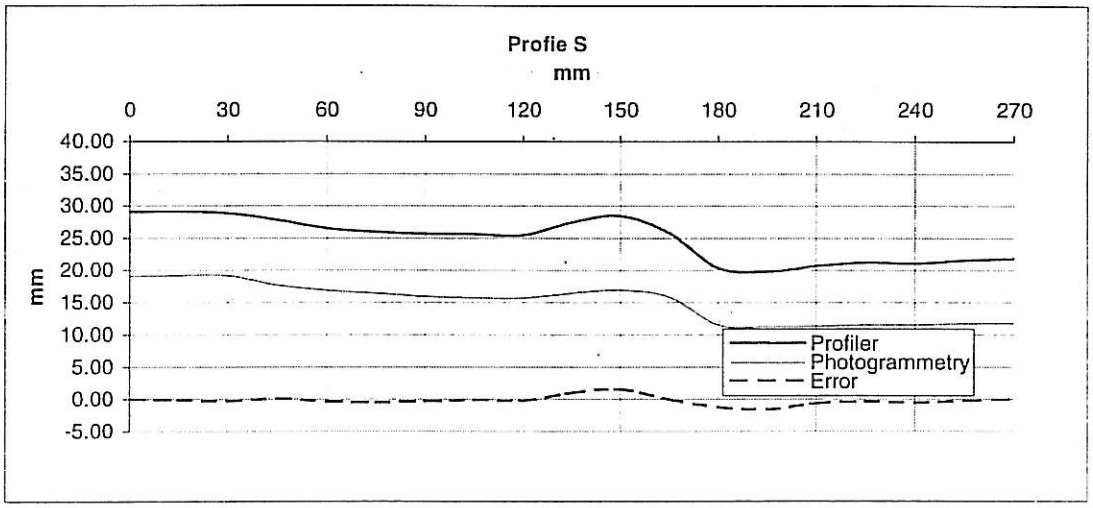
Profie S
mm
0
30
60
90
120
150
180
210
240
270
40.00
35.00
30.00
25.00
20.00
15.00
10.00
5.00
0.00
-5.00
mm
Profiler
Photogrammetry
Error

4.5 Contour Plot for Joint Surface

Surfer software (Version 16) is used to plot the contours for the model joint surface. Figure 4.2(a) and 4.2(b) show the plots using data from both methods of measurement, plotted at 1 mm contour interval. The changes of colour in the plot indicate the difference in topographic height of the joint surface. The darker colour implies the portion of lower topographic height and vice versa. Both plots show almost identical surface texture, especially in the area where there are significant changes in contour (usually referred to as troughs and peaks in surface roughness).

4.6 3 Dimensional Plot for Joint Surface

Again *Surfer* is used to plot the surface of the model joint in 3 dimensions, based on data obtained from both methods of measurement. This type of plot gives a better presentation of the surface. Views of the joint surface, in the form of orthographic projections from different angles and side projection, are shown in Figure 4.3(a) to 4.3(f). For ease of comparison, all the plots are done using a similar scale, i.e. 1inch: 40 map unit in x and y direction, and 1 inch: 15 map unit in z direction.

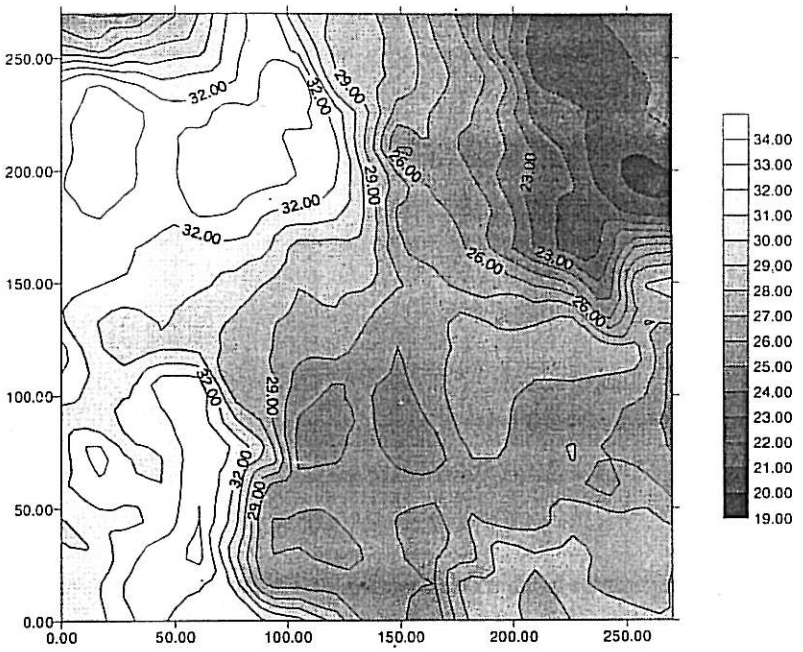

Figure 4.2(a): Contour plot (1 mm interval) for the joint surface based on data obtained using profiler

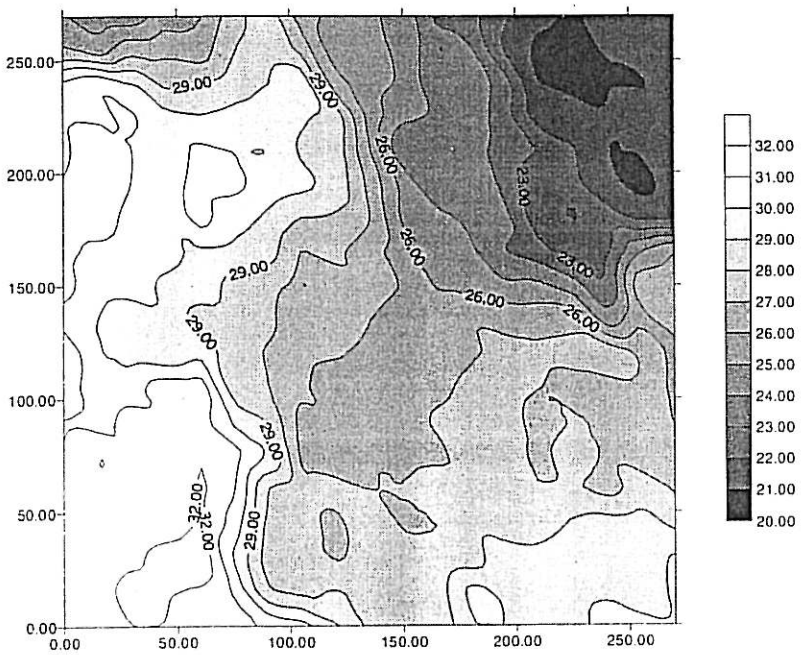

Figure 4.2(b): Contour plot (1 mm interval) for the joint surface based on data obtained using close-range photogrammetry

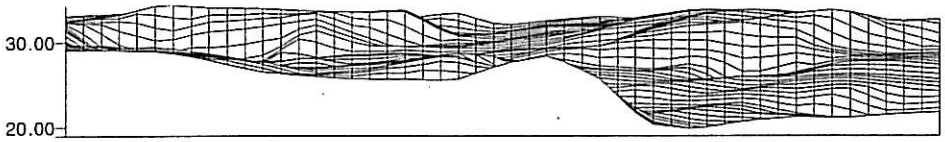

Figure 4.3(a): Side projection of the profiles based on data from profiler (plotted in mm)

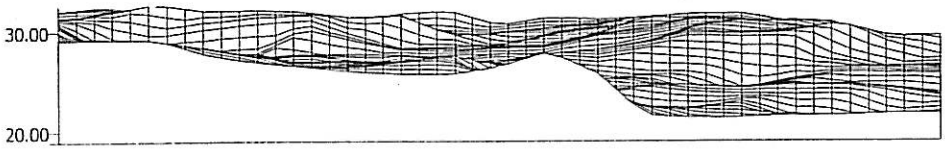

Figure 4.3(b): Side projection of the profiles based on data from photogrammetry (plotted in mm)

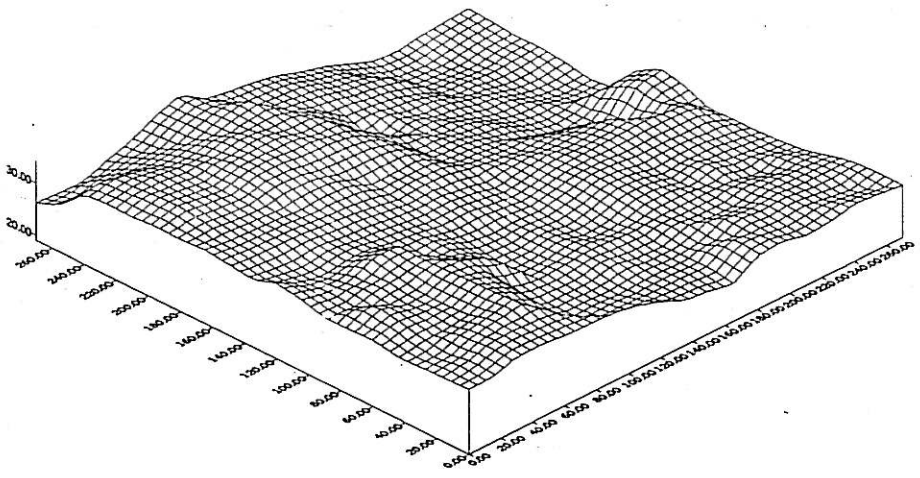

Figure 4.3(c): Orthographic projection of the profiles based on data from profiler (plotted in mm)

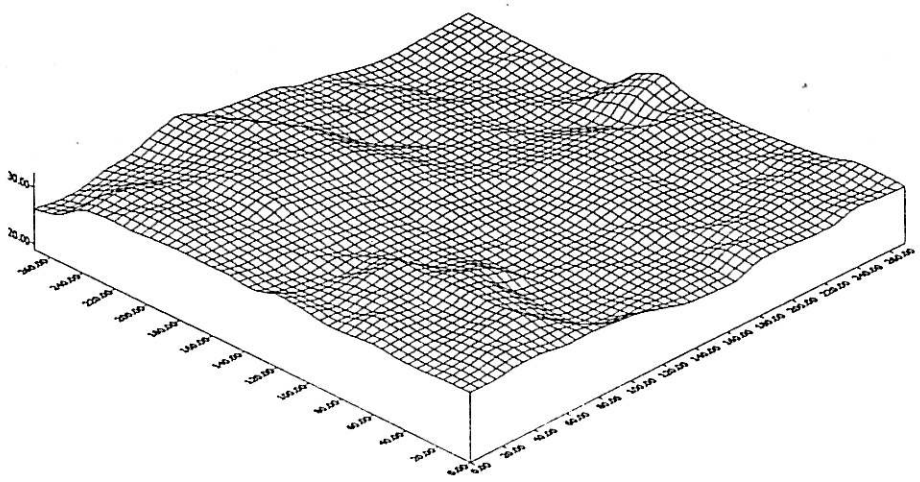

Figure 4.3(d): Orthographic projection of the profiles based on data from photogrammetry (plotted in mm)

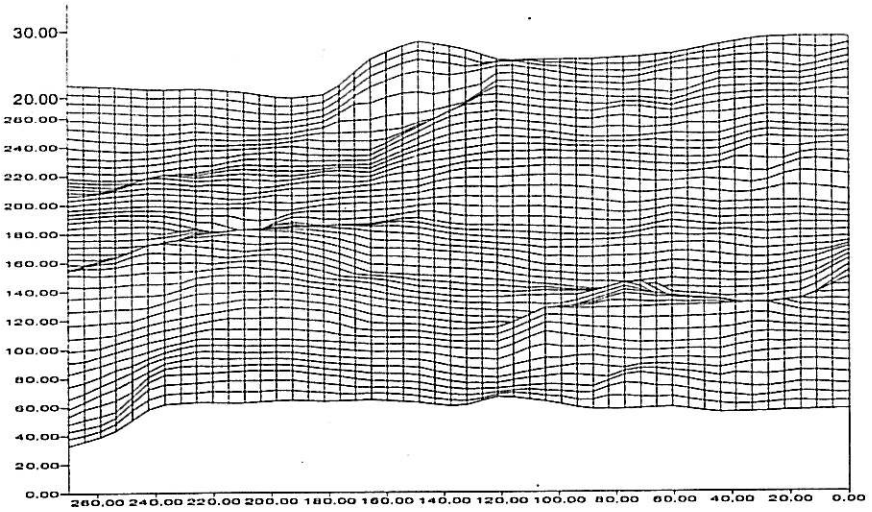

Figure 4.3(e): Orthographic projection of the profiles based on data from profiler (plotted in mm)

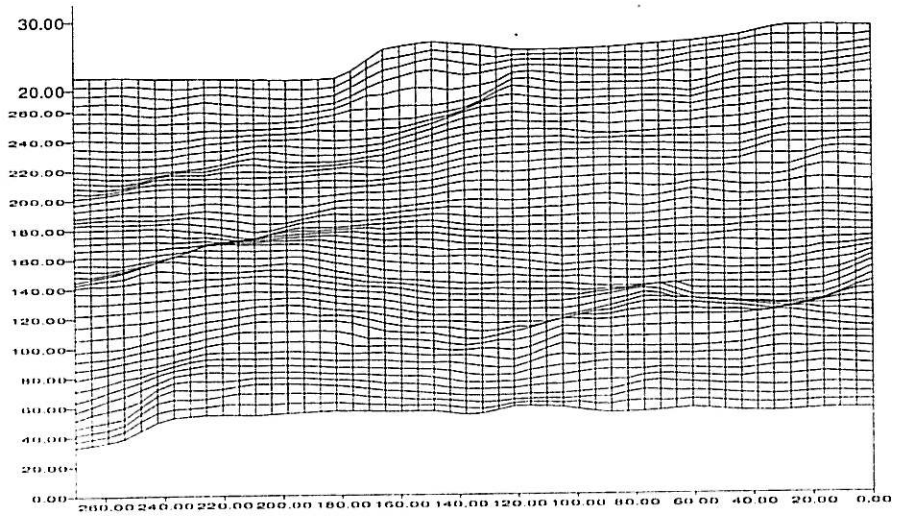

Figure 4.3(f): Orthographic projection of the profiles based on data from photogrammetry (plotted in mm)

4.7 Comparison of contact surface

Contact area in this case refers to the horizontal shear plane taken at the mean height of all the peaks and troughs on the model joint (see Section 3.5.3). The contact area, which basically represents the area just above the mean plane, is calculated using *Surfer* and shown in Figure 4.4. This comparison is to verify the difference in contact area between joint surfaces plotted using both data. Both Figures 4.4(a) and 4.4(b) are plotted using scale of 1inch: 45 map unit in x and y direction, and 1 inch: 6 map unit in z direction. The calculated contact area is 354.1cm^2 for the joint surface plotted using profiler and 361.2 cm^2 for photogrammetry. The difference in area is 7.1 cm^2 i.e. about 0.97% of the total area of the joint surface.

4.8 Comparison of Roughness Index

This comparison is to assess the degree of roughness of the joint surface produced by data from both methods and the assessment is based on three types of roughness index namely; k, *CLA* and *SD* (see Section 3.5.2). Table 4.5 shows the value of roughness index obtained from profiles measured using both methods and the difference in roughness index between both methods. In this comparison, data from profiler is used as reference. The standard deviations for the difference in the roughness index between the two methods of measurement are $SD = 0.23$, $k = 0.92$ and $CLA = 0.55$.

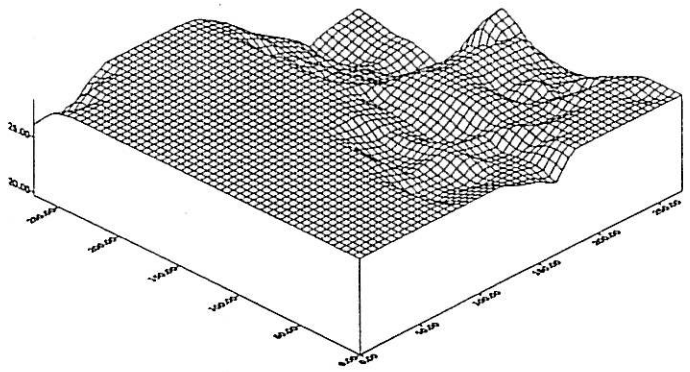

Figure 4.4(a): Contact area based on data from profiler (plotted in mm).

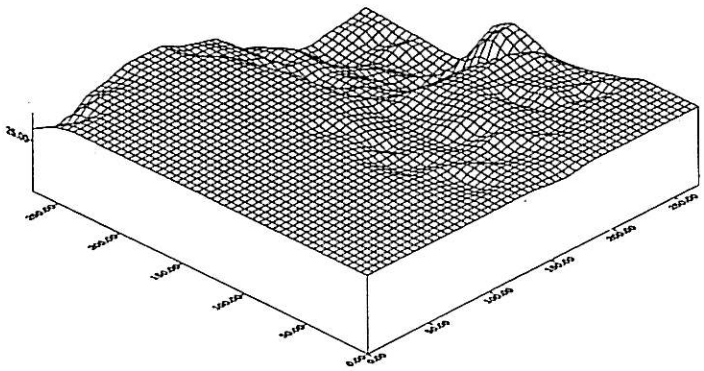

Figure 4.4(b):Contact area based on data from photogrammetry (plotted in mm).

Table 4.5: Comparison of Roughness Index

	Profiler						Different		
	S.P	*k*	*CLA*	S.P	*k*	*CLA*	S.P	*k*	*CLA*
Profile 1	2.01	6.85	3.95	1.79	5.33	2.63	0.23	1.52	1.32
Profile 2	2.20	6.44	2.68	2.41	7.09	2.69	-0.21	-0.65	0.00
Profile 3	2.43	7.66	2.71	2.67	8.49	3.27	-0.25	-0.83	-0.56
Profile 4	2.31	7.54	2.38	2.51	7.55	2.82	-0.21	0.00	-0.43
Profile 5	2.52	7.67	2.71	2.34	6.33	2.48	0.18	1.34	0.22
Profile 6	2.83	7.74	3.07	2.59	6.51	2.72	0.24	1.23	0.35
Profile 7	2.52	7.87	3.14	2.32	6.35	2.88	0.21	1.52	0.26
Profile 8	2.45	8.14	3.43	2.32	7.17	2.89	0.13	0.97	0.53
Profile 9	1.77	8.01	3.52	1.60	6.35	2.20	0.17	1.66	1.32
Profile 10	1.81	7.52	4.33	1.70	6.61	3.41	0.11	0.91	0.92
Profile 11	2.70	9.88	6.05	2.56	2.56	2.56	0.14	0.52	1.14
Profile 12	3.74	11.52	6.59	3.70	11.01	5.57	0.05	0.51	1.02
Profile 13	4.83	12.76	7.60	4.48	11.70	6.54	0.35	1.06	1.06
Profile 14	5.47	14.36	8.57	5.33	14.56	7.95	0.13	-0.21	0.62
Profile 15	5.42	13.84	7.96	5.23	14.04	7.34	0.19	-0.20	0.62
Profile 16	5.25	13.03	7.36	5.05	11.54	7.03	0.20	1.49	0.32
Profile 17	4.99	13.80	7.46	4.72	12.71	6.62	0.27	1.08	0.84
Profile 18	4.13	12.67	6.30	3.64	10.14	5.33	0.49	2.53	0.97
Profile 19	3.72	12.50	5.45	2.71	8.81	3.87	1.01	3.69	1.58
Profile A	1.79	7.39	5.48	1.26	5.01	3.76	0.53	2.38	1.72
Profile B	2.09	8.12	5.89	1.54	6.10	4.28	0.55	2.02	1.62
Profile C	1.87	7.70	6.01	1.65	7.19	5.11	0.22	0.51	0.90
Profile D	1.52	6.17	4.43	1.50	5.95	3.74	0.02	0.22	0.69
Profile E	1.67	5.61	3.47	1.55	5.39	3.33	0.12	0.22	0.14
Profile F	1.38	4.68	2.63	1.04	3.58	1.80	0.34	1.10	0.83
Profile G	2.31	6.96	3.79	1.91	5.74	2.98	0.40	1.21	0.80
Profile H	2.47	7.32	2.98	2.34	7.05	2.75	0.13	0.27	0.23
Profile I	1.94	6.08	2.41	1.63	5.03	2.04	0.31	1.04	0.38
Profile J	0.93	2.95	1.27	0.75	2.34	0.92	0.18	0.61	0.35
Profile K	0.79	3.64	2.47	0.52	2.38	1.61	0.26	1.26	0.87
Profile L	0.67	2.22	1.09	0.59	2.43	1.26	0.08	-0.21	-0.16
Profile M	1.70	5.28	2.48	1.41	4.91	2 31	0.30	0.37	0.17
Profile N	2.45	7.34	4.08	2.35	7.16	3.91	0.11	0.18	0.17
Profile O	3.17	8.74	4.84	3.16	8.77	4.69	0.02	-0.04	0.15
Profile P	3.70	9.33	5.15	3.46	9.42	4.82	0.23	-0.09	0.34
Profile Q	3.66	9.88	4.45	3.43	9.53	4.10	0.23	0.35	0.34
Profile R	3.59	10.03	5.52	3.10	8.60	4.37	0.49	1.43	1.15
Profile S	3.32	9.35	5.11	2.93	7.87	3.73	0.39	1.48	1.38
					Standard deviation:		***0.23***	***0.92***	***0.55***

4.9 Data from Measurement of Joint Surface In the Field

Measurement of joint surface in the field is carried out using close-range photogrammetry. The main objective of the field work is to assess the versatility and practicality of this method for measuring joint surface in field conditions.

The coordinates of the grid points marked on the measured joint surface in the field are listed in Appendix H. This data is accordingly analysed and formatted to obtain the 3D plot of the joint surface, using *Surfer*. The resulting plot shows a satisfactory presentation of the joint surface conditions particularly on features representing the peaks and troughs (see Figure 4.5(a) and (b)). However, the plot of joint surface contour in Figure 4.6, does give a satisfactory reflection of the surface as the surface is in an inclined position during image acquisition. This condition is probably due to the point of origin for the coordinate system of the object is being referred to the camera station on the left (left image is used as reference during processing of data using *Photo Modeler*). If required the measured surface of the object can be orientated using 3D transformation.

Figure 4.7 shows the typical shape of the five selected profiles (Profile A to Profile E) that clearly display the various peaks and troughs on the measured joint surface. Figure 4.8 shows the corresponding locations and distinctive features of the profiles plotted in Figure 4.7. Based on the plotted image, there are three major peaks (peak 1, 2, and 3) that can be readily recognised and these are clearly shown in the plotted profiles. Peak 1 occurs along the profile A and Peak 2 and 3 occur along the profile D. The surface characteristics can also be visualised in the orthographic projection produced using data acquired by close-range photogrammetry.

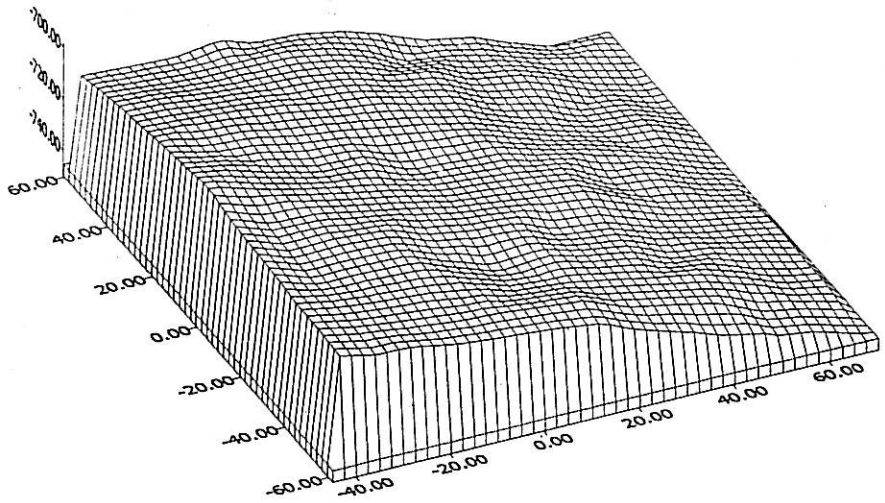

Figure 4.5(a): Orthographic projection of the joint surface based on field data obtained using photogrammetry (View A).

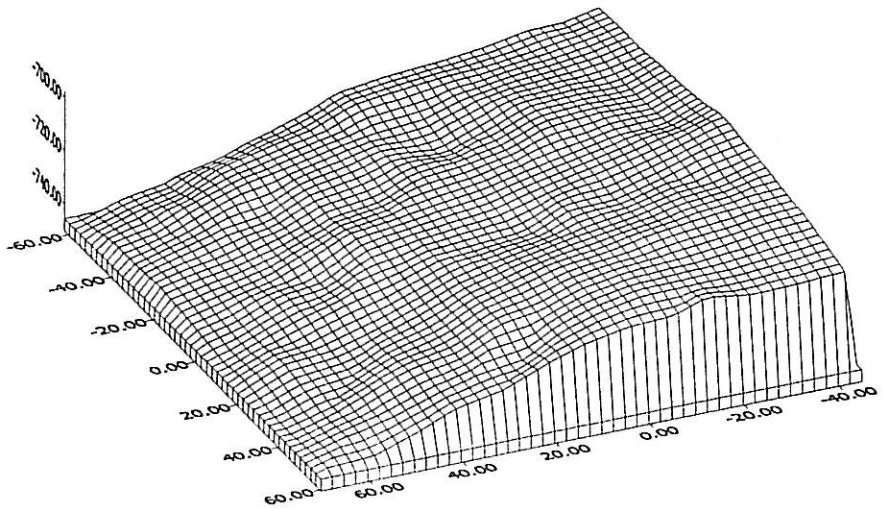

Figure 4.5(b): Orthographic projection of the joint surface based on field data obtained using photogrammetry (View B).

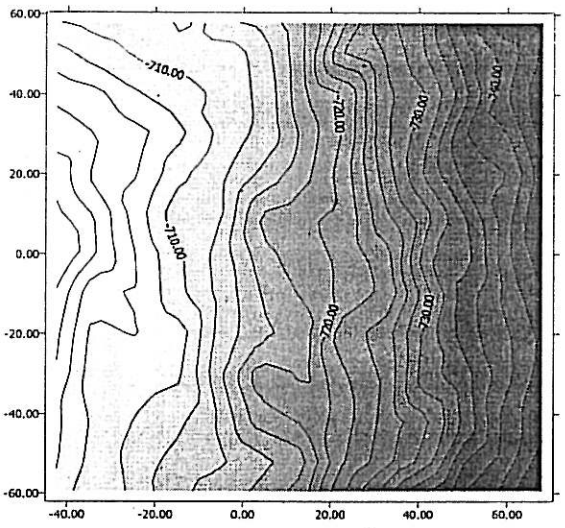

Figure 4.6: Plot of joint surface contour based on data obtained using photogrammetry.

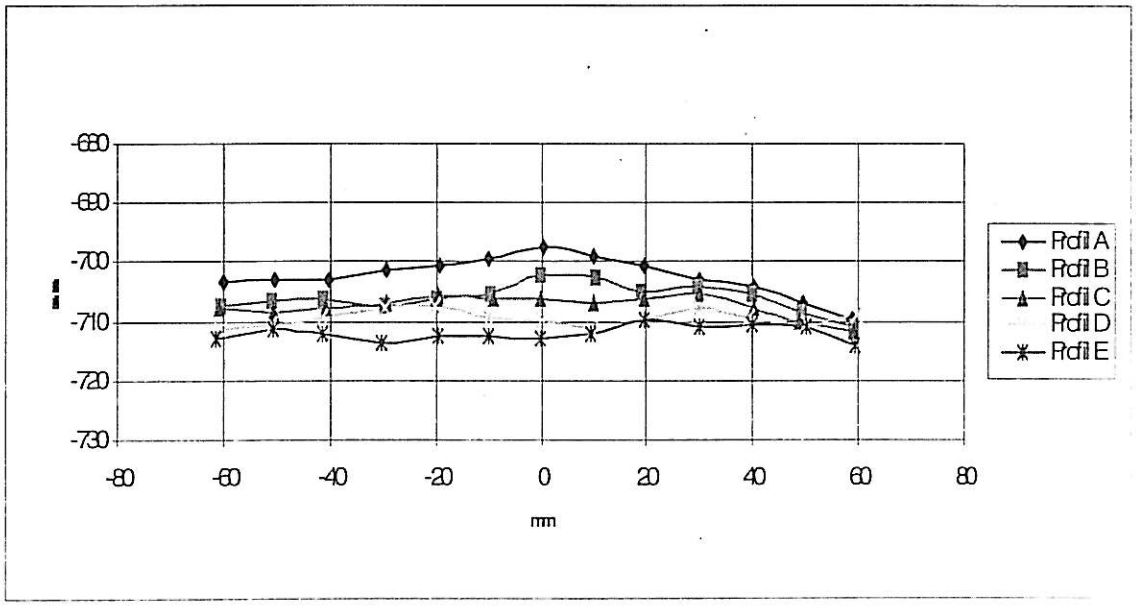

Figure 4.7: Selected profiles from the measurement of joint surface in the field.

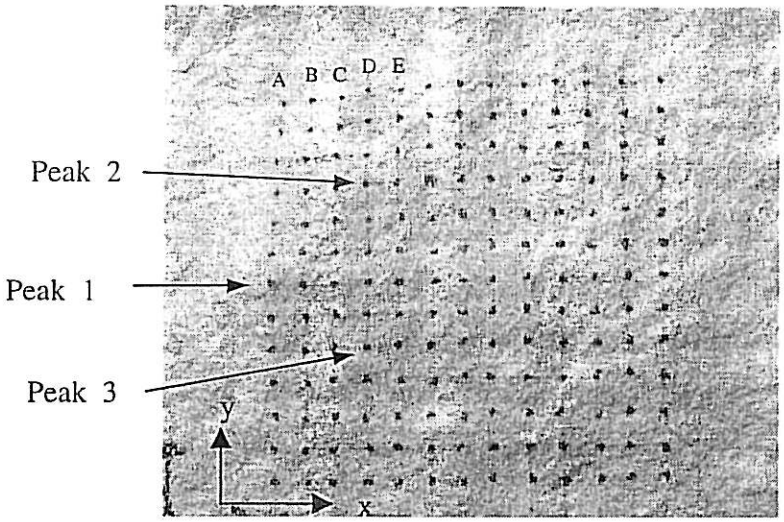

Figure 4.8: Locations and distinctive features of profiles A, B, C, D and E.

CHAPTER V

DISCUSSION AND CONCLUSION

5.1 Introduction

This study has shown that close-range photogrammetry exhibits positive characteristics as an alternative method for obtaining surface texture of joint surface. In this chapter, results of data analysis and the outcome of the study will be discussed and specifically, on the accuracy of measured data, advantages and applicability of close-range photogrammetry. Errors in data acquired and the probable sources of these errors will also be highlighted.

5.2 Accuracy of Data

From the comparison made on the contour of joint surface plotted using data obtained using both methods, contour for the photogrammetry method displays similar characteristics as that of the profiler. Similarity can be observed in detailed texture especially in the area where there are significant changes in contour height due to the occurrence of peaks and troughs.

3D plots and cross-sectional view along selected profiles of model joint also display strong similarities. Orthographic projection of joint surface, plotted using photogrammetry data, has highlighted the capability of this method in producing a more complete and detailed presentation of a surface. This comparison can be seen in Figure 4.3(c) and 4.3(d). Thus, it can be inferred that photogrammetry exhibits the ability to map a more complex joint surface and which could have been relatively difficult using profiler. Based on the laboratory work, some difficulties with the profiler have observed especially, when the peaks and troughs are relatively closed to each other. This type of surface texture will be difficult to profile particularly, when the width of the trough is

smaller than the diameter of the dial gauge plunger. It must be noted that this type of texture is common for joint surface in coarse-grained granite and it is known as *small-scale* roughness that contributes significantly to joint shear strength (see Section 2.1.2). Difficulty in measuring this type of texture may result in an imperfect presentation of the joint surface consequently, it affects the estimated values of *JRC* and angle *i*, which are the essential parameters for evaluating the shear strength of joint.

Some minor differences are observed between plots produced using both methods. Observation on the orthographic projections shows that these differences occur in the area with the highest peaks and the lowest troughs. The differences have been presented in numerical values in Section 4.4, and it is shown that the standard deviation for the photogrammetry method is 0.61 mm, with profiler data as reference. The standard deviation for each profile is presented in Figure 5.1, in the form of bar charts. The value of maximum standard deviation for all the profiles is 1.15 mm and this occurs in profile 19. This relatively high error can be attributed to the distortion of camera lens and will be discussed in Section 5.7.

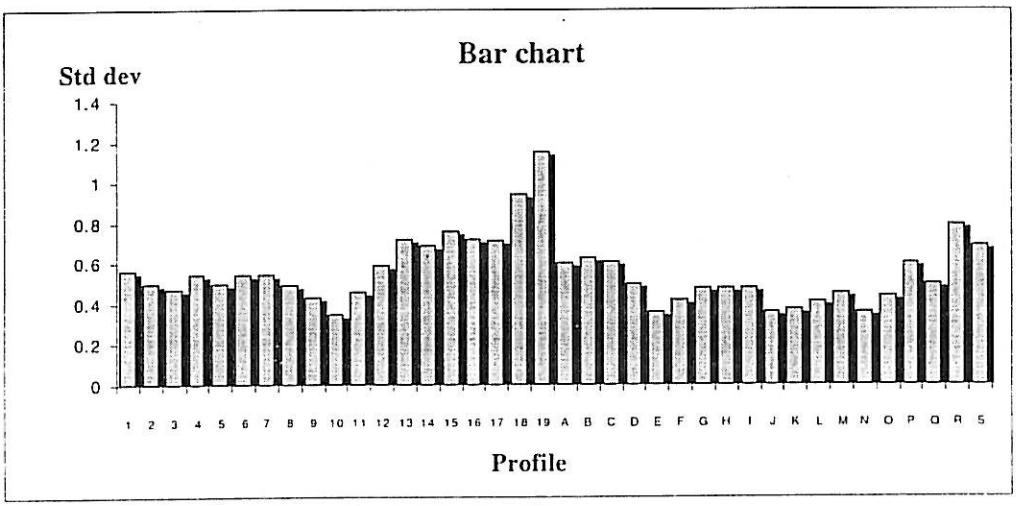

Figure 5.1: Bar chart for the standard deviation of profiles obtained using photogrammetry

For the roughness index, based on analysis (Table 4.4), it is found that the maximum difference in index *SD*, *k* and *CLA* occurs in those profiles listed in Table 5.1. It can be said that the errors mainly occur in those profiles located near the edge of the model joint block, i.e. profile 19 and profile A. Again it is thought that this error is due to the distortion of camera lenses.

Table 5.1: Value of maximum difference in roughness index

Roughness index	Maximum difference	Profile with maximum difference
SD	1.01	Profile 19
k	3.69	Profile 19
CLA	1.72	Profile A

Comparison on the area of contact surface, profiler method exhibits an area of 48.6% and photogrammetry exhibits an area of 49.5%, based on the total area of model joint. The difference of less than 1% between the methods shows that photogrammetry has the ability to produce a surface texture of similar quality as the profiler. A good estimation of the gross contact area between two interfacing rough joints is an important factor to be considered when conducting shear test on rock joint. This is due to the value of effective normal stress, acting on joint surface, is dependent of the actual contact between the rough joints. A fairly good estimate on the gross contact area can only be achieved if detailed texture of the joint surface and the approximate orientation of the shearing plane are known. The orientation of the shear plane is usually estimated using the normal/vertical displacement (δv) observed during shear test, which in return, is controlled by the degree of roughness of the joint being tested. It is therefore thought that the data of joint surface, which is obtained using photogrammetry, facilitates the process of estimating this contact area. Moreover, the use of digital image in photogrammetry method helps to expedite data processing and analysis. The digital data can also be used to present the joint surface in various types of plots and projections, which are essential for visual assessments.

In selecting specific method of measurement in engineering fields, would require information like nature of measurement, accuracy of data and versatility of equipments. Based on the nature of measurement and accuracy of data, photogrammetry seems to possess promising potentials for a number of applications in the field of engineering geology and rock mechanics. As discussed earlier, this method is suitable for detailed and accurate mapping of a joint surface and thus, enables good estimation of several parameters that are related to joint shear strength. Standard deviation of 0.61 mm, observed during comparison of all the measured profiles, is relatively small compared to the actual shape of irregularities on the measured model joint. It is thought that a better result would have been obtained if calibrations on lens distortion were carried out. This calibration is particularly important if the acquired profiles are to be used for estimating values of *JRC* and angle *i*. In other words, the degree of accuracy of photogrammetry method can be adjusted accordingly to suit specific application.

Method of joint surface measurement using profiler requires the profiling work along a given section to be undertaken repetitively to obtain data of high accuracy. For example, the height of grid point A5 in Appendix E, ranging between 31.66 mm and 31.94 mm for 10 measurements. The mean value for the 10 measurements is 31.79 mm. This implies that profiler produces varying heights although the measurement is taken at the same grid point. In addition, an accurate presentation of joint surface will only be possible if the number of measured profiles is larger in number. It is also noted that profiler, which consists of various mechanical components, is subjected to wear and tear and prone to human error. Repetitive measuring procedure can be difficult and time consuming and may not be effective under field conditions.

5.3 Time Required for Measurement and Data Processing

The time required in producing the required result is an important factor to be considered in selecting the appropriate method of measurement. In general, measurement work that involved acquiring and processing of large amount of data can be expedite with the help of computer and automated measuring device.

Based on the laboratory work conducted, measurement using profiler requires an about a week to obtain 10 sets of reading for a total number of 361 grid points. Processing and analysis of each set of data takes about 2 days to produce the respective profile and this is mainly due to the length of time required to key in the data into the computer.

For the close-range photogrammetry, image acquisition process and inclusive of equipments setting-up, requires less than 30 minutes. About 2 to 3 hours is required for data processing that involves down-loading of digital image into computer and the associated processes to produce object coordinates. However, this time duration does not include all the relevant preliminary work for photogrmmetry such as calibration of camera sensor and other procedures as discussed in Section 3.4.1. It must be noted that all the related preliminary work is done once only for the selected equipments and hard-wares. Time required for data processing depends on the type of computer softwares used. Most of the softwares used in this study are those commonly used in civil engineering field.

In the field, measurement of joint surface using close-range photogrammetry requires similar time duration as that in the laboratory. However, based on experience, it can be said that measurement in the field using profiler will definitely takes a longer time. This is mainly due to additional time required to set the profiler on unfavourable joint location and field conditions that may effect work progress.

Another advantages of photogrammetry method is the time required for measuring work is independent of the condition of joint surface, the number grid points and the area to be measured. This may not be the situation for profiler method. For example, an accurate presentation of a complex joint surface would require a significant number of profiles to be measured and thus, may takes a longer time. However, for photogrammetry, if joint exhibits suitable surface texture (i.e. significant contrast in colour between mineral grains) measurement process mainly involving image acquisition of the joint using pre-

calibrated digital camera. The process can be repeated on other joints in the study area and data (digital image) can be stored and processed at later stage in laboratory.

5.4 Equipment and Software for Photogrammetry

In general, the equipments required for image acquisition in surface texture measurement are similar to those used in the field of photogrammetry in topographic mapping. They are essentially a normal or digital camera and other related accessories. A compatible computer and related photogrammetry softwares are required for data processing and analysis. Most of the softwares are those commonly used in civil engineering field such as *Matrox Inspector*, *Surfer*, *CivilCad* and others.

A situation may arise when joint is located in an unfavourable condition so that marking of the grid points is difficult to undertake. In this case, a suitable slide-projector of sufficient light intensity, may be used to project grid points directly onto the joint surafce. However, if joint is within reach, grid points can be marked manually using suitable marker, so that these points can be easily recognised in the produced image.

5.5 Applicability of Photogrammetry

Factors such as measurement time, data processing, handling of equipments and accuracy of data for detailed mapping of joint surface, are among the advantages of photogrammetry method compared to profiler.

Ability to perform a non-contact measurement of joint surface, with minimal human and instrument interactions, helps to reduce error in the acquired data to a minimal level. In the case of profiler, equipment needs to be in direct contact with joint surface for measurement to be made thus may not be practical for certain orientation and location of joint in the field. However, these problems do not affect the performance of photogrammetry method, significantly.

For photogrammetry, provided the related equipments have been calibrated, and the texture of joint surface is able to produce the required image, then work in the field would only consist of image acquisition.

5.6 Application of Photogrammetry Method in Rock Engineering Field

Based on the nature of measurement undertaken in this study, besides mapping of joint surface, close-range photogrammetry may be used for similar applications that involve measurement of rock surface. Using the same concept adopted in this study, the proposed method can be tailored to suit specific measurement work on rock surface in a small, medium or large scale. Specifically, the method can be adopted to measure large-scale roughness or undulations on joint.

Application of photogrammetry in monitoring slope stability have also been highlighted by industries however, the method may need further refinements. It is thought that the concept can be refined to monitor small movements in unstable rock blocks (e.g. unstability due to wedge failure) exposed on cut slopes. In this case, the unstable blocks to be monitored can be marked using suitable target points (similar to the grid points used in this study). Provided that the block is a solid mass, any small movements of the block can be continuously or periodically monitored using close-range photogrammetry. The output data of this monitoring system can be linked to another system which may be use to trigger a suitable signal or alarm when the movement of the unstable block is deemed critical.

Another potential application of close-range photogrammetry is in quarry operation, where measurement of rock volume on quarry faces and stockpiles are important for production estimation. By marking suitable targets on the surface of rock mass (quarry face and stockpiles), its volume can be estimated using photogrammetry. However, this measurement depends on the locations, shape and size of the rock mass. Stockpiles in the form of small aggregates and relatively large quarry face may not be suitable.

5.7 Error in Photogrammetry Method

The associated errors in Photogrammetry have been highlighted in Section 4.4.1. Based on analysis of data, a number of factors have been identified as sources and origins for these errors.

In general, the main factor that determines the degree of accuracy of photogrammetry is the quality of camera used in image acquisition. In this aspect, camera lens is the important component that influences data accuracy.

From the bar charts on the standard deviations (Figure 5.1), it can be seen that the distribution is curve-shaped and the values of standard deviation are smaller for profiles located in the centre portion of the model surface (profile 9, 10, 11, J, K and L). For profiles located closer to the edges of the model surface (1, 19, A and R) exhibit a higher values of standard deviation. This phenomenon is most likely due to the distortion of camera lens.

Distortion in camera lens will result in shape of an image to be slightly different than the actual shape of the object. This means that lens distortion can have a certain effect on the coordinates of photo image and consequently, it affects the image coordinates. Majority of optical systems suffer setback from lens distortion. Use of high quality lenses may reduce this problem to a certain degree. The amount of error in image, due to lens distortion, also depends on focal length of camera. When a camera is set at minimum focal length (for DC 240 it is 6 mm), the amount of lens distortion will be at its maximum. It is for this particular reason that, in this study, the camera was set at maximum focal length (for DC 240 it is 18 mm) during image acquisition, so that the error due lens distortion is at minimum level. Calibration of camera lens is another alternative for reducing this type of error.

The second factor that may have contributed to error in photogrammetry method is camera resolution. Camera resolution can be divided into two main components: i.e. lens

resolution and camera sensor (CCD) resolution. A camera lens with higher resolution will give a clearer image. A bigger camera aperture, a larger number of pixels (e.g. 4 Mega pixels) and a finer pixel size, all contribute to producing an image of higher resolution. Based on aperture size and number of pixel, the digital camera used in this study can be categorised as medium resolution camera.

Besides that, initial data for photogrammetry method and computer softwares and programs used in the study may have affected, to a certain extent, the accuracy data. The coordinates for the target plate, which are measured using theodolite, do exhibit some error of their own (see Appendix A). This may affect the value of elements used in processing the camera relative orientation using *GAP* software. In this study, the pixel size is determined approximately and its accuracy has been affected by the unstable camera focal length for DC 240 is fixed with zoom type lens. This type of lens is less stable compared to lens with fixed focal length.

Data from profiler, which is not free of error, has been used as datum when verifying the accuracy of data obtained using photogrammetry. Close examination of data shows that each set of data produced using profiler does contain errors. Consequently, a procedure for data rejection has been undertaken mainly to discard unrepresentative data. The reason for using data from profiler as datum is mainly due to it is the most commonly used method in measuring joint surface.

5.8 Conclusion

The outcome of this study strongly indicates that close-range photogrammetry exhibits the appropriate capabilities and characteristics as an alternative tool for measuring texture of joint surface. Using some basic equipment like digital camera and computer, this method is capable of producing accurate image of joint surface in the form of plots and projections. The image, which is in the form of digital data, can be analysed accordingly for the purpose of estimating the value of various parameters that are related to the roughness and strength of joint.

In terms of accuracy, data for the 38 profiles, obtained using photogrammetry exhibits standard deviation of 0.61 mm when compared with data obtained using profiler. This is quite satisfactory for the purpose of verifying the applicability of this method as an alternative method for joint surface measurment.

When measured data is used to determine value of *JRC*, which requires data of high accuracy, the accuracy of data acquired using photogrammetry can be improved further using specific procedures and equipment. In this case, the use of large format camera with high quality lenses and sensor resolution is strongly recommended. In other words, the type of camera used in photgrammetry depends on the purpose of measurement and the degree of accuracy of data to be acquired. Or alternatively, the process for lens calibration can be carried out if accuracy is very critical.

This study has also demonstrated the capabilities of close-range photogrammetry for measuring joint surface in the field. It is superior to conventional profiler in terms of measuring process, versatility of equipment, amount and reliability of data. The related equipment and procedures are relatively easy to handle and with minimal human and environmental interactions. Thus, measurement work in the field can be carried out at a much shorter time. These aspects are essential where working area and joint locations in the field may not be in favourable conditions.

Data obtained using photogrammetry method consists of 3D image of an object in digital format. Data of this nature can be readily formatted to suit complex and tedious analysis using computer software. For instance it has been shown using photogrammetry data and suitable computer software, different plots of joint surface have been produced. These plots may be in the form of normal 2D cross-section and complex 3D orthographic projection. The 2D plot in particular, can be done along any specified section of the joint surface, and this helps in detailed assessment of the joint profile (e.g. roughness, *JRC* and angle *i*). The 3D plot on the other hand, facilitates in detailed evaluation on the texture of

the whole joint surface. Perhaps, this is useful in predicting the probable direction of shear on the joint surface.

Finally, it is concluded that close-range photogrammetry is suitable for measuring and mapping the texture of joint surface in rock. At this stage its application is mainly for measuring joint surface that exhibits small-scale roughness (asperities). Its concept can also be extended for other applications specifically, in those work related to measuring of rock surface, volume and movement.

References

Abdul Hamid Mohd Tahir (1990), *Asas Fotogrametri*, Universiti Teknologi Malaysia, Skudai, Johor, 118p.

Archambault, G., Flamand, R., Gentier, S., Riss, J. and Sirieix, C. (1996), Rock Joint Shear Mechanical Behavior with 3D Surfaces Morphology and Degradation During Shear Displacement, *Eurock'96*, Barla (ed.), Rotterdam. Balkema, p247-254.

Aydan, O. and Kawamoto, T. (1990), Discontinuities and Their Effect on Rock Mass, *Rock Joints*, Rotterdam, Balkema, p149-156.

Bandis, S.C. (1993), Engineering Properties and Characterisation of Rock Discontinuities, *Comprehensive Rock Engineering, Priciples, Practice and Projects.* Hudson *et al.* (eds.), Vol.1, Pergamon Press, p155-183.

Barton, N. (1976), The Shear Strength of Rock and Rock Joints, *International Journal of Rock Mechanics and Mining Sciences and Geomechanical Abstract,* No. 13, p79-255.

Barton, N. and Choubey, V. (1977), The Shear Strength of Rock Joints in Theory and Practice, *Rock Mechanics*, Vol.10, p1-54.

Barton, N. (1978), Suggested Methods for the Quantitative Description of Discontinuities in Rock Mass, International Society of Rock Mechanics Commission on Standardization of Laboratory and Field Test, *International Journal of Rock Mechanics and Mining Sciences and Geomechanical Abstracts*, No. 15, p68-319.

Barton, N and Bandis, S.C. (1982), Effect of Block Size on the Shear Behaviour of Jointed Rock, *Proc. of 23rd U.S. Symposium on Rock Mechanics*, Berkeley, California, p739-760.

Beavis, F.C. (1992), *Geologi Kejuruteraan*, Ibrahim Komoo dan Tajul Anuar Jamaluddin (Penterjemah), Dewan Bahasa dan Pustaka, Kuala Lumpur, p253.

Bell, F.G. (1992), *Engineering Geology*, London, Blackwell Scientific Publisher, 359p.

Brady B.H.G. and Brown E.T., (1985), *Rock Mechanics for Underground Mining*, 1st edition, George Allen & Unwin, London, 527p.

Carr, J.R. (1989), Fractal Characterization of Joint Surface Roughness in Welded Tuff at Yucca Mountain, Nevada, *Proceedings of 30th U.S. Symposium on Rock* Mechanics, Morgantown.

Chernychev, S.N. & Dearman, W.R. (1991), *Rock Fracture*, 1st. ed. ISBN 0-7505-1017-4, Butterworth-Heinemann Ltd., London, pp. 63p.

Cooper, M.A.R. and Robson, S. (1996), Theory of Close Range Photogrammetry, *Close Range Photogrammtery and Machine Vision*, Atkinson (ed.), Scotland, UK, Whittles Publishing, p9-51.

Cunha, A.P. and Muralha, J. (1990), About the Mechanical Behaviour of Joint Surfaces of Rock Masses, *Geotecnia*. **58**. p43-63.

Dowman, I.J. and Scott, P.J. (1980), Photogrammetric Theory, Techniques and Problems, *Development in Close Range Photogrammetry-1*. Atkinson (ed.), London, Applied Science Publishers, p15-37.

Dowman, I.J. (1996), Fundamentals of Digital Photogrammetry, *Close Range Photogrammtery and Machine Vision*, Atkinson (ed.), Scotland, UK, Whittles Publishing, p52-77.

Fecker, E. and Rengers, N. (1971), Measurement of Large Scale Roughness of Rock Planes by means of Profilograph and Geological Compass, *Proceedings on Symposium on Rock Fracture*, Nancy, France, p1-18.

Franklin, J.A. and Dusseault, M.B. (1989), *Rock Engineering*, New York, McGraw-Hill, 246p.

Goodman, R.E., Heuze, F.E. and Onishi, Y. (1972), Research on Strength-Deformability-Water Pressure Relationships for Faults in Direct Shear, *Final Report Contract ARPA No. H0210020*, US Bureau of Mines.

Goodman, R.E. and Richard, E. (1980), *Introduction to Rock Mechanics*, New York, John Wiley & sons, p335.

Hencher, S.R. and Richards, L.R. (1989), Laboratory Direct Shear Testing of Rock Discontinuities, *Ground Engineering*, p24-30.

ISRM, (1981), *Rock Characterisation Testing and Monitoring, ISRM Suggested Methods*, Inst. of Mining & Metallurgy, (Brown E.T. ed.), Pergamon Press, p. 211.

Kraus, K. (1993), Photogrammtery: Fundamentals and Standard Processes, Vol.1. Bonn, Dummler, 397p.

Lama, R.D. and Vutukuri, V.S. (1978), *Handbook on Mechanical Properties of Rock, Testing Techiques and Results*, Vol. 4, Clausthal, Trans Tech Publication, 515p.

Lamas, L.N. (1996), An Experimental and Analytical Study of the Roughness of Granite Joints, *Eurock '96*, Barla (ed.), Rotterdam, Balkema, p117-126.

Mohd For Mohd Amin, Teo, King Beng and Mushairry Mustaffar (2000), Preliminary Design Parameters Based on Laboratory Shear Test of Core Samples, *Proceedins on*

Annual Geological Conference 2000, Geological Society of Malaysia, G.H. Teh, Joy J. Pereira & T.F. Ng (eds.), Kuala Lumpur, p293-298.

Mohd For Mohd Amin, Teo, King Beng and Mushairry Mustaffar (2001), Joint Surface Measurement Using Close-range Photogrammetry, *Proceedings on 3rd Symposium on Engineering Geology and the Environment*, Edi Prasetyo, Herryal and Dodid (eds.), Yogyakarta, p294-301.

Muralha, J. (1991), Applications on Fractal Theory in Geotechnics." *Geotecnia. 63*, p43-74.

Mushairry Mustaffar (1997), A Refinement to Automated Photogrammetry." *Australian Surveyor*, Vol. 42. No.4, p166-171.

Mushairry Mustaffar (1999), Automated Surface Measurements Using Close Range Digital Photogrammetry, *Seminar Kejuruteraan Awam, 29-30 May*, Melaka.

Piggott, A.R. & Elsworth, D. (1995), A Comparison of Methods of Characterising Surface Roughness, *Fractured and Jointed Rock Masses*, Myer, Cook, Goodman & Tsang (Eds), Rotterdam, Balkema, p471-476.

Patton, F.D. (1966), *Multiple Mode of Shear Failure in Rock and Related Materials*, Ph D. Thesis, University of Illinios, 282p.

Power, M.C. and Hencher, S.R. (1996), A New Experimental Method for The Study of Real Area of Contact Between Joint Walls During Shear, *Rock Mechanics*, Aubertin, Hassani & Mitri (Eds), Balkema, Rotterdam, p1217-1221.

Richards, L.R. and Cowland, J.W. (1982), The Effect of Surface Roughness on the Field Shear Strength of Sheeting Joints in Hong Kong Granite, *Hong Kong Engineer*, Vol.10 Part 10, p39-43.

Teo King Beng (2002), *Pengukuran Tekstur Permukaan Kekar Batuan – Perbandingan Kaedah Fotogrametri Jarak Dekat dan Kaedah Konvesional*, Tesis Sarjana Kejuruteraan (Awam), Universiti Teknologi Malaysia, Skudai, Johor.

Tze, R. & Cruden, D.M. (1979), Estimating Joint Roughness Coefficient, *International Journal of Rock Mechanics & Geomechanics Abstracts*, Vol.16, Britain, Pergamon Press, p303-307.

Wolf, P.R. (1974), *Element of Photogrammetry*, New York, McGraw-Hill, 562p.

Wolf, P.R. (1983), *Elements of Photogrammetry*, 2nd edition, McGraw-Hill, 628p.

APPENDIX A: Coordinates of points on target plate

(semua nilai adalah dalam unit mm)

TARGET	X (dX)	Y (dY)	Z (dZ)
1	101.519	104.9398	9.8655
error	0	0	0
2	101.5861	104.9594	9.8634
error	0	0	-0.0001
3	101.656	104.9623	9.8637
error	0	0	0
4	101.7239	104.9876	9.8614
error	0	0	-0.0002
5	101.7958	104.9834	9.8649
error	0	0	-0.0002
6	101.8659	104.9907	9.8662
error	0	0	0
7	101.5169	104.9473	9.7935
error	0	0	0.0001
8	101.5875	104.938	9.7969
error	0	0	-0.0001
9	101.6521	104.9662	9.7943
error	0	0	0.0001
10	101.7276	104.9545	9.796
error	0	0	0.0002
11	101.7937	104.9866	9.7925
error	0	0	0.0002
12	101.8641	104.9917	9.7932
error	0	0	0.0002
13	101.5204	104.9193	9.728
error	0	0	0.0009
14	101.5892	104.9232	9.7304
error	0	0	0.0002
15	101.6561	104.9558	9.725
error	0	0	0.0003
16	101.7722	105.0839	9.7209
error	0	0.0001	0.0028
17	101.7995	104.9586	9.7257
error	0	0	0.0005
18	101.8681	104.9696	9.7271
error	0	0	0.0004
19	101.5214	104.9079	9.6603
error	0	0	0.0002
20	101.5916	104.9136	9.6598
error	0	0	0.0004
21	101.659	104.9418	9.6572
error	0	0	0.0004

TARGET	X (dX)	Y (dY)	Z (dZ)
22	101.7279	104.935	9.6606
error	0	0	-0.0001
23	101.7994	104.9522	9.6582
error	0	0	0.0001
24	101.8681	104.9656	9.6585
error	0	0	0.0002
25	101.5204	104.918	9.5851
error	0	0	0
26	101.5936	104.9006	9.5907
error	0	0	0.0002
27	101.6599	104.9324	9.5869
error	0	0	0
28	101.7317	104.925	9.5905
error	0	0	0.0001
29	101.7992	104.9486	9.5889
error	0	0	0
30	101.8699	104.9535	9.588
error	0	0	-0.0005
31	101.5262	104.8783	9.5206
error	0	0	0.0003
32	101.5933	104.8979	9.5188
error	0	0	0
33	101.6647	104.901	9.5204
error	0	0	0
34	101.7312	104.9223	9.5198
error	0	0	0.0001
35	101.8014	104.9304	9.5199
error	0	0	0.0003
36	101.8733	104.9289	9.5211
	0	0	0.0004

APPENDIX B: Specifications for Digital Camera Kodak DC 240

Model	: Kodak Digital Zoom DC 240
CCD resolution	: 1344 x 971 pixel
Image resolution	: 1280 x 960 pixel (high resolution), 640 x 480 pixel (normal resolution)
Storage	: 2 MB
Lens	: 6X auto focus zoom 3X optical zoom, 2X digital zoom
Digital Zoom	: 2X
Lens focal length	: 6 - 18 mm 39 – 117 mm equivalent to 35 mm camera format
Focus range	: 0.5 m – infinity, macro 0.25 – 0.5 m
Shutter speed	: ½ - 1/755 sec
Aperture range	: Wide: f/2.8 – f/16; Tele: f/4.5 – f/25.7
Equivalent ISO	: 140
Colour	: 24-bit.
Flash	: Effective area: Wide : 0.5 – 4 m Tele : 0.5 – 2.5 m
View finder	:Optical zoom (real image)
Power	: 4 AA size battery @ 6v equivalent
Tripod socket size	: ¼ inch
Weight	: 328g without battery
Dimension	: 133 x 51 x 76 mm

APPENDIX C: Coordinates for images obtained using Matrox Inspector

	Koordinat Imej Kiri		Koordinat Imej Kanan	
Label	Centroid X	Centroid Y	Centroid X	Centroid Y
2	-0.733	1.652	1.175	1.467
3	-0.5851	1.637	1.031	1.45
4	-0.4448	1.623	0.8827	1.434
5	-0.2965	1.612	0.7404	1.419
6	-0.1605	1.603	0.6021	1.404
7	-0.02126	1.593	0.4605	1.392
8	0.1201	1.57	0.3139	1.383
9	0.2366	1.554	0.1781	1.373
10	0.3582	1.538	0.0353	1.362
11	0.4822	1.516	-0.092	1.344
12	0.5963	1.504	-0.2248	1.333
13	-0.7296	1.494	-0.3555	1.319
14	0.7044	1.491	-0.4907	1.31
15	-0.5843	1.48	1.179	1.307
16	0.8163	1.468	-0.6056	1.3
17	-0.4368	1.465	1.033	1.287
18	-0.2937	1.455	-0.7089	1.28
19	0.9253	1.446	0.887	1.274
20	-0.1618	1.438	-0.8197	1.254
21	-0.02213	1.43	0.7494	1.252
22	1.029	1.426	-0.9264	1.242
23	0.1207	1.419	0.6076	1.239
24	1.132	1.419	0.463	1.23
25	0.2472	1.41	-1.035	1.224
26	1.241	1.403	0.3164	1.226
27	1.348	1.39	0.1859	1.213
28	0.3606	1.383	-1.153	1.208
29	1.45	1.379	0.04028	1.209
30	0.4817	1.365	-0.09319	1.195
31	0.5991	1.354	-0.2178	1.18
32	0.7146	1.335	-0.357	1.177
33	-0.7117	1.327	-0.4873	1.165
34	-0.5684	1.325	-0.6094	1.146
35	0.8247	1.321	1.19	1.141
36	-0.4212	1.303	-0.7135	1.126
37	0.9218	1.298	1.041	1.127
38	-0.2878	1.293	-0.8279	1.113
39	-0.1519	1.28	0.8925	1.114
40	1.026	1.282	-0.9427	1.099
41	-0.01483	1.27	0.7523	1.099
42	1.133	1.268	0.6101	1.092

Label	Centroid X	Centroid Y	Centroid X	Centroid Y
43	1.24	1.263	-1.044	1.087
44	0.1266	1.256	0.4547	1.09
45	1.349	1.254	-1.159	1.074
46	0.2574	1.247	0.3168	1.07
47	1.45	1.243	0.187	1.064
48	0.3647	1.226	0.03966	1.053
50	0.4804	1.213	-0.09308	1.04
51	0.5977	1.199	-0.2238	1.028
52	0.7123	1.192	-0.37	1.026
53	0.8295	1.176	-0.4839	1.012
54	0.9307	1.17	-0.6067	0.9912
55	-0.7059	1.165	-0.7202	0.9878
56	-0.5678	1.156	1.191	0.9797
57	1.028	1.151	-0.8327	0.967
58	-0.4179	1.14	1.036	0.9661
59	1.133	1.131	-0.9561	0.9588
60	-0.2835	1.131	0.8962	0.9531
61	-0.1482	1.124	-1.078	0.9522
62	1.239	1.122	0.7551	0.945
63	-0.009504	1.118	0.6077	0.938
64	0.1284	1.103	-1.178	0.9338
65	1.344	1.112	0.4603	0.9295
66	1.453	1.103	0.3177	0.9206
67	0.2513	1.097	0.1827	0.9109
68	0.3739	1.083	0.04632	0.9054
69	0.4809	1.07	-0.09352	0.8902
70	0.5938	1.057	-0.2397	0.8884
71	0.7131	1.041	-0.3651	0.8764
72	0.827	1.032	-0.4871	0.8658
73	0.9319	1.02	-0.6101	0.853
74	1.029	1.005	-0.7284	0.8428
75	-0.7093	0.9926	-0.8447	0.825
76	1.143	0.9918	-0.9627	0.8189
77	-0.5633	0.987	1.19	0.8108
78	1.241	0.9828	-1.075	0.8116
79	-0.4207	0.9788	1.046	0.8034
80	1.348	0.9749	-1.178	0.7985
81	-0.2855	0.9665	0.8945	0.7898
82	1.451	0.965	0.7558	0.7851
83	-0.1419	0.9583	0.6024	0.7735
84	-0.007092	0.9495	0.4626	0.7707
85	0.1324	0.9409	0.3186	0.761
86	0.2487	0.9312	0.185	0.753
87	0.3856	0.9235	0.05169	0.7398
88	0.4864	0.9044	-0.09057	0.7368
89	0.5841	0.8964	-0.2242	0.7305
90	0.7049	0.8936	-0.3629	0.7208

Label	Centroid X	Centroid Y	Centroid X	Centroid Y
91	0.822	0.8783	-0.487	0.7122
92	0.9334	0.8691	-0.6135	0.7004
93	1.038	0.8607	-0.7345	0.6907
94	1.146	0.8524	-0.8452	0.6814
95	1.237	0.8408	-0.9614	0.6734
96	-0.7075	0.8302	-1.081	0.6634
97	1.345	0.8307	-1.178	0.6529
98	-0.5586	0.8158	1.048	0.6367
99	1.446	0.8221	1.19	0.6395
100	-0.4243	0.8119	0.8954	0.6341
101	-0.2838	0.7996	0.7522	0.6208
102	-0.1436	0.7984	0.6076	0.6204
103	-0.003026	0.7892	0.3219	0.6051
104	0.1265	0.7813	0.4594	0.6041
105	0.2514	0.7739	0.1912	0.5964
106	0.3813	0.7641	0.04636	0.5952
107	0.4878	0.7516	-0.228	0.5788
108	0.5962	0.7492	-0.0942	0.5763
109	0.7063	0.7392	-0.3633	0.5671
110	0.8252	0.7329	-0.4861	0.5609
111	0.9302	0.7205	-0.612	0.551
112	1.032	0.7133	-0.7354	0.5468
113	1.142	0.7042	-0.8446	0.5327
114	1.238	0.6994	-0.9626	0.5321
115	1.34	0.6942	-1.076	0.521
116	1.443	0.682	-1.179	0.5132
117	-0.7063	0.6555	1.199	0.477
118	-0.5662	0.6492	0.8964	0.4657
119	-0.4237	0.6387	1.052	0.4657
120	-0.2886	0.6346	0.7608	0.4572
121	-0.1414	0.6323	0.324	0.4456
122	-0.009129	0.6227	0.462	0.4462
123	0.1206	0.6229	0.6116	0.4463
124	0.2435	0.6137	0.187	0.4384
125	0.3764	0.6081	-0.09062	0.431
126	0.4932	0.6059	0.04918	0.4203
127	0.7154	0.5886	-0.22	0.4208
128	0.5967	0.5893	-0.3529	0.4172
129	0.8262	0.581	-0.4798	0.4103
130	0.9355	0.5708	-0.6048	0.4005
131	1.034	0.5628	-0.7326	0.3928
132	1.143	0.5607	-0.8422	0.3811
133	1.248	0.556	-0.9572	0.3756
134	1.349	0.5444	-1.18	0.368
135	1.449	0.5403	-1.077	0.3693
136	-0.7115	0.4905	1.039	0.3195
137	-0.5681	0.4837	1.187	0.3218
138	-0.4264	0.4799	0.8958	0.3093

Label	Centroid X	Centroid Y	Centroid X	Centroid Y
139	-0.2848	0.4746	0.759	0.3008
140	-0.1522	0.4744	0.609	0.2938
141	-0.01446	0.4665	0.323	0.2853
142	0.1208	0.4629	0.4659	0.2853
143	0.2366	0.4581	0.1869	0.2768
144	0.3697	0.4518	-0.08479	0.273
145	0.4892	0.4517	-0.2166	0.2674
146	0.5979	0.4391	0.04616	0.267
147	0.7103	0.4317	-0.4738	0.2565
148	0.8279	0.4339	-0.346	0.259
149	0.9328	0.4259	-0.6006	0.2503
150	1.04	0.4204	-0.722	0.2426
151	1.145	0.4237	-0.8393	0.2398
152	1.248	0.4205	-0.9559	0.2363
153	1.371	0.4205	-1.069	0.2266
154	1.48	0.4124	-1.181	0.2243
155	-0.7072	0.3198	1.184	0.161
156	-0.5682	0.3112	1.033	0.1594
157	-0.4229	0.3121	0.7493	0.1363
158	-0.2867	0.3067	0.9002	0.1381
159	-0.1548	0.3079	0.1877	0.1262
160	-0.02132	0.3072	0.3196	0.1286
161	0.1128	0.3015	0.6059	0.1273
162	0.2346	0.2995	0.04706	0.1288
163	0.3632	0.3024	0.462	0.1249
164	0.49	0.3009	-0.08507	0.1169
165	0.6032	0.2947	-0.2147	0.1131
166	0.7173	0.2903	-0.3418	0.1073
167	0.8273	0.2829	-0.5931	0.09795
168	1.383	0.277	-0.4664	0.1011
169	0.9391	0.2792	-0.7199	0.09456
170	1.054	0.2758	-0.9507	0.08916
171	1.155	0.2774	-0.8343	0.08917
172	1.486	0.276	-1.064	0.08147
173	1.251	0.2678	-1.178	0.08067
174	-0.7126	0.1539	1.047	-0.01054
175	-0.5683	0.148	1.186	-0.01014
176	-0.4284	0.1504	0.6021	-0.01927
177	-0.1547	0.1485	0.7455	-0.01909
178	-0.288	0.1449	0.8969	-0.02148
179	-0.01831	0.1424	0.3178	-0.02613
180	0.1132	0.1447	0.455	-0.0223
181	0.3636	0.1449	0.05121	-0.03495
182	0.4833	0.1401	0.1867	-0.03303
183	0.2299	0.141	-0.08054	-0.04357
184	0.5958	0.1395	-0.3389	-0.04399
185	0.8378	0.1409	-0.2141	-0.04639
186	0.7205	0.1376	-0.5878	-0.05072

Label	Centroid X	Centroid Y	Centroid X	Centroid Y
187	0.9485	0.1386	-0.4629	-0.05001
188	1.064	0.1371	-0.7069	-0.05175
189	1.38	0.1352	-0.9423	-0.05539
190	1.173	0.1336	-0.8343	-0.05472
191	1.259	0.1304	-1.058	-0.06028
192	1.48	0.1334	-1.173	-0.0632
193	1.384	-0.008166	1.039	-0.1835
194	0.8377	-0.01318	1.192	-0.1799
195	1.066	-0.008426	0.6005	-0.1883
196	1.286	-0.01513	0.7463	-0.189
197	1.474	-0.01353	0.8894	-0.1939
198	-0.0223	-0.01886	0.3218	-0.1953
199	0.1105	-0.01339	0.4588	-0.1914
200	0.2348	-0.02055	-0.3343	-0.1986
201	0.3605	-0.01892	-0.2066	-0.1971
202	0.4765	-0.01525	0.05182	-0.197
203	0.5939	-0.01825	-0.5879	-0.1999
204	0.9549	-0.01355	-0.4597	-0.2006
205	1.178	-0.0146	-0.08056	-0.2
206	-0.7025	-0.02225	0.1913	-0.201
207	-0.5679	-0.01717	-0.945	-0.2037
208	-0.4308	-0.02196	-0.7163	-0.2067
209	-0.1515	-0.02385	-1.179	-0.203
210	0.719	-0.02049	-1.058	-0.208
211	-0.2919	-0.02203	-0.828	-0.2114
212	1.279	-0.1526	-0.8388	-0.3493
213	1.381	-0.1525	-0.7233	-0.3459
214	1.472	-0.1508	-0.5822	-0.3525
215	0.9533	-0.155	-0.4581	-0.348
216	1.062	-0.1551	-0.3332	-0.3483
217	1.173	-0.1577	-0.2043	-0.3466
218	0.5931	-0.1619	-0.07831	-0.3475
219	0.7198	-0.1627	0.05226	-0.3469
220	0.8417	-0.1607	0.1894	-0.348
221	0.3507	-0.1692	0.3226	-0.3477
222	0.4748	-0.1735	0.4545	-0.3463
223	-0.01954	-0.1766	0.6005	-0.3472
224	0.1121	-0.173	0.7516	-0.3492
225	0.2323	-0.1708	0.8966	-0.3503
226	-0.1373	-0.1795	1.04	-0.3519
227	-0.2732	-0.1826	1.192	-0.3486
228	-0.5714	-0.1911	-1.178	-0.3532
229	-0.4218	-0.1905	-1.06	-0.359
230	-0.7061	-0.1957	-0.9477	-0.3549
231	1.379	-0.2885	-1.171	-0.4878
232	1.473	-0.2864	-1.057	-0.4917
233	1.174	-0.2973	-0.9529	-0.4921
234	1.277	-0.2925	-0.8359	-0.4963

Label	Centroid X	Centroid Y	Centroid X	Centroid Y
235	1.059	-0.2997	-0.721	-0.4936
236	0.8426	-0.3036	-0.3295	-0.4967
237	0.9552	-0.3035	-0.2034	-0.4988
238	0.5921	-0.3062	0.05216	-0.5005
239	0.7233	-0.3082	-0.5911	-0.5013
240	0.3557	-0.319	-0.4624	-0.5015
241	0.4775	-0.3181	-0.0756	-0.5058
242	0.2277	-0.3216	0.1884	-0.503
243	0.1165	-0.3333	0.3221	-0.5056
244	-0.1402	-0.3403	0.4589	-0.5091
245	-0.01326	-0.3409	0.6089	-0.5119
246	-0.2788	-0.3491	0.7507	-0.5135
247	-0.418	-0.3496	0.8951	-0.5133
248	-0.7109	-0.3612	1.047	-0.5169
249	-0.5632	-0.3544	1.194	-0.5177
250	1.476	-0.4234	-1.17	-0.6327
251	1.376	-0.435	-1.068	-0.6355
252	1.271	-0.4372	-0.9477	-0.6399
253	1.057	-0.4469	-0.832	-0.6463
254	1.174	-0.4443	-0.7209	-0.6492
255	0.9513	-0.45	-0.6012	-0.6496
256	0.8415	-0.4535	-0.3257	-0.6517
257	0.7128	-0.4578	-0.1992	-0.6537
258	0.4815	-0.4673	-0.47	-0.6568
259	0.5961	-0.4666	-0.07242	-0.6574
260	0.3542	-0.473	0.05742	-0.6593
261	0.2306	-0.4816	0.1866	-0.6651
262	0.1201	-0.4935	0.3228	-0.6643
263	-0.003976	-0.4954	0.4608	-0.6702
264	-0.1341	-0.5046	0.6041	-0.6663
265	-0.2776	-0.5089	0.7464	-0.6756
266	-0.4138	-0.5176	0.8899	-0.6759
267	-0.5575	-0.5222	1.048	-0.6867
268	-0.7082	-0.5249	1.195	-0.6834
269	1.477	-0.564	-1.174	-0.7798
270	1.384	-0.572	-1.06	-0.7871
271	1.271	-0.578	-0.9477	-0.7866
272	1.17	-0.5788	-0.8287	-0.7906
273	1.06	-0.5933	-0.7228	-0.7998
274	0.9467	-0.5938	-0.5958	-0.801
275	0.834	-0.6033	-0.4562	-0.8079
276	0.5955	-0.609	-0.3272	-0.8057
277	0.7232	-0.6144	-0.2044	-0.8106
278	0.4781	-0.6254	-0.07389	-0.8101
279	0.3555	-0.6294	0.05186	-0.8121
280	0.2328	-0.6339	0.1855	-0.8242
281	0.1054	-0.6489	0.3201	-0.8291
282	-0.004314	-0.6561	0.4614	-0.8351

Label	Centroid X	Centroid Y	Centroid X	Centroid Y
283	-0.1359	-0.6649	0.7512	-0.8399
284	-0.2756	-0.6682	0.6072	-0.8412
285	-0.4173	-0.6757	0.899	-0.8403
286	-0.5546	-0.6908	1.045	-0.8501
287	-0.7087	-0.6973	1.194	-0.8563
288	1.483	-0.7088	-1.167	-0.9208
289	1.387	-0.7176	-1.056	-0.9251
290	1.283	-0.7186	-0.9429	-0.9308
291	1.177	-0.7322	-0.8308	-0.9436
292	1.062	-0.7334	-0.7155	-0.9482
293	0.9447	-0.7447	-0.5898	-0.9527
294	0.8349	-0.7566	-0.4557	-0.9468
295	0.7181	-0.7575	-0.3248	-0.9527
296	0.5974	-0.7643	-0.2012	-0.958
297	0.4811	-0.7729	-0.07628	-0.9683
298	0.3514	-0.7768	0.0587	-0.9668
299	0.233	-0.7885	0.1934	-0.9789
300	0.1015	-0.8004	0.3217	-0.9869
301	-0.007555	-0.8151	0.4648	-0.9942
302	-0.1295	-0.8325	0.6097	-0.9993
303	-0.2751	-0.8402	0.7495	-1.009
304	-0.4163	-0.8448	0.8926	-1.014
305	1.489	-0.8509	1.041	-1.015
306	-0.5567	-0.8528	1.195	-1.025
307	-0.7073	-0.8594	-1.167	-1.066
308	1.385	-0.858	-1.054	-1.075
309	1.283	-0.8617	-0.9461	-1.086
310	1.182	-0.8752	-0.838	-1.092
311	1.066	-0.8792	-0.7214	-1.1
312	0.9563	-0.8967	-0.5863	-1.103
313	0.7162	-0.9074	-0.4469	-1.099
314	0.8377	-0.9078	-0.3243	-1.108
315	0.5968	-0.9165	-0.1991	-1.118
316	0.4769	-0.9316	-0.0751	-1.125
318	0.352	-0.9423	0.05398	-1.129
319	0.231	-0.9502	0.1908	-1.136
320	0.106	-0.9634	0.3304	-1.151
321	-0.01495	-0.9783	0.6018	-1.158
322	1.489	-0.9874	0.4569	-1.159
323	-0.1296	-0.9966	0.7467	-1.17
324	1.383	-0.9917	0.894	-1.17
325	-0.2701	-1.003	1.041	-1.189
326	1.284	-1.001	1.186	-1.194
327	-0.4117	-1.014	-1.169	-1.21
328	1.174	-1.015	-1.057	-1.22
329	-0.5596	-1.022	-0.9516	-1.231
330	1.066	-1.025	-0.8329	-1.24
331	-0.7101	-1.025	-0.7134	-1.245

Label	Centroid X	Centroid Y	Centroid X	Centroid Y
332	0.9556	-1.036	-0.592	-1.25
333	0.8465	-1.045	-0.4534	-1.254
334	0.7181	-1.055	-0.3255	-1.26
335	0.5997	-1.063	-0.2047	-1.271
336	0.4791	-1.075	-0.07545	-1.269
337	0.3588	-1.092	0.05379	-1.282
338	0.2332	-1.1	0.1915	-1.293
339	0.1047	-1.119	0.3182	-1.307
340	1.486	-1.126	0.4591	-1.313
341	-0.0103	-1.133	0.6036	-1.321
342	1.386	-1.136	0.7481	-1.332
343	-0.1347	-1.149	0.8954	-1.336
344	1.288	-1.145	1.043	-1.343
345	-0.2715	-1.166	-1.167	-1.35
346	1.171	-1.164	1.189	-1.358
347	1.063	-1.17	-1.053	-1.358
348	-0.4108	-1.18	-0.9469	-1.372
349	-0.5581	-1.189	-0.8311	-1.381
350	0.9592	-1.183	-0.7081	-1.391
351	0.8407	-1.192	-0.5899	-1.396
352	-0.709	-1.201	-0.4671	-1.408
353	0.7101	-1.201	-0.3409	-1.415
354	0.5967	-1.216	-0.2074	-1.422
355	0.4804	-1.228	-0.07139	-1.43
356	0.3657	-1.248	0.05958	-1.438
357	0.2477	-1.263	0.1892	-1.446
358	0.1223	-1.278	0.3199	-1.465
359	-0.00419	-1.288	0.4641	-1.474
360	-0.14	-1.304	0.6033	-1.485
361	-0.2732	-1.321	0.748	-1.499
364	-0.4138	-1.341	0.8901	-1.506
365	-0.5578	-1.346	1.038	-1.518
367	-0.7076	-1.36	1.19	-1.527

APPENDIX D: 3 dimensional matrix transformation

$$
\begin{vmatrix}
xp & yp & zp & 1 & 0 & 0 & 0 & 0 & 0 & 0 & 0 & 0 \\
0 & 0 & 0 & 0 & xp & yp & zp & 1 & 0 & 0 & 0 & 0 \\
0 & 0 & 0 & 0 & 0 & 0 & 0 & 0 & xp & yp & zp & 1 \\
xq & yq & zq & 1 & 0 & 0 & 0 & 0 & 0 & 0 & 0 & 0 \\
0 & 0 & 0 & 0 & xq & yq & zq & 1 & 0 & 0 & 0 & \\
0 & 0 & 0 & 0 & 0 & 0 & 0 & 0 & xq & yq & zq & 1 \\
xr & yr & zr & 1 & 0 & 0 & 0 & 0 & 0 & 0 & 0 & 0 \\
0 & 0 & 0 & 0 & xr & yr & zr & 1 & 0 & 0 & 0 & 0 \\
0 & 0 & 0 & 0 & 0 & 0 & 0 & 0 & xr & yr & zr & 1 \\
xs & ys & zs & 1 & 0 & 0 & 0 & 0 & 0 & 0 & 0 & 0 \\
0 & 0 & 0 & 0 & xs & ys & zs & 1 & 0 & 0 & 0 & 0 \\
0 & 0 & 0 & 0 & 0 & 0 & 0 & 0 & xs & ys & zs & 1
\end{vmatrix}
\begin{vmatrix} sm11 \\ sm12 \\ sm13 \\ Tx \\ sm21 \\ sm22 \\ sm23 \\ Ty \\ sm31 \\ sm32 \\ sm33 \\ Tz \end{vmatrix}
=
\begin{vmatrix} Xp \\ Yp \\ Zp \\ Xq \\ Yq \\ Zq \\ Xr \\ Yr \\ Zr \\ Xs \\ Ys \\ Zs \end{vmatrix}
$$

di mana:

xp = 101582.1003	yp = 9561.5612	zp = 95.9274
xq = 101573.0613	yq = 9836.7990	zq = 49.3167
xr = 101826.8110	yr = 9836.5196	zr = 0.7496
xs = 101834.9752	ys = 9562.5067	zs = 49.9210
Xp = 0	Yp = 0	Zp = 31.4356
Xq = 0	Yq = 270	Zq = 26.1250
Xr = 270	Yr = 0	Zr = 29.1700
Xs = 270	Ys = 270	Zs = 21.7950

Nota: Nilai-nilai koordinat di atas adalah dalam unit mm

Hasil bahagi bagi matrik di atas adalah seperti berikut:

sm11 = 1.129312059	sm21 = -0.087117815	sm31 = 0.127899996
sm12 = 0.094746654	sm22 = 0.900150849	sm32 = 0.113058547
sm13 = 0.340479952	sm23 = -0.460344999	sm33 = 0.756746789
Tx = -115656.4781	Ty = 286.9229069	Tz = -14114.52355

APPENDIX E: Analysis for rejection of observations for data obtained using profiler

Profil A

	A1	y		A2	y		A3	y		A4	y		A5	y		A6	y	
1	31.340	-0.107	accept	31.290	-0.028	accept	30.980	-0.078	accept	30.800	-0.104	accept	31.700	31.382	31.382	31.430	-0.097	accept
2	31.450	0.003	accept	31.290	-0.028	accept	30.980	-0.078	accept	30.850	-0.054	accept	31.660	31.342	31.342	31.380	-0.147	accept
3	31.420	-0.027	accept	31.270	-0.048	accept	31.020	-0.038	accept	30.900	-0.004	accept	31.800	31.482	31.482	31.520	-0.007	accept
4	31.550	0.103	accept	31.340	0.022	accept	31.050	-0.008	accept	30.880	-0.024	accept	31.760	31.442	31.442	31.570	0.043	accept
5	31.420	-0.027	accept	31.300	-0.018	accept	31.060	0.002	accept	30.900	-0.004	accept	31.800	31.482	31.482	31.550	0.023	accept
6	31.440	-0.007	accept	31.300	-0.018	accept	31.080	0.022	accept	30.960	0.056	accept	31.850	31.532	31.532	31.580	0.053	accept
7	31.470	0.023	accept	31.300	-0.018	accept	31.020	-0.038	accept	30.950	0.046	accept	31.760	31.442	31.442	31.580	0.053	accept
8	31.480	0.033	accept	31.420	0.102	reject	31.120	0.062	accept	30.980	0.076	accept	31.820	31.502	31.502	31.560	0.033	accept
9	31.420	-0.027	accept	31.330	0.012	accept	31.100	0.042	accept	30.850	-0.054	accept	31.790	31.472	31.472	31.500	-0.027	accept
10	31.480	0.033	accept	31.340	0.022	accept	31.170	0.112	accept	30.970	0.066	accept	31.940	31.622	31.622	31.600	0.073	accept
STDEV	0.055			0.043			0.061			0.060			0.077			0.072		
MIN	31.447			31.318	31.307		31.058			30.904			31.788			31.527		
z	0.124			0.096			0.139			0.136			0.175			0.162		

A7	y		A8	y		A9	y		A10	y		A11	y		A12	y	
31.460	-0.038	accept	32.750	-0.100	accept	33.440	-0.070	accept	31.840	-0.072	accept	32.580	-0.129	accept	32.680	-0.342	accept
31.480	-0.018	accept	32.720	-0.130	accept	33.450	-0.060	accept	31.840	-0.072	accept	32.530	-0.179	accept	32.740	-0.282	accept
31.450	-0.048	accept	32.680	-0.170	accept	33.500	-0.010	accept	31.900	-0.012	accept	32.540	-0.169	accept	32.800	-0.222	accept
31.500	0.002	accept	32.740	-0.110	accept	33.500	-0.010	accept	31.920	0.008	accept	32.620	-0.089	accept	33.920	0.898	accept
31.340	-0.158	accept	32.730	-0.120	accept	33.520	0.010	accept	31.970	0.058	accept	32.580	-0.129	accept	32.760	-0.262	accept
31.550	0.052	accept	32.730	-0.120	accept	33.500	-0.010	accept	31.940	0.028	accept	32.610	-0.099	accept	32.960	-0.062	accept
31.580	0.082	accept	32.830	-0.020	accept	33.560	0.050	accept	31.950	0.038	accept	32.680	-0.029	accept	32.720	-0.302	accept
31.570	0.072	accept	33.780	0.930	reject	33.600	0.090	accept	31.940	0.028	accept	33.660	0.951	reject	33.970	0.948	accept
31.460	-0.038	accept	32.710	-0.140	accept	33.420	-0.090	accept	31.850	-0.062	accept	32.590	-0.119	accept	32.740	-0.282	accept
31.590	0.092	accept	32.830	-0.020	accept	33.610	0.100	accept	31.970	0.058	accept	32.700	-0.009	accept	32.930	-0.092	accept
0.077			0.330			0.065			0.052			0.338			0.495		
31.498			32.850	32.747		33.510			31.912			32.709	32.603		33.022		
0.174			0.747			0.146			0.117			0.766			1.119		

	B1	y		B2	y		B3	y		B4	y		B5	y		B6	y	
1	31.550	-0.003	accept	31.880	-0.019	accept	30.920	-0.042	accept	31.600	0.020	accept	32.970	0.125	accept	33.590	-0.029	accept
2	31.550	-0.003	accept	31.880	-0.019	accept	30.980	0.018	accept	31.680	0.100	accept	32.880	0.035	accept	33.620	0.001	accept
3	31.500	-0.053	accept	31.820	-0.079	accept	30.900	-0.062	accept	31.510	-0.070	accept	32.800	-0.045	accept	33.560	-0.059	accept
4	31.480	-0.073	accept	31.850	-0.049	accept	30.880	-0.082	accept	31.450	-0.130	accept	32.780	-0.065	accept	33.550	-0.069	accept
5	31.580	0.027	accept	32.000	0.101	accept	31.050	0.088	accept	31.640	0.060	accept	32.930	0.085	accept	33.690	0.071	accept
6	31.420	-0.133	accept	31.850	-0.049	accept	30.910	-0.052	accept	31.520	-0.060	accept	32.670	-0.175	accept	33.560	-0.059	accept
7	31.530	-0.023	accept	31.810	-0.089	accept	30.960	-0.002	accept	31.580	0.000	accept	32.840	-0.005	accept	33.600	-0.019	accept
8	31.620	0.067	accept	32.000	0.101	accept	31.030	0.068	accept	31.630	0.050	accept	32.930	0.085	accept	33.760	0.141	accept
9	31.520	-0.033	accept	31.800	-0.099	accept	30.910	-0.052	accept	31.530	-0.050	accept	32.790	-0.055	accept	33.550	-0.069	accept
10	31.780	0.227	reject	32.100	0.201	accept	31.080	0.118	accept	31.660	0.080	accept	32.860	0.015	accept	33.710	0.091	accept
STDEV	0.097			0.100			0.070			0.075			0.089			0.075		
MIN	31.553	31.528		31.899			30.962			31.580			32.845			33.619		
z	0.219			0.227			0.159			0.170			0.202			0.170		

B7	y		B8	y		B9	y		B10	y		B11	y		B12	y	
31.290	0.001	accept	31.680	0.027	accept	31.170	-0.061	accept	30.980	-0.033	accept	32.160	0.033	accept	32.430	0.111	accept
31.220	-0.069	accept	31.680	0.027	accept	31.250	0.019	accept	31.090	0.077	accept	32.140	0.013	accept	32.320	0.001	accept
31.160	-0.129	accept	31.610	-0.043	accept	31.120	-0.111	accept	30.810	-0.203	accept	32.060	-0.067	accept	32.260	-0.059	accept
31.350	0.061	accept	31.580	-0.073	accept	31.120	-0.111	accept	31.000	-0.013	accept	32.060	-0.067	accept	32.320	0.001	accept
31.370	0.081	accept	31.730	0.077	accept	31.400	0.169	accept	31.170	0.157	accept	32.200	0.073	accept	32.450	0.131	accept
31.130	-0.159	accept	31.580	-0.073	accept	31.280	0.049	accept	30.910	-0.103	accept	32.080	-0.047	accept	32.240	-0.079	accept
31.200	-0.089	accept	31.660	0.007	accept	31.170	-0.061	accept	31.080	0.067	accept	32.110	-0.017	accept	32.300	-0.019	accept
31.250	-0.039	accept	31.720	0.067	accept	31.260	0.029	accept	31.020	0.007	accept	32.190	0.063	accept	32.370	0.051	accept
31.160	-0.129	accept	31.600	-0.053	accept	31.170	-0.061	accept	30.970	-0.043	accept	32.070	-0.057	accept	32.400	0.081	accept
31.760	0.471	reject	31.690	0.037	accept	31.370	0.139	accept	31.100	0.087	accept	32.200	0.073	accept	32.100	-0.219	accept
0.184			0.056			0.098			0.104			0.058			0.104		
31.289	31.237		31.653			31.231			31.013			32.127			32.319		
0.416			0.128			0.223			0.236			0.132			0.234		

	C1	y		C2	y		C3	y		C4	y		C5	y		C6	y	
1	33.000	-0.009	accept	33.300	-0.045	accept	32.800	-0.054	accept	31.640	-0.029	accept	32.120	-0.057	accept	31.710	-0.099	accept
2	32.850	-0.159	accept	33.250	-0.095	accept	32.750	-0.104	accept	31.650	-0.019	accept	32.100	-0.077	accept	31.630	-0.179	accept
3	32.970	-0.039	accept	33.350	0.005	accept	32.700	-0.154	accept	31.650	-0.019	accept	32.180	0.003	accept	31.720	-0.089	accept
4	32.940	-0.069	accept	33.260	-0.085	accept	32.760	-0.094	accept	31.600	-0.069	accept	32.100	-0.077	accept	31.730	-0.079	accept
5	33.000	-0.009	accept	33.350	0.005	accept	32.880	0.026	accept	31.630	-0.039	accept	32.240	0.063	accept	31.900	0.091	accept
6	33.120	0.111	accept	33.480	0.135	accept	33.040	0.186	accept	31.760	0.091	accept	32.250	0.073	accept	32.000	0.191	accept
7	32.970	-0.039	accept	33.340	-0.005	accept	32.880	0.026	accept	31.600	-0.069	accept	32.200	0.023	accept	31.900	0.091	accept
8	33.070	0.061	accept	33.410	0.065	accept	32.970	0.116	accept	31.800	0.131	accept	32.230	0.053	accept	31.850	0.041	accept
9	32.970	-0.039	accept	33.340	-0.005	accept	32.890	0.036	accept	31.660	-0.009	accept	32.120	-0.057	accept	31.850	0.041	accept
10	33.200	0.191	accept	33.370	0.025	accept	32.870	0.016	accept	31.700	0.031	accept	32.230	0.053	accept	31.800	-0.009	accept
STDEV	0.098			0.068			0.104			0.066			0.061			0.112		
MIN	33.009			33.345			32.854			31.669			32.177			31.809		
z	0.223			0.154			0.235			0.149			0.139			0.253		

C7	y		C8	y		C9	y		C10	y		C11	y		C12	y	
32.480	0.024	accept	31.420	-0.233	accept	30.200	0.104	accept	30.570	-0.012	accept	31.980	0.037	accept	32.030	-0.006	accept
32.260	-0.196	reject	31.720	0.067	accept	30.100	0.004	accept	30.480	-0.102	accept	31.840	-0.103	accept	31.870	-0.166	accept
32.450	-0.006	accept	31.740	0.087	accept	30.200	0.104	accept	30.540	-0.042	accept	31.920	-0.023	accept	31.950	-0.086	accept
32.400	-0.056	accept	31.200	-0.453	accept	30.140	0.044	accept	30.500	-0.082	accept	31.900	-0.043	accept	32.000	-0.036	accept
32.470	0.014	accept	31.550	-0.103	accept	30.200	0.104	accept	30.580	-0.002	accept	31.850	-0.093	accept	32.040	0.004	accept
32.580	0.124	accept	32.240	0.587	accept	30.340	0.244	accept	30.650	0.068	accept	32.000	0.057	accept	32.180	0.144	accept
32.460	0.004	accept	31.720	0.067	accept	30.120	0.024	accept	30.650	0.068	accept	32.000	0.057	accept	32.070	0.034	accept
32.520	0.064	accept	31.530	-0.123	accept	30.270	0.174	accept	30.640	0.058	accept	32.030	0.087	accept	32.100	0.064	accept
32.470	0.014	accept	31.630	-0.023	accept	29.170	-0.926	reject	30.550	-0.032	accept	31.940	-0.003	accept	32.040	0.004	accept
32.470	0.014	accept	31.780	0.127	accept	30.220	0.124	accept	30.660	0.078	accept	31.970	0.027	accept	32.080	0.044	accept
0.083			0.271			0.333			0.066			0.065			0.084		
32.456	32.478		31.653			30.096	30.199		30.582			31.943			32.036		
0.188			0.614			0.753			0.148			0.147			0.191		

	D1	y		D2	y		D3	y		D4	y		D5	y		D6	y	
1	32.920	-0.087	accept	33.350	-0.016	accept	33.500	-0.144	accept	32.140	-0.133	accept	32.040	0.033	accept	31.930	-0.049	accept
2	32.980	-0.027	accept	33.310	-0.056	accept	33.600	-0.044	accept	32.180	-0.093	accept	31.940	-0.067	accept	31.970	-0.009	accept
3	33.020	0.013	accept	33.400	0.034	accept	33.580	-0.064	accept	32.230	-0.043	accept	32.000	-0.007	accept	31.970	-0.009	accept
4	32.980	-0.027	accept	33.370	0.004	accept	33.600	-0.044	accept	32.220	-0.053	accept	32.000	-0.007	accept	31.980	0.001	accept
5	32.920	-0.087	accept	33.200	-0.166	reject	33.770	0.126	accept	32.410	0.137	accept	31.960	-0.047	accept	31.930	-0.049	accept
6	33.030	0.023	accept	33.430	0.064	accept	33.690	0.046	accept	32.300	0.027	accept	32.030	0.023	accept	32.000	0.021	accept
7	32.970	-0.037	accept	33.370	0.004	accept	33.570	-0.074	accept	32.220	-0.053	accept	32.000	-0.007	accept	31.980	0.001	accept
8	33.030	0.023	accept	33.440	0.074	accept	33.680	0.036	accept	32.320	0.047	accept	32.040	0.033	accept	32.050	0.071	accept
9	33.020	0.013	accept	33.410	0.044	accept	33.670	0.026	accept	32.290	0.017	accept	32.000	-0.007	accept	31.900	-0.079	accept
10	33.200	0.193	reject	33.380	0.014	accept	33.780	0.136	accept	32.420	0.147	accept	32.060	0.053	accept	32.080	0.101	accept
STDEV	0.079			0.070			0.090			0.093			0.037			0.055		
MIN	33.007	33.069		33.366	33.384		33.644			32.273			32.007			31.979		
z	0.179			0.158			0.203			0.210			0.084			0.124		

D7	y		D8	y		D9	y		D10	y		D11	y		D12	y	
32.850	0.011	accept	33.730	-0.062	accept	30.440	-0.474	accept	31.100	0.016	accept	31.740	-0.054	accept	31.840	0.039	accept
32.800	-0.039	accept	33.760	-0.032	accept	30.480	-0.434	accept	31.080	-0.004	accept	31.760	-0.034	accept	31.740	-0.061	accept
32.800	-0.039	accept	33.800	0.008	accept	30.520	-0.394	accept	31.110	0.026	accept	31.790	-0.004	accept	31.780	-0.021	accept
32.670	-0.169	accept	33.770	-0.022	accept	30.510	-0.404	accept	31.120	0.036	accept	31.780	-0.014	accept	31.780	-0.021	accept
32.880	0.041	accept	33.870	0.078	accept	30.480	-0.434	accept	31.000	-0.084	accept	31.770	-0.024	accept	31.740	-0.061	accept
32.730	-0.109	accept	33.830	0.038	accept	30.470	-0.444	accept	31.160	0.076	accept	31.820	0.026	accept	31.880	0.079	accept
32.900	0.061	accept	33.760	-0.032	accept	30.490	-0.424	accept	31.080	-0.004	accept	31.760	-0.034	accept	31.740	-0.061	accept
32.950	0.111	accept	33.830	0.038	accept	32.590	1.676	accept	31.170	0.086	accept	31.840	0.046	accept	31.880	0.079	accept
32.900	0.061	accept	33.720	-0.072	accept	30.570	-0.344	accept	30.820	-0.264	reject	31.800	0.006	accept	31.810	0.009	accept
32.910	0.071	accept	33.850	0.058	accept	32.590	1.676	accept	31.200	0.116	accept	31.880	0.086	accept	31.820	0.019	accept
0.088			0.052			0.884			0.108			0.042			0.054		
32.839			33.792			30.914			31.084	31.113		31.794			31.801		
0.200			0.117			2.000			0.245			0.096			0.123		

	E1	y		E2	y		E3	y		E4	y		E5	y		E6	y	
1	32.430	-0.084	accept	33.020	-0.017	accept	34.480	-0.077	accept	33.900	-0.260	accept	33.960	-0.022	accept	33.550	-0.148	accept
2	32.460	-0.054	accept	32.970	-0.067	accept	34.500	-0.057	accept	34.000	-0.160	accept	33.860	-0.122	accept	33.550	-0.148	accept
3	32.530	0.016	accept	33.020	-0.017	accept	34.600	0.043	accept	34.300	0.140	accept	34.030	0.048	accept	33.850	0.152	accept
4	32.450	-0.064	accept	33.000	-0.037	accept	34.500	-0.057	accept	34.000	-0.160	accept	33.950	-0.032	accept	33.570	-0.128	accept
5	32.520	0.006	accept	33.000	-0.037	accept	34.560	0.003	accept	34.250	0.090	accept	34.000	0.018	accept	33.780	0.082	accept
6	32.550	0.036	accept	33.050	0.013	accept	34.580	0.023	accept	34.060	-0.100	accept	34.000	0.018	accept	33.700	0.002	accept
7	32.460	-0.054	accept	33.020	-0.017	accept	34.500	-0.057	accept	34.200	0.040	accept	33.950	-0.032	accept	33.540	-0.158	accept
8	32.480	-0.034	accept	33.080	0.043	accept	34.570	0.013	accept	34.200	0.040	accept	33.940	-0.042	accept	33.660	-0.038	accept
9	32.600	0.086	accept	33.100	0.063	accept	34.640	0.083	accept	34.340	0.180	accept	34.050	0.068	accept	33.930	0.232	accept
10	32.660	0.146	accept	33.110	0.073	accept	34.640	0.083	accept	34.350	0.190	accept	34.080	0.098	accept	33.850	0.152	accept
STDEV	0.073			0.046			0.060			0.159			0.064			0.147		
MIN	32.514			33.037			34.557			34.160			33.982			33.698		
z	0.166			0.105			0.135			0.360			0.144			0.332		

E7	y		E8	y		E9	y		E10	y		E11	y		E12	y	
33.520	-0.016	accept	33.780	0.019	accept	30.780	-0.001	accept	30.360	-0.010	accept	31.260	0.014	accept	31.290	-0.054	accept
33.550	0.014	accept	33.780	0.019	accept	30.780	-0.001	accept	30.300	-0.070	accept	31.170	-0.076	accept	31.250	-0.094	accept
33.540	0.004	accept	33.750	-0.011	accept	30.730	-0.051	accept	30.340	-0.030	accept	31.230	-0.016	accept	31.360	0.016	accept
33.530	-0.006	accept	33.710	-0.051	accept	30.910	0.129	accept	30.360	-0.010	accept	31.300	0.054	accept	31.250	-0.094	accept
33.480	-0.056	accept	33.690	-0.071	accept	30.660	-0.121	accept	30.380	0.010	accept	31.230	-0.016	accept	31.400	0.056	accept
33.500	-0.036	accept	33.730	-0.031	accept	30.800	0.019	accept	30.400	0.030	accept	31.280	0.034	accept	31.370	0.026	accept
33.590	0.054	accept	33.730	-0.031	accept	30.840	0.059	accept	30.370	0.000	accept	31.240	-0.006	accept	31.280	-0.064	accept
33.580	0.044	accept	33.790	0.029	accept	30.850	0.069	accept	30.340	-0.030	accept	31.200	-0.046	accept	31.370	0.026	accept
33.590	0.054	accept	33.900	0.139	reject	30.670	-0.111	accept	30.450	0.080	accept	31.260	0.014	accept	31.440	0.096	accept
33.480	-0.056	accept	33.750	-0.011	accept	30.790	0.009	accept	30.400	0.030	accept	31.290	0.044	accept	31.430	0.086	accept
0.042			0.058			0.078			0.041			0.041			0.072		
33.536			33.761	33.746		30.781			30.370			31.246			31.344		
0.095			0.132			0.177			0.093			0.092			0.162		

	F1	y		F2	y		F3	y		F4	y		F5	y		F6	y	
1	32.320	-0.028	accept	32.030	-0.020	accept	30.300	-0.282	accept	31.720	-0.243	accept	32.500	0.074	accept	33.220	0.072	accept
2	32.320	-0.028	accept	32.000	-0.050	accept	30.420	-0.162	accept	31.800	-0.163	accept	32.400	-0.026	accept	33.240	0.092	accept
3	32.330	-0.018	accept	31.520	-0.530	reject	30.740	0.158	accept	31.880	-0.083	accept	32.430	0.004	accept	33.000	-0.148	accept
4	32.350	0.002	accept	32.100	0.050	accept	30.480	-0.102	accept	31.930	-0.033	accept	32.350	-0.076	accept	33.200	0.052	accept
5	32.290	-0.058	accept	32.130	0.080	accept	30.680	0.098	accept	32.020	0.057	accept	32.430	0.004	accept	33.290	0.142	accept
6	32.370	0.022	accept	32.180	0.130	accept	30.660	0.078	accept	32.000	0.037	accept	32.400	-0.026	accept	33.280	0.132	accept
7	32.410	0.062	accept	32.220	0.170	accept	30.590	0.008	accept	32.060	0.097	accept	32.470	0.044	accept	33.330	0.182	accept
8	32.340	-0.008	accept	31.880	-0.170	accept	30.670	0.088	accept	32.050	0.087	accept	32.440	0.014	accept	33.310	0.162	accept
9	32.350	0.002	accept	32.120	0.070	accept	30.530	-0.052	accept	32.100	0.137	accept	32.430	0.004	accept	33.290	0.142	accept
10	32.400	0.052	accept	32.320	0.270	accept	30.750	0.168	accept	32.070	0.107	accept	32.410	-0.016	accept	32.320	-0.828	reject
STDEV	0.037			0.222			0.147			0.127			0.041			0.306		
MIN	32.348			32.050	32.109		30.582			31.963			32.426			33.148	33.240	
z	0.084			0.503			0.333			0.288			0.092			0.691		

F7	y		F8	y		F9	y		F10	y		F11	y		F12	y	
30.840	-0.268	accept	29.180	0.010	accept	29.680	-0.017	accept	29.980	-0.025	accept	30.810	0.022	accept	31.720	0.048	accept
31.290	0.182	accept	29.210	0.040	accept	29.600	-0.097	accept	29.930	-0.075	accept	30.750	-0.038	accept	31.590	-0.082	accept
30.570	-0.538	reject	29.250	0.080	accept	29.670	-0.027	accept	30.030	0.025	accept	30.790	0.002	accept	31.630	-0.042	accept
31.100	-0.008	accept	29.040	-0.130	accept	29.670	-0.027	accept	29.970	-0.035	accept	30.720	-0.068	accept	31.650	-0.022	accept
31.250	0.142	accept	29.150	-0.020	accept	29.720	0.023	accept	30.030	0.025	accept	30.780	-0.008	accept	31.560	-0.112	accept
31.160	0.052	accept	29.120	-0.050	accept	29.700	0.003	accept	30.000	-0.005	accept	30.780	-0.008	accept	31.620	-0.052	accept
31.280	0.172	accept	29.210	0.040	accept	29.750	0.053	accept	30.050	0.045	accept	30.830	0.042	accept	31.790	0.118	accept
31.260	0.152	accept	29.210	0.040	accept	29.730	0.033	accept	30.030	0.025	accept	30.830	0.042	accept	31.740	0.068	accept
31.080	-0.028	accept	29.160	-0.010	accept	29.750	0.053	accept	30.000	-0.005	accept	30.790	0.002	accept	31.740	0.068	accept
31.250	0.142	accept	29.170	0.000	accept	29.700	0.003	accept	30.030	0.025	accept	30.800	0.012	accept	31.680	0.008	accept
0.234			0.059			0.045			0.037			0.034			0.074		
31.108	31.168		29.170			29.697			30.005			30.788			31.672		
0.528			0.133			0.102			0.083			0.077			0.168		

	G1	y		G2	y		G3	y		G4	y		G5	y		G6	y	
1	32.140	0.017	accept	27.530	-0.223	accept	26.900	0.005	accept	26.800	-0.119	accept	27.660	-0.193	accept	31.060	-0.318	reject
2	32.000	-0.123	accept	27.570	-0.183	accept	26.760	-0.135	accept	26.780	-0.139	accept	27.700	-0.153	accept	31.350	-0.028	accept
3	32.120	-0.003	accept	27.710	-0.043	accept	26.860	-0.035	accept	27.000	0.081	accept	27.860	0.007	accept	31.400	0.022	accept
4	32.110	-0.013	accept	27.650	-0.103	accept	26.820	-0.075	accept	26.900	-0.019	accept	27.820	-0.033	accept	31.350	-0.028	accept
5	32.060	-0.063	accept	27.850	0.097	accept	26.970	0.075	accept	26.900	-0.019	accept	27.860	0.007	accept	31.400	0.022	accept
6	32.160	0.037	accept	27.930	0.177	accept	26.900	0.005	accept	27.000	0.081	accept	27.900	0.047	accept	31.450	0.072	accept
7	32.180	0.057	accept	27.770	0.017	accept	26.940	0.045	accept	27.000	0.081	accept	27.880	0.027	accept	31.400	0.022	accept
8	32.140	0.017	accept	28.000	0.247	accept	27.030	0.135	accept	27.000	0.081	accept	27.900	0.047	accept	31.550	0.172	accept
9	32.120	-0.003	accept	27.650	-0.103	accept	26.850	-0.045	accept	26.910	-0.009	accept	27.860	0.007	accept	31.420	0.042	accept
10	32.200	0.077	accept	27.870	0.117	accept	26.920	0.025	accept	26.900	-0.019	accept	28.090	0.237	accept	31.400	0.022	accept
STDEV	0.058			0.157			0.077			0.082			0.117			0.125		
MIN	32.123			27.753			26.895			26.919			27.853			31.378	31.413	
z	0.131			0.355			0.175			0.186			0.265			0.283		

G7	y		G8	y		G9	y		G10	y		G11	y		G12	y	
29.490	-0.148	accept	29.480	-0.084	accept	29.080	-0.131	accept	29.210	-0.044	accept	29.850	-0.126	accept	31.280	-0.033	accept
29.630	-0.008	accept	29.460	-0.104	accept	29.030	-0.181	accept	29.120	-0.134	accept	29.780	-0.196	accept	31.150	-0.163	accept
29.700	0.062	accept	29.600	0.036	accept	29.260	0.049	accept	29.290	0.036	accept	30.020	0.044	accept	31.300	-0.013	accept
29.590	-0.048	accept	29.530	-0.034	accept	29.210	-0.001	accept	29.210	-0.044	accept	30.070	0.094	accept	31.270	-0.043	accept
29.550	-0.088	accept	29.540	-0.024	accept	29.270	0.059	accept	29.220	-0.034	accept	29.960	-0.016	accept	31.360	0.047	accept
29.740	0.102	accept	29.600	0.036	accept	29.270	0.059	accept	29.270	0.016	accept	30.000	0.024	accept	31.340	0.027	accept
29.650	0.012	accept	29.580	0.016	accept	29.220	0.009	accept	29.270	0.016	accept	30.000	0.024	accept	31.430	0.117	accept
29.740	0.102	accept	29.640	0.076	accept	29.310	0.099	accept	29.270	0.016	accept	30.050	0.074	accept	31.250	-0.063	accept
29.600	-0.038	accept	29.590	0.026	accept	29.250	0.039	accept	29.340	0.086	accept	30.030	0.054	accept	31.320	0.007	accept
29.690		accept	29.620	0.056	accept	29.210	-0.001	accept	29.340	0.086	accept	30.000	0.024	accept	31.430	0.117	accept
0.082			0.060			0.089			0.067			0.092			0.084		
29.638			29.564			29.211			29.254			29.976			31.313		
0.186			0.135			0.200			0.150			0.207			0.191		

	H1	y		H2	y		H3	y		H4	y		H5	y		H6	y	
1	31.280	-0.034	accept	27.620	-0.122	accept	26.930	-0.072	accept	26.900	-0.033	accept	27.140	-0.039	accept	26.510	-0.107	accept
2	31.160	-0.154	accept	27.640	-0.102	accept	26.940	-0.062	accept	26.800	-0.133	accept	27.100	-0.079	accept	26.540	-0.077	accept
3	31.230	-0.084	accept	27.610	-0.132	accept	27.070	0.068	accept	26.970	0.037	accept	27.180	0.001	accept	26.590	-0.027	accept
4	31.320	0.006	accept	27.800	0.058	accept	26.980	-0.022	accept	26.900	-0.033	accept	27.200	0.021	accept	26.590	-0.027	accept
5	31.300	-0.014	accept	27.800	0.058	accept	26.950	-0.052	accept	26.920	-0.013	accept	27.180	0.001	accept	26.700	0.083	accept
6	31.340	0.026	accept	27.810	0.068	accept	27.090	0.088	accept	26.920	-0.013	accept	27.200	0.021	accept	26.640	0.023	accept
7	31.400	0.086	accept	27.760	0.018	accept	26.910	-0.092	accept	27.070	0.137	accept	27.130	-0.049	accept	26.630	0.013	accept
8	31.360	0.046	accept	27.750	0.008	accept	27.050	0.048	accept	26.900	-0.033	accept	27.180	0.001	accept	26.560	-0.057	accept
9	31.350	0.036	accept	27.780	0.038	accept	27.000	-0.002	accept	26.950	0.017	accept	27.260	0.081	accept	26.710	0.093	accept
10	31.400	0.086	accept	27.850	0.108	accept	27.100	0.098	accept	27.000	0.067	accept	27.220	0.041	accept	26.700	0.083	accept
STDEV	0.075			0.087			0.071			0.072			0.046			0.071		
MIN	31.314			27.742			27.002			26.933			27.179			26.617		
z	0.170			0.196			0.160			0.162			0.105			0.160		

H7	y		H8	y		H9	y		H10	y		H11	y		H12	y	
26.880	-0.019	accept	27.550	-0.013	accept	28.260	0.004	accept	28.730	-0.040	accept	29.040	0.015	accept	29.410	0.035	accept
26.880	-0.019	accept	27.470	-0.093	accept	28.200	-0.056	accept	28.680	-0.090	accept	28.960	-0.065	accept	29.300	-0.075	accept
26.910	0.011	accept	27.660	0.097	accept	28.170	-0.086	accept	28.700	-0.070	accept	29.130	0.105	accept	29.430	0.055	accept
26.900	0.001	accept	27.530	-0.033	accept	28.300	0.044	accept	28.810	0.040	accept	28.930	-0.095	accept	29.330	-0.045	accept
26.900	0.001	accept	27.530	-0.033	accept	28.270	0.014	accept	28.810	0.040	accept	28.980	-0.045	accept	29.430	0.055	accept
26.880	-0.019	accept	27.580	0.017	accept	28.280	0.024	accept	28.820	0.050	accept	29.000	-0.025	accept	29.290	-0.085	accept
26.910	0.011	accept	27.600	0.037	accept	28.300	0.044	accept	28.820	0.050	accept	29.070	0.045	accept	29.260	-0.115	accept
26.860	-0.039	accept	27.530	-0.033	accept	28.200	-0.056	accept	28.800	0.030	accept	28.930	-0.045	accept	29.400	0.025	accept
26.940	0.041	accept	27.580	0.017	accept	28.330	0.074	accept	28.810	0.040	accept	29.080	0.055	accept	29.480	0.105	accept
26.930	0.031	accept	27.600	0.037	accept	28.250	-0.006	accept	28.720	-0.050	accept	29.080	0.055	accept	29.420	0.045	accept
0.025			0.053			0.051			0.056			0.064			0.074		
26.899			27.563			28.256			28.770			29.025			29.375		
0.056			0.119			0.116			0.126			0.146			0.167		

	I1	y		I2	y		I3	y		I4	y		I5	y		I6	y	
1	29.700	-0.046	accept	27.640	-0.045	accept	26.600	-0.008	accept	26.750	-0.168	accept	27.470	-0.091	accept	26.450	-0.224	accept
2	29.580	-0.166	accept	27.540	-0.145	reject	26.530	-0.078	accept	26.810	-0.108	accept	27.440	-0.121	accept	26.500	-0.174	accept
3	29.670	-0.076	accept	27.680	-0.005	accept	26.600	-0.008	accept	26.950	0.032	accept	27.610	0.049	accept	26.740	0.066	accept
4	29.780	0.034	accept	27.660	-0.025	accept	26.580	-0.028	accept	26.870	-0.048	accept	27.600	0.039	accept	26.640	-0.034	accept
5	29.720	-0.026	accept	27.700	0.015	accept	26.600	-0.008	accept	26.920	0.002	accept	27.520	-0.041	accept	26.670	-0.004	accept
6	29.780	0.034	accept	27.740	0.055	accept	26.590	-0.018	accept	26.950	0.032	accept	27.530	-0.031	accept	26.780	0.106	accept
7	29.780	0.034	accept	27.690	0.005	accept	26.570	-0.038	accept	26.930	0.012	accept	27.520	-0.041	accept	26.730	0.056	accept
8	29.860	0.114	accept	27.730	0.045	accept	26.700	0.092	accept	26.900	-0.018	accept	27.700	0.139	accept	26.700	0.026	accept
9	29.790	0.044	accept	27.720	0.035	accept	26.710	0.102	accept	26.950	0.032	accept	27.640	0.079	accept	26.720	0.046	accept
10	29.800	0.054	accept	27.750	0.065	accept	26.600	-0.008	accept	27.150	0.232	accept	27.580	0.019	accept	26.810	0.136	accept
STDEV	0.080			0.062			0.056			0.105			0.080			0.116		
MIN	29.746			27.685	27.701		26.608			26.918			27.561			26.674		
z	0.181			0.140			0.126			0.238			0.180			0.263		

I7	y		I8	y		I9	y		I10	y		I11	y		I12	y	
26.420	-0.085	accept	26.880	-0.056	accept	28.400	0.027	accept	28.890	-0.033	accept	29.370	-0.077	accept	29.280	-0.186	accept
26.390	-0.115	accept	26.800	-0.136	accept	28.270	-0.103	accept	28.860	-0.063	accept	29.350	-0.097	accept	29.370	-0.096	accept
26.520	0.015	accept	26.830	-0.106	accept	28.390	0.017	accept	28.900	-0.023	accept	29.500	0.053	accept	29.500	0.034	accept
26.450	-0.055	accept	26.940	0.004	accept	28.300	-0.073	accept	28.820	-0.103	accept	29.430	-0.017	accept	29.400	-0.066	accept
26.550	0.045	accept	26.920	-0.016	accept	28.440	0.067	accept	28.940	0.017	accept	29.480	0.033	accept	29.520	0.054	accept
26.560	0.055	accept	26.930	-0.006	accept	28.420	0.047	accept	29.020	0.097	accept	29.490	0.043	accept	29.540	0.074	accept
26.540	0.035	accept	27.020	0.084	accept	28.370	-0.003	accept	28.900	-0.023	accept	29.400	-0.047	accept	29.490	0.024	accept
26.530	0.025	accept	26.980	0.044	accept	28.320	-0.053	accept	29.000	0.077	accept	29.440	-0.007	accept	29.520	0.054	accept
26.530	0.025	accept	27.000	0.064	accept	28.450	0.077	accept	28.880	-0.043	accept	29.500	0.053	accept	29.420	-0.046	accept
26.560	0.055	accept	27.060	0.124	accept	28.370	-0.003	accept	29.020	0.097	accept	29.510	0.063	accept	29.620	0.154	accept
0.062			0.083			0.060			0.070			0.058			0.098		
26.505			26.936			28.373			28.923			29.447			29.466		
0.140			0.187			0.136			0.157			0.131			0.222		

	J1	y		J2	y		J3	y		J4	y		J5	y		J6	y	
1	27.680	0.013	accept	27.410	0.073	accept	27.180	0.177	accept	28.070	0.116	accept	28.170	0.224	reject	27.700	0.100	accept
2	27.610	-0.057	accept	27.270	-0.067	accept	26.900	-0.103	accept	27.920	-0.034	accept	27.860	-0.086	accept	27.650	0.050	accept
3	27.680	0.013	accept	27.330	-0.007	accept	26.940	-0.063	accept	27.970	0.016	accept	27.960	0.014	accept	27.480	-0.120	accept
4	27.600	-0.067	accept	27.260	-0.077	accept	26.920	-0.083	accept	27.860	-0.094	accept	27.880	-0.066	accept	27.400	-0.200	accept
5	27.640	-0.027	accept	27.280	-0.057	accept	27.000	-0.003	accept	27.880	-0.074	accept	27.900	-0.046	accept	27.630	0.030	accept
6	27.660	-0.007	accept	27.330	-0.007	accept	26.930	-0.073	accept	27.940	-0.014	accept	27.950	0.004	accept	27.670	0.070	accept
7	27.680	0.013	accept	27.360	0.023	accept	27.070	0.067	accept	27.980	0.026	accept	27.870	-0.076	accept	27.470	-0.130	accept
8	27.720	0.053	accept	27.390	0.053	accept	27.000	-0.003	accept	28.000	0.046	accept	27.950	0.004	accept	27.750	0.150	accept
9	27.680	0.013	accept	27.340	0.003	accept	27.060	0.057	accept	27.970	0.016	accept	27.920	-0.026	accept	27.490	-0.110	accept
10	27.720	0.053	accept	27.400	0.063	accept	27.030	0.027	accept	27.950	-0.004	accept	28.000	0.054	accept	27.760	0.160	accept
STDEV	0.041			0.054			0.086			0.060			0.090			0.129		
MIN	27.667			27.337			27.003			27.954			27.946	27.921		27.600		
z	0.092			0.123			0.195			0.136			0.205			0.292		

J7	y		J8	y		J9	y		J10	y		J11	y		J12	y	
27.250	0.051	accept	27.100	-0.015	accept	27.620	0.007	accept	28.060	-0.028	accept	29.270	0.005	accept	29.580	-0.010	accept
27.120	-0.079	accept	27.080	-0.035	accept	27.580	-0.033	accept	28.020	-0.068	accept	29.230	-0.035	accept	29.570	-0.020	accept
27.160	-0.039	accept	27.120	0.005	accept	27.630	0.017	accept	28.090	0.002	accept	29.270	0.005	accept	29.590	0.000	accept
27.150	-0.049	accept	27.070	-0.045	accept	27.540	-0.073	accept	28.000	-0.088	accept	29.210	-0.055	accept	29.550	-0.040	accept
27.170	-0.029	accept	27.070	-0.045	accept	27.510	-0.103	accept	28.100	0.012	accept	29.200	-0.065	accept	29.540	-0.050	accept
27.220	0.021	accept	27.130	0.015	accept	27.650	0.037	accept	28.140	0.052	accept	29.270	0.005	accept	29.610	0.020	accept
27.220	0.021	accept	27.130	0.015	accept	27.640	0.027	accept	28.040	-0.048	accept	29.300	0.035	accept	29.630	0.040	accept
27.250	0.051	accept	27.150	0.035	accept	27.660	0.047	accept	28.250	0.162	reject	29.300	0.035	accept	29.650	0.060	accept
27.200	0.001	accept	27.100	-0.015	accept	27.640	0.027	accept	28.100	0.012	accept	29.270	0.005	accept	29.610	0.020	accept
27.250	0.051	accept	27.200	0.085	accept	27.660	0.047	accept	28.080	-0.008	accept	29.330	0.065	accept	29.570	-0.020	accept
0.047			0.040			0.052			0.071			0.041			0.035		
27.199			27.115			27.613			28.088	28.070		29.265			29.590		
0.106			0.091			0.118			0.160			0.093			0.079		

	K1	y		K2	y		K3	y		K4	y		K5	y		K6	y	
1	27.160	-0.015	accept	27.250	-0.064	accept	26.910	-0.078	accept	26.750	-0.061	accept	27.540	-0.048	accept	26.100	-0.126	accept
2	27.100	-0.075	accept	27.250	-0.064	accept	26.800	-0.188	accept	26.700	-0.111	accept	27.500	-0.088	accept	26.150	-0.076	accept
3	27.200	0.025	accept	27.300	-0.014	accept	27.030	0.042	accept	26.800	-0.011	accept	27.580	-0.008	accept	26.240	0.014	accept
4	27.050	-0.125	accept	27.270	-0.044	accept	26.950	-0.038	accept	26.730	-0.081	accept	27.550	-0.038	accept	26.150	-0.076	accept
5	27.180	0.005	accept	27.300	-0.014	accept	26.960	-0.028	accept	26.760	-0.051	accept	27.580	-0.008	accept	26.230	0.004	accept
6	27.150	-0.025	accept	27.300	-0.014	accept	26.970	-0.018	accept	26.840	0.029	accept	27.600	0.012	accept	26.240	0.014	accept
7	27.220	0.045	accept	27.300	-0.014	accept	27.000	0.012	accept	26.870	0.059	accept	27.600	0.012	accept	26.290	0.064	accept
8	27.270	0.095	accept	27.430	0.116	accept	27.120	0.132	accept	26.920	0.109	accept	27.680	0.092	accept	26.290	0.064	accept
9	27.200	0.025	accept	27.330	0.016	accept	27.060	0.072	accept	26.840	0.029	accept	27.610	0.022	accept	26.270	0.044	accept
10	27.220	0.045	accept	27.410	0.096	accept	27.080	0.092	accept	26.900	0.089	accept	27.640	0.052	accept	26.300	0.074	accept
STDEV	0.064			0.061			0.092			0.075			0.051			0.069		
MIN	27.175			27.314			26.988			26.811			27.588			26.226		
z	0.144			0.139			0.209			0.169			0.116			0.157		

K7	y		K8	y		K9	y		K10	y		K11	y		K12	y	
26.230	-0.111	accept	26.700	-0.045	accept	26.870	-0.034	accept	26.830	-0.086	accept	28.000	-0.086	accept	26.680	-0.261	reject
26.240	-0.101	accept	26.760	0.015	accept	26.830	-0.074	accept	26.880	-0.036	accept	28.050	-0.036	accept	26.850	-0.091	accept
26.350	0.009	accept	26.730	-0.015	accept	26.830	-0.074	accept	26.900	-0.016	accept	28.080	-0.006	accept	26.880	-0.061	accept
26.370	0.029	accept	26.710	-0.035	accept	26.960	0.056	accept	26.920	0.004	accept	28.120	0.034	accept	27.060	0.119	accept
26.270	-0.071	accept	26.700	-0.045	accept	26.930	0.026	accept	26.900	-0.016	accept	28.130	0.044	accept	26.970	0.029	accept
26.420	0.079	accept	26.740	-0.005	accept	26.940	0.036	accept	26.930	0.014	accept	28.090	0.004	accept	27.000	0.059	accept
26.360	0.019	accept	26.780	0.035	accept	26.900	-0.004	accept	27.010	0.094	accept	28.100	0.014	accept	27.030	0.089	accept
26.360	0.019	accept	26.770	0.025	accept	26.910	0.006	accept	26.970	0.054	accept	28.070	-0.016	accept	26.930	-0.011	accept
26.320	-0.021	accept	26.790	0.045	accept	26.870	-0.034	accept	26.880	-0.036	accept	28.080	-0.006	accept	26.980	0.039	accept
26.490	0.149	accept	26.770	0.025	accept	27.000	0.096	accept	26.940	0.024	accept	28.140	0.054	accept	27.030	0.089	accept
0.080			0.034			0.055			0.051			0.041			0.114		
26.341			26.745			26.904			26.916			28.086			26.941	26.970	
0.182			0.076			0.125			0.114			0.093			0.257		

	L1	y		L2	y		L3	y		L4	y		L5	y		L6	y	
1	25.220	-0.998	accept	25.550	-1.394	accept	25.930	-0.922	accept	25.400	-1.218	accept	24.980	-2.341	accept	24.820	-1.694	accept
2	26.550	0.332	accept	27.430	0.486	accept	27.120	0.268	accept	27.060	0.442	accept	28.250	0.929	accept	27.100	0.586	accept
3	26.630	0.412	accept	27.510	0.566	accept	27.220	0.368	accept	27.150	0.532	accept	28.320	0.999	accept	27.180	0.666	accept
4	25.200	-1.018	accept	25.520	-1.424	accept	25.960	-0.892	accept	25.320	-1.298	accept	24.940	-2.381	accept	24.840	-1.674	accept
5	26.620	0.402	accept	27.540	0.596	accept	27.290	0.438	accept	27.120	0.502	accept	28.340	1.019	accept	27.270	0.756	accept
6	26.620	0.402	accept	27.540	0.596	accept	27.230	0.378	accept	27.160	0.542	accept	28.320	0.999	accept	27.290	0.776	accept
7	26.650	0.432	accept	27.570	0.626	accept	27.250	0.398	accept	27.150	0.532	accept	28.320	0.999	accept	27.300	0.786	accept
8	26.700	0.482	accept	27.560	0.616	accept	27.260	0.408	accept	27.170	0.552	accept	28.350	1.029	accept	27.230	0.716	accept
9	26.650	0.432	accept	27.580	0.636	accept	27.260	0.408	accept	27.190	0.572	accept	28.350	1.029	accept	27.170	0.656	accept
10	25.340	-0.878	accept	25.640	-1.304	accept	26.000	-0.852	accept	25.460	-1.158	accept	25.040	-2.281	accept	24.940	-1.574	accept
STDEV	0.668			0.950			0.615			0.846			1.611			1.139		
MIN	26.218			26.944			26.852			26.618			27.321			26.514		
z	1.510			2.148			1.391			1.915			3.645			2.576		

L7	y		L8	y		L9	y		L10	y		L11	y		L12	y	
26.200	-1.037	accept	26.300	-1.362	accept	26.830	-0.778	accept	27.780	-0.031	accept	27.780	0.579	accept	28.150	1.385	accept
27.550	0.313	accept	28.180	0.518	accept	27.760	0.152	accept	27.750	-0.061	accept	26.840	-0.361	accept	26.100	-0.665	accept
27.600	0.363	accept	28.250	0.588	accept	27.840	0.232	accept	27.850	0.039	accept	26.950	-0.251	accept	26.150	-0.615	accept
26.070	-1.167	accept	26.120	-1.542	accept	26.920	-0.688	accept	27.850	0.039	accept	27.880	0.679	accept	28.260	1.495	accept
27.740	0.503	accept	28.280	0.618	accept	27.940	0.332	accept	27.680	-0.131	accept	26.920	-0.281	accept	26.050	-0.715	accept
27.750	0.513	accept	28.300	0.638	accept	27.960	0.352	accept	27.850	0.039	accept	26.940	-0.261	accept	26.170	-0.595	accept
27.740	0.503	accept	28.320	0.658	accept	27.970	0.362	accept	27.850	0.039	accept	26.940	-0.261	accept	26.080	-0.685	accept
27.750	0.513	accept	28.310	0.648	accept	27.930	0.322	accept	27.850	0.039	accept	26.950	-0.251	accept	26.180	-0.585	accept
27.710	0.473	accept	28.320	0.658	accept	27.910	0.302	accept	27.880	0.069	accept	26.950	-0.251	accept	26.160	-0.605	accept
26.260	-0.977	accept	26.240	-1.422	accept	27.020	-0.588	accept	27.770	-0.041	accept	27.860	0.659	accept	28.350	1.585	accept
0.736			0.997			0.479			0.063			0.443			1.029		
27.237			27.662			27.608			27.811			27.201			26.765		
1.665			2.255			1.083			0.143			1.002			2.327		

	M1	y		M2	y		M3	y		M4	y		M5	y		M6	y	
1	29.170	-0.073	accept	29.690	-0.083	accept	27.300	-0.124	accept	27.880	-0.216	reject	27.460	-0.177	reject	28.050	-0.051	accept
2	29.180	-0.063	accept	29.680	-0.093	accept	27.320	-0.104	accept	28.040	-0.056	accept	27.600	-0.037	accept	28.100	-0.001	accept
3	29.200	-0.043	accept	29.750	-0.023	accept	27.450	0.026	accept	28.130	0.034	accept	27.650	0.013	accept	28.150	0.049	accept
4	29.190	-0.053	accept	29.750	-0.023	accept	27.440	0.016	accept	28.090	-0.006	accept	27.660	0.023	accept	28.130	0.029	accept
5	29.270	0.027	accept	29.780	0.007	accept	27.480	0.056	accept	28.150	0.054	accept	27.660	0.023	accept	28.050	-0.051	accept
6	29.250	0.007	accept	29.830	0.057	accept	27.410	-0.014	accept	28.100	0.004	accept	27.650	0.013	accept	27.980	-0.121	accept
7	29.230	-0.013	accept	29.730	-0.043	accept	27.430	0.006	accept	28.110	0.014	accept	27.580	-0.057	accept	27.970	-0.131	accept
8	29.330	0.087	accept	29.800	0.027	accept	27.470	0.046	accept	28.160	0.064	accept	27.700	0.063	accept	28.160	0.059	accept
9	29.310	0.067	accept	29.850	0.077	accept	27.520	0.096	accept	28.150	0.054	accept	27.700	0.063	accept	28.190	0.089	accept
10	29.300	0.057	accept	29.870	0.097	accept	27.420	-0.004	accept	28.150	0.054	accept	27.710	0.073	accept	28.230	0.129	accept
STDEV	0.058			0.065			0.068			0.084			0.075			0.087		
MIN	29.243			29.773			27.424			28.096	28.120		27.637	27.657		28.101		
z	0.131			0.147			0.154			0.191			0.170			0.197		

M7	y		M8	y		M9	y		M10	y		M11	y		M12	y	
28.550	-0.086	accept	28.630	-0.124	reject	28.300	-0.046	accept	28.100	-0.077	accept	26.450	-0.034	accept	25.810	-0.174	accept
28.560	-0.076	accept	28.740	-0.014	accept	28.220	-0.126	accept	28.100	-0.077	accept	26.420	-0.064	accept	25.920	-0.064	accept
28.610	-0.026	accept	28.720	-0.034	accept	28.360	0.014	accept	28.150	-0.027	accept	26.470	-0.014	accept	25.880	-0.104	accept
28.600	-0.036	accept	28.750	-0.004	accept	28.390	0.044	accept	28.150	-0.027	accept	26.470	-0.014	accept	25.970	-0.014	accept
28.680	0.044	accept	28.770	0.016	accept	28.400	0.054	accept	28.210	0.033	accept	26.530	0.046	accept	26.110	0.126	accept
28.650	0.014	accept	28.800	0.046	accept	28.370	0.024	accept	28.230	0.053	accept	26.480	-0.004	accept	26.000	0.016	accept
28.630	-0.006	accept	28.780	0.026	accept	28.300	-0.046	accept	28.200	0.023	accept	26.460	-0.024	accept	26.000	0.016	accept
28.690	0.054	accept	28.740	-0.014	accept	28.340	-0.006	accept	28.240	0.063	accept	26.500	0.016	accept	26.070	0.086	accept
28.680	0.044	accept	28.810	0.056	accept	28.360	0.014	accept	28.160	-0.017	accept	26.500	0.016	accept	26.060	0.076	accept
28.710	0.074	accept	28.800	0.046	accept	28.420	0.074	accept	28.230	0.053	accept	26.560	0.076	accept	26.020	0.036	accept
0.055			0.053			0.059			0.053			0.040			0.092		
28.636			28.754	28.768		28.346			28.177			26.484			25.984		
0.125			0.120			0.134			0.119			0.091			0.208		

	N1	y		N2	y		N3	y		N4	y		N5	y		N6	y	
1	29.570	-0.073	accept	29.240	-0.119	accept	29.530	-0.156	accept	27.350	-0.126	accept	27.440	-0.125	accept	28.060	-0.045	accept
2	29.520	-0.123	accept	29.240	-0.119	accept	29.580	-0.106	accept	27.370	-0.106	accept	27.370	-0.195	accept	28.000	-0.105	accept
3	29.590	-0.053	accept	29.310	-0.049	accept	29.630	-0.056	accept	27.420	-0.056	accept	27.520	-0.045	accept	28.070	-0.035	accept
4	29.600	-0.043	accept	29.320	-0.039	accept	29.660	-0.026	accept	27.450	-0.026	accept	27.520	-0.045	accept	28.070	-0.035	accept
5	29.620	-0.023	accept	29.400	0.041	accept	29.720	0.034	accept	27.500	0.024	accept	27.580	0.015	accept	28.090	-0.015	accept
6	29.620	-0.023	accept	29.360	0.001	accept	29.780	0.094	accept	27.470	-0.006	accept	27.590	0.025	accept	28.190	0.085	accept
7	29.730	0.087	accept	29.430	0.071	accept	29.700	0.014	accept	27.550	0.074	accept	27.620	0.055	accept	28.120	0.015	accept
8	29.710	0.067	accept	29.420	0.061	accept	29.730	0.044	accept	27.550	0.074	accept	27.630	0.065	accept	28.130	0.025	accept
9	29.720	0.077	accept	29.400	0.041	accept	29.750	0.064	accept	27.500	0.024	accept	27.630	0.065	accept	28.100	-0.005	accept
10	29.750	0.107	accept	29.470	0.111	accept	29.780	0.094	accept	27.600	0.124	accept	27.750	0.185	accept	28.220	0.115	accept
STDEV	0.079			0.079			0.085			0.081			0.108			0.064		
MIN	29.643			29.359			29.686			27.476			27.565			28.105		
z	0.178			0.180			0.191			0.182			0.243			0.145		

N7	y		N8	y		N9	y		N10	y		N11	y		N12	y	
28.230	-0.091	accept	28.480	-0.071	accept	28.450	-0.075	accept	27.510	-0.076	accept	26.610	-0.105	accept	24.530	0.048	accept
28.200	-0.121	accept	28.420	-0.131	accept	28.420	-0.105	accept	27.480	-0.106	accept	26.630	-0.085	accept	24.380	-0.102	accept
28.270	-0.051	accept	28.450	-0.101	accept	28.480	-0.045	accept	27.540	-0.046	accept	26.680	-0.035	accept	24.330	-0.152	accept
28.300	-0.021	accept	28.480	-0.071	accept	28.490	-0.035	accept	27.560	-0.026	accept	26.750	0.035	accept	24.570	0.088	accept
28.350	0.029	accept	28.550	-0.001	accept	28.550	0.025	accept	27.630	0.044	accept	26.770	0.055	accept	24.530	0.048	accept
28.320	-0.001	accept	28.510	-0.041	accept	28.520	-0.005	accept	27.600	0.014	accept	26.780	0.065	accept	24.440	-0.042	accept
28.390	0.069	accept	28.690	0.139	accept	28.580	0.055	accept	27.640	0.054	accept	26.780	0.065	accept	24.510	0.028	accept
28.380	0.059	accept	28.580	0.029	accept	28.580	0.055	accept	27.630	0.044	accept	26.700	-0.015	accept	24.540	0.058	accept
28.350	0.029	accept	28.700	0.149	accept	28.550	0.025	accept	27.620	0.034	accept	26.500	-0.215	accept	24.420	-0.062	accept
28.420	0.099	accept	28.650	0.099	accept	28.630	0.105	accept	27.650	0.064	accept	26.950	0.235	accept	24.570	0.088	accept
0.071			0.101			0.065			0.060			0.122			0.084		
28.321			28.551			28.525			27.586			26.715			24.482		
0.161			0.228			0.147			0.135			0.276			0.190		

	O1	y		O2	y		O3	y		O4	y		O5	y		O6	y	
1	28.500	-0.044	accept	28.700	-0.092	accept	29.030	-0.133	accept	27.320	-0.115	accept	27.530	-0.079	accept	27.030	0.015	accept
2	28.420	-0.124	accept	28.700	-0.092	accept	29.000	-0.163	accept	27.300	-0.135	accept	27.520	-0.089	accept	26.920	-0.095	accept
3	28.550	0.006	accept	28.750	-0.042	accept	29.100	-0.063	accept	27.430	-0.005	accept	27.580	-0.029	accept	27.020	0.005	accept
4	28.550	0.006	accept	28.750	-0.042	accept	29.260	0.097	accept	27.450	0.015	accept	27.550	-0.059	accept	26.960	-0.055	accept
5	28.510	-0.034	accept	28.780	-0.012	accept	29.130	-0.033	accept	27.430	-0.005	accept	27.830	0.221	reject	26.950	-0.065	accept
6	28.640	0.096	accept	28.820	0.028	accept	29.120	-0.043	accept	27.530	0.095	accept	27.550	-0.059	accept	27.030	0.015	accept
7	28.570	0.026	accept	28.820	0.028	accept	29.170	0.007	accept	27.500	0.065	accept	27.690	0.081	accept	27.090	0.075	accept
8	28.540	-0.004	accept	28.800	0.008	accept	29.130	-0.033	accept	27.410	-0.025	accept	27.570	-0.039	accept	27.050	0.035	accept
9	28.580	0.036	accept	28.850	0.058	accept	29.320	0.157	accept	27.460	0.025	accept	27.630	0.021	accept	27.020	0.005	accept
10	28.580	0.036	accept	28.950	0.158	accept	29.370	0.207	accept	27.520	0.085	accept	27.640	0.031	accept	27.080	0.065	accept
STDEV	0.059			0.075			0.120			0.077			0.094			0.056		
MIN	28.544			28.792			29.163			27.435			27.609	27.584		27.015		
z	0.133			0.170			0.271			0.174			0.214			0.126		

O7	y		O8	y		O9	y		O10	y		O11	y		O12	y	
26.870	-0.086	accept	27.810	-0.101	accept	28.640	0.050	accept	27.680	-0.098	accept	25.900	0.144	accept	22.900	0.043	accept
26.920	-0.036	accept	27.880	-0.031	accept	28.480	-0.110	accept	27.680	-0.098	accept	25.580	-0.176	accept	22.780	-0.077	accept
26.920	-0.036	accept	27.800	-0.111	accept	28.480	-0.110	accept	27.750	-0.028	accept	25.920	0.164	accept	22.880	0.023	accept
27.000	0.044	accept	27.870	-0.041	accept	28.510	-0.080	accept	27.780	0.002	accept	25.710	-0.046	accept	22.850	-0.007	accept
26.970	0.014	accept	27.970	0.059	accept	28.580	-0.010	accept	27.780	0.002	accept	25.660	-0.096	accept	22.810	-0.047	accept
26.960	0.004	accept	28.040	0.129	accept	28.530	-0.060	accept	27.780	0.002	accept	25.730	-0.026	accept	22.770	-0.087	accept
26.980	0.024	accept	28.050	0.139	accept	28.640	0.050	accept	27.830	0.052	accept	25.610	-0.146	accept	22.830	-0.027	accept
27.020	0.064	accept	27.900	-0.011	accept	28.630	0.040	accept	27.830	0.052	accept	25.870	0.114	accept	22.890	0.033	accept
26.920	-0.036	accept	27.870	-0.041	accept	28.660	0.070	accept	27.820	0.042	accept	25.710	-0.046	accept	22.970	0.113	accept
27.000	0.044	accept	27.920	0.009	accept	28.750	0.160	accept	27.850	0.072	accept	25.870	0.114	accept	22.890	0.033	accept
0.047			0.086			0.089			0.060			0.125			0.061		
26.956			27.911			28.590			27.778			25.756			22.857		
0.107			0.194			0.201			0.136			0.282			0.139		

	P1	y		P2	y		P3	y		P4	y		P5	y		P6	y	
1	28.760	-0.214	accept	28.860	-0.452	reject	29.270	-0.099	accept	0.285	-0.002	accept	27.340	-0.094	accept	27.970	-0.319	reject
2	28.880	-0.094	accept	29.200	-0.112	accept	29.250	-0.119	accept	0.286	-0.001	accept	27.340	-0.094	accept	28.240	-0.049	accept
3	28.900	-0.074	accept	29.630	0.318	accept	29.440	0.071	accept	0.286	-0.001	accept	27.440	0.006	accept	28.200	-0.089	accept
4	29.030	0.056	accept	29.350	0.038	accept	29.320	-0.049	accept	0.288	0.001	accept	27.440	0.006	accept	28.380	0.091	accept
5	29.070	0.096	accept	29.410	0.098	accept	29.410	0.041	accept	0.288	0.001	accept	27.480	0.046	accept	28.400	0.111	accept
6	28.940	-0.034	accept	29.240	-0.072	accept	29.320	-0.049	accept	0.287	0.000	accept	27.460	0.026	accept	28.310	0.021	accept
7	29.090	0.116	accept	29.430	0.118	accept	29.430	0.061	accept	0.288	0.001	accept	27.470	0.036	accept	28.420	0.131	accept
8	29.020	0.046	accept	29.370	0.058	accept	29.380	0.011	accept	0.287	0.000	accept	27.470	0.036	accept	28.250	-0.039	accept
9	29.000	0.026	accept	29.320	0.008	accept	29.360	-0.009	accept	0.288	0.001	accept	27.420	-0.014	accept	28.340	0.051	accept
10	29.050	0.076	accept	29.310	-0.002	accept	29.510	0.141	accept	0.287	0.000	accept	27.480	0.046	accept	28.380	0.091	accept
STDEV	0.103			0.198			0.081			0.001			0.053			0.134		
MIN	28.974			29.312	29.362		29.369			0.287			27.434			28.289	28.324	
z	0.233			0.447			0.184			0.002			0.120			0.304		

P7	y		P8	y		P9	y		P10	y		P11	y		P12	y	
27.140	-0.195	accept	27.750	-0.177	accept	28.740	-0.089	accept	28.020	-0.244	accept	24.840	-0.118	accept	21.400	-0.102	accept
27.270	-0.065	accept	27.840	-0.087	accept	28.750	-0.079	accept	28.200	-0.064	accept	24.900	-0.058	accept	21.440	-0.062	accept
27.250	-0.085	accept	27.850	-0.077	accept	28.930	0.101	accept	28.120	-0.144	accept	24.920	-0.038	accept	21.520	0.018	accept
27.380	0.045	accept	27.970	0.043	accept	28.830	0.001	accept	28.370	0.106	accept	25.000	0.042	accept	21.500	-0.002	accept
27.430	0.095	accept	27.710	-0.217	accept	28.870	0.041	accept	28.400	0.136	accept	24.980	0.022	accept	21.530	0.028	accept
27.330	-0.005	accept	28.000	0.073	accept	28.800	-0.029	accept	28.240	-0.024	accept	24.940	-0.018	accept	21.500	-0.002	accept
27.430	0.095	accept	28.100	0.173	accept	28.870	0.041	accept	28.320	0.056	accept	25.000	0.042	accept	21.540	0.038	accept
27.390	0.055	accept	28.040	0.113	accept	28.820	-0.009	accept	28.310	0.046	accept	25.020	0.062	accept	21.530	0.028	accept
27.350	0.015	accept	27.950	0.023	accept	28.820	-0.009	accept	28.300	0.036	accept	24.980	0.022	accept	21.530	0.028	accept
27.380	0.045	accept	28.060	0.133	accept	28.860	0.031	accept	28.360	0.096	accept	25.000	0.042	accept	21.530	0.028	accept
0.091			0.133			0.057			0.120			0.057			0.046		
27.335			27.927			28.829			28.264			24.958			21.502		
0.206			0.302			0.130			0.272			0.129			0.104		

	Q1	y		Q2	y		Q3	y		Q4	y		Q5	y		Q6	y	
1	29.910	-0.109	accept	28.460	-0.185	accept	28.670	-0.144	accept	28.220	-0.343	accept	26.120	-0.196	accept	26.700	-0.196	accept
2	29.920	-0.099	accept	28.540	-0.105	accept	28.700	-0.114	accept	28.370	-0.193	accept	26.170	-0.146	accept	26.760	-0.136	accept
3	29.950	-0.069	accept	28.580	-0.065	accept	28.780	-0.034	accept	28.570	0.007	accept	26.330	0.014	accept	26.920	0.024	accept
4	29.960	-0.059	accept	28.580	-0.065	accept	28.760	-0.054	accept	28.410	-0.153	accept	26.250	-0.066	accept	26.840	-0.056	accept
5	30.000	-0.019	accept	28.610	-0.035	accept	28.800	-0.014	accept	28.530	-0.033	accept	26.290	-0.026	accept	26.880	-0.016	accept
6	30.180	0.161	accept	28.810	0.165	accept	28.920	0.106	accept	28.840	0.277	accept	26.410	0.094	accept	26.970	0.074	accept
7	30.050	0.031	accept	28.670	0.025	accept	28.880	0.066	accept	28.580	0.017	accept	26.370	0.054	accept	26.940	0.044	accept
8	30.050	0.031	accept	28.690	0.045	accept	28.850	0.036	accept	28.680	0.117	accept	26.380	0.064	accept	26.950	0.054	accept
9	30.110	0.091	accept	28.760	0.115	accept	28.900	0.086	accept	28.660	0.097	accept	26.420	0.104	accept	27.000	0.104	accept
10	30.060	0.041	accept	28.750	0.105	accept	28.880	0.066	accept	28.770	0.207	accept	26.420	0.104	accept	27.000	0.104	accept
STDEV	0.087			0.110			0.086			0.189			0.107			0.102		
MIN	30.019			28.645			28.814			28.563			26.316			26.896		
z	0.197			0.249			0.195			0.428			0.241			0.230		

Q7	y		Q8	y		Q9	y		Q10	y		Q11	y		Q12	y	
27.240	-0.121	accept	27.630	-0.112	accept	28.680	-0.092	accept	24.320	-0.069	accept	22.720	0.000	accept	21.810	-0.150	accept
27.230	-0.131	accept	27.630	-0.112	accept	28.740	-0.032	accept	24.180	-0.209	accept	22.570	-0.150	accept	21.830	-0.130	accept
27.290	-0.071	accept	27.700	-0.042	accept	28.740	-0.032	accept	24.320	-0.069	accept	22.640	-0.080	accept	21.900	-0.060	accept
27.270	-0.091	accept	27.650	-0.092	accept	28.800	0.028	accept	24.370	-0.019	accept	22.650	-0.070	accept	21.930	-0.030	accept
27.320	-0.041	accept	27.730	-0.012	accept	28.870	0.098	accept	24.450	0.061	accept	22.650	-0.070	accept	21.880	-0.080	accept
27.400	0.039	accept	27.790	0.048	accept	28.810	0.038	accept	24.470	0.081	accept	22.800	0.080	accept	22.070	0.110	accept
27.410	0.049	accept	27.810	0.068	accept	28.650	-0.122	accept	24.530	0.141	accept	22.730	0.010	accept	22.070	0.110	accept
27.370	0.009	accept	27.830	0.088	accept	28.780	0.008	accept	24.350	-0.039	accept	22.730	0.010	accept	22.000	0.040	accept
27.540	0.179	accept	27.800	0.058	accept	28.900	0.128	accept	24.420	0.031	accept	22.810	0.090	accept	22.110	0.150	accept
27.540	0.179	accept	27.850	0.108	accept	28.750	-0.022	accept	24.480	0.091	accept	22.900	0.180	accept	22.000	0.040	accept
0.113			0.085			0.078			0.102			0.098			0.106		
27.361			27.742			28.772			24.389			22.720			21.960		
0.256			0.192			0.175			0.232			0.221			0.239		

	R1	y		R2	y		R3	y		R4	y		R5	y		R6	y	
1	29.470	-0.157	accept	27.810	-0.115	accept	28.600	-0.135	accept	28.190	-0.115	accept	27.660	-0.118	accept	26.210	-0.096	accept
2	29.660	0.033	accept	27.900	-0.025	accept	28.680	-0.055	accept	28.280	-0.025	accept	27.720	-0.058	accept	26.250	-0.056	accept
3	29.620	-0.007	accept	27.940	0.015	accept	28.740	0.005	accept	28.320	0.015	accept	27.800	0.022	accept	26.310	0.004	accept
4	29.430	-0.197	accept	27.650	-0.275	reject	28.570	-0.165	accept	28.130	-0.175	accept	27.670	-0.108	accept	26.160	-0.146	accept
5	29.640	0.013	accept	27.960	0.035	accept	28.760	0.025	accept	28.350	0.045	accept	27.810	0.032	accept	26.320	0.014	accept
6	29.700	0.073	accept	28.000	0.075	accept	28.790	0.055	accept	28.320	0.015	accept	27.730	-0.048	accept	26.290	-0.016	accept
7	29.660	0.033	accept	28.030	0.105	accept	28.780	0.045	accept	28.370	0.065	accept	27.820	0.042	accept	26.380	0.074	accept
8	29.730	0.103	accept	28.050	0.125	accept	28.830	0.095	accept	28.430	0.125	accept	27.870	0.092	accept	26.400	0.094	accept
9	29.650	0.023	accept	27.910	-0.015	accept	28.760	0.025	accept	28.370	0.065	accept	27.800	0.022	accept	26.340	0.034	accept
10	29.710	0.083	accept	28.000	0.075	accept	28.840	0.105	accept	28.290	-0.015	accept	27.900	0.122	accept	26.400	0.094	accept
STDEV	0.100			0.120			0.091			0.089			0.081			0.081		
MIN	29.627			27.925	27.956		28.735			28.305			27.778			26.306		
z	0.225			0.271			0.206			0.201			0.182			0.182		

R7	y		R8	y		R9	y		R10	y		R11	y		R12	y	
26.420	-0.108	accept	27.610	0.030	accept	28.430	-0.113	accept	27.230	-0.025	accept	27.950	-0.102	accept	24.210	-1.125	reject
26.520	-0.008	accept	27.530	-0.050	accept	28.500	-0.043	accept	27.180	-0.075	accept	28.000	-0.052	accept	25.300	-0.035	accept
26.540	0.012	accept	27.490	-0.090	accept	28.540	-0.003	accept	27.210	-0.045	accept	28.060	0.008	accept	25.420	0.085	accept
26.320	-0.208	accept	27.480	-0.100	accept	28.410	-0.133	accept	27.110	-0.145	accept	27.920	-0.132	accept	25.440	0.105	accept
26.570	0.042	accept	27.550	-0.030	accept	28.580	0.037	accept	27.420	0.165	accept	28.110	0.058	accept	25.490	0.155	accept
26.570	0.042	accept	27.630	0.050	accept	28.500	-0.043	accept	27.180	-0.075	accept	28.080	0.028	accept	25.320	-0.015	accept
26.610	0.082	accept	27.620	0.040	accept	28.580	0.037	accept	27.330	0.075	accept	28.000	-0.052	accept	25.460	0.125	accept
26.650	0.122	accept	27.650	0.070	accept	28.640	0.097	accept	27.310	0.055	accept	28.170	0.118	accept	25.500	0.165	accept
26.520	-0.008	accept	27.520	-0.060	accept	28.590	0.047	accept	27.280	0.025	accept	28.080	0.028	accept	25.620	0.285	accept
26.560	0.032	accept	27.720	0.140	accept	28.660	0.117	accept	27.300	0.045	accept	28.150	0.098	accept	25.590	0.255	accept
0.095			0.078			0.083			0.090			0.083			0.408		
26.528			27.580			28.543			27.255			28.052			25.335	25.460	
0.215			0.176			0.188			0.204			0.187			0.923		

	S1	y		S2	y		S3	y		S4	y		S5	y		S6	y	
1	29.050	-0.020	accept	29.110	0.008	accept	28.820	-0.064	accept	28.000	0.205	accept	26.500	-0.017	accept	25.850	-0.110	accept
2	29.000	-0.070	accept	29.000	-0.102	accept	28.840	-0.044	accept	27.750	-0.045	accept	26.490	-0.027	accept	25.900	-0.060	accept
3	29.070	0.000	accept	29.160	0.058	accept	28.900	0.016	accept	27.960	0.165	accept	26.560	0.043	accept	26.000	0.040	accept
4	29.100	0.030	accept	29.060	-0.042	accept	28.850	-0.034	accept	27.910	0.115	accept	26.510	-0.007	accept	25.940	-0.020	accept
5	29.170	0.100	accept	29.200	0.098	accept	28.960	0.076	accept	27.950	0.155	accept	26.550	0.033	accept	26.000	0.040	accept
6	28.880	-0.190	accept	28.920	-0.182	accept	28.740	-0.144	accept	27.560	-0.235	accept	26.320	-0.197	accept	25.820	-0.140	accept
7	29.120	0.050	accept	29.170	0.068	accept	28.940	0.056	accept	27.660	-0.135	accept	26.600	0.083	accept	26.050	0.090	accept
8	29.000	-0.070	accept	29.000	-0.102	accept	28.820	-0.064	accept	27.640	-0.155	accept	26.480	-0.037	accept	25.890	-0.070	accept
9	29.070	0.000	accept	29.100	-0.002	accept	28.870	-0.014	accept	27.900	0.105	accept	26.460	-0.057	accept	25.970	0.010	accept
10	29.240	0.170	accept	29.300	0.198	accept	29.100	0.216	accept	27.620	-0.175	accept	26.700	0.183	accept	26.180	0.220	accept
STDEV	0.099			0.112			0.099			0.166			0.099			0.106		
MIN	29.070			29.102			28.884			27.795			26.517			25.960		
z	0.224			0.253			0.224			0.375			0.223			0.239		

S7	y		S8	y		S9	y		S10	y		S11	y		S12	y	
25.580	-0.087	accept	25.610	-0.044	accept	25.530	0.026	accept	27.350	0.071	accept	28.410	-0.068	accept	25.760	-0.041	accept
25.570	-0.097	accept	25.610	-0.044	accept	25.530	0.026	accept	27.490	0.211	accept	28.440	-0.038	accept	25.500	-0.301	accept
25.670	0.003	accept	25.770	0.116	accept	25.500	-0.004	accept	27.340	0.061	accept	28.490	0.012	accept	25.470	-0.331	accept
25.630	-0.037	accept	25.630	-0.024	accept	25.570	0.066	accept	27.410	0.131	accept	28.440	-0.038	accept	26.080	0.279	accept
25.730	0.063	accept	25.700	0.046	accept	25.440	-0.064	accept	27.580	0.301	accept	28.510	0.032	accept	25.780	-0.021	accept
25.560	-0.107	accept	25.580	-0.074	accept	25.600	0.096	accept	27.340	0.061	accept	28.320	-0.158	accept	25.560	-0.241	accept
25.770	0.103	accept	25.670	0.016	accept	25.480	-0.024	accept	25.620	-1.659	reject	28.580	0.102	accept	26.180	0.379	accept
25.650	-0.017	accept	25.610	-0.044	accept	25.490	-0.014	accept	27.520	0.241	accept	28.480	0.002	accept	25.690	-0.111	accept
25.630	-0.037	accept	25.600	-0.054	accept	25.420	-0.084	accept	27.550	0.271	accept	28.440	-0.038	accept	25.720	-0.081	accept
25.880	0.213	accept	25.760	0.106	accept	25.480	-0.024	accept	27.590	0.311	accept	28.670	0.192	accept	26.270	0.469	accept
0.101			0.068			0.055			0.591			0.096			0.283		
25.667			25.654			25.504			27.279	27.463		28.478			25.801		
0.228			0.154			0.125			1.337			0.216			0.640		

A13	y		A14	y		A15	y		A16	y		A17	y		A18	y	
32.680	-0.065	accept	32.880	-0.088	accept	32.500	-0.026	accept	32.650	-0.137	accept	32.280	-0.046	accept	27.850	-0.142	accept
32.670	-0.075	accept	32.890	-0.078	accept	32.430	-0.096	accept	32.630	-0.157	accept	32.240	-0.086	accept	28.040	0.048	accept
32.720	-0.025	accept	32.920	-0.048	accept	32.540	0.014	accept	32.660	-0.127	accept	32.260	-0.066	accept	27.850	-0.142	accept
32.740	-0.005	accept	33.000	0.032	accept	32.530	0.004	accept	32.690	-0.097	accept	32.300	-0.026	accept	27.980	-0.012	accept
32.770	0.025	accept	32.980	0.012	accept	32.580	0.054	accept	33.700	0.913	reject	32.300	-0.026	accept	28.020	0.028	accept
32.780	0.035	accept	33.020	0.052	accept	32.530	0.004	accept	32.710	-0.077	accept	32.370	0.044	accept	28.080	0.088	accept
32.770	0.025	accept	33.040	0.072	accept	32.540	0.014	accept	32.700	-0.087	accept	32.310	-0.016	accept	28.040	0.048	accept
32.810	0.065	accept	33.000	0.032	accept	32.580	0.054	accept	32.750	-0.037	accept	32.350	0.024	accept	28.050	0.058	accept
32.710	-0.035	accept	32.920	-0.048	accept	32.470	-0.056	accept	32.640	-0.147	accept	32.270	-0.056	accept	27.980	-0.012	accept
32.800	0.055	accept	33.030	0.062	accept	32.560	0.034	accept	32.740	-0.047	accept	32.580	0.254	reject	28.030	0.038	accept
0.049			0.060			0.048			0.323			0.098			0.081		
32.745			32.968			32.526			32.787	32.686		32.326	32.298		27.992		
0.110			0.136			0.108			0.732			0.221			0.182		

A19	y	
25.980	-0.145	accept
26.180	0.055	accept
26.120	-0.005	accept
26.120	-0.005	accept
26.140	0.015	accept
26.200	0.075	accept
26.150	0.025	accept
26.160	0.035	accept
26.050	-0.075	accept
26.150	0.025	accept
0.065		
26.125		
0.147		

B13	y		B14	y		B15	y		B16	y		B17	y		B18	y	
33.120	0.005	accept	34.000	0.052	accept	33.910	0.033	accept	33.380	-0.036	accept	33.190	0.534	accept	27.240	0.039	accept
33.150	0.035	accept	34.000	0.052	accept	33.900	0.023	accept	33.430	0.014	accept	33.150	0.494	accept	27.110	-0.091	accept
33.060	-0.055	accept	33.850	-0.098	accept	33.780	-0.097	accept	33.320	-0.096	accept	33.060	0.404	accept	27.200	-0.001	accept
33.040	-0.075	accept	33.900	-0.048	accept	33.800	-0.077	accept	33.370	-0.046	accept	33.070	0.414	accept	27.240	0.039	accept
33.160	0.045	accept	34.060	0.112	accept	33.950	0.073	accept	33.500	0.084	accept	33.220	0.564	accept	27.330	0.129	accept
33.070	-0.045	accept	33.850	-0.098	accept	33.820	-0.057	accept	33.380	-0.036	accept	33.100	0.444	accept	27.150	-0.051	accept
33.150	0.035	accept	33.940	-0.008	accept	33.850	-0.027	accept	33.400	-0.016	accept	33.140	0.484	accept	27.270	0.069	accept
33.200	0.085	accept	34.020	0.072	accept	33.970	0.093	accept	33.480	0.064	accept	33.240	0.584	accept	27.220	0.019	accept
33.100	-0.015	accept	33.840	-0.108	accept	33.830	-0.047	accept	33.340	-0.076	accept	28.100	-4.556	reject	27.000	-0.201	accept
33.100	-0.015	accept	34.020	0.072	accept	33.960	0.083	accept	33.560	0.144	accept	33.290	0.634	accept	27.250	0.049	accept
0.050			0.083			0.070			0.076			1.603			0.093		
33.115			33.948			33.877			33.416			32.656	33.162		27.201		
0.114			0.187			0.158			0.172			3.625			0.211		

B19	y	
25.830	0.007	accept
25.950	0.127	accept
25.790	-0.033	accept
25.740	-0.083	accept
25.870	0.047	accept
25.820	-0.003	accept
25.870	0.047	accept
25.850	0.027	accept
25.780	-0.043	accept
25.730	-0.093	accept
0.067		
25.823		
0.150		

C13	y		C14	y		C15	y		C16	y		C17	y		C18	y	
32.470	0.046	accept	33.150	-0.013	accept	33.120	0.006	accept	33.410	0.025	accept	32.260	16.082	accept	28.680	0.004	accept
32.300	-0.124	accept	33.070	-0.093	accept	32.970	-0.144	accept	33.330	-0.055	accept	31.880	15.702	accept	28.510	-0.166	accept
32.370	-0.054	accept	33.140	-0.023	accept	33.140	0.026	accept	33.350	-0.035	accept	31.920	15.742	accept	28.600	-0.076	accept
32.360	-0.064	accept	33.120	-0.043	accept	32.980	-0.134	accept	33.330	-0.055	accept	31.810	15.632	accept	28.590	-0.086	accept
32.420	-0.004	accept	33.180	0.017	accept	33.100	-0.014	accept	33.410	0.025	accept	32.300	16.122	accept	28.680	0.004	accept
32.530	0.106	accept	33.260	0.097	accept	33.190	0.076	accept	33.470	0.085	accept	0.324	-15.854	accept	28.960	0.284	accept
32.410	-0.014	accept	33.150	-0.013	accept	33.140	0.026	accept	33.390	0.005	accept	0.320	-15.858	accept	28.610	-0.066	accept
32.530	0.106	accept	33.250	0.087	accept	33.260	0.146	accept	33.440	0.055	accept	0.323	-15.855	accept	28.850	0.174	accept
32.430	0.006	accept	33.100	-0.063	accept	33.060	-0.054	accept	33.370	-0.015	accept	0.319	-15.859	accept	28.620	-0.056	accept
32.420	-0.004	accept	33.210	0.047	accept	33.180	0.066	accept	33.350	-0.035	accept	0.325	-15.853	accept	28.660	-0.016	accept
0.072			0.062			0.091			0.047			16.714			0.133		
32.424			33.163			33.114			33.385			16.178			28.676		
0.164			0.141			0.206			0.107			37.808			0.301		

C19	y	
25.710	0.022	accept
25.540	-0.148	accept
25.600	-0.088	accept
25.640	-0.048	accept
25.620	-0.068	accept
25.840	0.152	accept
25.670	-0.018	accept
25.910	0.222	accept
25.670	-0.018	accept
25.680	-0.008	accept
0.111		
25.688		
0.250		

D13	y		D14	y		D15	y		D16	y		D17	y		D18	y	
32.140	-0.006	accept	32.520	0.011	accept	32.520	0.026	accept	32.560	-0.049	accept	31.080	-0.053	accept	29.150	-0.070	accept
32.110	-0.036	accept	32.480	-0.029	accept	32.480	-0.014	accept	32.580	-0.029	accept	31.000	-0.133	accept	29.170	-0.050	accept
32.140	-0.006	accept	32.420	-0.089	accept	32.490	-0.004	accept	32.570	-0.039	accept	31.300	0.167	accept	29.220	0.000	accept
32.140	-0.006	accept	32.480	-0.029	accept	32.470	-0.024	accept	32.590	-0.019	accept	31.070	-0.063	accept	29.240	0.020	accept
32.120	-0.026	accept	32.480	-0.029	accept	32.450	-0.044	accept	32.540	-0.069	accept	30.810	-0.323	accept	29.170	-0.050	accept
32.170	0.024	accept	32.580	0.071	accept	32.520	0.026	accept	32.720	0.111	accept	31.120	-0.013	accept	29.260	0.040	accept
32.120	-0.026	accept	32.480	-0.029	accept	32.470	-0.024	accept	32.620	0.011	accept	31.690	0.557	reject	29.180	-0.040	accept
32.180	0.034	accept	32.580	0.071	accept	32.510	0.016	accept	32.650	0.041	accept	31.090	-0.043	accept	29.270	0.050	accept
32.140	-0.006	accept	32.520	0.011	accept	32.510	0.016	accept	32.530	-0.079	accept	31.030	-0.103	accept	29.230	0.010	accept
32.200	0.054	accept	32.550	0.041	accept	32.520	0.026	accept	32.730	0.121	accept	31.140	0.007	accept	29.310	0.090	accept
0.029			0.051			0.025			0.071			0.231			0.052		
32.146			32.509			32.494			32.609			31.133	31.071		29.220		
0.065			0.115			0.058			0.160			0.522			0.117		

D19	y	
27.370	-0.101	accept
27.400	-0.071	accept
27.500	0.029	accept
27.400	-0.071	accept
27.440	-0.031	accept
27.450	-0.021	accept
27.410	-0.061	accept
27.620	0.149	accept
27.510	0.039	accept
27.610	0.139	accept
0.088		
27.471		
0.198		

E13	y		E14	y		E15	y		E16	y		E17	y		E18	y	
33.130	0.012	accept	33.780	0.001	accept	33.650	0.004	accept	32.510	-0.048	accept	31.450	0.018	accept	29.330	-0.125	accept
33.100	-0.018	accept	33.720	-0.059	accept	33.600	-0.046	accept	32.500	-0.058	accept	31.430	-0.002	accept	29.380	-0.075	accept
33.100	-0.018	accept	33.730	-0.049	accept	33.620	-0.026	accept	32.540	-0.018	accept	31.390	-0.042	accept	29.400	-0.055	accept
33.120	0.002	accept	33.780	0.001	accept	33.640	-0.006	accept	32.600	0.042	accept	31.340	-0.092	accept	29.330	-0.125	accept
33.000	-0.118	reject	33.760	-0.019	accept	33.630	-0.016	accept	32.600	0.042	accept	31.430	-0.002	accept	29.410	-0.045	accept
33.140	0.022	accept	33.820	0.041	accept	33.660	0.014	accept	32.580	0.022	accept	31.480	0.048	accept	29.400	-0.055	accept
33.120	0.002	accept	33.750	-0.029	accept	33.580	-0.066	accept	32.450	-0.108	accept	31.500	0.068	accept	29.330	-0.125	accept
33.170	0.052	accept	33.850	0.071	accept	33.670	0.024	accept	32.550	-0.008	accept	31.430	-0.002	accept	29.410	-0.045	accept
33.150	0.032	accept	33.790	0.011	accept	33.710	0.064	accept	32.650	0.092	accept	31.450	0.018	accept	29.820	0.365	accept
33.150	0.032	accept	33.810	0.031	accept	33.700	0.054	accept	32.600	0.042	accept	31.420	-0.012	accept	29.740	0.285	accept
0.047			0.041			0.041			0.060			0.045			0.175		
33.118	33.131		33.779			33.646			32.558			31.432			29.455		
0.107			0.092			0.093			0.135			0.101			0.397		

E19	y	
28.910	-0.036	accept
28.870	-0.076	accept
29.000	0.054	accept
28.850	-0.096	accept
29.000	0.054	accept
29.000	0.054	accept
28.840	-0.106	accept
28.940	-0.006	accept
29.050	0.104	accept
29.000	0.054	accept
0.075		
28.946		
0.169		

F13	y		F14	y		F15	y		F16	y		F17	y		F18	y	
33.020	0.056	accept	34.060	0.214	accept	33.980	0.158	accept	33.640	-0.098	accept	31.800	0.052	accept	31.640	0.024	accept
32.920	-0.044	accept	33.970	0.124	accept	33.850	0.028	accept	33.680	-0.058	accept	31.450	-0.298	accept	31.550	-0.066	accept
33.000	0.036	accept	34.000	0.154	accept	33.880	0.058	accept	33.740	0.002	accept	31.600	-0.148	accept	31.600	-0.016	accept
32.860	-0.104	accept	34.000	0.154	accept	33.710	-0.112	accept	33.720	-0.018	accept	31.300	-0.448	accept	31.600	-0.016	accept
32.960	-0.004	accept	34.080	0.234	accept	33.720	-0.102	accept	33.730	-0.008	accept	32.030	0.282	accept	31.610	-0.006	accept
32.950	-0.014	accept	33.970	0.124	accept	33.810	-0.012	accept	33.730	-0.008	accept	32.000	0.252	accept	31.600	-0.016	accept
33.020	0.056	accept	34.100	0.254	accept	33.870	0.048	accept	33.760	0.022	accept	32.080	0.332	accept	31.620	0.004	accept
33.000	0.036	accept	34.060	0.214	accept	33.850	0.028	accept	33.790	0.052	accept	31.900	0.152	accept	31.680	0.064	accept
32.950	-0.014	accept	33.140	-0.706	accept	33.760	-0.062	accept	33.830	0.092	accept	31.370	-0.378	accept	31.610	-0.006	accept
32.960	-0.004	accept	33.080	-0.766	accept	33.790	-0.032	accept	33.760	0.022	accept	31.950	0.202	accept	31.650	0.034	accept
0.049			0.391			0.082			0.053			0.293			0.035		
32.964			33.846			33.822			33.738			31.748			31.616		
0.112			0.884			0.185			0.121			0.663			0.079		

F19	y	
31.200	-0.113	accept
31.000	-0.313	accept
31.410	0.097	accept
31.260	-0.053	accept
31.250	-0.063	accept
31.270	-0.043	accept
31.330	0.017	accept
31.300	-0.013	accept
31.530	0.217	accept
31.580	0.267	accept
0.166		
31.313		
0.375		

G13	y		G14	y		G15	y		G16	y		G17	y		G18	y	
31.760	-0.124	accept	33.120	-0.139	accept	33.660	-0.192	accept	33.230	-0.062	accept	33.320	0.052	accept	32.550	-0.162	accept
31.800	-0.084	accept	33.070	-0.189	accept	33.780	-0.072	accept	33.180	-0.112	accept	33.220	-0.048	accept	32.600	-0.112	accept
31.870	-0.014	accept	33.280	0.021	accept	34.050	0.198	accept	33.270	-0.022	accept	33.190	-0.078	accept	32.700	-0.012	accept
31.860	-0.024	accept	33.300	0.041	accept	33.820	-0.032	accept	33.250	-0.042	accept	33.200	-0.068	accept	32.740	0.028	accept
31.880	-0.004	accept	33.210	-0.049	accept	33.860	0.008	accept	33.310	0.018	accept	33.430	0.162	accept	32.790	0.078	accept
31.920	0.036	accept	33.200	-0.059	accept	33.850	-0.002	accept	33.290	-0.002	accept	33.120	-0.148	accept	32.720	0.008	accept
32.000	0.116	accept	33.430	0.171	accept	33.920	0.068	accept	33.330	0.038	accept	33.220	-0.048	accept	32.750	0.038	accept
31.940	0.056	accept	33.320	0.061	accept	33.880	0.028	accept	33.330	0.038	accept	33.230	-0.038	accept	32.750	0.038	accept
31.900	0.016	accept	33.340	0.081	accept	33.850	-0.002	accept	33.350	0.058	accept	33.240	-0.028	accept	32.750	0.038	accept
31.910	0.026	accept	33.320	0.061	accept	33.850	-0.002	accept	33.380	0.088	accept	33.510	0.242	accept	32.770	0.058	accept
0.068			0.109			0.099			0.061			0.119			0.077		
31.884			33.259			33.852			33.292			33.268			32.712		
0.155			0.246			0.223			0.137			0.269			0.174		

G19	y	
32.770	-0.124	accept
32.800	-0.094	accept
32.900	0.006	accept
32.860	-0.034	accept
32.900	0.006	accept
33.000	0.106	accept
32.920	0.026	accept
32.920	0.026	accept
32.940	0.046	accept
32.930	0.036	accept
0.068		
32.894		
0.153		

H13	y		H14	y		H15	y		H16	y		H17	y		H18	y	
31.410	-0.105	accept	33.000	-0.037	accept	32.400	-0.122	accept	33.320	-0.056	accept	33.930	-0.005	accept	31.900	0.467	accept
31.510	-0.005	accept	32.900	-0.137	reject	32.620	0.098	accept	33.270	-0.106	accept	33.860	-0.075	accept	31.780	0.347	accept
31.440	-0.075	accept	33.040	0.003	accept	32.620	0.098	accept	33.320	-0.056	accept	33.920	-0.015	accept	32.220	0.787	accept
31.670	0.155	accept	33.070	0.033	accept	32.400	-0.122	accept	33.420	0.044	accept	33.960	0.025	accept	31.470	0.037	accept
31.480	-0.035	accept	33.050	0.013	accept	32.610	0.088	accept	33.410	0.034	accept	34.000	0.065	accept	31.050	-0.383	accept
31.510	-0.005	accept	33.070	0.033	accept	32.420	-0.102	accept	33.420	0.044	accept	33.960	0.025	accept	31.100	-0.333	accept
31.500	-0.015	accept	33.070	0.033	accept	32.470	-0.052	accept	33.410	0.034	accept	33.920	-0.015	accept	31.250	-0.183	accept
31.460	-0.055	accept	33.040	0.003	accept	32.680	0.158	accept	33.370	-0.006	accept	33.900	-0.035	accept	31.250	-0.183	accept
31.650	0.135	accept	33.100	0.063	accept	32.490	-0.032	accept	33.400	0.024	accept	33.970	0.035	accept	31.140	-0.293	accept
31.520	0.005	accept	33.030	-0.007	accept	32.510	-0.012	accept	33.420	0.044	accept	33.930	-0.005	accept	31.170	-0.263	accept
0.084			0.055			0.103			0.054			0.040			0.400		
31.515			33.037	33.052		32.522			33.376			33.935			31.433		
0.190			0.125			0.234			0.122			0.089			0.904		

H19	y	
29.810	-0.043	accept
29.800	-0.053	accept
29.830	-0.023	accept
29.770	-0.083	accept
29.820	-0.033	accept
29.900	0.047	accept
29.890	0.037	accept
29.860	0.007	accept
29.900	0.047	accept
29.950	0.097	accept
0.056		
29.853		
0.127		

I13	y		I14	y		I15	y		I16	y		I17	y		I18	y	
31.100	-0.162	accept	32.300	0.114	accept	32.310	-0.270	accept	32.110	0.248	accept	29.050	-0.233	accept	28.430	-0.254	accept
31.180	-0.082	accept	31.840	-0.346	accept	32.500	-0.080	accept	31.800	-0.062	accept	29.180	-0.103	accept	28.570	-0.114	accept
31.260	-0.002	accept	32.090	-0.096	accept	32.580	0.000	accept	31.800	-0.062	accept	29.320	0.037	accept	28.660	-0.024	accept
31.270	0.008	accept	32.330	0.144	accept	32.520	-0.060	accept	31.850	-0.012	accept	29.230	-0.053	accept	28.650	-0.034	accept
31.270	0.008	accept	32.160	-0.026	accept	32.600	0.020	accept	31.720	-0.142	accept	29.320	0.037	accept	28.810	0.126	accept
31.300	0.038	accept	32.170	-0.016	accept	32.700	0.120	accept	31.740	-0.122	accept	29.300	0.017	accept	28.790	0.106	accept
31.240	-0.022	accept	32.080	-0.106	accept	32.630	0.050	accept	31.540	-0.322	accept	29.400	0.117	accept	28.670	-0.014	accept
31.320	0.058	accept	32.410	0.224	accept	32.600	0.020	accept	32.020	0.158	accept	29.280	-0.003	accept	28.720	0.036	accept
31.360	0.098	accept	32.330	0.144	accept	32.580	0.000	accept	31.970	0.108	accept	29.350	0.067	accept	28.740	0.056	accept
31.320	0.058	accept	32.150	-0.036	accept	32.780	0.200	accept	32.070	0.208	accept	29.400	0.117	accept	28.800	0.116	accept
0.076			0.166			0.125			0.179			0.107			0.118		
31.262			32.186			32.580			31.862			29.283			28.684		
0.171			0.375			0.283			0.405			0.242			0.266		

I19	y	
28.700	-0.150	accept
28.740	-0.110	accept
28.920	0.070	accept
28.770	-0.080	accept
28.900	0.050	accept
28.800	-0.050	accept
28.870	0.020	accept
28.820	-0.030	accept
28.850	0.000	accept
29.130	0.280	reject
0.120		
28.850		
0.272		

J13	y		J14	y		J15	y		J16	y		J17	y		J18	y	
30.020	0.069	accept	29.830	0.104	accept	28.750	-0.026	accept	29.380	0.044	accept	28.530	0.041	accept	28.250	0.002	accept
29.900	-0.051	accept	29.690	-0.036	accept	28.770	-0.006	accept	29.200	-0.136	accept	28.480	-0.009	accept	28.230	-0.018	accept
29.920	-0.031	accept	29.720	-0.006	accept	28.750	-0.026	accept	29.230	-0.106	accept	28.450	-0.039	accept	28.260	0.012	accept
29.880	-0.071	accept	29.610	-0.116	accept	28.810	0.034	accept	29.150	-0.186	accept	28.450	-0.039	accept	28.210	-0.038	accept
29.930	-0.021	accept	29.730	0.004	accept	28.760	-0.016	accept	29.370	0.034	accept	28.380	-0.109	accept	28.220	-0.028	accept
30.000	0.049	accept	29.710	-0.016	accept	28.840	0.064	accept	29.440	0.104	accept	28.520	0.031	accept	28.320	0.072	accept
29.950	-0.001	accept	29.750	0.024	accept	28.800	0.024	accept	29.440	0.104	accept	28.480	-0.009	accept	28.300	0.052	accept
29.950	-0.001	accept	29.740	0.014	accept	28.700	-0.076	accept	29.500	0.164	accept	28.560	0.071	accept	28.330	0.082	accept
29.900	-0.051	accept	29.710	-0.016	accept	28.790	0.014	accept	29.170	-0.166	accept	28.520	0.031	accept	28.140	-0.108	accept
30.060	0.109	accept	29.770	0.044	accept	28.790	0.014	accept	29.480	0.144	accept	28.520	0.031	accept	28.220	-0.028	accept
0.058			0.057			0.039			0.135			0.052			0.058		
29.951			29.726			28.776			29.336			28.489			28.248		
0.132			0.128			0.088			0.306			0.118			0.130		

J19	y	
28.190	-0.059	accept
28.240	-0.009	accept
28.290	0.041	accept
28.180	-0.069	accept
28.290	0.041	accept
28.280	0.031	accept
28.270	0.021	accept
28.230	-0.019	accept
28.240	-0.009	accept
28.280	0.031	accept
0.040		
28.249		
0.091		

K13	y		K14	y		K15	y		K16	y		K17	y		K18	y	
26.400	-0.189	accept	27.170	-0.159	accept	24.300	-0.150	accept	26.070	-0.221	reject	27.400	-0.286	accept	27.730	-0.048	accept
26.500	-0.089	accept	27.300	-0.029	accept	24.560	0.110	accept	26.200	-0.091	accept	27.740	0.054	accept	27.730	-0.048	accept
26.610	0.021	accept	27.100	-0.229	accept	24.530	0.080	accept	26.310	0.019	accept	27.590	-0.096	accept	27.740	-0.038	accept
26.630	0.041	accept	27.300	-0.029	accept	24.560	0.110	accept	26.260	-0.031	accept	27.750	0.064	accept	27.750	-0.028	accept
26.600	0.011	accept	27.360	0.031	accept	24.410	-0.040	accept	26.330	0.039	accept	27.610	-0.076	accept	27.750	-0.028	accept
26.550	-0.039	accept	27.410	0.081	accept	24.500	0.050	accept	26.320	0.029	accept	27.680	-0.006	accept	27.750	-0.028	accept
26.630	0.041	accept	27.390	0.061	accept	24.530	0.080	accept	26.350	0.059	accept	27.970	0.284	accept	27.730	-0.048	accept
26.630	0.041	accept	27.400	0.071	accept	24.320	-0.130	accept	26.400	0.109	accept	27.580	-0.106	accept	27.870	0.092	accept
26.640	0.051	accept	27.400	0.071	accept	24.410	-0.040	accept	26.290	-0.001	accept	27.740	0.054	accept	27.930	0.152	accept
26.700	0.111	accept	27.460	0.131	accept	24.380	-0.070	accept	26.380	0.089	accept	27.800	0.114	accept	27.800	0.022	accept
0.085			0.114			0.098			0.097			0.153			0.069		
26.589			27.329			24.450			26.291	26.316		27.686			27.778		
0.193			0.259			0.222			0.219			0.347			0.156		

K19	y	
27.250	-0.061	accept
27.270	-0.041	accept
27.270	-0.041	accept
27.270	-0.041	accept
27.310	-0.001	accept
27.300	-0.011	accept
27.330	0.019	accept
27.360	0.049	accept
27.400	0.089	accept
27.350	0.039	accept
0.048		
27.311		
0.109		

L13	y		L14	y		L15	y		L16	y		L17	y		L18	y	
27.610	1.033	accept	27.340	1.752	accept	28.500	2.513	accept	27.110	1.203	accept	27.170	0.825	accept	27.480	1.349	accept
26.000	-0.577	accept	24.780	-0.808	accept	24.880	-1.107	accept	25.300	-0.607	accept	25.850	-0.495	accept	25.430	-0.701	accept
26.150	-0.427	accept	24.830	-0.758	accept	24.930	-1.057	accept	25.360	-0.547	accept	25.950	-0.395	accept	25.640	-0.491	accept
27.650	1.073	accept	27.250	1.662	accept	28.300	2.313	accept	27.050	1.143	accept	27.220	0.875	accept	27.480	1.349	accept
26.100	-0.477	accept	24.860	-0.728	accept	24.980	-1.007	accept	25.350	-0.557	accept	26.000	-0.345	accept	25.510	-0.621	accept
26.050	-0.527	accept	24.860	-0.728	accept	24.930	-1.057	accept	25.530	-0.377	accept	26.000	-0.345	accept	25.520	-0.611	accept
26.130	-0.447	accept	24.870	-0.718	accept	24.980	-1.007	accept	25.370	-0.537	accept	26.000	-0.345	accept	25.500	-0.631	accept
26.130	-0.447	accept	24.890	-0.698	accept	24.940	-1.047	accept	25.370	-0.537	accept	25.980	-0.365	accept	25.570	-0.561	accept
26.150	-0.427	accept	24.900	-0.688	accept	25.000	-0.987	accept	25.380	-0.527	accept	26.000	-0.345	accept	25.570	-0.561	accept
27.800	1.223	accept	27.300	1.712	accept	28.430	2.443	accept	27.250	1.343	accept	27.280	0.935	accept	27.610	1.479	accept
0.769			1.180			1.673			0.852			0.608			0.963		
26.577			25.588			25.987			25.907			26.345			26.131		
1.739			2.669			3.784			1.927			1.376			2.178		

L19	y	
26.560	0.854	accept
25.240	-0.466	accept
25.300	-0.406	accept
26.600	0.894	accept
25.310	-0.396	accept
25.330	-0.376	accept
25.310	-0.396	accept
25.330	-0.376	accept
25.370	-0.336	accept
26.710	1.004	accept
0.635		
25.706		
1.436		

M13	y		M14	y		M15	y		M16	y		M17	y		M18	y	
25.300	-0.149	reject	25.180	-0.171	accept	24.440	-0.121	accept	25.070	-0.125	accept	25.550	-0.099	accept	24.960	-0.091	accept
25.420	-0.029	accept	25.330	-0.021	accept	24.550	-0.011	accept	25.170	-0.025	accept	25.530	-0.119	accept	25.000	-0.051	accept
25.420	-0.029	accept	25.250	-0.101	accept	24.570	0.009	accept	25.170	-0.025	accept	25.600	-0.049	accept	25.000	-0.051	accept
25.470	0.021	accept	25.370	0.019	accept	24.600	0.039	accept	25.170	-0.025	accept	25.660	0.011	accept	25.040	-0.011	accept
25.470	0.021	accept	25.410	0.059	accept	24.640	0.079	accept	25.190	-0.005	accept	25.670	0.021	accept	25.100	0.049	accept
25.430	-0.019	accept	25.330	-0.021	accept	24.540	-0.021	accept	25.200	0.005	accept	25.650	0.001	accept	25.050	-0.001	accept
25.470	0.021	accept	25.400	0.049	accept	24.550	-0.011	accept	25.180	-0.015	accept	25.640	-0.009	accept	25.060	0.009	accept
25.480	0.031	accept	25.410	0.059	accept	24.590	0.029	accept	25.270	0.075	accept	25.700	0.051	accept	25.070	0.019	accept
25.530	0.081	accept	25.430	0.079	accept	24.630	0.069	accept	25.240	0.045	accept	25.720	0.071	accept	25.110	0.059	accept
25.500	0.051	accept	25.400	0.049	accept	24.500	-0.061	accept	25.290	0.095	accept	25.770	0.121	accept	25.120	0.069	accept
0.063			0.081			0.060			0.062			0.074			0.052		
25.449	25.466		25.351			24.561			25.195			25.649			25.051		
0.142			0.183			0.136			0.140			0.167			0.118		

M19	y	
24.350	-0.130	reject
24.420	-0.060	accept
24.480	0.000	accept
24.500	0.020	accept
24.490	0.010	accept
24.490	0.010	accept
24.480	0.000	accept
24.520	0.040	accept
24.520	0.040	accept
24.550	0.070	accept
0.057		
24.480	24.494	
0.129		

N13	y		N14	y		N15	y		N16	y		N17	y		N18	y	
24.730	-0.091	accept	23.740	-0.095	accept	24.110	-0.106	accept	23.680	-0.069	accept	24.450	-0.052	accept	22.320	0.005	accept
24.700	-0.121	accept	23.800	-0.035	accept	24.130	-0.086	accept	23.640	-0.109	accept	24.410	-0.092	accept	22.020	-0.295	reject
24.730	-0.091	accept	23.780	-0.055	accept	24.130	-0.086	accept	23.670	-0.079	accept	24.400	-0.102	accept	22.250	-0.065	accept
24.790	-0.031	accept	23.800	-0.035	accept	24.250	0.034	accept	23.740	-0.009	accept	24.500	-0.002	accept	22.370	0.055	accept
24.870	0.049	accept	23.870	0.035	accept	24.240	0.024	accept	23.790	0.041	accept	24.550	0.048	accept	22.390	0.075	accept
24.800	-0.021	accept	23.830	-0.005	accept	24.180	-0.036	accept	23.730	-0.019	accept	24.480	-0.022	accept	22.340	0.025	accept
24.920	0.099	accept	23.870	0.035	accept	24.330	0.114	accept	23.810	0.061	accept	24.590	0.088	accept	22.380	0.065	accept
24.900	0.079	accept	23.880	0.045	accept	24.240	0.024	accept	23.780	0.031	accept	24.540	0.038	accept	22.270	-0.045	accept
24.880	0.059	accept	23.880	0.045	accept	24.200	-0.016	accept	23.810	0.061	accept	24.570	0.068	accept	22.430	0.115	accept
24.890	0.069	accept	23.900	0.065	accept	24.350	0.134	accept	23.840	0.091	accept	24.530	0.028	accept	22.380	0.065	accept
0.081			0.053			0.082			0.068			0.066			0.117		
24.821			23.835			24.216			23.749			24.502			22.315	22.348	
0.184			0.120			0.186			0.154			0.149			0.266		

N19	y	
22.730	0.058	accept
22.500	-0.172	accept
22.550	-0.122	accept
22.730	0.058	accept
22.740	0.068	accept
22.570	-0.102	accept
22.730	0.058	accept
22.750	0.078	accept
22.640	-0.032	accept
22.780	0.108	accept
0.099		
22.672		
0.224		

O13	y		O14	y		O15	y		O16	y		O17	y		O18	y	
22.740	0.070	accept	22.500	-0.018	accept	22.700	-0.135	accept	21.530	-0.019	accept	20.880	0.015	accept	20.400	-0.028	accept
22.570	-0.100	accept	22.400	-0.118	reject	22.760	-0.075	accept	21.460	-0.089	accept	21.070	0.205	accept	20.350	-0.078	accept
22.680	0.010	accept	22.500	-0.018	accept	22.780	-0.055	accept	21.510	-0.039	accept	20.850	-0.015	accept	20.360	-0.068	accept
22.170	-0.500	accept	22.510	-0.008	accept	22.760	-0.075	accept	21.530	-0.019	accept	20.800	-0.065	accept	20.360	-0.068	accept
22.730	0.060	accept	22.520	0.002	accept	22.910	0.075	accept	21.550	0.001	accept	20.730	-0.135	accept	20.420	-0.008	accept
22.710	0.040	accept	22.550	0.032	accept	22.870	0.035	accept	21.580	0.031	accept	20.580	-0.285	accept	20.500	0.072	accept
22.940	0.270	accept	22.550	0.032	accept	22.890	0.055	accept	21.580	0.031	accept	20.920	0.055	accept	20.500	0.072	accept
22.770	0.100	accept	22.530	0.012	accept	22.900	0.065	accept	21.540	-0.009	accept	21.250	0.385	accept	20.420	-0.008	accept
22.970	0.300	accept	22.560	0.042	accept	22.880	0.045	accept	21.600	0.051	accept	20.920	0.055	accept	20.450	0.022	accept
22.420	-0.250	accept	22.560	0.042	accept	22.900	0.065	accept	21.610	0.061	accept	20.650	-0.215	accept	20.520	0.092	accept
0.237			0.048			0.077			0.045			0.196			0.063		
22.670			22.518	22.531		22.835			21.549			20.865			20.428		
0.536			0.108			0.173			0.103			0.444			0.142		

O19	y	
20.820	0.001	accept
20.750	-0.069	accept
20.870	0.051	accept
20.850	0.031	accept
20.730	-0.089	accept
20.920	0.101	accept
20.790	-0.029	accept
20.800	-0.019	accept
20.810	-0.009	accept
20.850	0.031	accept
0.056		
20.819		
0.128		

P13	y		P14	y		P15	y		P16	y		P17	y		P18	y	
21.400	-0.178	accept	22.170	0.016	accept	21.650	-0.040	accept	21.330	-0.112	accept	20.250	-0.122	accept	19.910	-0.118	reject
21.500	-0.078	accept	22.000	-0.154	accept	21.680	-0.010	accept	21.400	-0.042	accept	20.280	-0.092	accept	20.000	-0.028	accept
21.530	-0.048	accept	22.280	0.126	accept	21.750	0.060	accept	21.460	0.018	accept	20.300	-0.072	accept	20.020	-0.008	accept
21.630	0.052	accept	22.120	-0.034	accept	21.710	0.020	accept	21.410	-0.032	accept	20.450	0.078	accept	20.000	-0.028	accept
21.650	0.072	accept	22.140	-0.014	accept	21.600	-0.090	accept	21.470	0.028	accept	20.400	0.028	accept	20.040	0.012	accept
21.560	-0.018	accept	22.160	0.006	accept	21.690	0.000	accept	21.490	0.048	accept	20.460	0.088	accept	20.070	0.042	accept
21.680	0.102	accept	22.100	-0.054	accept	21.640	-0.050	accept	21.470	0.028	accept	20.340	-0.032	accept	20.040	0.012	accept
21.610	0.032	accept	22.200	0.046	accept	21.630	-0.060	accept	21.400	-0.042	accept	20.340	-0.032	accept	20.060	0.032	accept
21.610	0.032	accept	22.200	0.046	accept	21.850	0.160	accept	21.490	0.048	accept	20.420	0.048	accept	20.060	0.032	accept
21.610	0.032	accept	22.170	0.016	accept	21.700	0.010	accept	21.500	0.058	accept	20.480	0.108	accept	20.080	0.052	accept
0.083			0.074			0.071			0.055			0.081			0.050		
21.578			22.154			21.690			21.442			20.372			20.028	20.041	
0.187			0.166			0.161			0.124			0.183			0.113		

P19	y	
20.220	-0.161	reject
20.400	0.019	accept
20.380	-0.001	accept
20.330	-0.051	accept
20.400	0.019	accept
20.420	0.039	accept
20.400	0.019	accept
20.400	0.019	accept
20.410	0.029	accept
20.450	0.069	accept
0.064		
20.381	20.399	
0.145		

Q13	y		Q14	y		Q15	y		Q16	y		Q17	y		Q18	y	
21.470	-0.156	accept	20.360	-0.111	accept	20.150	-0.141	accept	20.560	-0.153	accept	19.930	-0.210	accept	20.410	-0.137	accept
21.500	-0.126	accept	20.300	-0.171	accept	20.150	-0.141	accept	20.550	-0.163	accept	20.030	-0.110	accept	20.420	-0.127	accept
21.580	-0.046	accept	20.450	-0.021	accept	20.260	-0.031	accept	20.650	-0.063	accept	20.120	-0.020	accept	20.480	-0.067	accept
21.570	-0.056	accept	20.420	-0.051	accept	20.200	-0.091	accept	20.640	-0.073	accept	20.080	-0.060	accept	20.520	-0.027	accept
21.630	0.004	accept	20.460	-0.011	accept	20.290	-0.001	accept	20.720	0.007	accept	20.130	-0.010	accept	20.550	0.003	accept
21.760	0.134	accept	20.530	0.059	accept	20.430	0.139	accept	20.800	0.087	accept	20.330	0.190	accept	20.600	0.053	accept
21.630	0.004	accept	20.550	0.079	accept	20.340	0.049	accept	20.720	0.007	accept	20.170	0.030	accept	20.610	0.063	accept
21.700	0.074	accept	20.550	0.079	accept	20.340	0.049	accept	20.850	0.137	accept	20.200	0.060	accept	20.570	0.023	accept
21.710	0.084	accept	20.610	0.139	accept	20.410	0.119	accept	20.790	0.077	accept	20.250	0.110	accept	20.700	0.153	accept
21.710	0.084	accept	20.480	0.009	accept	20.340	0.049	accept	20.850	0.137	accept	20.160	0.020	accept	20.610	0.063	accept
0.096			0.094			0.100			0.111			0.112			0.091		
21.626			20.471			20.291			20.713			20.140			20.547		
0.217			0.213			0.226			0.251			0.254			0.206		

Q19	y	
21.150	-0.070	accept
21.000	-0.220	accept
21.070	-0.150	accept
21.200	-0.020	accept
21.240	0.020	accept
21.360	0.140	accept
21.150	-0.070	accept
21.130	-0.090	accept
21.250	0.030	accept
21.650	0.430	reject
0.181		
21.220	21.172	
0.410		

R13	y		R14	y		R15	y		R16	y		R17	y		R18	y	
20.630	-0.077	accept	19.480	-0.113	accept	19.830	-0.209	accept	20.740	-0.206	accept	20.770	-0.136	accept	21.170	-0.120	accept
20.720	0.013	accept	19.560	-0.033	accept	19.900	-0.139	accept	20.900	-0.046	accept	20.840	-0.066	accept	21.240	-0.050	accept
20.720	0.013	accept	19.590	-0.003	accept	20.110	0.071	accept	20.960	0.014	accept	20.870	-0.036	accept	21.270	-0.020	accept
20.420	-0.287	accept	19.410	-0.183	accept	19.940	-0.099	accept	20.780	-0.166	accept	20.860	-0.046	accept	21.160	-0.130	accept
20.780	0.073	accept	19.640	0.047	accept	19.960	-0.079	accept	21.000	0.054	accept	20.900	-0.006	accept	21.300	0.010	accept
20.900	0.193	accept	19.600	0.007	accept	19.940	-0.099	accept	21.000	0.054	accept	20.980	0.074	accept	21.310	0.020	reject
20.560	-0.147	accept	19.660	0.067	accept	20.290	0.251	accept	21.040	0.094	accept	21.000	0.094	accept	21.370	0.080	accept
20.850	0.143	accept	19.670	0.077	accept	20.260	0.221	accept	21.050	0.104	accept	21.020	0.114	accept	21.380	0.090	accept
20.670	-0.037	accept	19.620	0.027	accept	20.130	0.091	accept	20.950	0.004	accept	20.900	-0.006	accept	21.340	0.050	accept
20.820	0.113	accept	19.700	0.107	accept	20.030	-0.009	accept	21.040	0.094	accept	20.920	0.014	accept	21.360	0.070	accept
0.144			0.090			0.154			0.109			0.077			0.079		
20.707			19.593			20.039			20.946			20.906			21.290	21.288	
0.326			0.203			0.349			0.246			0.175			0.179		

R19	y	
21.520	0.034	accept
21.430	-0.056	accept
21.440	-0.046	accept
21.150	-0.336	accept
21.670	0.184	accept
21.480	-0.006	accept
21.400	-0.086	accept
21.420	-0.066	accept
21.630	0.144	accept
21.720	0.234	accept
0.163		
21.486		
0.370		

S13	y		S14	y		S15	y		S16	y		S17	y		S18	y	
20.300	-0.075	accept	19.720	-0.032	accept	20.730	0.010	accept	21.120	-0.083	accept	21.040	-0.073	accept	21.470	-0.065	accept
20.260	-0.115	accept	19.690	-0.062	accept	20.650	-0.070	accept	21.160	-0.043	accept	21.030	-0.083	accept	21.460	-0.075	accept
20.300	-0.075	accept	19.810	0.058	accept	20.750	0.030	accept	21.350	0.147	accept	21.080	-0.033	accept	21.570	0.035	accept
20.420	0.045	accept	19.710	-0.042	accept	20.760	0.040	accept	21.200	-0.003	accept	21.070	-0.043	accept	21.520	-0.015	accept
20.640	0.265	accept	19.840	0.088	accept	20.760	0.040	accept	21.300	0.097	accept	21.150	0.037	accept	21.570	0.035	accept
20.220	-0.155	accept	19.520	-0.232	accept	20.520	-0.200	accept	21.000	-0.203	accept	20.960	-0.153	accept	21.400	-0.135	accept
20.400	0.025	accept	19.810	0.058	accept	20.750	0.030	accept	21.250	0.047	accept	21.200	0.087	accept	21.620	0.085	accept
20.410	0.035	accept	19.730	-0.022	accept	20.650	-0.070	accept	21.090	-0.113	accept	21.020	-0.093	accept	21.500	-0.035	accept
20.320	-0.055	accept	19.740	-0.012	accept	20.730	0.010	accept	21.170	-0.033	accept	21.070	-0.043	accept	21.580	0.045	accept
20.480	0.105	accept	19.950	0.198	accept	20.900	0.180	accept	21.390	0.187	accept	21.510	0.397	reject	21.660	0.125	accept
0.123			0.113			0.099			0.121			0.155			0.079		
20.375			19.752			20.720			21.203			21.113	21.069		21.535		
0.279			0.255			0.223			0.274			0.350			0.180		

S19	y	
21.720	-0.075	accept
21.730	-0.065	accept
21.780	-0.015	accept
21.760	-0.035	accept
21.880	0.085	accept
21.630	-0.165	accept
21.850	0.055	accept
21.770	-0.025	accept
21.830	0.035	accept
22.000	0.205	accept
0.101		
21.795		
0.230		

APPENDIX F: Output data obtained using Intersection Programme

Titik	X	Y	Z
A19	101573.0613	9836.798973	-104901.6833
B19	101587.5452	9837.183211	-104905.2109
C19	101601.4459	9837.613464	-104907.6069
D19	101616.03	9837.729727	-104908.4685
E19	101629.9825	9838.735091	-104910.5827
F19	101644.0253	9839.220138	-104910.8699
G19	101658.7407	9838.570404	-104911.6822
H19	101672.4337	9838.485257	-104916.8256
I19	101686.5222	9838.515459	-104920.4402
J19	101701.0177	9838.01845	-104923.4283
K19	101714.6349	9838.34621	-104926.3824
L19	101728.5922	9838.371693	-104931.1743
M19	101742.6432	9837.680052	-104934.124
N19	101757.0645	9837.016634	-104938.056
O19	101770.947	9836.546742	-104941.53
P19	101784.5366	9836.845608	-104944.3213
Q19	101798.7409	9836.565901	-104946.1931
R19	101813.0755	9836.484928	-104948.4006
S19	101826.811	9836.51963	-104950.2504
A18	101573.5752	9822.166137	-104898.3263
B18	101587.7604	9822.38658	-104901.6406
C18	101602	9822.360074	-104902.4031
D18	101616.3855	9822.724309	-104904.8134
E18	101630.1164	9822.697698	-104907.5785
F18	101644.2137	9823.321676	-104907.9471
G18	101659.2575	9823.779491	-104909.6744
H18	101673.4801	9824.045808	-104913.3021
I18	101687.352	9823.022912	-104918.5342
J18	101701.3102	9822.881845	-104920.8981
K18	101715.413	9823.054908	-104924.1804
L18	101730.0315	9822.336517	-104928.3416
M18	101743.6628	9822.229158	-104930.9381
N18	101757.3108	9821.300541	-104936.1455
O18	101771.3531	9820.88495	-104939.888
P18	101785.4404	9820.692547	-104942.4883
Q18	101799.2415	9821.353555	-104944.233
R18	101813.532	9821.341534	-104945.942
S18	101827.3501	9821.546356	-104948.1393
A17	101575.0012	9806.770802	-104891.9708
B17	101588.5792	9807.748011	-104893.5938
C17	101603.2583	9807.200573	-104896.9813
D17	101617.089	9807.290178	-104901.256

Titik	X	Y	Z
E17	101631.0678	9807.826188	-104903.5109
F17	101645.2125	9807.557782	-104905.0956
G17	101660.2156	9807.978003	-104907.0138
H17	101674.1464	9808.249079	-104908.2613
I17	101687.7979	9807.43315	-104914.9144
J17	101701.5813	9807.416927	-104918.5414
K17	101715.6777	9807.362306	-104921.7158
L17	101730.279	9807.573237	-104926.3095
M17	101744.3399	9806.988336	-104927.9521
N17	101757.7663	9807.641849	-104931.9637
O17	101771.909	9806.746538	-104937.5853
P17	101785.9215	9805.946865	-104940.3522
Q17	101799.8161	9806.083004	-104942.391
R17	101814.0503	9806.052502	-104944.8433
S17	101828.4486	9806.076748	-104946.2687
A16	101575.8448	9792.067752	-104889.224
B16	101589.1137	9792.440106	-104891.5551
C16	101603.7399	9792.163034	-104893.5096
D16	101617.4759	9792.128403	-104896.9867
E16	101631.4553	9792.783744	-104899.778
F16	101645.879	9793.068979	-104901.9026
G16	101660.5987	9793.03368	-104904.0773
H16	101674.2412	9793.302125	-104907.029
I16	101688.1614	9793.227228	-104909.8559
J16	101701.9264	9792.675093	-104916.0544
K16	101716.0414	9792.76532	-104920.5134
L16	101730.5187	9792.189885	-104923.2336
M16	101744.585	9792.16377	-104925.9073
N16	101758.4923	9791.923301	-104929.8595
O16	101772.224	9791.481923	-104934.6895
P16	101787.007	9791.03633	-104936.9725
Q16	101800.4517	9790.858113	-104939.9942
R16	101814.3047	9790.951442	-104941.2922
S16	101828.7201	9790.936032	-104944.0818
A15	101575.9816	9776.346525	-104887.0549
B15	101589.7158	9776.750329	-104887.9585
C15	101603.9296	9776.941055	-104891.5213
D15	101617.7172	9776.81916	-104894.6963
E15	101632.139	9776.983135	-104895.9649
F15	101646.3684	9777.089308	-104898.7415
G15	101661.2933	9777.303686	-104901.2095
H15	101674.5602	9777.24682	-104904.9785
I15	101690.0179	9777.350971	-104907.956
J15	101702.8862	9776.633899	-104913.2526
K15	101716.0052	9776.27208	-104919.4842
L15	101730.422	9776.760086	-104921.8644
M15	101744.6862	9776.326494	-104923.9738
N15	101759.0815	9776.246939	-104927.3665

Titik	X	Y	Z
O15	101772.8355	9775.865297	-104930.4722
P15	101787.543	9775.883176	-104934.1677
Q15	101800.4572	9775.378603	-104937.7263
R15	101815.0425	9775.38211	-104940.0995
S15	101828.7205	9775.171617	-104941.9717
A14	101576.4826	9761.422875	-104884.4584
B14	101590.6238	9761.277257	-104885.8153
C14	101604.0321	9761.677996	-104889.2902
D14	101618.2723	9761.144965	-104892.1612
E14	101632.3757	9761.897347	-104893.626
F14	101647.119	9761.695015	-104896.1099
G14	101661.2834	9761.795509	-104899.4008
H14	101675.1233	9761.733511	-104902.1881
I14	101689.9611	9761.802226	-104905.4457
J14	101703.1854	9760.925211	-104910.1493
K14	101716.9776	9761.609062	-104915.2206
L14	101731.198	9761.023608	-104919.8548
M14	101745.4054	9761.120575	-104921.4951
N14	101759.0601	9760.331603	-104924.758
O14	101773.1091	9760.592276	-104929.2225
P14	101787.4678	9760.058373	-104931.6389
Q14	101800.9082	9760.308891	-104935.188
R14	101815.1697	9760.036015	-104938.3629
S14	101828.8626	9759.453086	-104939.7109
A13	101576.9777	9745.662251	-104881.7894
B13	101590.3897	9745.489678	-104883.8383
C13	101604.6343	9745.292663	-104887.3594
D13	101618.37	9745.365693	-104890.3959
E13	101633.0344	9745.998885	-104891.2653
F13	101647.328	9745.856173	-104895.039
G13	101661.4698	9746.321746	-104898.2484
H13	101675.3592	9746.144097	-104901.6962
I13	101690.3173	9746.028511	-104904.3278
J13	101704.0811	9746.349728	-104907.6619
K13	101717.5111	9744.75109	-104912.7445
L13	101731.9799	9745.543432	-104915.8672
M13	101745.9453	9745.40944	-104919.0466
N13	101759.8979	9744.822111	-104921.8911
O13	101773.7831	9744.181827	-104926.7047
P13	101788.3211	9744.491848	-104929.8508
Q13	101801.8638	9744.629731	-104931.4447
R13	101816.2429	9743.847707	-104934.9294
S13	101830.0221	9744.075801	-104937.2664
A12	101576.9369	9730.390606	-104879.7005
B12	101590.8368	9730.166585	-104882.6443
C12	101604.8466	9730.488003	-104885.438
D12	101619.1447	9730.411705	-104888.0839
E12	101632.939	9730.495249	-104891.089

Titik	X	Y	Z
P10	101790.2863	9699.58463	-104917.1891
Q10	101803.5003	9698.83251	-104922.5101
R10	101818.5898	9699.830164	-104923.1544
S10	101831.8045	9699.816847	-104924.5443
A9	101578.9287	9684.199491	-104872.0874
B9	101592.3561	9683.730084	-104876.8248
C9	101606.0306	9683.588229	-104879.8716
D9	101620.1712	9683.069791	-104882.6894
E9	101634.4173	9683.327325	-104884.2988
F9	101648.5097	9683.614959	-104888.4535
G9	101663.0558	9683.698436	-104891.656
H9	101677.0224	9683.302873	-104894.7031
I9	101691.2871	9683.377346	-104897.418
J9	101704.8831	9683.279542	-104900.3464
K9	101718.9388	9683.147589	-104903.3487
L9	101733.9126	9682.811158	-104905.7357
M9	101748.0255	9683.565153	-104907.3988
N9	101762.3617	9683.784812	-104909.3001
O9	101776.5321	9684.156024	-104911.8588
P9	101790.9652	9683.78582	-104914.0573
Q9	101804.9647	9683.571587	-104915.902
R9	101818.6805	9684.250552	-104919.2364
S9	101832.143	9683.814038	-104923.2141
A8	101579.0922	9668.186719	-104870.024
B8	101592.4648	9667.651707	-104874.353
C8	101607.0782	9667.951864	-104876.3152
D8	101621.6737	9668.830837	-104877.4671
E8	101635.647	9669.1016	-104879.92
F8	101649.3226	9668.075722	-104886.4297
G8	101663.6259	9668.376333	-104889.2584
H8	101677.2628	9668.229687	-104892.6658
I8	101691.0532	9668.135767	-104896.2227
J8	101705.2347	9667.884712	-104898.3033
K8	101719.2621	9668.404131	-104901.0979
L8	101734.2182	9668.368268	-104903.0815
M8	101748.6719	9668.623097	-104904.5993
N8	101762.3793	9669.025428	-104906.5884
O8	101776.6247	9668.799214	-104909.7862
P8	101791.2761	9668.453649	-104912.6606
Q8	101805.2668	9668.656063	-104915.0054
R8	101818.8881	9668.597842	-104917.0891
S8	101832.3341	9668.541163	-104920.8994
A7	101579.2521	9653.186108	-104869.0005
B7	101593.564	9653.141428	-104871.8057
C7	101607.6147	9653.516945	-104873.0735
D7	101621.7356	9653.169176	-104875.8568
E7	101635.8995	9653.729596	-104878.0367
F7	101649.8742	9652.827997	-104882.349

Titik	X	Y	Z
G7	101664.1911	9652.918251	-104885.858
H7	101677.4539	9653.088457	-104891.1359
I7	101691.8284	9653.100261	-104893.4079
J7	101705.9239	9652.723836	-104895.8896
K7	101719.5552	9653.464004	-104898.7676
L7	101734.761	9653.437888	-104900 1569
M7	101749.0574	9653.639702	-104901.9914
N7	101763.0734	9653.456531	-104904.2892
O7	101777.2221	9653.134686	-104908.4419
P7	101791.6153	9653.356348	-104909.941
Q7	101805.3862	9653.547361	-104912.5748
R7	101819.4765	9653.466426	-104915.5114
S7	101832.8001	9653.396336	-104918.4228
A6	101579.9042	9637.990862	-104866.5615
B6	101594.1435	9638.20235	-104867.5895
C6	101608.4943	9637.885345	-104870.9342
D6	101622.3604	9637.758612	-104873.8225
E6	101636.7857	9638.031326	-104875.03
F6	101650.6106	9638.265307	-104877.9573
G6	101664.5789	9637.496139	-104882.1464
H6	101678.2124	9637.311687	-104888.7806
I6	101692.2851	9637.510986	-104891.5472
J6	101706.7151	9637.701204	-104893.4218
K6	101720.4405	9637.462682	-104896.3422
L6	101734.3515	9637.639708	-104898.5156
M6	101749.3729	9638.197972	-104899.6615
N6	101763.2713	9637.978645	-104902.3903
O6	101777.1646	9638.099612	-104905.6759
P6	101791.706	9638.038408	-104906.9482
Q6	101805.0703	9638.172612	-104910.2048
R6	101819.6811	9637.615616	-104913.3314
S6]	101833.3077	9638.426678	-104915.6211
A5	101580.2007	9622.384478	-104863.6602
B5	101595.0037	9622.251746	-104865.901
C5	101608.641	9622.745479	-104868.8672
D5	101623.0127	9622.702587	-104871.6979
E5	101636.9997	9622.682827	-104872.5372
F5	101651.1807	9622.664999	-104876.169
G5	101664.4091	9621.504396	-104882.6605
H5	101678.7141	9622.103333	-104885 952
I5	101692.5561	9622 021579	-104888 3136
J5	101706.7739	9622 11494	-104891 0784
K5	101720.5174	9622 832125	-104893 405
L5	101735.3513	9622.187074	-104894 7488
M5	101749.1259	9622 371312	-104897 6029
N5	101763 3772	9622 458886	-104900 4241
O5	101777 882	9622 130995	-104903 0204
P5	101792 0668	9622.982749	-104905 4265

Titik	X	Y	Z
Q5	101805.8804	9622.794233	-104908.5774
R5	101820.2492	9623.019105	-104909.5869
S5	101833.6117	9622.945062	-104912.7891
A4	101580.8765	9607.268655	-104862.1246
B4	101595.3256	9607.313137	-104864.2627
C4	101609.2438	9607.1816	-104866.9553
D4	101623.4048	9606.736516	-104868.8824
E4	101638.1098	9607.046407	-104870.3941
F4	101651.5532	9607.011337	-104874.7223
G4	101664.4914	9606.918444	-104880.7665
H4	101679.1926	9606.991121	-104883.7985
I4	101692.7672	9607.091672	-104886.7025
J4	101707.2765	9607.014175	-104888.0554
K4	101721.3097	9607.219022	-104891.4432
L4	101735.7447	9606.97438	-104893.705
M4	101749.598	9606.843243	-104895.1343
N4	101763.7545	9606.84415	-104898.4503
O4	101778.4632	9607.291325	-104900.6014
P4	101792.7124	9607.213277	-104901.7992
Q4	101806.558	9607.782444	-104903.9592
R4	101820.4725	9607.811591	-104906.2626
S4	101834.2627	9607.586598	-104909.5405
A3	101581.0871	9591.893331	-104859.9729
B3	101595.5807	9591.441501	-104862.293
C3	101609.9567	9591.411774	-104863.6977
D3	101623.9796	9591.776555	-104865.2008
E3	101638.3171	9591.667849	-104867.2531
F3	101651.516	9591.155294	-104873.3159
G3	101665.5337	9591.068302	-104878.8716
H3	101679.4545	9591.105487	-104881.509
I3	101693.2827	9590.79613	-104884.2656
J3	101707.4041	9591.117026	-104886.0565
K3	101721.4466	9591.658348	-104888.448
L3	101735.8505	9591.675742	-104891.1245
M3	101750.5644	9590.993053	-104893.1843
N3	101764.4279	9591.704592	-104893.7921
O3	101778.6102	9592.504358	-104896.8538
P3	101793.1644	9592.395527	-104898.455
Q3	101806.9025	9592.903434	-104901.6187
R3	101820.6934	9592.228324	-104903.9023
S3	101834.345	9592.670237	-104905.3809
A2	101581.5269	9576.305638	-104857.2015
B2	101596.0336	9576.247788	-104859.4173
C2	101610.2719	9576.354022	-104860.5693
D2	101624.4342	9576.234418	-104863.5181
E2	101638.5982	9576.55844	-104866.3107
F2	101652.0599	9576.565873	-104869.8769
G2	101665.6129	9575.783016	-104875.7784

Titik	X	Y	Z
H2	101679.9684	9576.176597	-104878.7636
I2	101693.9225	9576.126999	-104880.5671
J2	101707.8787	9576.885586	-104883.4823
K2	101721.9963	9576.849973	-104885.7165
L2	101736.3676	9576.551218	-104888.5311
M2	101750.9013	9577.133923	-104888.6097
N2	101764.8214	9577.068346	-104891.7003
O2	101779.032	9577.140033	-104894.5046
P2	101793.094	9577.117521	-104897.0122
Q2	101807.3535	9577.821901	-104899.1264
R2	101820.9562	9577.86707	-104901.9437
S2	101834.7869	9577.792132	-104903.1725
A1	101582.1003	9561.56122	-104855.0726
B1	101596.5514	9561.58091	-104857.6262
C1	101610.5539	9561.231988	-104859.0507
D1	101624.7477	9561.532268	-104861.5826
E1	101638.7772	9561.32245	-104865.0372
F1	101652.9696	9561.818626	-104867.2323
G1	101666.7927	9561.374877	-104870.1635
H1	101680.778	9561.462635	-104873.1618
I1	101694.6499	9561.215943	-104877.1566
J1	101708.551	9561.161672	-104881.2846
K1	101722.4076	9561.155938	-104884.1426
L1	101736.0703	9561.436868	-104886.6748
M1	101750.9555	9561.73255	-104886.9126
N1	101765.6289	9561.787819	-104889.3155
O1	101779.1709	9561.72302	-104892.2726
P1	101793.2237	9561.346678	-104894.7369
Q1	101807.6113	9562.659633	-104895.5742
R1	101821.1613	9562.409547	-104898.4819
S1	101834.9752	9562.506664	-104901.079

APPENDIX G: Profiles obtained from profiler and photogrammetry method

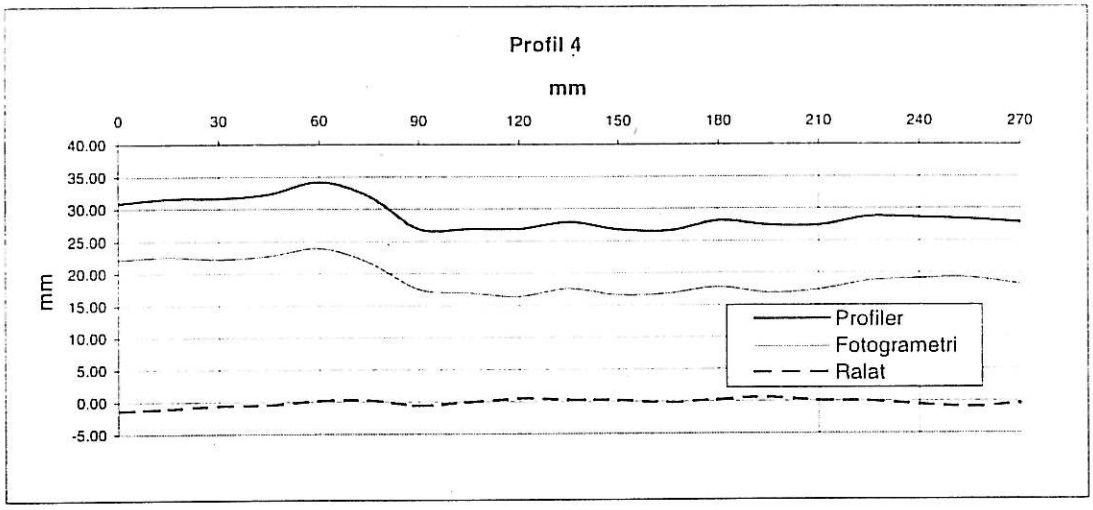
Profil 4
mm
0
30
60
90
120
150
180
210
240
270
40.00
35.00
30.00
25.00
20.00
15.00
10.00
5.00
0.00
-5.00
mm
Profiler
Fotogrametri
Ralat

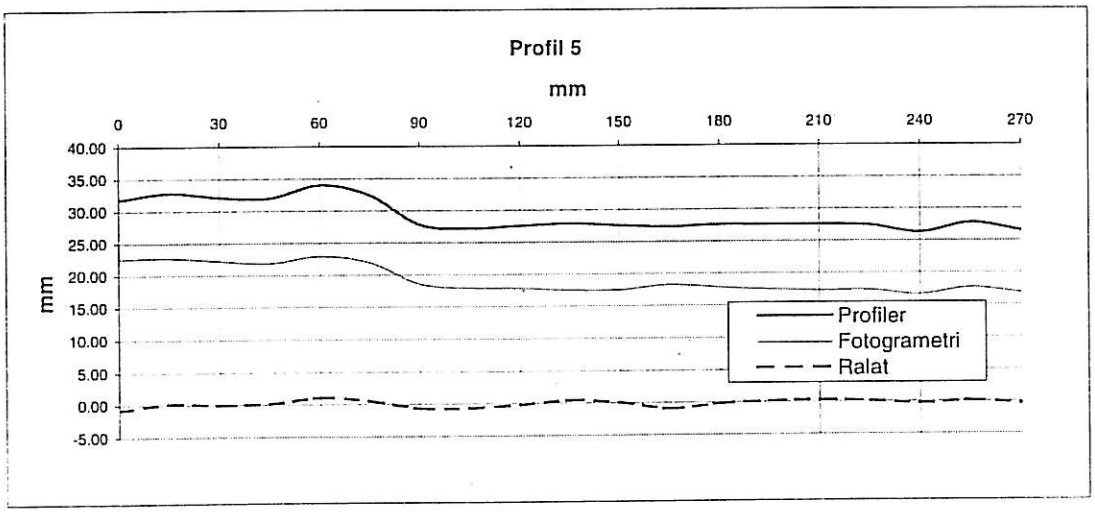
Profil 5
mm
0
30
60
90
120
150
180
210
240
270
40.00
35.00
30.00
25.00
20.00
15.00
10.00
5.00
0.00
-5.00
mm
Profiler
Fotogrametri
Ralat

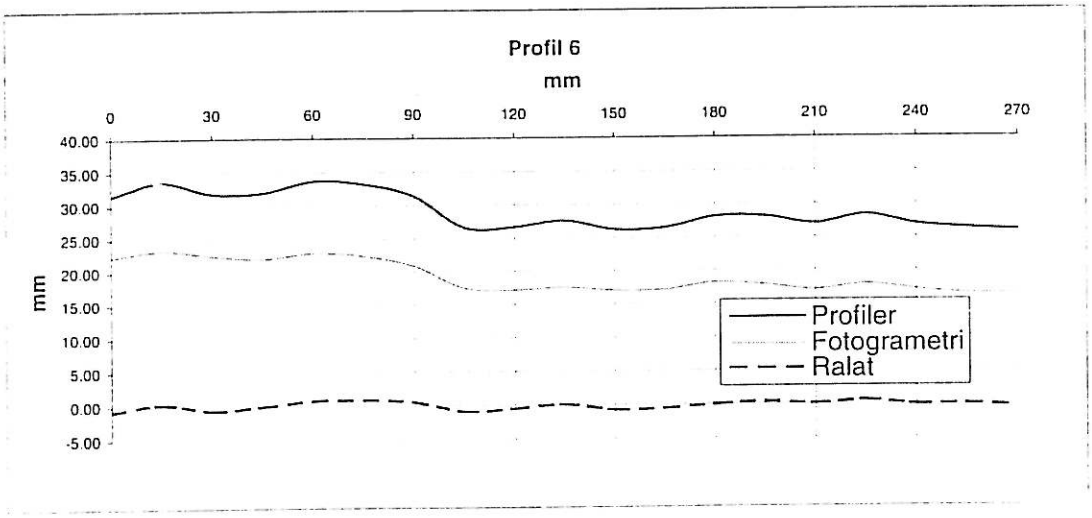
Profil 6
mm
0
30
60
90
120
150
180
210
240
270
40.00
35.00
30.00
25.00
20.00
15.00
10.00
5.00
0.00
-5.00
mm
Profiler
Fotogrametri
Ralat

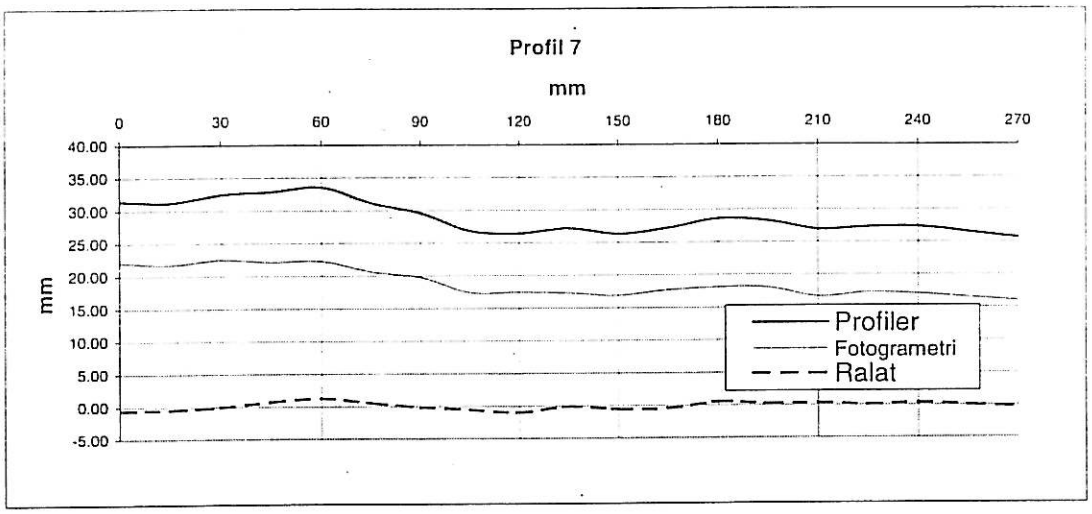
Profil 7
mm
0
30
60
90
120
150
180
210
240
270
40.00
35.00
30.00
25.00
20.00
15.00
10.00
5.00
0.00
-5.00
mm
Profiler
Fotogrametri
Ralat

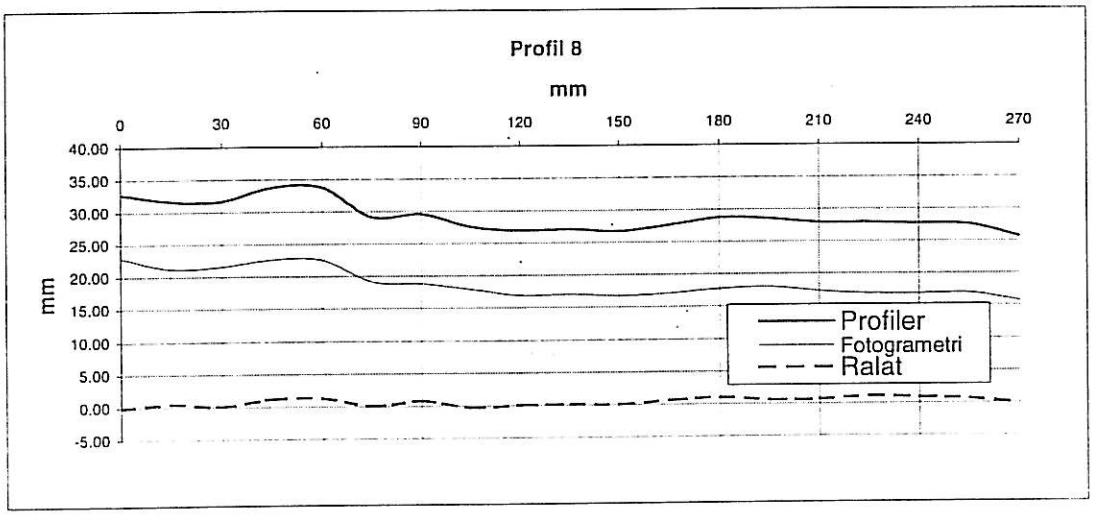
Profil 8
mm
0
30
60
90
120
150
180
210
240
270
40.00
35.00
30.00
25.00
20.00
15.00
10.00
5.00
0.00
-5.00
mm
Profiler
Fotogrametri
Ralat

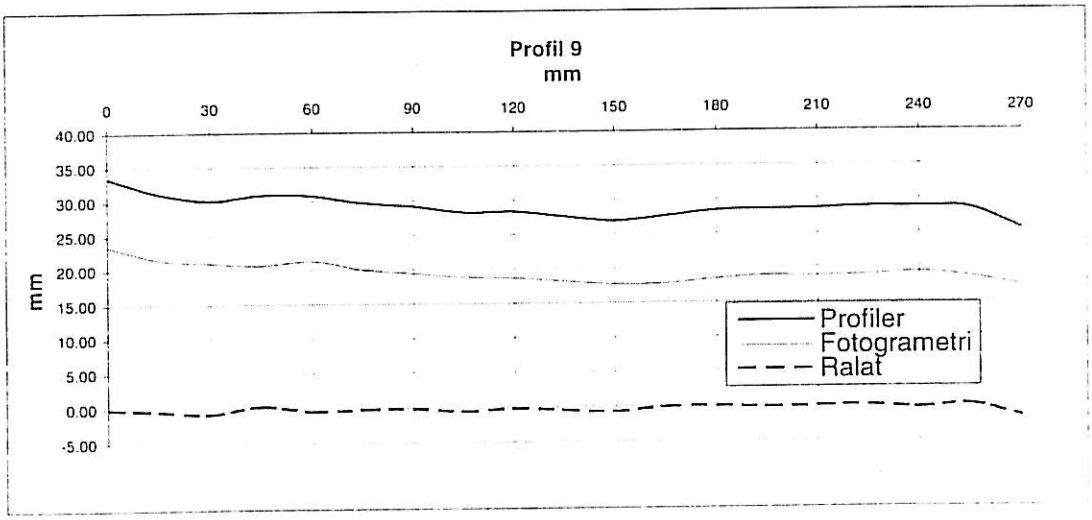
Profil 9
mm
0
30
60
90
120
150
180
210
240
270
40.00
35.00
30.00
25.00
20.00
15.00
10.00
5.00
0.00
-5.00
mm
Profiler
Fotogrametri
Ralat

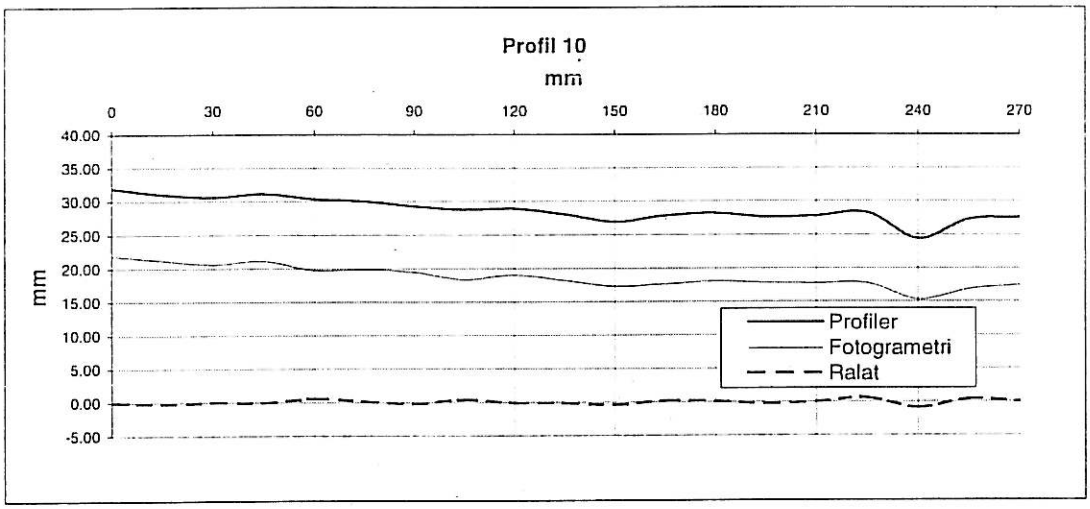
Profil 10
mm
0
30
60
90
120
150
180
210
240
270
40.00
35.00
30.00
25.00
20.00
15.00
10.00
5.00
0.00
-5.00
mm
Profiler
Fotogrametri
Ralat

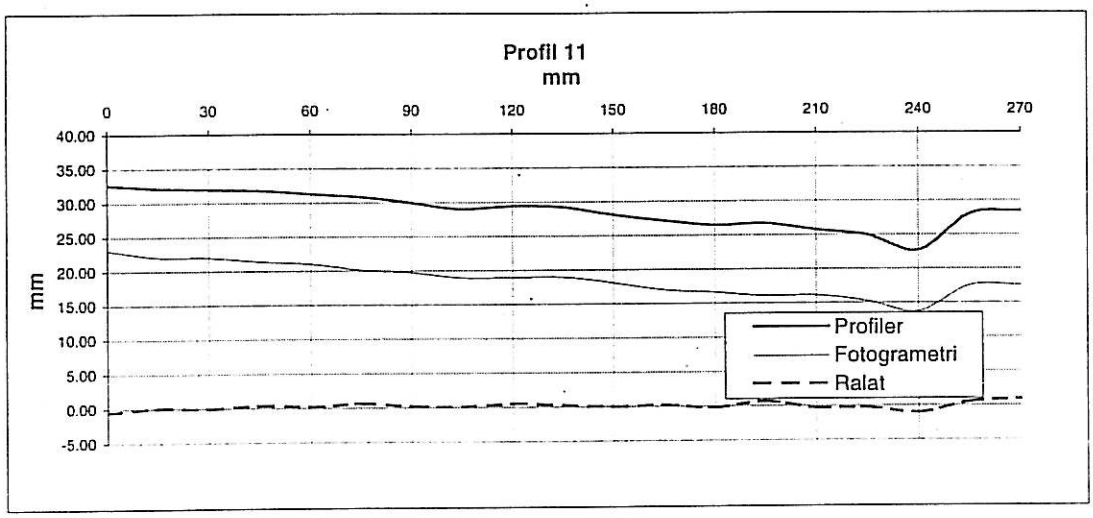
Profil 11
mm
0
30
60
90
120
150
180
210
240
270
40.00
35.00
30.00
25.00
20.00
15.00
10.00
5.00
0.00
-5.00
mm
Profiler
Fotogrametri
Ralat

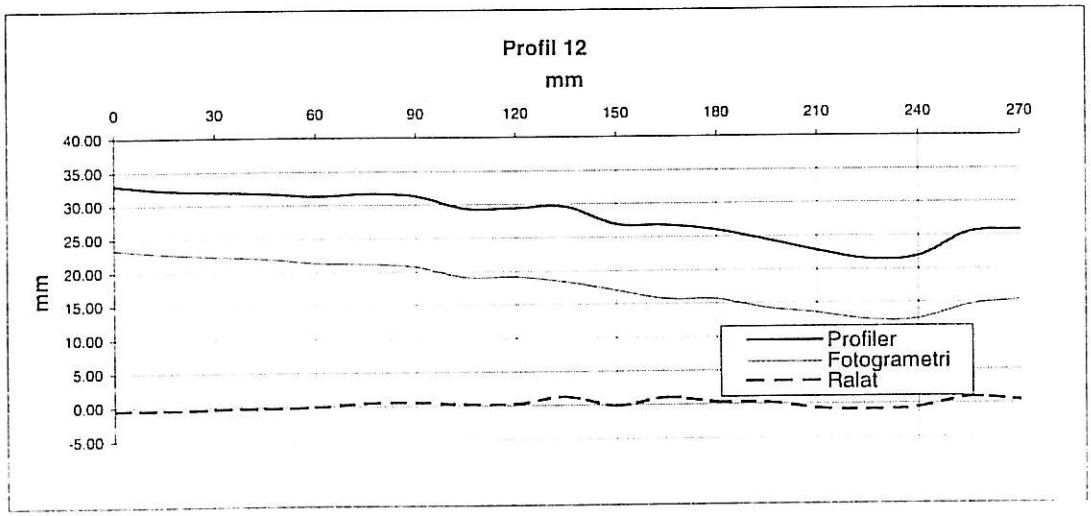
Profil 12
mm
0
30
60
90
120
150
180
210
240
270
40.00
35.00
30.00
25.00
20.00
15.00
10.00
5.00
0.00
-5.00
mm
Profiler
Fotogrametri
Ralat

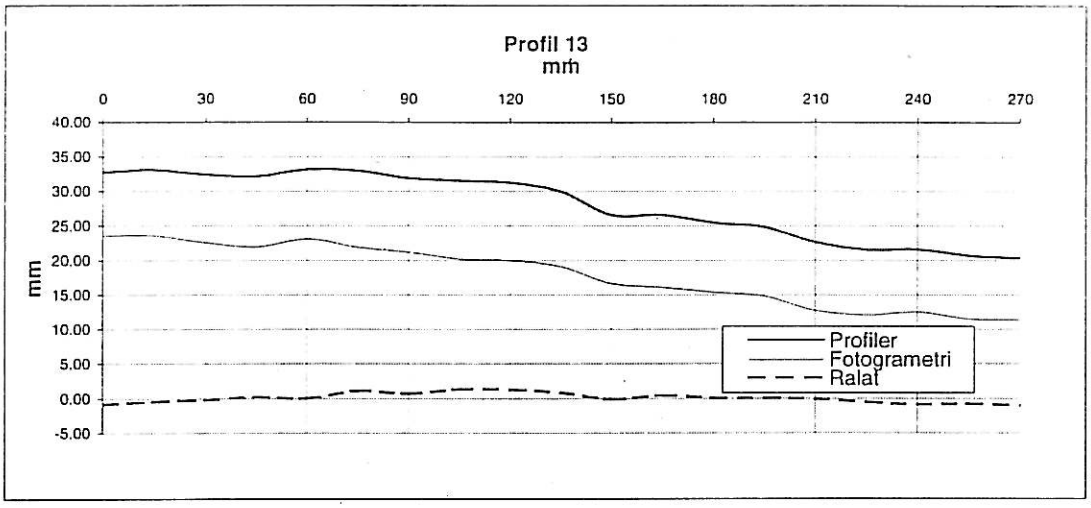
Profil 13
mm
0
30
60
90
120
150
180
210
240
270
40.00
35.00
30.00
25.00
20.00
15.00
10.00
5.00
0.00
-5.00
mm
Profiler
Fotogrametri
Ralat

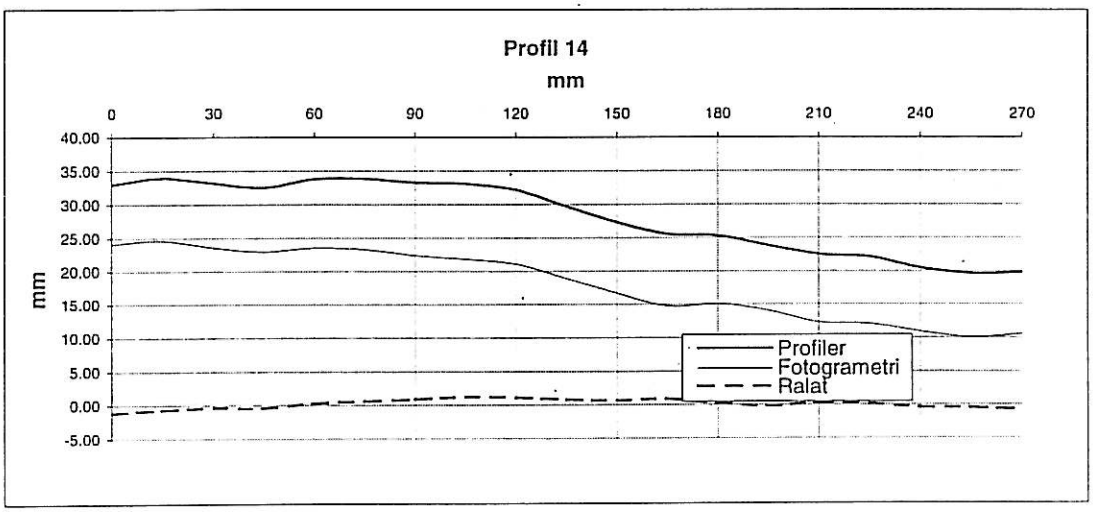
Profil 14
mm
0
30
60
90
120
150
180
210
240
270
40.00
35.00
30.00
25.00
20.00
15.00
10.00
5.00
0.00
-5.00
mm
Profiler
Fotogrametri
Ralat

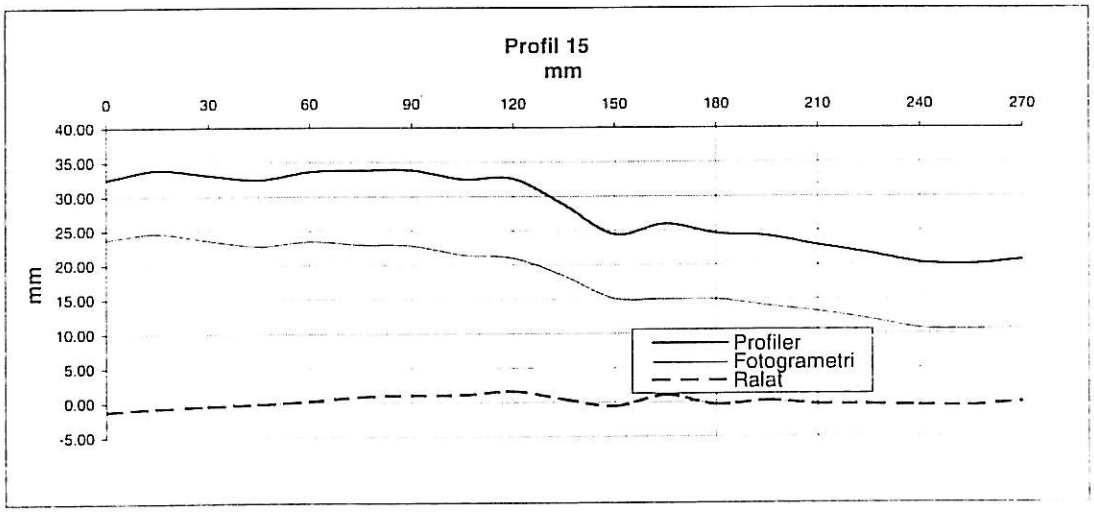
Profil 15
mm
0
30
60
90
120
150
180
210
240
270
40.00
35.00
30.00
25.00
20.00
15.00
10.00
5.00
0.00
-5.00
mm
Profiler
Fotogrametri
Ralat

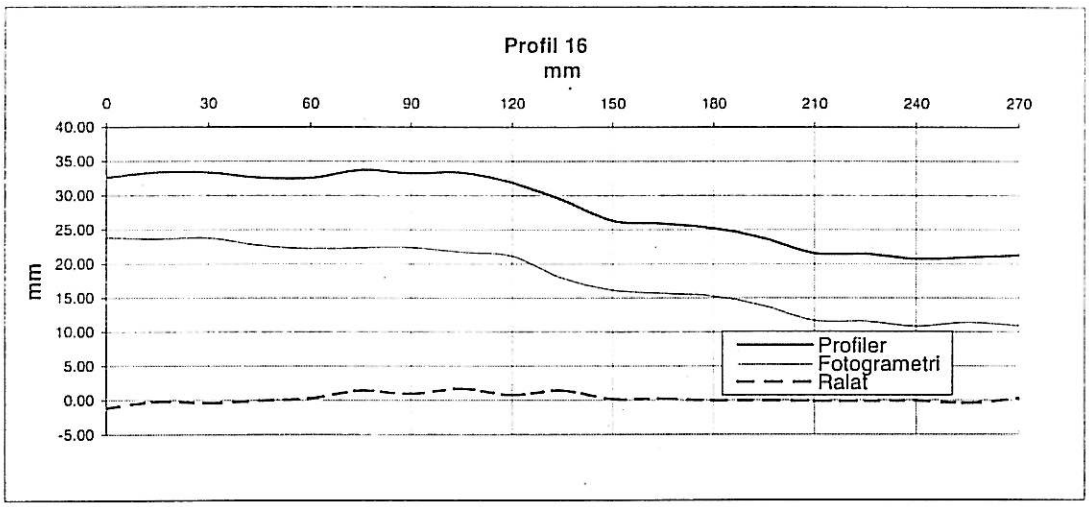
Profil 16
mm
0
30
60
90
120
150
180
210
240
270
40.00
35.00
30.00
25.00
20.00
15.00
10.00
5.00
0.00
-5.00
mm
Profiler
Fotogrametri
Ralat

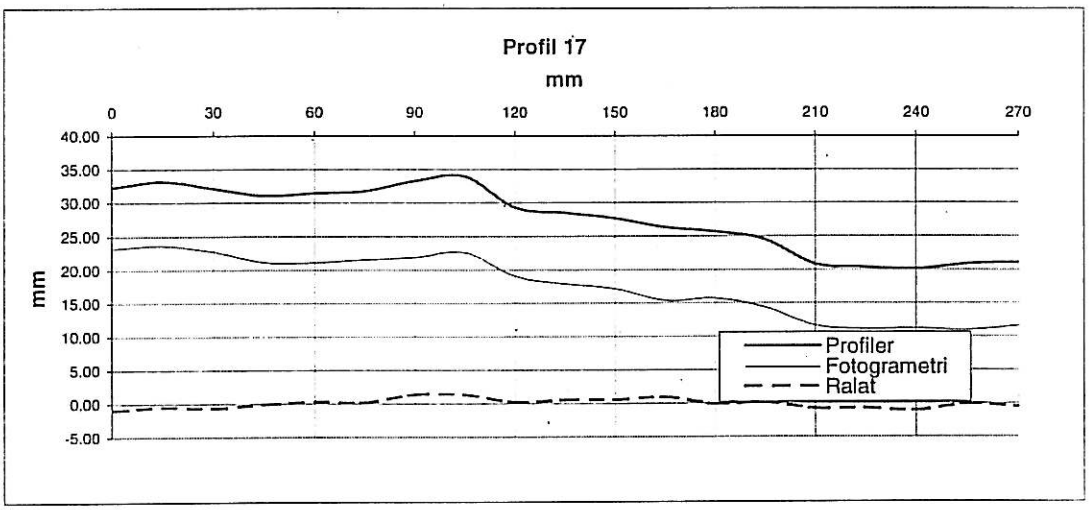
Profil 17
mm
0
30
60
90
120
150
180
210
240
270
40.00
35.00
30.00
25.00
20.00
15.00
10.00
5.00
0.00
-5.00
mm
Profiler
Fotogrametri
Ralat

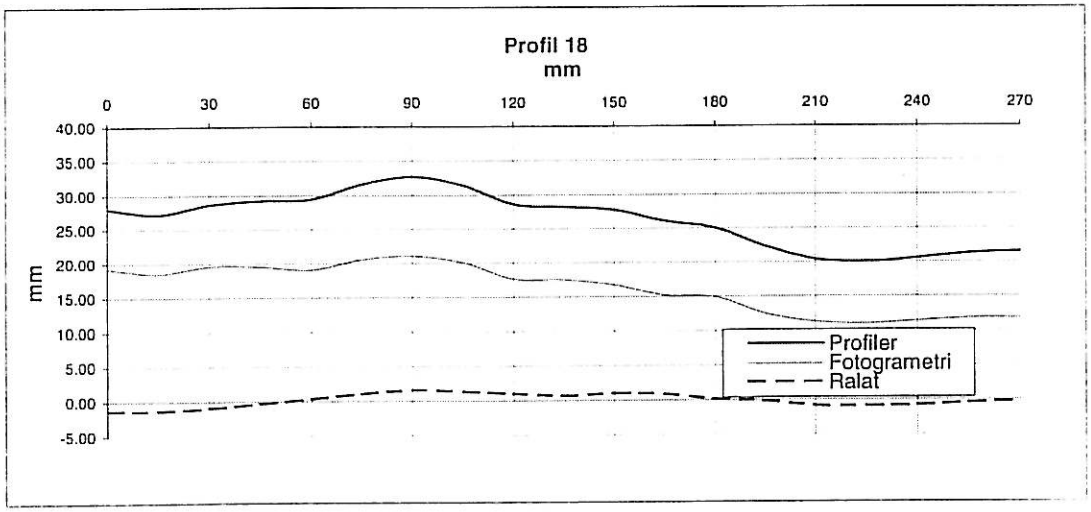
Profil 18
mm
0
30
60
90
120
150
180
210
240
270
40.00
35.00
30.00
25.00
20.00
15.00
10.00
5.00
0.00
-5.00
mm
Profiler
Fotogrametri
Ralat

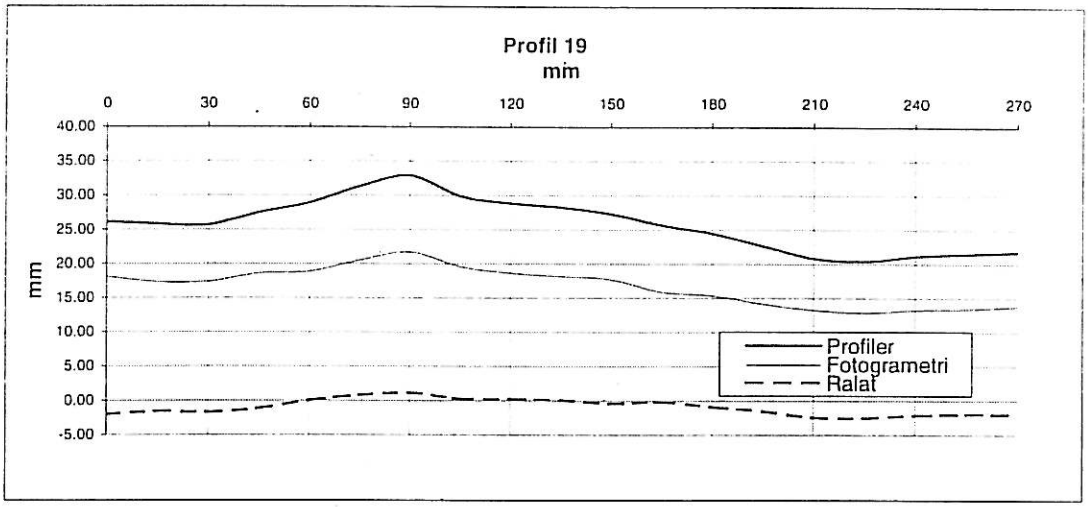
Profil 19
mm
0
30
60
90
120
150
180
210
240
270
40.00
35.00
30.00
25.00
20.00
15.00
10.00
5.00
0.00
-5.00
mm
Profiler
Fotogrametri
Ralat

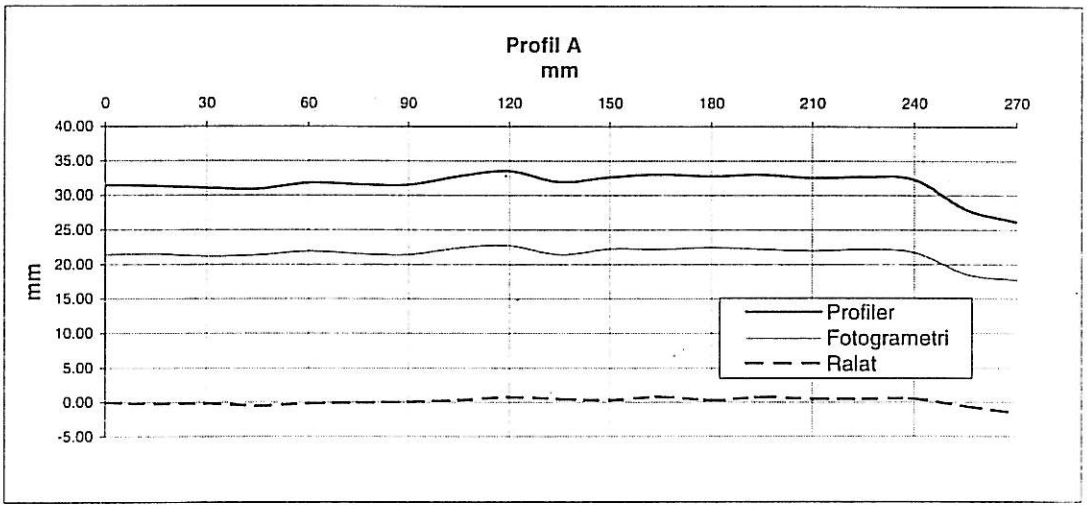
Profil A
mm
0
30
60
90
120
150
180
210
240
270
40.00
35.00
30.00
25.00
20.00
15.00
10.00
5.00
0.00
-5.00
mm
Profiler
Fotogrametri
Ralat

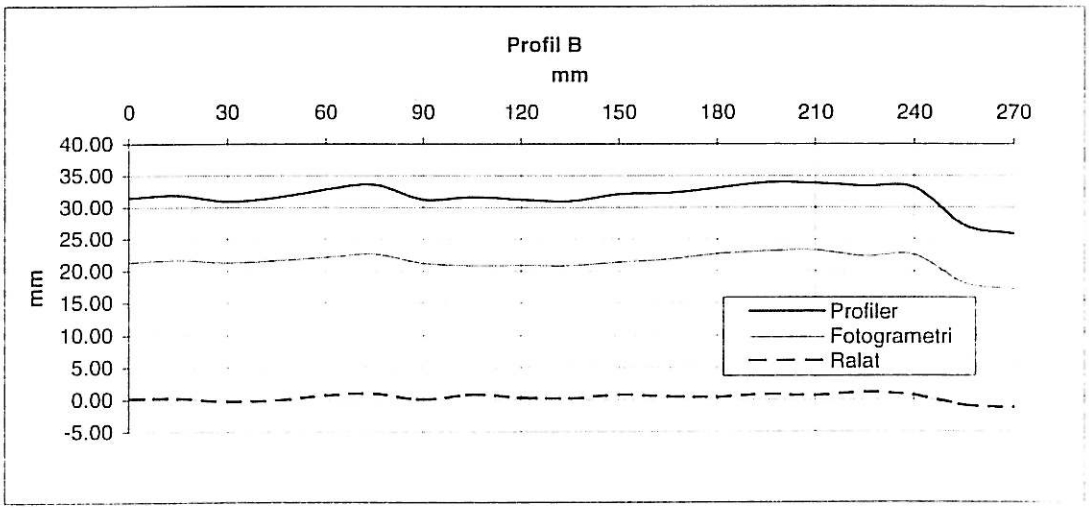
Profil B
mm
0
30
60
90
120
150
180
210
240
270
40.00
35.00
30.00
25.00
20.00
15.00
10.00
5.00
0.00
-5.00
mm
Profiler
Fotogrametri
Ralat

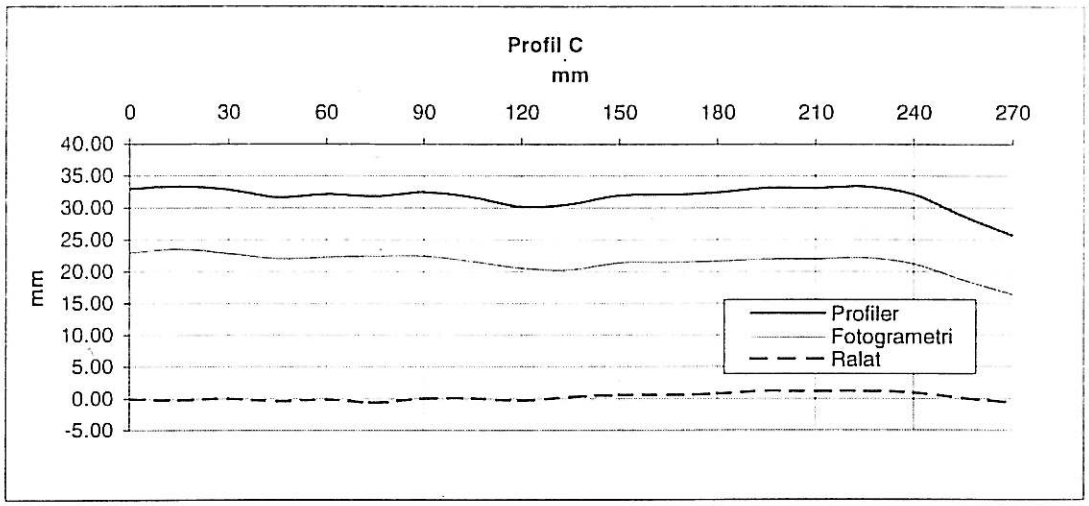
Profil C
mm
0
30
60
90
120
150
180
210
240
270
40.00
35.00
30.00
25.00
20.00
15.00
10.00
5.00
0.00
-5.00
mm
Profiler
Fotogrametri
Ralat

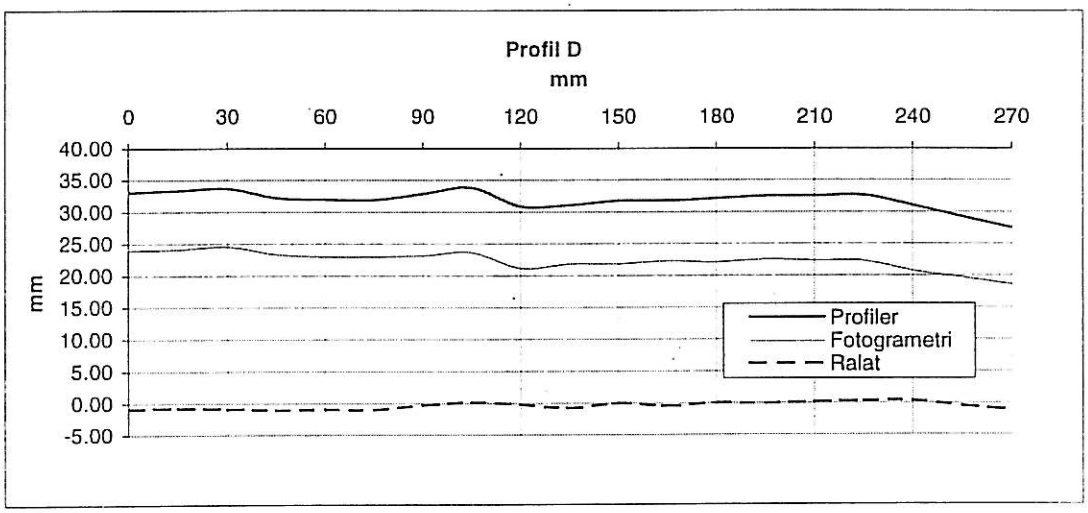
Profil D
mm
0
30
60
90
120
150
180
210
240
270
40.00
35.00
30.00
25.00
20.00
15.00
10.00
5.00
0.00
-5.00
mm
Profiler
Fotogrametri
Ralat

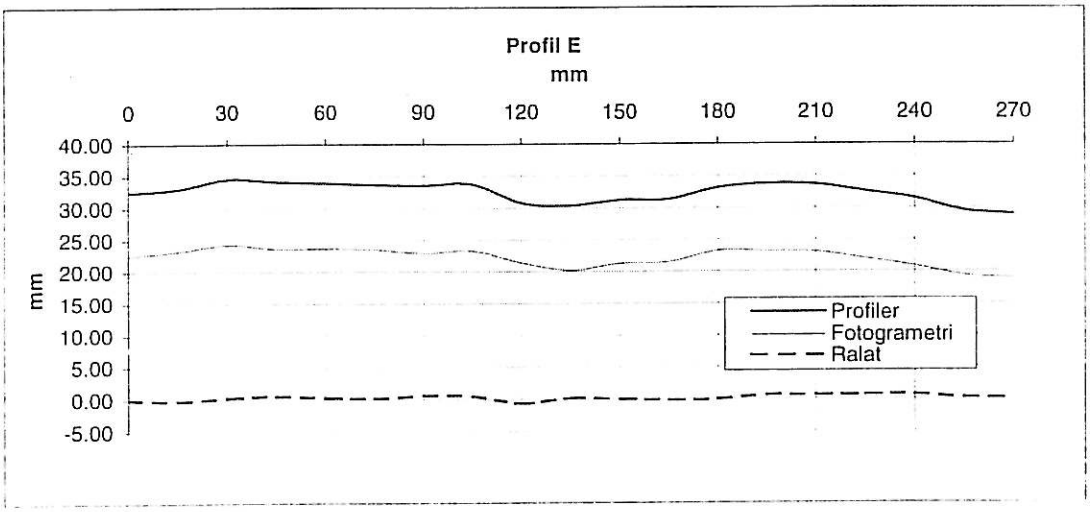
Profil E
mm
0
30
60
90
120
150
180
210
240
270
40.00
35.00
30.00
25.00
20.00
15.00
10.00
5.00
0.00
-5.00
mm
Profiler
Fotogrametri
Ralat

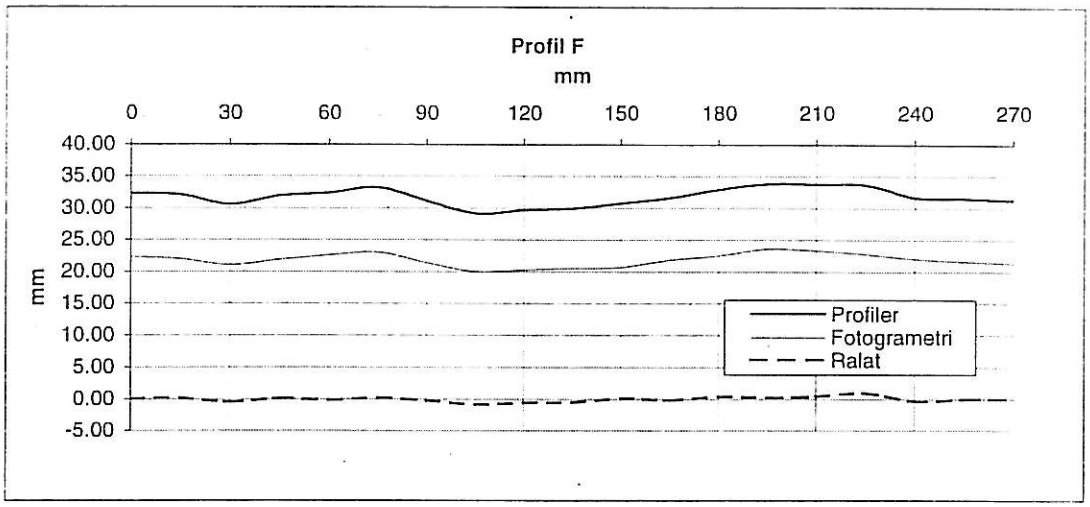
Profil F
mm
0
30
60
90
120
150
180
210
240
270
40.00
35.00
30.00
25.00
20.00
15.00
10.00
5.00
0.00
-5.00
mm
Profiler
Fotogrametri
Ralat

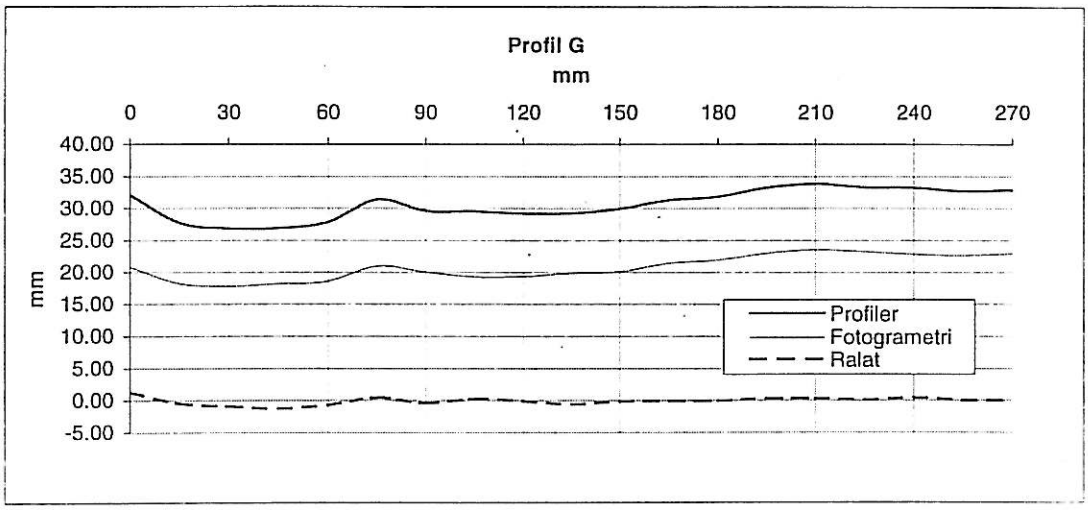
Profil G
mm
0
30
60
90
120
150
180
210
240
270
40.00
35.00
30.00
25.00
20.00
15.00
10.00
5.00
0.00
-5.00
mm
Profiler
Fotogrametri
Ralat

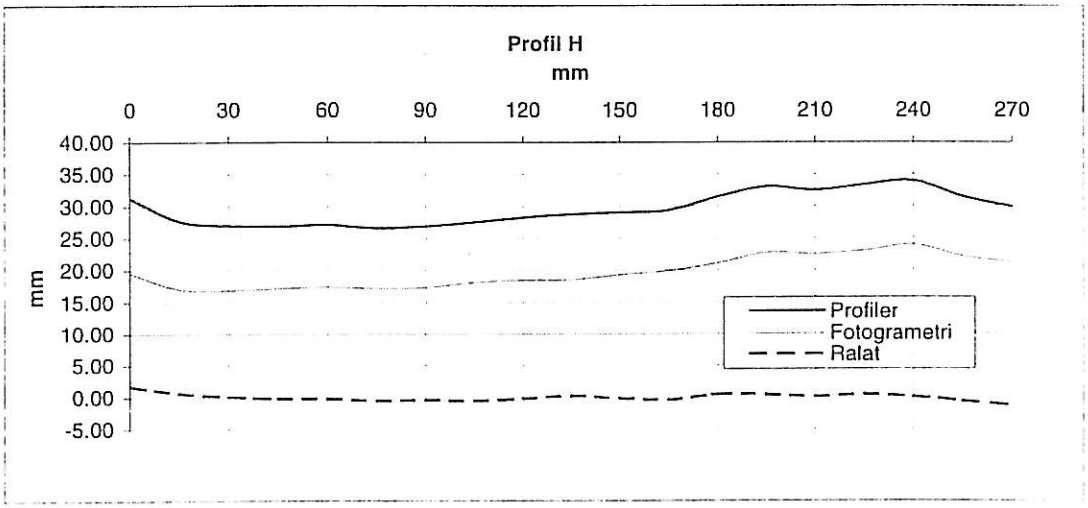
Profil H
mm
0
30
60
90
120
150
180
210
240
270
40.00
35.00
30.00
25.00
20.00
15.00
10.00
5.00
0.00
-5.00
mm
Profiler
Fotogrametri
Ralat

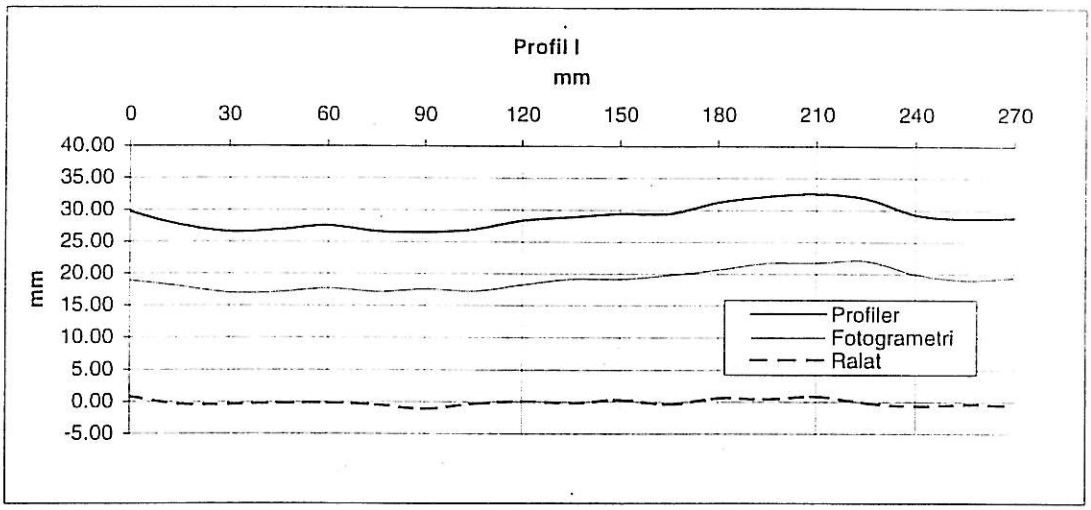
Profil I
mm
0
30
60
90
120
150
180
210
240
270
40.00
35.00
30.00
25.00
20.00
15.00
10.00
5.00
0.00
-5.00
mm
Profiler
Fotogrametri
Ralat

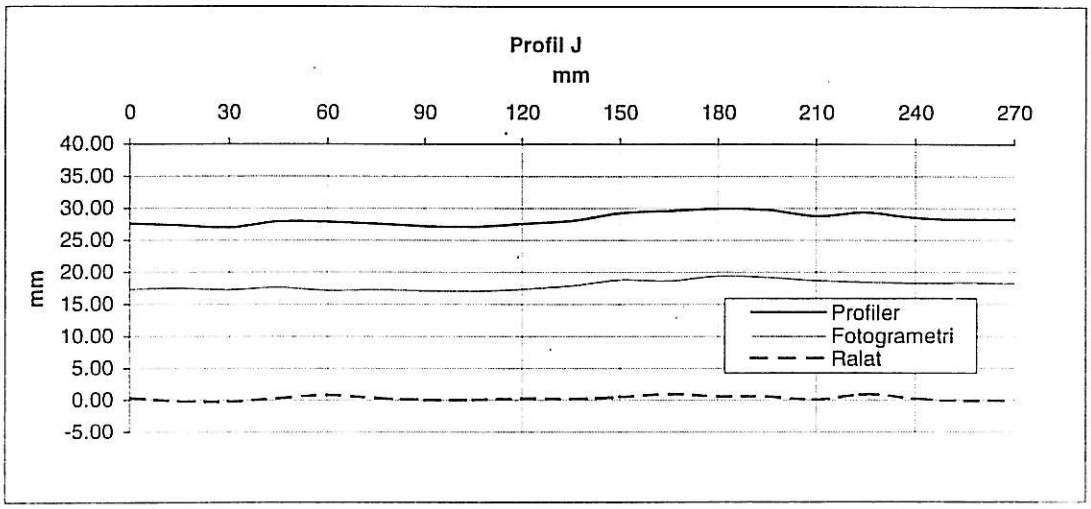
Profil J
mm
0
30
60
90
120
150
180
210
240
270
40.00
35.00
30.00
25.00
20.00
15.00
10.00
5.00
0.00
-5.00
mm
Profiler
Fotogrametri
Ralat

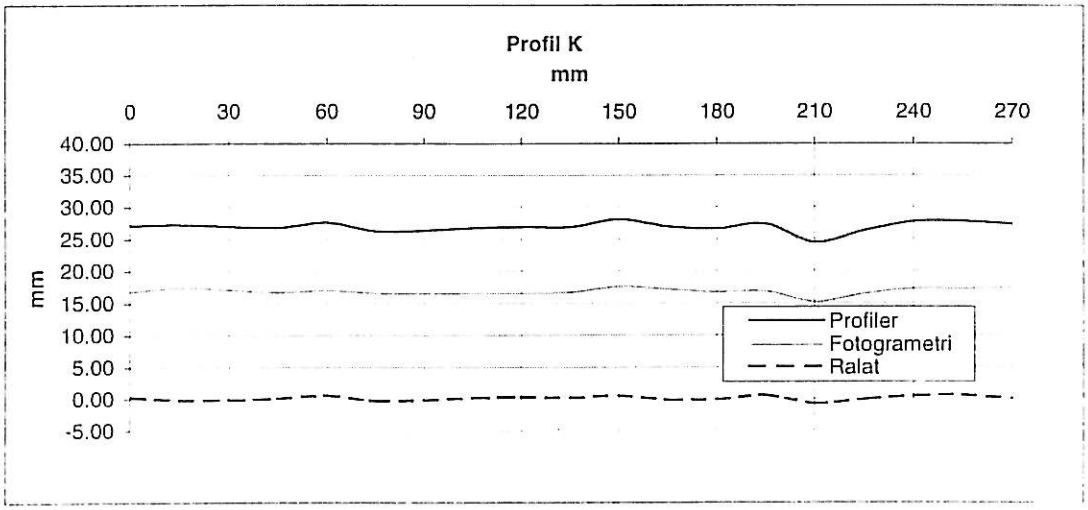
Profil K
mm
0
30
60
90
120
150
180
210
240
270
40.00
35.00
30.00
25.00
20.00
15.00
10.00
5.00
0.00
-5.00
mm
Profiler
Fotogrametri
Ralat

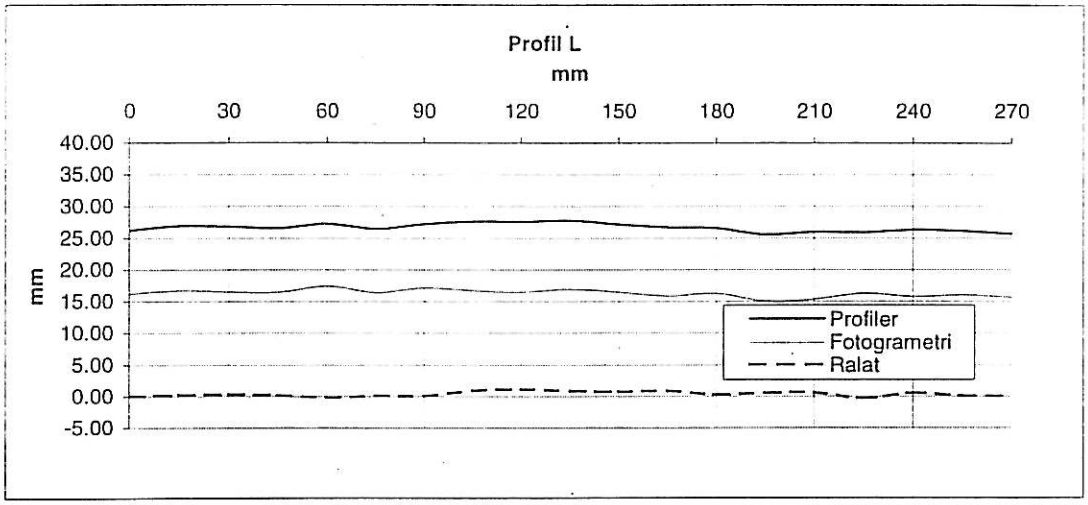
Profil L
mm
0
30
60
90
120
150
180
210
240
270
40.00
35.00
30.00
25.00
20.00
15.00
10.00
5.00
0.00
-5.00
mm
Profiler
Fotogrametri
Ralat

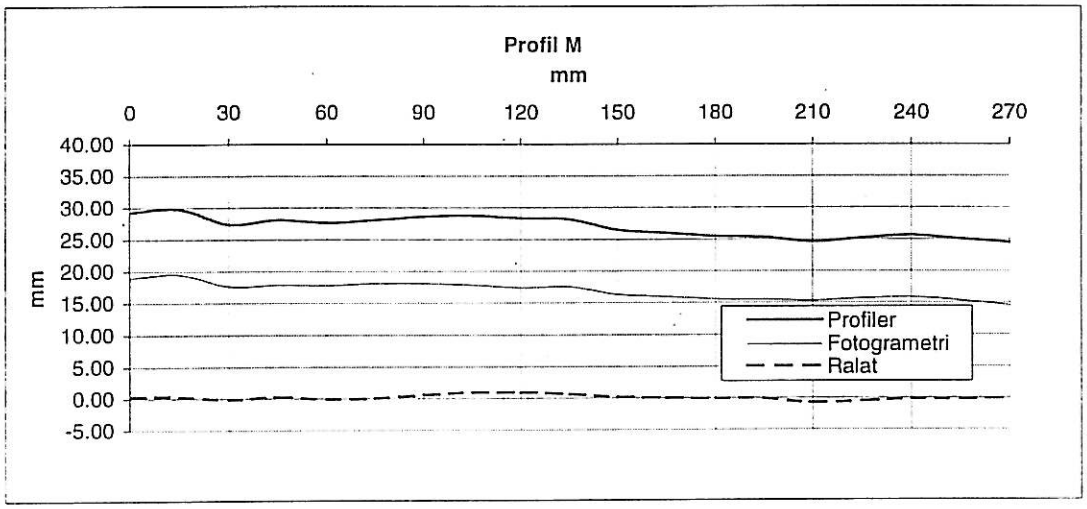
Profil M
mm
0
30
60
90
120
150
180
210
240
270
40.00
35.00
30.00
25.00
20.00
15.00
10.00
5.00
0.00
-5.00
mm
Profiler
Fotogrametri
Ralat

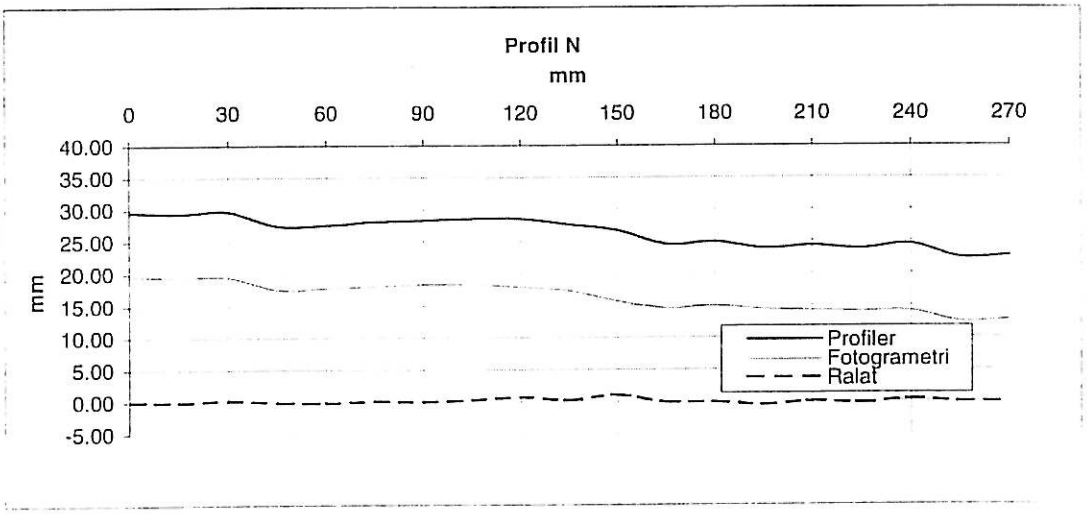
Profil N
mm
0
30
60
90
120
150
180
210
240
270
40.00
35.00
30.00
25.00
20.00
15.00
10.00
5.00
0.00
-5.00
mm
Profiler
Fotogrametri
Ralat

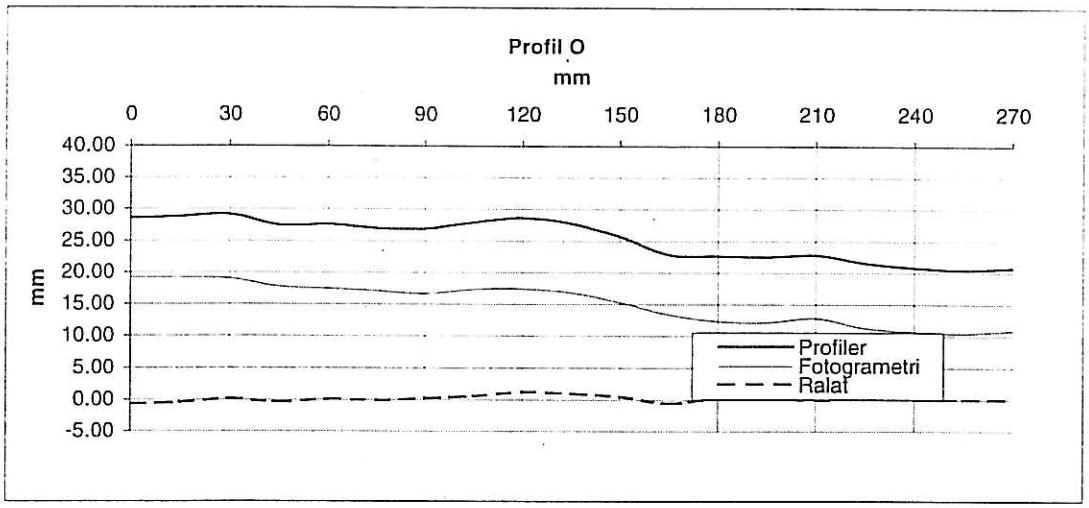
Profil O
mm
0
30
60
90
120
150
180
210
240
270
40.00
35.00
30.00
25.00
20.00
15.00
10.00
5.00
0.00
-5.00
mm
Profiler
Fotogrametri
Ralat

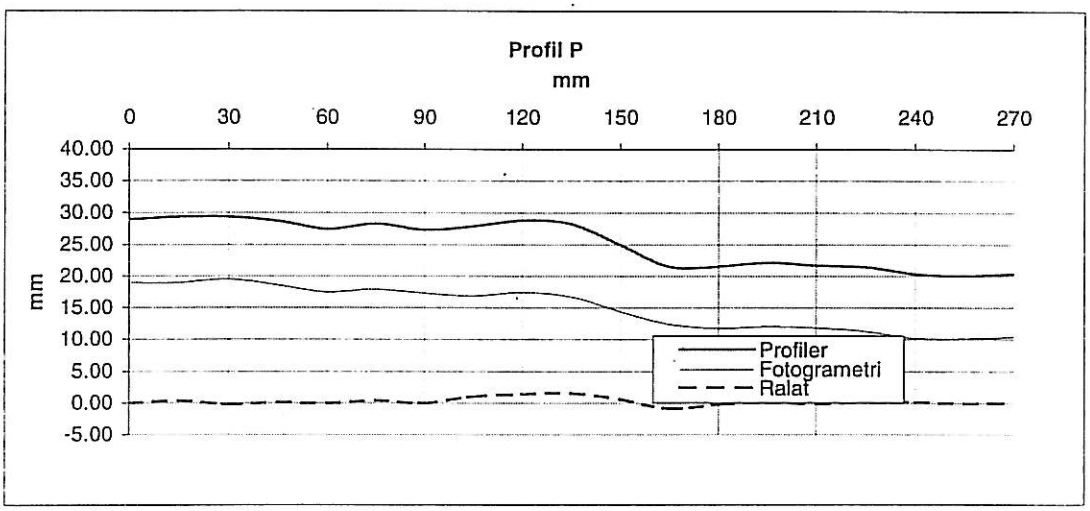
Profil P
mm
0
30
60
90
120
150
180
210
240
270
40.00
35.00
30.00
25.00
20.00
15.00
10.00
5.00
0.00
-5.00
mm
Profiler
Fotogrametri
Ralat

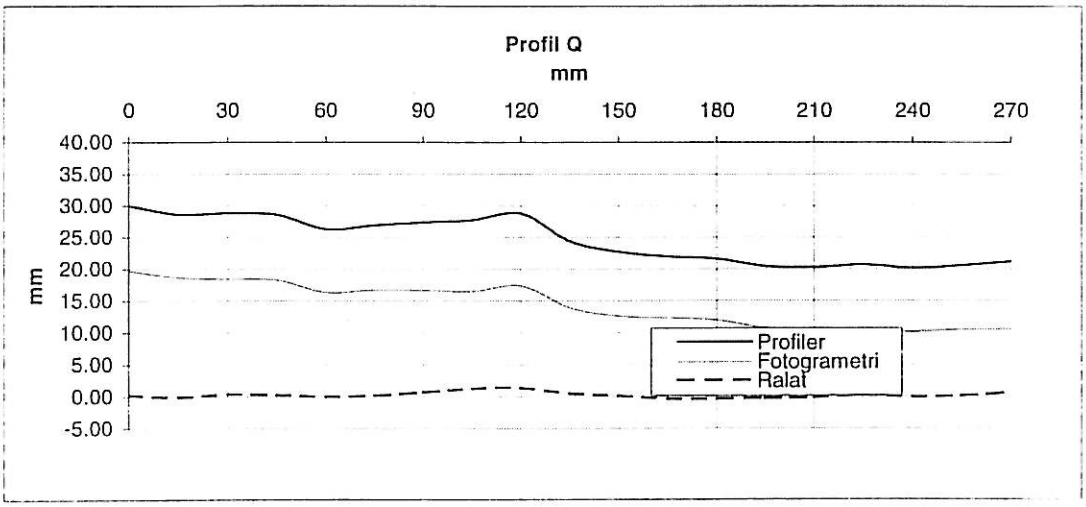
Profil Q
mm
0
30
60
90
120
150
180
210
240
270
40.00
35.00
30.00
25.00
20.00
15.00
10.00
5.00
0.00
-5.00
mm
Profiler
Fotogrametri
Ralat

APPENDIX H: Coordinates for joint surface obtained using photogrammetry method in the field

(semua nilai dalam unit mm)

X	Y	Z
-44.426	58.676	-709.937
-34.492	59.049	-710.986
-24.119	59.074	-711.793
-13.048	59.643	-709
-4.835	59.288	-714.183
5.107	59.873	-715.159
14.736	60.512	-718.544
22.698	59.533	-722.949
31.544	59.215	-728.887
40.761	59.853	-731.998
48.613	59.037	-737.786
58.207	59.763	-743.839
69.334	59.17	-744.709
-43.61	49.459	-706.865
-33.838	49.116	-708.663
-23.42	48.964	-710.196
-13.541	50.034	-710.513
-3.152	50.001	-710.804
6.219	50.605	-713.798
14.168	50.381	-718.087
22.215	50.016	-725.765
31.909	50.226	-727.875
40.724	50.13	-731.514
49.568	49.651	-736.463
59.232	49.281	-740.54
69.408	50.014	-745.064
-43.43	40.136	-704.373
-33.734	39.992	-705.337
-23.957	40.255	-707.892
-13.604	39.319	-709.377
-3.717	39.949	-710.447
6.249	40.754	-713.315
14.581	40.549	-718.195
23.904	40.529	-720.544
31.408	39.197	-726.993
42.282	39.979	-730.092
49.033	39.767	-734.245
59.178	39.681	-741.437
69.111	40.685	-746.057
-43	29.924	-702.929
-33.11	29.785	-704.054
-23.323	29.947	-705.513

X	Y	Z
-13.486	30.139	-707.778
-3.656	30.203	-711.023
6.229	30.15	-713.001
15.3	30.07	-717.242
23.76	29.997	-720.578
32.074	29.872	-727.439
41.909	29.996	-731.431
49.897	29.34	-737.771
59.646	29.522	-739.561
69.01	29.568	-745.468
-42.627	19.685	-700.681
-33.126	19.032	-704.823
-23.82	19.734	-706.01
-14.12	19.527	-709.684
-3.236	19.475	-712.187
5.819	18.487	-715.302
14.783	19.569	-717.721
23.255	19.951	-721.027
32.103	19.433	-726.683
40.822	19.683	-731.88
50.261	19.295	-736.48
60.599	19.703	-738.04
69.292	18.683	-744.202
-43.068	9.892	-699.246
-33.04	10.19	-702.526
-24.469	10.097	-706.987
-15.19	9.656	-711.181
-4.67	9.508	-711.978
4.328	8.734	-718.593
14.181	9.171	-719.671
23.757	9.339	-720.689
32.486	9.522	-725.516
41.722	9.611	-729.243
50.121	8.685	-733.52
59.695	9.14	-739.105
69.494	9.101	-745.442
-41.97	0.592	-697.453
-33.013	-0.053	-702.245
-24.276	-0.224	-706.142
-14.051	0.051	-709.862
-5.272	-0.153	-712.799
5.327	-0.348	-717.569

X	Y	Z
13.698	-0.619	-718.901
23.382	-0.667	-720.637
33.339	-0.406	-723.444
41.981	-1.405	-731.618
51.124	-0.671	-733.338
60.263	-0.727	-739.708
69.844	-0.92	-743.932
-43.566	-9.967	-699.607
-34.097	-9.578	-705.584
-23.8	-9.155	-706.223
-14.595	-9.92	-709.464
-5.295	-10.151	-712.517
4.693	-10.123	-716.285
13.745	-9.864	-718.285
23.245	-10.132	-720.652
33.382	-9.652	-722.705
42.288	-10.789	-729.349
50.637	-10.66	-735.063
60.303	-10.629	-738.68
70.473	-11.141	-742.597
-43.658	-19.339	-700.615
-34.673	-20.036	-706.317
-24.34	-19.615	-705.888
-13.521	-20.226	-707.315
-5.686	-19.584	-712.624
4.22	-19.849	-715.545
14.219	-19.37	-717.007
21.797	-20.101	-722.813
32.501	-19.539	-724.934
41.837	-20.503	-730.885
51.318	-21.026	-735.14
60.832	-20.762	-737.947
70.234	-20.223	-741.333
-43.665	-29.516	-701.357
-34.146	-29.75	-707.183
-25.261	-29.511	-706.875
-13.985	-29.859	-707.681
-5.235	-30.323	-713.687
3.722	-30.539	-719.275
14.776	-29.851	-717.671
21.738	-30.549	-721.269
32.49	-31.112	-724.26
41.365	-31.576	-731.07
51.224	-30.578	-733.437
60.714	-30.302	-737.686
70.447	-31.347	-742.32
-43.709	-40.219	-703.078
-34.735	-41.513	-706.09
-25.372	-40.739	-707.925

X	Y	Z
-15.591	-41.536	-709.186
-5.681	-41.563	-711.97
3.168	-41.563	-716.711
14.254	-42.143	-718.256
22.297	-41.07	-720.869
32.584	-41.631	-724.631
41.689	-41.638	-727.501
51.91	-42.982	-733.294
59.773	-41.635	-738.849
69.241	-42.444	-741.723
-44.325	-50.375	-703.059
-34.625	-50.932	-706.471
-26.424	-50.641	-708.377
-14.415	-50.978	-710.748
-5.608	-50.685	-711.411
4.738	-51.756	-713.487
13.261	-51.474	-715.086
22.298	-51.798	-721.514
32.6	-51.849	-725.222
41.853	-51.61	-728.765
50.882	-52.473	-736.401
59.329	-52.187	-738.87
68.977	-53.297	-743.891
-44.815	-60.022	-703.54
-34.743	-60.612	-707.573
-26.654	-60.804	-707.911
-16.039	-60.598	-711.23
-6.164	-61.385	-713.107
4.348	-61.397	-714.652
13.753	-61.413	-717.172
20.819	-60.671	-722.647
31.205	-61.053	-728.536
40.187	-61.94	-734.866
50.072	-61.992	-738.468
58.883	-61.187	-740.526
68.004	-61.254	-745.555